

PROPELLER EXCITED BOSSING FORCES

Albert L. Jenks, Jr.

and

Robert P. Metzger

Library
U. S. Naval Postgraduate School
Monterey, California



PROPELLER EXCITED BOSSING FORCES

by

ALBERT L. JENKS, JR., LIEUTENANT, U.S. NAVY
//

B.S., U.S. Naval Academy
(1949)

ROBERT P. METZGER, LIEUTENANT, U.S. NAVY

B.S., U.S. Naval Academy
(1947)

SUBMITTED IN PARTIAL FULFILLMENT

OF THE REQUIREMENTS FOR THE

DEGREE OF NAVAL

ENGINEER

at the

MASSACHUSETTS INSTITUTE OF

TECHNOLOGY

MAY 1955

PROPELLER EXCITED BOSSING FORCES

by

Albert L. Jenks, Jr., Lieutenant, U.S. Navy

Robert P. Metzger, Lieutenant, U.S. Navy

Submitted to the Department of Naval Architecture and Marine Engineering on 20 May 1955 in partial fulfillment of the requirements for the degree of Naval Engineer.

ABSTRACT

The objective of this thesis has been the investigation of the influence of various design and operational parameters on the magnitude and phase relationship of propeller excited bossing forces. The investigation was confined to the hydrodynamically induced forces normal to the bossing.

A model bossing was installed upstream of a four-bladed Troost propeller in the test section of the MIT Marine Propeller Tunnel. The magnitudes of the forces were determined by comparison of the response of the bossing system as instrumentation readings with readings representing the application of known forces to the bossing. Phase relationships were obtained by combining angular measurements computed from the instrumentation readings with direct angular readings, taken by means of properly timed strobe lights.

The major conclusions of this investigation are:

(1) The hydrodynamically induced vibratory force normal to the bossing is a function of propeller thrust, water velocity, clearance, and bossing length.

(2) The generally accepted law of similitude for scaling bossing forces is substantially in error for the forces measured in this investigation.

(3) The phase angle relationship between the measured force and the propeller blade is relatively insensitive to clearance, but varies with propeller thrust and bossing length.

The major recommendations resulting from this thesis are:

PROPELLER EXCITED HOSSING FORCES

by

Albert L. Jenks, Jr., Lieutenant, U.S. Navy
Robert P. Metzger, Lieutenant, U.S. Navy

Submitted to the Department of Naval Architecture and
Marine Engineering on 20 May 1955 in partial fulfill-
ment of the requirements for the degree of Naval Engineer.

ABSTRACT

The objective of this thesis has been the investi-
gation of the influence of various design and operational
parameters on the magnitude and phase relationship of pro-
peller excited hosing forces. The investigation was con-
fined to the hydrodynamically induced forces normal to the
hosing.

A model hosing was installed upstream of a four-
bladed tractor propeller in the test section of the MIT Marine
Propeller Tunnel. The magnitudes of the forces were deter-
mined by comparison of the response of the hosing system
as instrumentation readings with readings representing the
application of known forces to the hosing. Phase relation-
ships were obtained by combining angular measurements com-
puted from the instrumentation readings with direct angular
readings, taken by means of properly fixed stereo lights.

The major conclusions of this investigation are:

(1) The hydrodynamically induced hosing force
normal to the hosing is a function of propeller thrust,
water velocity, clearance, and hosing length.

(2) The generally accepted law of similarity for
hosing hosing forces is substantially in error for the
forces measured in this investigation.

(3) The phase angle relationship between the
measured force and the propeller blade is relatively in-
sensitive to clearance, but varies with propeller thrust
and hosing length.

The major recommendations resulting from this
thesis are:

- (1) Investigate the existing law of similitude,
- (2) Verify the conclusion that the magnitude of the force is a function of the water velocity, and
- (3) Investigate the effect of variable wake on the magnitude of the vibratory force and its phase angle.

Thesis Supervisor: Frank M. Lewis

Title: Professor of Marine Engineering

- (1) Investigate the existing law of similitude.
- (2) Verify the conclusion that the magnitude of the force is a function of the water velocity, and
- (3) Investigate the effect of variable wave on the magnitude of the vibratory force and its phase angle.

Title: Professor of Marine Engineering
 Thesis Supervisor: Frank W. Lewis

Cambridge, Massachusetts
20 May 1955

Secretary of the Faculty
Massachusetts Institute of Technology
Cambridge 39, Massachusetts

Dear Sir:

In accordance with the requirement for the
Degree of Naval Engineer, we submit herewith a thesis
entitled: "Propeller Excited Bossing Forces".

Respectfully yours,

ACKNOWLEDGEMENT

Without the patient guidance and engineering genius of Professor Frank M. Lewis, this investigation would not have been possible.

TABLE OF CONTENTS

<u>Title</u>	<u>Page</u>
I. Introduction	1
II. Apparatus	11
General	11
A. Propeller Tunnel	15
B. Propeller	16
C. Bossing	17
D. Horizontal Arm	20
E. Mounting	20
F. Detector System	24
G. Calibrator	30
H. Phase System	37
I. Speed Control	39
III. Procedure	42
IV. Results	49
V. Discussion of Results	62
VI. Conclusions	69
VII. Recommendations	71
VIII. Appendix	74
A. Details of Procedure	75
1. Determination of an Acceptable Calibration and Measure Pro- cedure	75
2. Details of Force Determination	87
3. Details of Phase Angle De- termination	95
B. Sample Calculation	103
C. Original Data and Calculations	109
D. Bibliography	157

TABLE OF CONTENTS

<u>Page</u>	<u>Title</u>
I	I. Introduction
11	II. Apparatus
11	General
12	A. Propeller Tunnel
16	B. Propeller
17	C. Hoisting
20	D. Horizontal Arm
20	E. Mounting
24	F. Detector System
30	G. Calibrator
37	H. Phase System
39	I. Speed Control
42	III. Procedure
49	IV. Results
62	V. Discussion of Results
69	VI. Conclusions
71	VII. Recommendations
74	VIII. Appendix
75	A. Details of Procedure
	1. Determination of an Acceptable
	Calibration and Residue Pro-
75	cedure
87	2. Details of Force Determination
	3. Details of Phase Angle De-
92	termination
102	B. Sample Calculation
109	C. Original Data and Calculations
127	D. Bibliography

LIST OF FIGURES

	Page
I Creation of Force	4
II Propeller and Bossing in Test Section	12
III Bossing System as Mounted in Test Section	13
IV Propeller Testing Tunnel at M.I.T.	14
V Bossing	18
VI Bossing, Nose Piece, and Spacer Rings	12
VII Horizontal Arm	21
VIII Mountings	23
IX Wiring Diagram of Detector Circuit	25
X Detector	26
XI Instrumentation Arrangement	27
XII Calibrator	31
XIII Lever Arms	33
XIV Calibrator in Position for a Calibration Run	34
XV Calibration Set-up	35
XVI Calibrator in Position for a Measurement Run	38
XVII Telescope Mounted in Test Section Window	38
XVIII Propeller Tunnel Speed Control Circuit ...	40
XIX Tuning Fork	34
XX Force Determination	44
XXI Plot of Force vs Thrust for Short Bossing	52
XXII Plot of Force vs Thrust for Long Bossing..	53

LIST OF FIGURES

Page	Figure
1	I Creation of Force
12	II Propeller and housing in Test Section
13	III Housing system as mounted in Test Section
14	IV Propeller Testing Tunnel at N.S.T.
15	V Housing
16	VI Housing, hose piece, and spacer rings
21	VII Horizontal Arm
23	VIII Mountings
25	IX Wiring Diagram of Detector Circuit
26	X Detector
27	XI Instrumentation Arrangement
31	XII Calibrator
33	XIII Lever Arm
34	XIV Calibrator in Position for a Calibration Run
35	XV Calibration Set-up
36	XVI Calibrator in Position for a Measurement Run
38	XVII Telescope mounted in Test Section Window
40	XVIII Propeller Tunnel Speed Control Circuit
42	XIX Tuning Fork
44	XX Force Determination
52	XXI Plot of Force vs Thrust for short housing
53	XXII Plot of Force vs Thrust for long housing

LIST OF FIGURES
(continued)

	Page
XXIII Plot of Force vs Clearance	54
XXIV Plot of Force vs Clearance, Semi-Log	55
XXV Plot of Force vs Thrust, Short Bossing with Variable Water Velocity	56
XXVI Plot of Force vs Water Velocity, Short Bossing	57
XXVII Bossing Clearance	88
XXVIII Force Measured	88
XXIX Force Sign Convention	89
XXX Phase Angle Relationships for Calibration and Measurement	97
XXXI Composite Phase Angle Diagram	98
XXXII Calibration Curve for Short Bossing, Clearance 1.00"	145
XXXIII Calibration Curve for Short Bossing, Clearance 1.00"	146
XXXIV Calibration Curve for Short Bossing, Clearances of 1.00", 2.00", 3.00"	147
XXXV Calibration Curve for Short Bossing, Clearances of 1.50", 2.25", 2.75"	148
XXXVI Plot of RPM vs Resultant Reading for Short Bossing, Clearance 2.00"	149
XXXVII Calibration Curve for Short Bossing, Clearance 2.00", Variable RPM	150
XXXVIII Calibration Curve for Short Bossing, Clearance 2.00", Variable RPM	151
XXXIX Calibration Curve for Short Bossing, Clearance 2.00", Variable RPM	152

LIST OF FIGURES
(continued)

Page	
24	XXIII Plot of Force vs Clearance
25	XXIV Plot of Force vs Clearance, Inclined
26	XXV Plot of Force vs Thrust, Short Bearing with Variable Water Velocity
27	XXVI Plot of Force vs Water Velocity, Short Bearing
28	XXVII Bearing Clearance
29	XXVIII Force Measured
30	XXIX Force Sign Convention
31	XXX Phase Angle Relationships for Calibration and Measurement
32	XXXI Composite Phase Angle Diagram
145	XXXII Calibration Curve for Short Bearing, Clearance 1.00"
146	XXXIII Calibration Curve for Short Bearing, Clearance 1.00"
147	XXXIV Calibration Curve for Short Bearing, Clearances of 1.00", 1.50", 2.00"
148	XXXV Calibration Curve for Short Bearing, Clearances of 1.50", 2.50", 3.75"
149	XXXVI Plot of HFM vs Resonant Bearing for Short Bearing, Clearance 1.00"
150	XXXVII Calibration Curve for Short Bearing, Clearance 2.00", Variable RPM
151	XXXVIII Calibration Curve for Short Bearing, Clearance 2.50", Variable RPM
152	XXXIX Calibration Curve for Short Bearing, Clearance 3.00", Variable RPM

LIST OF FIGURES
(continued)

	Page
XL Plot of J vs Thrust	153
XLI Calibration Curve for Long Bossing, Clearance 1.00", 1.25", 1.50"	154
XLII Calibration Curve for Long Bossing, Clearance, 1.50", 1.75", 2.00", 2.25", 2.50"	155
XLIII Calibration Curve for Long Bossing, Clearances of 2.50", 2.75", 3.00"	156

(5441100)

Page 10

123 Plot of J vs Thrust 123

XLI Calibration Curve for Long Boiling, Clearance 1.50", 1.75", 1.90" 124

XLII Calibration Curve for Long Boiling, Clearance 1.50", 1.75", 1.90", 2.25", 2.50" 125

XLIII Calibration Curve for Long Boiling, Clearances of 2.50", 2.75", 3.00" 126

LIST OF TABLES

		Page
I	Calibration Run No. 1, Short Bossing, Clearance 1.00"	110
II	Calibration Run No. 2, Short Bossing, Clearance 1.00"	112
III	Measurement Run No. 1, Short Bossing, Clearance 1.00"	113
IV	Calibration Run No. 3, Short Bossing, Clearance 1.50"	114
V	Measurement Run No. 2, Short Bossing, Clearance 1.50"	115
VI	Measurement Run No. 3, Short Bossing, Clearance 1.75"	116
VII	Calibration Run No. 4, Short Bossing, Clearance 2.00"	117
VIII	Calibration Run No. 4, Short Bossing, Clearance 2.00"	119
IX	Measurement Run No. 8, Short Bossing, Clearance 2.00"	121
X	Calibration Run No. 5, Short Bossing, Clearance 2.25"	122
XI	Measurement Run No. 4, Short Bossing, Clearance 2.25"	123
XII	Measurement Run No. 5, Short Bossing, Clearance 2.50"	124
XIII	Calibration Run No. 6, Short Bossing, Clearance 2.75"	125
XIV	Measurement Run No. 6, Short Bossing, Clearance 2.75"	126
XV	Calibration Run No. 7, Short Bossing, Clearance 3.00"	127

LIST OF TABLES

110	Calibration Run No. 1, Short Boring, Clearance 1.00"	I
112	Calibration Run No. 2, Short Boring, Clearance 1.00"	II
113	Measurement Run No. 1, Short Boring, Clearance 1.00"	III
114	Calibration Run No. 3, Short Boring, Clearance 1.50"	IV
115	Measurement Run No. 2, Short Boring, Clearance 1.50"	V
116	Measurement Run No. 3, Short Boring, Clearance 1.75"	VI
117	Calibration Run No. 4, Short Boring, Clearance 2.00"	VII
118	Calibration Run No. 4, Short Boring, Clearance 2.00"	VIII
121	Measurement Run No. 5, Short Boring, Clearance 2.00"	IX
122	Calibration Run No. 5, Short Boring, Clearance 2.25"	X
123	Measurement Run No. 4, Short Boring, Clearance 2.25"	XI
124	Measurement Run No. 5, Short Boring, Clearance 2.50"	XII
125	Calibration Run No. 6, Short Boring, Clearance 2.75"	XIII
126	Measurement Run No. 6, Short Boring, Clearance 2.75"	XIV
127	Calibration Run No. 7, Short Boring, Clearance 3.00"	XV

LIST OF TABLES
(continued)

	Page
XVI Measurement Run No. 7, Short Bossing, Clearance 3.00"	128
XVII Measurement Run No. 9, Short Bossing, Clearance 2.00"	129
XVIII Measurement Run No. 10, Short Bossing, Clearance 2.00"	130
XIX Calibration Run No. 8, Long Bossing, Clearance 1.00"	131
XX Calibration Run No. 9, Long Bossing, Clearance 1.50"	132
XXI Calibration Run No. 10, Long Bossing, Clearance 2.00"	133
XXII Calibration Run No. 11, Long Bossing, Clearance 2.50"	134
XXIII Calibration Run No. 12, Long Bossing, Clearance 3.00"	135
XXIV Measurement Run No. 11, Long Bossing, Clearance 1.00"	136
XXV Measurement Run No. 12, Long Bossing, Clearance 1.25"	137
XXVI Measurement Run No. 13, Long Bossing, Clearance 1.50"	138
XXVII Measurement Run No. 14, Long Bossing, Clearance 1.75"	139
XXVIII Measurement Run No. 15, Long Bossing, Clearance 2.00"	140
XXIX Measurement Run No. 16, Long Bossing, Clearance 2.25"	141
XXX Measurement Run No. 17, Long Bossing, Clearance 2.50"	142

LIST OF TABLES
(continued)

Page

138	XVI	Measurement Run No. 8, Short Boring, Clearance 3.00"
139	XVII	Measurement Run No. 9, Short Boring, Clearance 3.00"
139	XVIII	Measurement Run No. 10, Short Boring, Clearance 3.00"
139	XIX	Calibration Run No. 8, Long Boring, Clearance 1.00"
139	XX	Calibration Run No. 9, Long Boring, Clearance 1.00"
139	XXI	Calibration Run No. 10, Long Boring, Clearance 2.00"
139	XXII	Calibration Run No. 11, Long Boring, Clearance 2.50"
139	XXIII	Calibration Run No. 12, Long Boring, Clearance 3.00"
139	XXIV	Measurement Run No. 11, Long Boring, Clearance 1.00"
139	XXV	Measurement Run No. 12, Long Boring, Clearance 1.50"
139	XXVI	Measurement Run No. 13, Long Boring, Clearance 1.50"
139	XXVII	Measurement Run No. 14, Long Boring, Clearance 1.50"
140	XXVIII	Measurement Run No. 15, Long Boring, Clearance 1.50"
141	XXIX	Measurement Run No. 16, Long Boring, Clearance 2.50"
141	XXX	Measurement Run No. 17, Long Boring, Clearance 2.50"

LIST OF TABLES
(continued)

	Page
XXXI Measurement Run No. 18, Long Bossing, Clearance 2.75"	143
XXXII Measurement Run No. 19, Long Bossing, Clearance 3.00"	144
XXXIII Summary of Phase Angles for Short Bossing	58
XXXIV Summary of Phase Angles for Long Bossing	59
XXXV Summary of Phase Angles and Forces	60
XXXVI Comparison of Force by Law of Similitude ..	61

LIST OF TABLES
(continued)

Page

141	XXXXI Measurement of the α and β rays of Radium Clearance 2.75
142	XXXXII Measurement of the α and β rays of Radium Clearance 2.75
143	XXXXIII Summary of phase angles for short passing
144	XXXXIV Summary of phase angles for long passing
145	XXXXV Summary of phase angles and factors
146	XXXXVI Comparison of factors by law of diffraction
147	XXXXVII Summary of phase angles for short passing
148	XXXXVIII Summary of phase angles for long passing
149	XXXXIX Summary of phase angles and factors
150	XXXXX Comparison of factors by law of diffraction
151	XXXXXI Summary of phase angles for short passing
152	XXXXXII Summary of phase angles for long passing
153	XXXXXIII Summary of phase angles and factors
154	XXXXXIV Comparison of factors by law of diffraction
155	XXXXXV Summary of phase angles for short passing
156	XXXXXVI Summary of phase angles for long passing
157	XXXXXVII Summary of phase angles and factors
158	XXXXXVIII Comparison of factors by law of diffraction
159	XXXXXIX Summary of phase angles for short passing
160	XXXXXX Summary of phase angles for long passing
161	XXXXXXI Summary of phase angles and factors
162	XXXXXXII Comparison of factors by law of diffraction

I. INTRODUCTION

A. GENERAL.

Theoretically for any system to vibrate at other than its natural frequency a driving force constitutes a necessary condition. The resultant vibration is a function of the frequency and magnitude of the driving or exciting force. Any periodic force acting externally or internally on the system may constitute the excitation. Considering a ship underway as the system the possible sources of excitation are numerous. The magnitude of a majority of these driving forces are such, or can be made such, that they are negligible. The rotating propeller constitutes a source of excitation which is of substantial magnitude. In geared-turbine and electric drive vessels this form of excitation is predominant and in many cases the sole source of vibration from a practical standpoint.

Propeller excited vibrations may be subdivided into two distinct groups: (1) those of once per revolution frequency which result from propeller unbalance and (2) those of blade frequency. (Blade frequency equals the number of propeller blades times the shaft speed.) Observations and previous investigations have shown that

I. INTRODUCTION

A. GENERAL.

Theoretically for any system to vibrate at other than its natural frequency a driving force constitutes a necessary condition. The resultant vibration is a function of the frequency and magnitude of the driving or exciting force. Any periodic force acting externally or internally on the system may constitute the excitation.

Considering a ship underway as the system the possible sources of excitation are numerous. The magnitude of a majority of these driving forces are such, or can be made such, that they are negligible. The rotating propeller constitutes a source of excitation which is of substantial magnitude. In geared-turbine and electric drive vessels this form of excitation is predominant and in many cases the sole source of vibration from a practical standpoint. Propeller excited vibrations may be subdivided into

two distinct groups: (1) those of once per revolution frequency which result from propeller unbalance and (2) those of blade frequency. (Blade frequency equals the number of propeller blades times the shaft speed.) Observations and previous investigations have shown that

the excitation frequency of ship hull vibrations is that of blade frequency. Further reference to propeller excited vibrations will be to excitation of blade frequency unless specified otherwise.

The propeller forces exciting hull vibrations are caused by hydrodynamic forces acting on the propeller alone and/or by the interaction of the hydrodynamic forces acting on the propeller, hull, and appendages. In general, it has been established that the excitation forces of blade frequency are transmitted to the vessel by means of: (1) shaft bearing and (2) hydrodynamically generated pressure fluctuations acting directly on the hull or its appendages.

To clearly define the source of excitation of the blade frequency vibrations, the total vibratory force acting on a vessel is separated into bearing forces and surface forces. The surface force is more completely defined by specifying the surface upon which it acts. For example, a single screw vessel may have hull surface and rudder surface forces while the twin screw vessel may have, in addition, bossing surface forces or strut surface forces. Sometimes, the hull surface forces are referred to as hull suction forces.

The bearing forces are caused principally by the wake variation across the propeller disc. From past investigations it has been generally concluded that in

The excitation frequency of ship hull vibrations is that of blade frequency. Further reference is made to blade frequency which will be the excitation of blade frequency unless specified otherwise.

The propeller forces exciting hull vibrations are

caused by hydrodynamic forces acting on the propeller along and/or by the rotation of the hydrodynamic forces acting on the propeller, hull, and appendages. In general, it has been established that the excitation forces of blade

frequency are transmitted to the vessel by means of: (1) shaft bending and (2) hydrodynamically generated pressure fluctuations acting directly on the hull or its appendages.

To clarify define the source of excitation of the

blade frequency vibrations, the total vibratory force acting on a vessel is separated into bearing forces and surface forces. The surface force is more completely defined by specifying the surface upon which it acts. For example, a single screw vessel may have hull surface and under surface forces while the two screw vessel may have, in addition, bearing surface forces or strut surface forces. Sometimes, the hull surface forces are referred to as hull excitation forces.

The bearing forces are caused principally by the

wake variation across the propeller disc. From past investigations it has been generally concluded that in

both single and twin screw vessels the bearing forces are a minor source of hull vibration. The hull surface forces in single screw vessels or the bossing surface forces, if bossing are fitted, in twin screw vessels are the predominant sources of excitation.

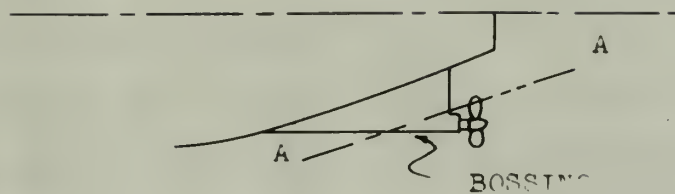
A reasonable theoretical solution to the problem of calculating the surface forces is non-existent. A qualitative explanation of the creation of this surface force is based on the concept of circulation. Referring to Fig. 1, in position (1) the circulation is entirely around the blade element as shown. This causes a negative pressure on the forward face and a positive pressure on the after or driving face of the propeller blade. As the blade element approaches the bossing or hull surface there is a shift in the circulation to some path as shown in position (2). The shift in circulation is caused by the introduction of the structure in the path of circulation. The change in circulation is accompanied by a tangential momentum change. To produce this change a force acts on the system of hull and propeller. As the blade moves past the structure the circulation is restored to its original value with an accompanying reversal of momentum and force. Thus, a periodic force is imparted to the hull and the propeller. The forces imparted directly to the hull are the surface forces. Those imparted to the propeller result in bearing forces.

both single and twin screw vessels the bearing forces are a minor source of hull vibration. The hull surface forces in single screw vessels or the bearing surface forces, if bearing are lifted, in twin screw vessels are the dominant sources of excitation.

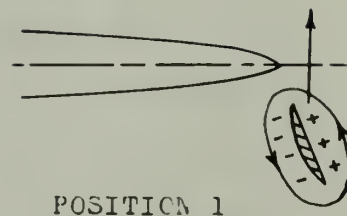
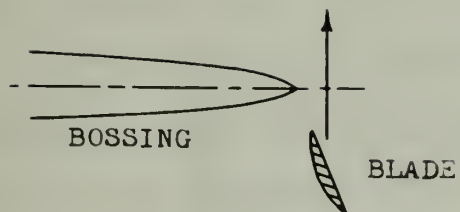
A reasonable theoretical solution to the problem of calculating the surface forces is non-existent. A qualitative explanation of the direction of this surface force is based on the concept of circulation. Referring to Fig. 1, in position (1) the circulation is entirely around the blade element as shown. This causes a negative pressure on the forward face and a positive pressure on the after or driving face of the propeller blade. As the blade element approaches the bearing or hull surface there is a shift in the circulation to some path as shown in position (2). The shift in circulation is caused by the introduction of the structure in the path of circulation. The change in circulation is accompanied by a tangential momentum change. To produce this change a force acts on the system of hull and propeller. As the blade moves past the structure the circulation is restored to its original value with an accompanying reversal of momentum and force. Thus, a periodic force is imparted to the hull and the propeller. The forces imparted directly to the hull are the surface forces. Those imparted to the propeller result in bearing forces.

FIGURE I

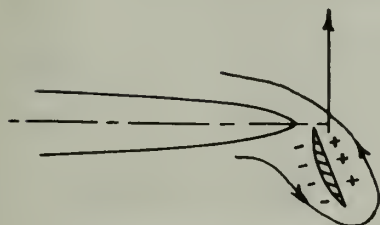
CREATION OF FORCE



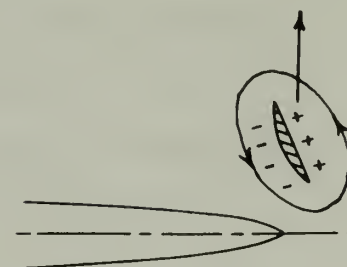
SECTION A-A



POSITION 1



POSITION 2



POSITION 3

The composition of the actual periodic force system described above is not definitely known but is seen to be a complex system. In order to permit an experimental analysis of the force system it is necessary to replace the actual system with a simplified force system which is considered to be practically equivalent. In adopting such a system only the blade frequency vibrations are considered. In the past investigations an equivalent system consisting of six components was adopted: vertical, transverse, and longitudinal forces and couples about the vertical, transverse, and longitudinal axes. From past work it has been seen that the predominant components are the vertical and horizontal forces and the couple about the longitudinal axis. It should be emphasized that these components of the adopted system are nominal, simple harmonic forces which are nearly equivalent to the actual total force system. Thus, it seems entirely feasible to reduce the entire problem of propeller excited vibrations to individual investigations of predominant equivalent force components acting on one of the known sources of vibration, i.e. bossing surface, hull surface, rudder surface, or bearings.

B. PREVIOUS WORK

In the past four basic approaches have been used to determine information regarding propeller excited hull vibrations. The basic approaches are: (1) electrical analogy,

The composition of the actual periodic force system described above is not definitely known but is seen to be a complex system. In order to permit an experimental analysis of the force system it is necessary to replace the actual system with a simplified force system which is considered to be practically equivalent. In adopting such a system only the blade frequency vibrations are considered. In the past investigations an equivalent system consisting of six components was adopted: vertical, transverse, and longitudinal forces and couples about the vertical, transverse, and longitudinal axes. From past work it has been seen that the predominant components are the vertical and horizontal forces and the couple about the longitudinal axis. It should be emphasized that these components of the adopted system are nominal, simple harmonic forces which are nearly equivalent to the actual total force system. Thus, it seems entirely feasible to reduce the entire problem of propeller excited vibrations to individual investigations of predominant equivalent force components acting on one of the known sources of vibration, i.e., passing surface, hull surface, rudder surface, or bearings.

B. PREVIOUS WORK

In the past four basic approaches have been used to determine information regarding propeller excited hull vibrations. The basic approaches are: (1) electrical analogy,

(2) full scale shipboard measurements, (3) self propelled model testing, and (4) propeller tunnel investigations.

Professor F. M. Lewis has computed the pressure variations on an infinite plane wall, parallel to the propeller axis by an electrical analogy^{(10)*}. The analogy consisted of magnetic measurement of the field strength of an electrical model of a propeller in which current varying conductors replaced vortex filaments. From the basic data, pressure contours could be plotted and these in turn integrated to determine the magnitude of the total vibratory force. It is also possible by this method to deduce the total mean longitudinal component of the pressure, which should correspond to the thrust deduction. This method provides the order of magnitude of the forces only. The broad assumption required for solution of the problem exclude the possibility of refined results.

The literature available on ship vibration indicates that numerous shipboard vibratory measurements have been made^{(19), (18), (4)}. The purpose of many of these investigations has been to correlate data for verification of the design formulas used in the calculations of the natural frequency of the hull structure. The shipboard vibratory investigations in which the ob-

* Numbers in parentheses refer to References.

(1) full scale shipboard measurements, (2) full scale
 model testing, and (3) propeller tunnel investi-
 gations.

Professor F. W. Lewis has computed the pressure
 variations on an infinite plane wall, parallel to the
 propeller axis by an electrical analogy⁽¹⁰⁾. The
 analogy consisted of magnetic measurement of the field
 strength of an electrical model of a propeller in which
 current carrying conductors replaced vortex filaments.
 From the basic data, pressure contours could be plotted
 and these in turn integrated to determine the magnitude
 of the total vibratory force. It is also possible by
 this method to deduce the total mean longitudinal com-
 ponent of the pressure, which should correspond to the
 thrust deduction. This method provides the order of
 magnitude of the forces only. The fixed assumption re-
 quired for solution of the problem exclude the possibility
 of refined results.

The literature available on ship vibration indi-
 cates that numerous shipboard vibratory measurements
 have been made^{(11),(12),(13)}. The purpose of many of
 these investigations has been to correlate data for
 verification of the design formulas used in the cal-
 culations of the natural frequency of the hull structure.
 The shipboard vibratory investigations in which the ob-

* Numbers in parentheses refer to references.

jective was to determine information regarding the source and magnitude of the excitation forces are few. Measurements of the vertical excitation forces on the OLD COLONY MARINER were made in 1952 and on the GOPHER MARINER at a later date.⁽¹¹⁾ Obviously, some shipboard measurements are necessary to establish laws of similitude so that model testing will be of significance, but full scale basic research is impractical.

Professor Lewis conducted research on the propeller excited vibration problem by means of self-propelled models under the sponsorship of the Society of Naval Architects and Marine Engineers in the early 1930's⁽¹⁰⁾. A continuation of this work, again by the use of self-propelled models, has been conducted recently under the sponsorship of Panel H-8 of the Society of Naval Architects and Marine Engineers⁽¹¹⁾. Practically all of the information available on this subject is a result of this research with the self-propelled models. The system employed consists of a hull balance system. An adjustable vibration generator and a vibration detector are mounted on the model. The magnitude and direction of the vibratory force applied to the model by the vibration generator is controllable. The procedure would be to run the model at the desired advance coefficient, adjust the vibration generator to give a zero output from the vibration pick-up, and then interpret the vibration generator settings to calculate the vibratory

objective was to determine information regarding the source
 and magnitude of the excitation forces are low. Measure-
 ments of the vertical excitation forces on the OLD COLONY
 WHEEL were made in 1952 and on the COPIES WHEEL in 1954.
 Later work, (11) however, was shipboard measurements
 are necessary to establish laws of vibration on this
 model testing will be of significance, but full scale basic
 research is impractical.
 Professor Lewis conducted research on the shipboard
 excited vibration problem by means of self-propelled models
 under the sponsorship of the Society of Naval Architects
 and Marine Engineers in the early 1950's. (10) A continuation
 of this work, again by the use of self-propelled models, has
 been conducted recently under the sponsorship of Panel H-2
 of the Society of Naval Architects and Marine Engineers. (11)
 Practically all of the information available on this sub-
 ject is a result of this research with the self-propelled
 models. The system employed consists of a hull balance
 system. An adjustable vibration generator and a vibration
 detector are mounted on the model. The magnitude and
 direction of the vibratory force applied to the model by
 the vibration generator is controllable. The procedure
 would be to run the model at the desired advance co-
 efficient, adjust the vibration generator to give a test
 output from the vibration pick-up, and then inspect
 the vibration generator settings to eliminate the vibratory

excitation force. The vibration detector (pick-up) can be adjusted to respond to either vertical, transverse, or torsional motion. This approach to the problem has yielded good results but has many disadvantages from an operational standpoint. The employment of self-propelled models is expensive, cumbersome, and requires some type of ship model tank facilities.

The basic approach to the problem which is the most convenient experimentally is that of a propeller tunnel investigation. Two methods have been employed in the propeller tunnel approach: (1) measurement of forces, (2) measurement of pressures. To the authors' knowledge there is no published information indicating that propeller tunnel investigations of propeller excited vibrations have been conducted at other than Massachusetts Institute of Technology. Five theses have been written concerning different phases of propeller excited vibrations since 1941. Pinkerton and Arnold⁽¹⁴⁾ and Reece and Lansdowne⁽¹⁵⁾ measured, directly, the vibratory force acting on a scale model of a ship's bossing. The three remaining theses measured the pressure field in various locations near the rotating propeller. Ellis and Henderson⁽⁷⁾ measured the pressure distribution on a model bossing and integrated the pressure contours over the area of the bossing to find the total bossing surface force. Dinsmore and Hooper⁽⁶⁾

excitation force. The vibrator detector (pick-up) can be adjusted to respond to either vertical, transverse, or torsional motion. This approach to the problem has yielded good results but has many disadvantages from an operational standpoint. The employment of self-powered models is expensive, cumbersome, and requires some type of ship model tank facilities.

The basic approach to the problem which is the most convenient experimentally is that of a propeller tunnel investigation. Two methods have been employed in the propeller tunnel approach: (1) measurement of forces, (2)

measurement of pressures. To the author's knowledge there is no published information indicating that propeller tunnel investigations of propellers excited vibrations have been conducted at other than Massachusetts Institute of Technology. Five theses have been written concerning

different phases of propeller excited vibrations since 1941. Pinkerton and Arnold (14) and Pace and Landstone (15) measured, directly, the vibratory force acting on a scale model of a ship's housing. The three remaining theses

measured the pressure field in various locations near the rotating propeller. Ellis and Wadsworth (7) measured the pressure distribution on a model housing and investigated the pressure contours over the area of the housing to find the total bending surface force. Lindsay and Hootner (8)

measured the pressure field on a flat surface directly above the propeller simulating the ship's hull. The pressure contours could be integrated to find the hull surface forces. McClure and Mavor⁽¹³⁾ used, what was essentially, a pressure probe to measure pressure at various locations in an attempt to define the pressure field surrounding the propeller. All these methods involved tedious data reduction techniques, such as analysis of cathode ray oscilloscope presentations, graphical harmonic analysis, and graphical integration of pressure contours. As a result of these time consuming data reduction methods the amount of useful information and systematic testing has actually been extremely small.

C. OBJECTIVE.

The importance of reducing hull vibrations in all types of vessels needs no emphasis. Before vibration free designs can be made it is necessary to understand the mechanism of propeller excitation and to understand this mechanism additional research is necessary. The current technical interest in this problem is evidenced by⁽¹¹⁾ and the fact that a research program is now at the David Taylor Model Basin under the general advice of Research Panel H-8 of the Society of Naval Architects and Marine Engineers.

measured the pressure field on a flat surface directly above the propeller simulating the ship's hull. The pressure contours could be integrated to find the hull surface forces. McClure and Geyer (11) used, what was essentially, a pressure probe to measure pressure at various locations in an attempt to define the pressure field surrounding the propeller. All these methods involved tedious data reduction techniques, such as analysis of cathode ray oscilloscope presentations, graphical harmonic analysis, and graphical integration of pressure contours. As a result of these time consuming data reduction methods the amount of useful information and systematic testing has actually been extremely small.

C. OBJECTIVE.

The importance of reducing hull vibrations in all types of vessels needs no emphasis. Before vibration free design can be made it is necessary to understand the mechanism of propeller excitation and to understand this mechanism additional research is necessary. The current technical interest in this problem is evidenced by (11) and the fact that a research program is now at the David Taylor Model Basin under the general advice of Research Vessel H-8 of the Society of Naval Architects and Marine Engineers.

From an examination of the scope of the problem and the results of previous investigations it becomes apparent that a complete understanding of the design parameters affecting propeller excitation and their relative importance is lacking. By employment of a propeller tunnel it should be possible to investigate separately the various sources of excitation and their relationships to design or operational parameters. As discussed earlier an equivalent force system consisting of nominal simple harmonic forces may be employed and therefore each excitation source can be examined for the simple harmonic forces constituting the equivalent system. For example, an investigation of the bossing surface forces could be confined to the force normal to the bossing. A model bossing has recently been designed and developed at the Marine Propeller Tunnel at the Massachusetts Institute of Technology for use in such an investigation.

The objectives of this thesis are: (1) to assemble a satisfactory detector system for measurement of the vibratory forces normal to the bossing, (2) to arrive at an acceptable method of system calibration, and (3) to investigate as many of the variables affecting the magnitude of the vibratory forces as time permitted.

From an examination of the scope of the problem and the results of previous investigations it became apparent that a complete understanding of the design parameters affecting propeller excitation and their relative importance is lacking. By employment of a propeller tunnel it should be possible to investigate separately the various sources of excitation and their relationship to design or operational parameters. As discussed earlier an equivalent force system consisting of multiple simple harmonic forces may be employed and therefore each excitation source can be examined for the simple harmonic forces constituting the equivalent system. For example, an investigation of the bearing surface forces could be confined to the force normal to the bearing. A model bearing has recently been designed and developed at the Marine Propeller Tunnel at the Massachusetts Institute of Technology for use in such an investigation.

The objectives of this thesis are: (1) to assemble a satisfactory detector system for measurement of the vibratory forces normal to the bearing, (2) to arrive at an acceptable method of system calibration, and (3) to investigate as many of the variables affecting the magnitude of the vibratory forces as time permitted.

II. DESCRIPTION OF APPARATUS

GENERAL

The measurement of the vibratory force normal to the bossing was made by placing a cast aluminum bossing upstream of the propeller in the test section of the propeller tunnel. See Figures II, III, and IV. The hydrodynamically induced vibratory forces cause a rotational displacement of the bossing. This displacement is proportional to the magnitude and frequency of the excitation or vibratory force normal to the bossing. The motion of the bossing is transmitted through a hollow steel shaft to the horizontal arm and finally, by means of a vertical rod, to the moveable coil of the detector unit. See Figure III. The horizontal arm and bossing are clamped to the center portion of the hollow steel shaft which is clamped at its ends to the inside of the propeller tunnel. The dimensions of the hollow shaft are such that it responds only to the applied moment, resulting in an angular displacement or twist of the shaft with negligible bending.

The relative motion of the moveable coil in the detector, with respect to the field of a fixed energized

II. DESCRIPTION OF APPARATUS

GENERAL

The measurement of the vibratory force normal to the bearing was made by placing a cast aluminum bearing unit in the propeller in the test section of the propeller tunnel. See Figures II, III, and IV. The hydrodynamically induced vibratory forces cause a rotational displacement of the bearing. This displacement is proportional to the magnitude and frequency of the excitation or vibratory force normal to the bearing. The motion of the bearing is transmitted through a hollow steel shaft to the horizontal arm and finally, by means of a vertical rod, to the movable coil of the detector unit. See Figure III. The horizontal arm and bearing are clamped to the center portion of the hollow steel shaft which is clamped at its ends to the inside of the propeller tunnel. The dimensions of the hollow shaft are such that it responds only to the applied moment, resulting in an angular displacement or twist of the shaft with negligible bending. The relative motion of the movable coil in the detector, with respect to the field of a fixed magnetized

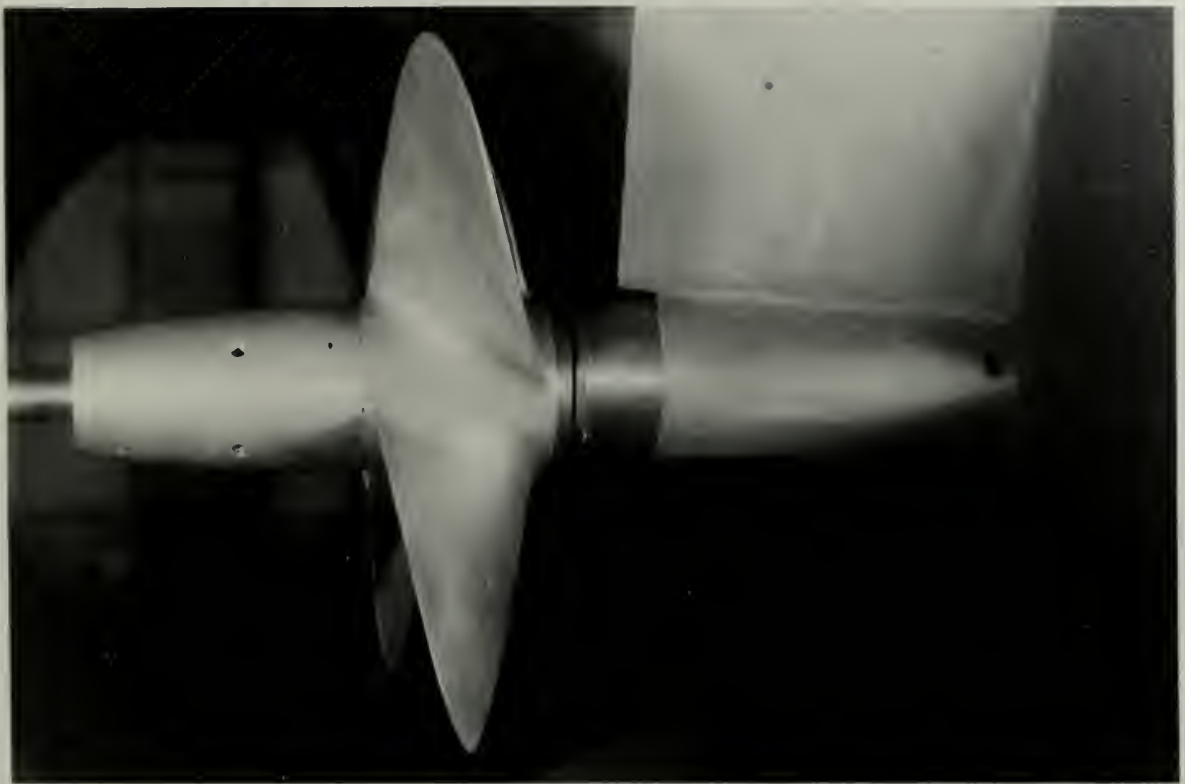


Fig. II. Propeller and Bossing mounted in test section of tunnel. (Note hole in bossing at 0.7 radius for attachment of wire from calibrator. One inch spacer is attached to bossing.)

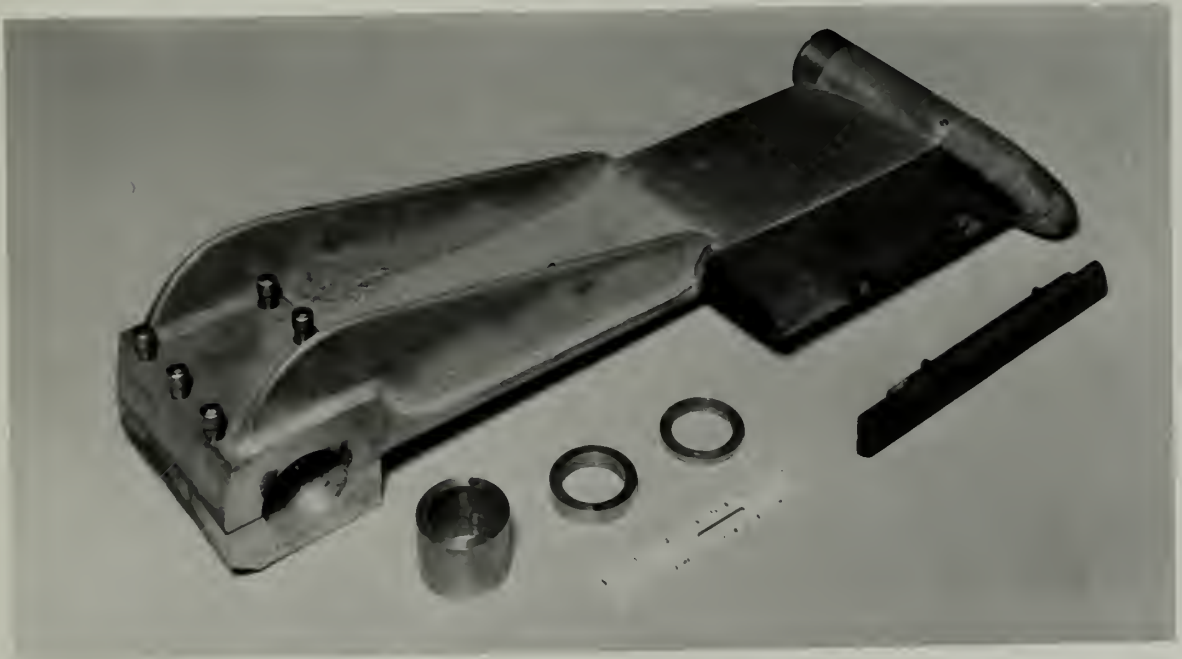
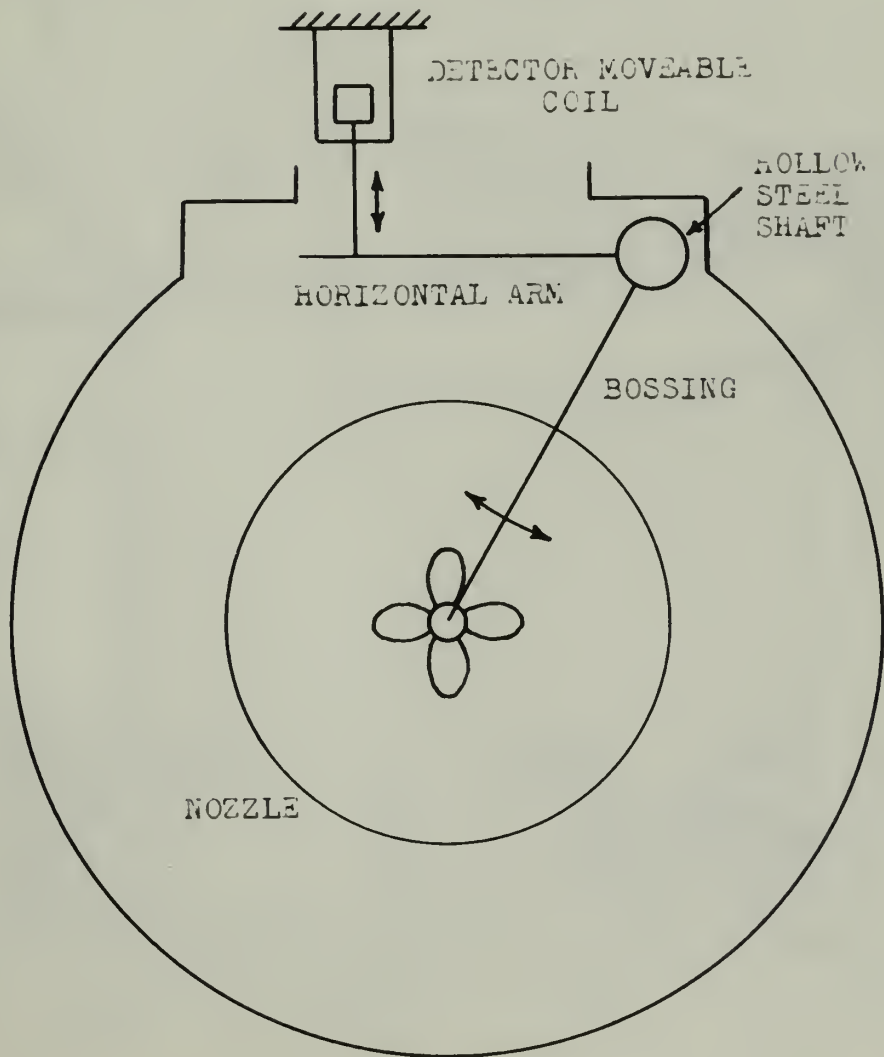
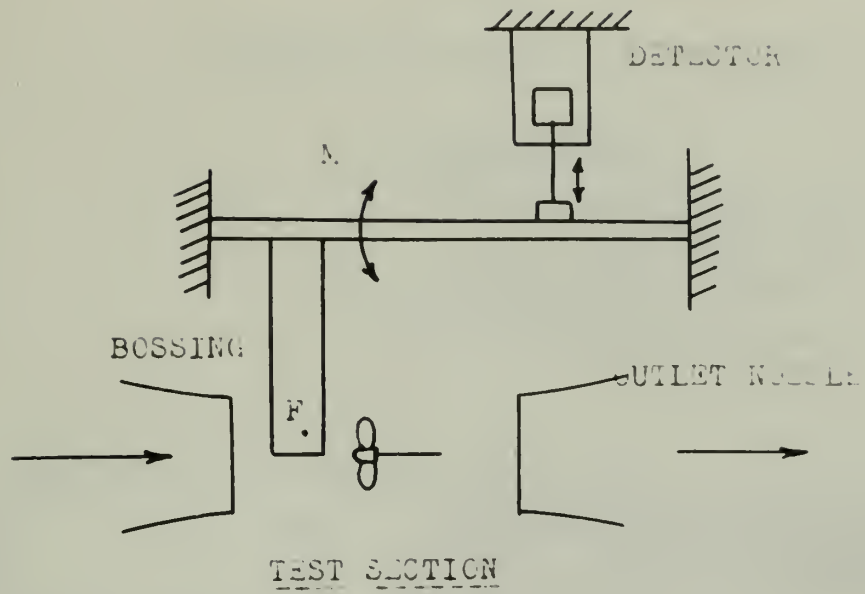


Fig. VI. Bossing, nose pieces, and spacer rings. (One inch spacer attached.)

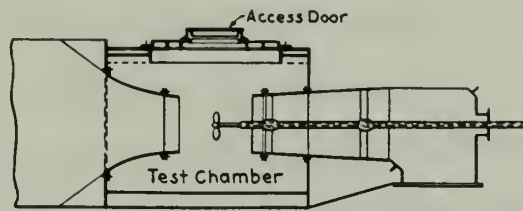
FIGURE III



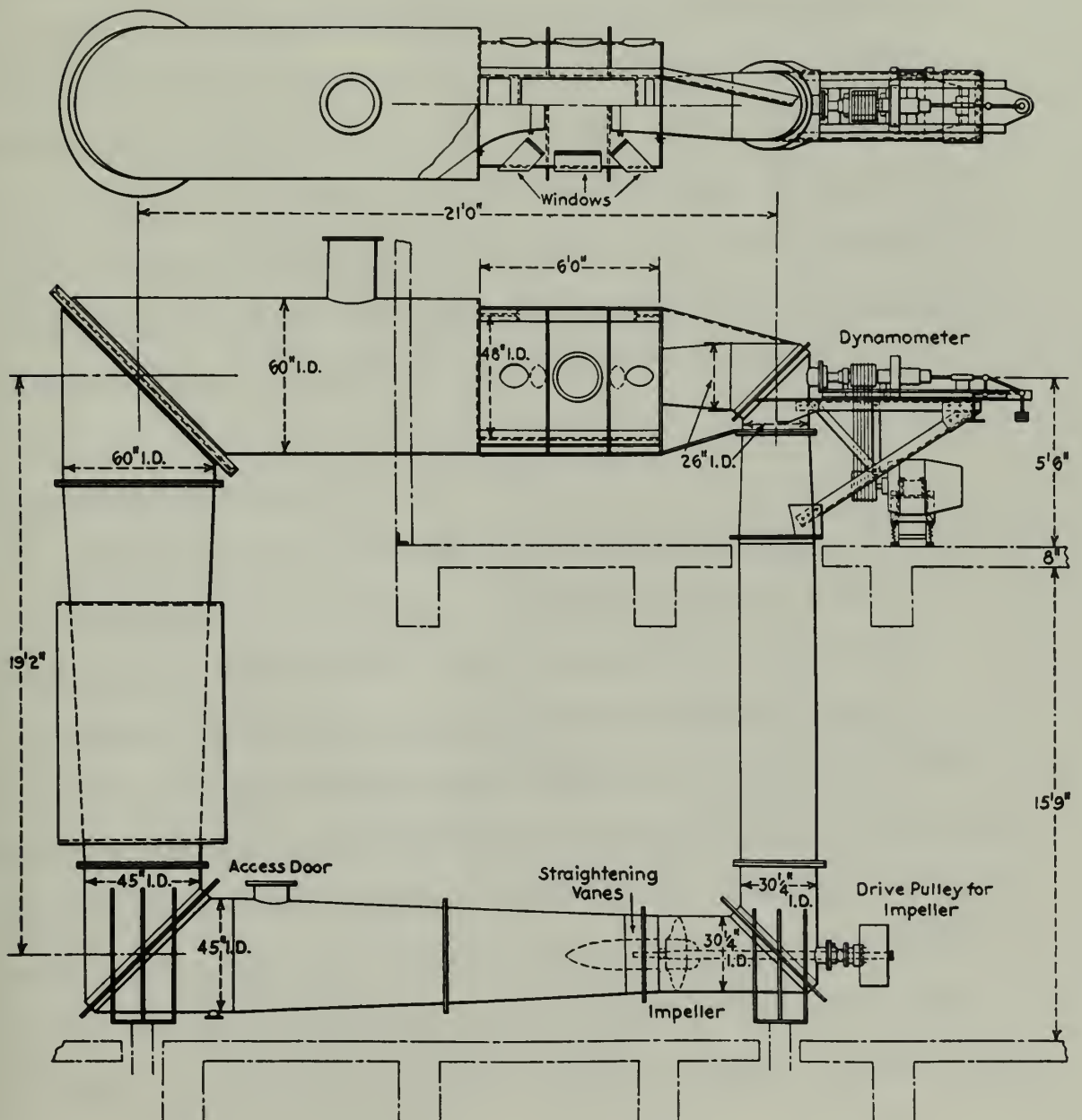
LOOKING UPSTREAM FROM OUTLET NOZZLE

FIGURE IV

PROPELLER TESTING TUNNEL AT M. I. T.



Vertical Cross-Section Through Nozzle



coil, results in the generation of a voltage proportional to the velocity of the moveable coil. If simple harmonic motion is assumed, this voltage is also proportional to the displacement of the bossing. The output of the detector, after amplification, is used to energize the moveable coil of an AC galvanometer. This instrument is essentially a wattmeter in which the magnetizing coil is energized by the output of a sine wave generator. The magnitude of the unknown force and its phase relationship to the propeller blade position is determined by comparison of the resultant galvanometer deflections with readings representing forces of known magnitude. Such known forces and deflections are plotted as calibration curves.

A. PROPELLER TUNNEL

The tests were made at the Massachusetts Institute of Technology, in the marine propeller tunnel, which is described in detail in⁽⁹⁾ and illustrated in Fig. IV. In general, it consists of a closed circuit of large diameter tubing, through which water is circulated by an impeller located in the bottom, horizontal leg. The upper leg includes a test chamber in which the propeller is run. Water enters the test chamber through a converging nozzle twenty inches in diameter at its outlet. The propeller is driven by a shaft entering the test chamber through the

coil, results in the generation of a voltage proportional to the velocity of the movable coil. If simple harmonic motion is assumed, this voltage is also proportional to the displacement of the housing. The output of the detector, after amplification, is used to energize the movable coil of an AC galvanometer. This instrument is essentially a wattmeter in which the magnetizing coil is energized by the output of a sine wave generator. The magnitude of the unknown force and its phase relationship to the propeller blade position is determined by comparison of the resultant galvanometer deflections with readings representing forces of known magnitude. Such known forces and deflections are plotted as calibration curves.

A. PROPELLER TUNNEL

The tests were made at the Massachusetts Institute of Technology, in the marine propeller tunnel, which is described in detail in (7) and illustrated in Fig. IV. In general, it consists of a closed circuit of large diameter tubing, through which water is circulated by an impeller located in the bottom, horizontal leg. The upper leg includes a test chamber in which the propeller is run. Water enters the test chamber through a converging nozzle twenty inches in diameter at its outlet. The propeller is driven by a shaft entering the test chamber through the

receiving nozzle. Speed control of both the water velocity and the propeller is by the Ward-Leonard System. A single 100-horsepower induction motor drives three generators, one for the impeller, one for the dynamometer, and one for excitation. A 75-horsepower motor drives the impeller and a 40-horsepower motor drives the dynamometer.

Water velocity in the test section is measured by using the differential pressure in the inlet nozzle. This pressure differential is transmitted to a gage containing a heavy hydrocarbon which has been calibrated by pitot tube measurements. Propeller revolutions are determined by an electric clock counter mechanism and torque is measured by reading the angular twist in a calibrated shaft. Thrust measurements are determined by a weighted balance arm in 30-pound increments while the differentials are converted into oil pressure and are read on a mercury column.

B. PROPELLER

The propeller used throughout the investigation was a twelve inch model of a 22-foot Troost merchant type propeller designed for an ore carrier. It has the following characteristics:

Material:	Cast Aluminum
Diameter:	11.82 inches
No. of Blades:	4
Pitch Ratio (p/d):	0.957
Mean Width Ratio:	0.248
Blade Thickness Fraction:	0.05

receiving nozzle. Speed control of both the water velocity and the propeller is by the Ward-Leonard system. A single 100-horsepower induction motor drives three generators, one for the impeller, one for the dynamometer, and one for excitation. A 75-horsepower motor drives the impeller and a 40-horsepower motor drives the dynamometer.

Water velocity in the test section is measured by using the differential pressure in the inlet nozzle. This pressure differential is transmitted to a gage containing a heavy hydrocarbon which has been calibrated by other tube measurements. Propeller revolutions are determined by an electric clock counter mechanism and torque is measured by reading the angular twist in a calibrated shaft. Thrust measurements are determined by a weighted balance arm in 30-pound increments while the differentials are converted into oil pressure and are read on a mercury column.

8. PROPELLER

The propeller used throughout the investigation was a twelve inch model of a 12-foot Thrust Research type propeller designed for an air carrier. It has the following characteristics:

Material:	Cast Aluminum
Length:	11.5 inches
No. of Blades:	4
Pitch Ratio (p/d):	0.927
Mean Width Ratio:	0.118
Blade Thickness:	
Fraction:	0.02

C. BOSSING

The bossing consists of an aluminum casting fitted with detachable wooden nose pieces for varying its length and shape. See Fig. VI. The cast aluminum portion has been machined and hand filed to the dimensions shown in Fig. V.

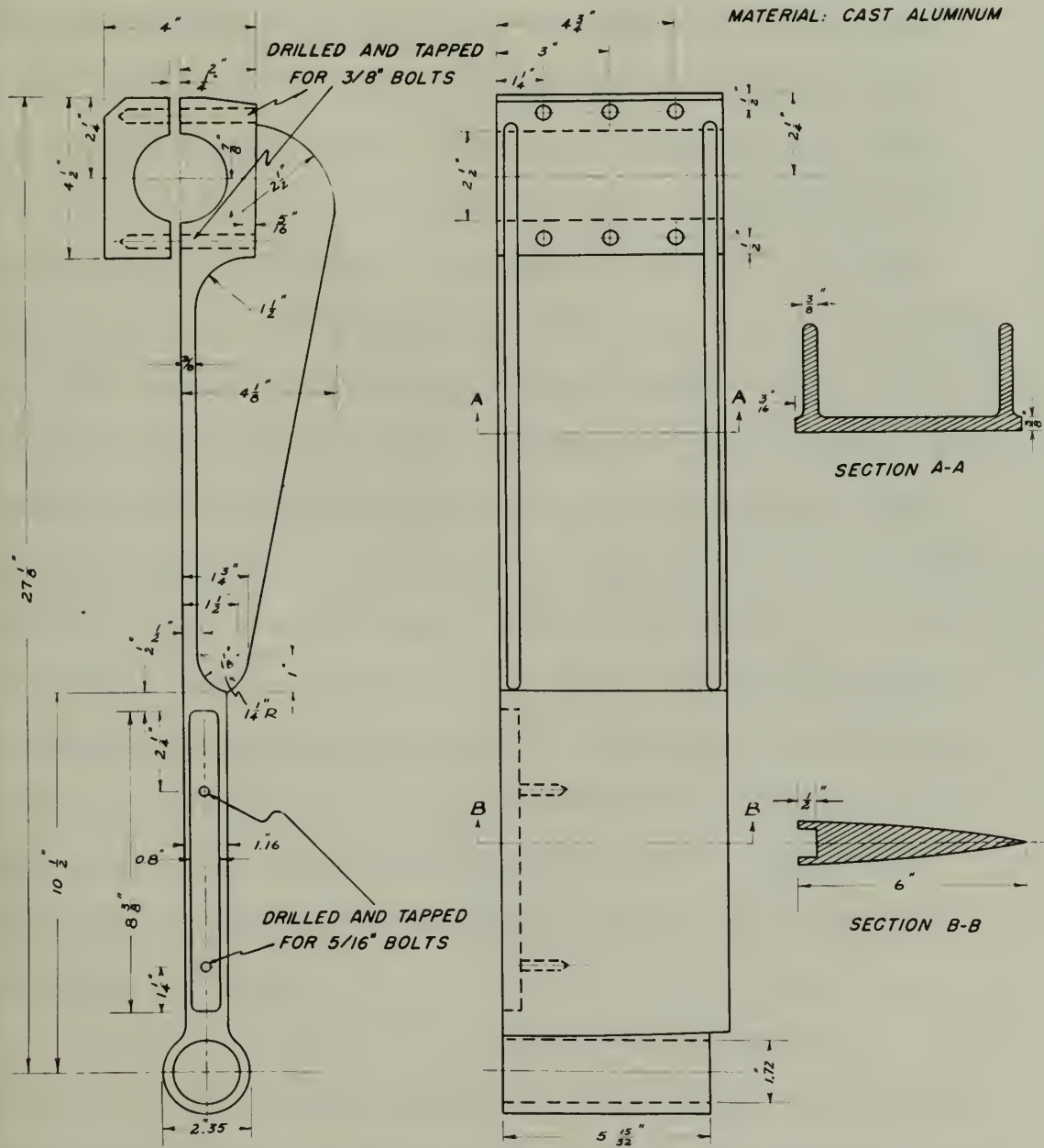
As shown in Figs. V and VI the aluminum portion consists of three different shapes or sections: the hub section, airfoil section, and channel section. The hub or cylindrically shaped section houses a removable, spherically seated bearing designed to support a propeller shaft extension if used. The bossing and bearing are so designed that it is possible to vary the clearance between the airfoil section of the bossing and the propeller while the bearing remains fixed in relation to the propeller shaft extension. This is accomplished by attaching cylindrical spacer rings to lengthen the hub portion of the bossing. When the clearance is varied between the propeller and the bossing the spacers are inserted to maintain a constant clearance between propeller hub and bossing hub whether the bearing is in use or not. The forward or leading edge of the hub is fitted with a removable, wooden fair-water or nose piece. Fig. VI shows the bossing, several spacer rings and the wooden nose pieces.

The housing consists of an aluminum casting fitted with detachable wooden nose pieces for varying its length and shape. See Fig. VI. The cast aluminum portion has been machined and hand filed to the dimensions shown in

Fig. V.

As shown in Fig. V and VI the aluminum portion consists of three different shapes or sections: the hub section, airfoil section, and channel section. The hub or cylindrically shaped section houses a removable, spherically seated bearing designed to support a propeller shaft extension if used. The housing and bearing are so designed that it is possible to vary the clearance between the airfoil section of the housing and the propeller while the housing remains fixed in relation to the propeller shaft extension. This is accomplished by attaching cylindrical spacer rings to lengthen the hub portion of the housing. When the clearance is varied between the propeller and the housing the spacers are inserted to maintain a constant clearance between propeller hub and housing hub whether the bearing is in use or not. The forward or leading edge of the hub is fitted with a removable, wooden fair-water or nose piece. Fig. VI shows the housing, several spacer rings and the wooden nose piece.

FIGURE V
BOSSING



The airfoil or hydrofoil section extends from the hub to the channel section. The length of the airfoil section is such that with the bossing positioned in the test chamber of the propeller tunnel it extends radially beyond the water jet between the two nozzles. The aluminum portion of the airfoil section takes the form of the U.S. Navy Standard Strut Section. The forebody, as previously mentioned, consists of wooden nose pieces of various lengths, which complete the streamlined shape of the airfoil section. For these investigations two such pieces were employed. The first, or long nose piece, represents the forebody of the Navy Standard Strut Section, giving the bossing an overall length of 9-3/8 inches. The second, or short nose piece, has a semi-circular cross-section of diameter equal to the thickness of the aluminum bossing at the forward edge. Thus it represents the minimum overall length possible with this aluminum afterbody. In subsequent discussions any reference made to the long bossing is to be interpreted as referring to the aluminum casting with the long nose piece attached. Similarly, the short bossing is the aluminum section with the short nose piece in place.

For the section of bossing outside the flow a modified channel shape is used to maintain maximum stiffness with minimum weight. At the upper end, provision is made for clamping the bossing to the hollow steel shaft. See Fig. V.

The airfoil or hydrofoil section extends from the

hub to the channel section. The length of the airfoil section is such that with the housing positioned in the test chamber of the propeller tunnel it extends radially

beyond the water jet between the two nozzles. The

aluminum portion of the airfoil section takes the form of the U.S. Navy Standard Strut Section. The forebody, as previously mentioned, consists of wooden nose pieces of various lengths, which complete the streamlined shape

of the airfoil section. For these investigations two such pieces were employed. The first, or long nose piece, represents the forebody of the Navy Standard Strut Section,

giving the housing an overall length of 9-3/8 inches. The

second, or short nose piece, has a semi-circular cross-section of diameter equal to the thickness of the aluminum housing at the forward edge. Thus it represents the minimum overall length possible with this aluminum afterbody.

In subsequent discussions any reference made to the long housing is to be interpreted as referring to the aluminum

casting with the long nose piece attached. Similarly,

the short housing is the aluminum section with the short

nose piece in place.

For the section of housing outside the flow

modified channel shape is used to maintain maximum stiffness with minimum weight. At the upper end, provision is made for clamping the housing to the hollow steel shaft.

See Fig. V.

D. HORIZONTAL ARM

The horizontal arm is mounted transversely near the top of the propeller tunnel as shown in Fig. III. It is clamped to the hollow steel shaft at approximately the center of the propeller tunnel hatch. The angular displacement of twist of the steel shaft causes a rotation of the horizontal arm and a resulting vertical displacement of the unclamped end, where it is connected to the moveable coil of the detector. The linkage between the moveable coil of the detector and the horizontal arm is a 3/8-inch rod with a rigid coupling for easy disassembly.

The arm is an aluminum casting, having an I-beam cross section to give maximum stiffness with minimum weight. The casting has been machined to the dimensions shown in Fig. VII for clamping to the hollow steel shaft.

E. MOUNTING

Both the horizontal arm and the bossing were clamped to a hollow steel shaft having an inside diameter of 2-1/4 inches, an outside diameter of 2-1/2 inches, and a length of 30 inches. Dimensioning of the steel shaft was such as to provide a large bending stiffness with suitable torsional stiffness for the magnitude of forces anticipated. The shaft was rigidly clamped to the inside top of the propeller tunnel test section at two points each approximately thirteen inches

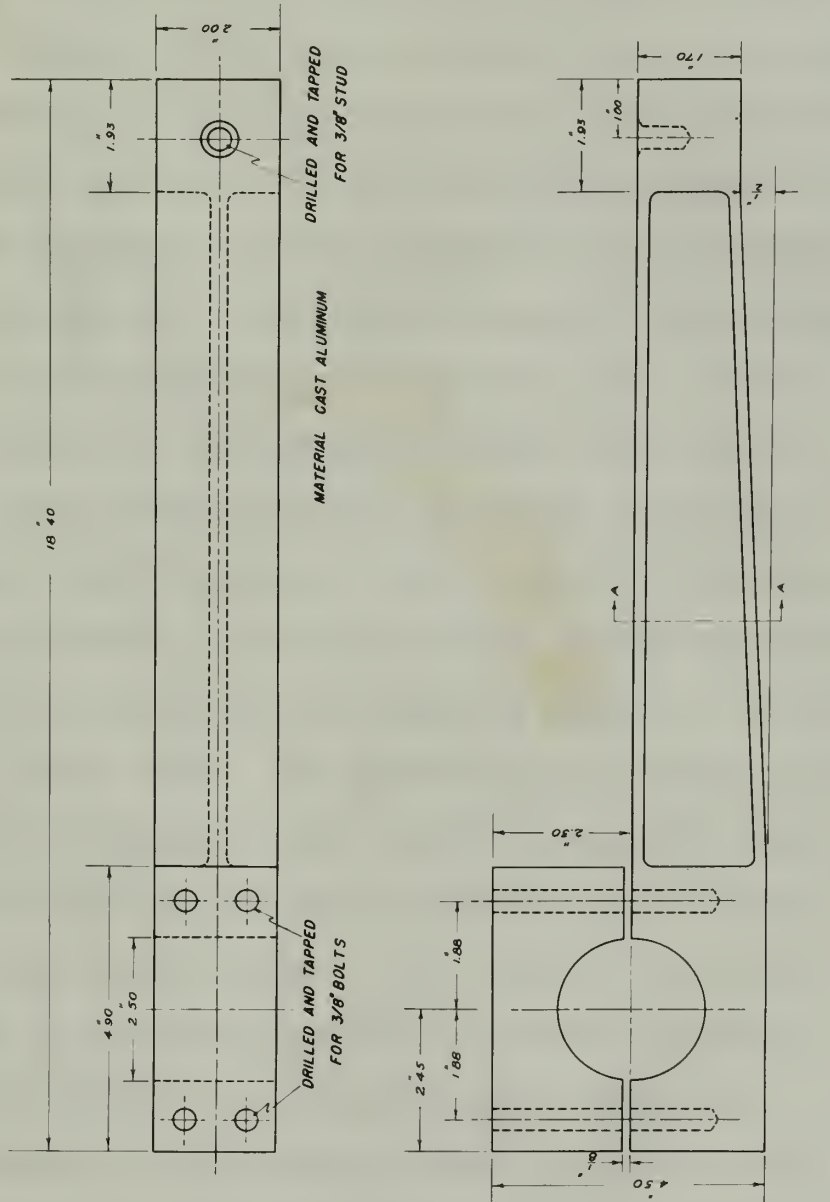
D. HORIZONTAL ARM

The horizontal arm is mounted transversely near the top of the propeller tunnel as shown in Fig. III. It is clamped to the hollow steel shaft at approximately the center of the propeller tunnel hatch. The angular displacement of twist of the steel shaft causes a rotation of the horizontal arm and a resulting vertical displacement of the unclamped end, which is connected to the movable coil of the detector. The linkage between the movable coil of the detector and the horizontal arm is a 3/8-inch rod with a rigid coupling for easy disassembly. The arm is an aluminum casting, having an I-beam cross section to give maximum stiffness with minimum weight. The casting has been machined to the dimensions shown in Fig. VII for clamping to the hollow steel shaft.

E. MOUNTING

Both the horizontal arm and the housing were clamped to a hollow steel shaft having an inside diameter of 2-1/4 inches, an outside diameter of 2-1/2 inches, and a length of 30 inches. Extending at the steel shaft was such as to provide a large bending stiffness with suitable torsional stiffness for the magnitude of forces anticipated. The shaft was rigidly clamped to the inside top of the propeller tunnel hatch section at two points each approximately thirteen inches

FIGURE VII
HORIZONTAL ARM



from the point where the horizontal arm was mounted. See Fig. III.

The shaft was clamped in two cast bronze mountings, machined to the dimensions shown in Fig. VIII. The bronze mountings are bolted to the inside top of the propeller tunnel test section and so positioned that the hollow steel shaft is parallel to the propeller shaft. Once installed, the cast bronze mountings and the hollow steel shaft remained in the propeller tunnel throughout the investigation. The horizontal arm was permanently clamped to the hollow steel shaft in the desired location just below the propeller tunnel hatch. Thus the horizontal arm, hollow steel shaft, and bronze mountings remained in position throughout the investigation. The bossing was shifted to various locations on the hollow steel shaft and removed from the test section whenever required and/or at the completion of a day's work. The detector and calibrator were clamped to the propeller tunnel hatch coaming for easy removal and in the case of the calibrator, ease of relocation to the control panel. See Figs. XIV and XVI. The positions of the detector unit and the calibrator were carefully marked to facilitate exact relocation.

In addition to the bossing system mounting as described above, the propeller mounting and the mounting for the frictionless bearing pulley should be mentioned.

from the point where the horizontal arm was mounted. See

Fig. III.

The shaft was clamped in two cast bronze mountings,

machined to the dimensions shown in Fig. VIII. The bronze

mountings are bolted to the inside top of the propeller

tunnel test section and so positioned that the hollow steel

shaft is parallel to the propeller shaft. Once installed,

the cast bronze mountings and the hollow steel shaft re-

mained in the propeller tunnel throughout the investigation.

The horizontal arm was permanently clamped to the hollow

steel shaft in the desired location just below the pro-

PELLER tunnel hatch. Thus the horizontal arm, hollow

steel shaft, and bronze mountings remained in position

throughout the investigation. The passing was shifted

to various locations on the hollow steel shaft and removed

from the test section whenever required and/or at the con-

clusion of a day's work. The detector and calibrator were

clamped to the propeller tunnel hatch coaming for easy

removal and in the case of the calibrator, ease of re-

location to the control panel. See Figs. XIV and XVI.

The positions of the detector unit and the calibrator

were carefully marked to facilitate exact relocation.

In addition to the passing system mounting as de-

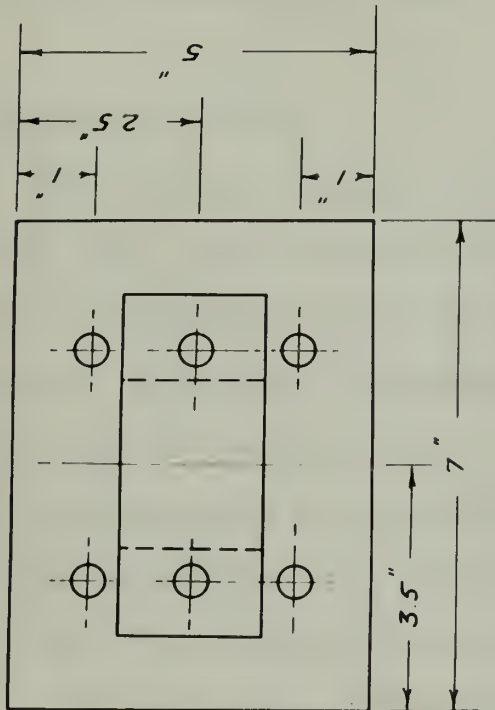
scribed above, the propeller mounting and the mounting

for the frictionless bearing pulley should be mentioned.

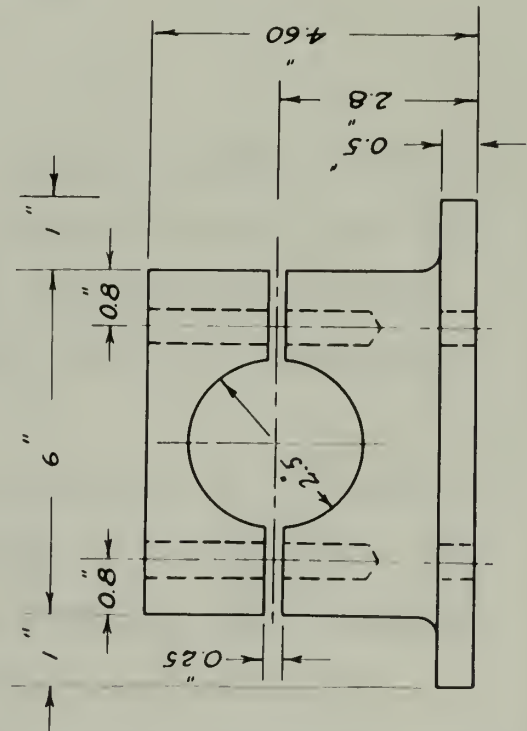
MOUNTINGS

MATERIAL: CAST BRONZE

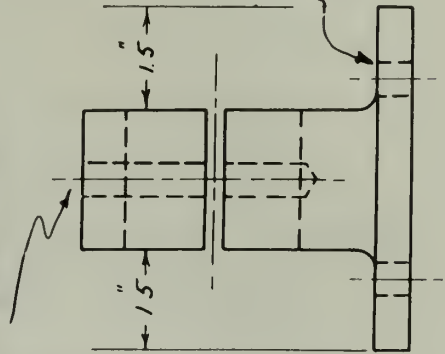
FIGURE VIII



DRILL AND TAP FOR
3/8" ALLEN HEAD BOLTS



DRILL FOR
3/8" BOLTS



Propeller mounting refers to keying the propeller to the propeller shaft for the measurement runs. The important point is that the propeller and propeller shaft were carefully marked to insure correct angular mounting of the propeller. This was required for the method employed in determining phase angle relationships. See Appendix A.

The frictionless bearing pulley was mounted in such a location as to insure normal attachment of the calibration wire to the bossing. See Fig. XV. A channel beam was bolted between the two nozzles of the test chamber. See Fig. IV. The pulley was then mounted on the channel in such a fashion that removal and reinstallation was easily accomplished when desired.

F. DETECTOR SYSTEM

The wiring diagram of the detector system is shown in Fig. IX. From the wiring diagram it can be seen that the instrumentation consisted of five major components: detector, amplifier, galvanometer, sine wave generator, and cathode ray oscilloscope.

The detector is described in detail in (10) and illustrated in Fig. X. It consists of a fixed coil, (E), energized by a lead acid storage battery, and a moveable coil, (F), containing 8000 turns of No. 36 enameled copper wire. The moveable coil is positioned within the

Propeller mounting refers to keying the propeller to the propeller shaft for the measurement runs. The important point is that the propeller and propeller shaft were carefully marked to insure correct angular mounting of the propeller. This was required for the method employed in determining phase angle relationships. See Appendix A.

The frictionless bearing pulley was mounted in such a location as to insure normal attachment of the calibration wire to the bearing. See Fig. XV. A channel beam was bolted between the two nozzles of the test chamber. See Fig. IV. The pulley was then mounted on the channel in such a fashion that removal and reinstallation was easily accomplished when desired.

F. DETECTOR SYSTEM

The wiring diagram of the detector system is shown in Fig. IM. From the wiring diagram it can be seen that the instrumentation consisted of five major components: detector, amplifier, galvanometer, sine wave generator, and cathode ray oscilloscope.

The detector is described in detail in (10) and illustrated in Fig. X. It consists of a fixed coil, (E), energized by a lead acid storage battery, and a movable coil, (F), containing 8000 turns of No. 36 enameled copper wire. The movable coil is positioned within the

FIGURE IX
WIRING DIAGRAM OF DETECTOR CIRCUIT

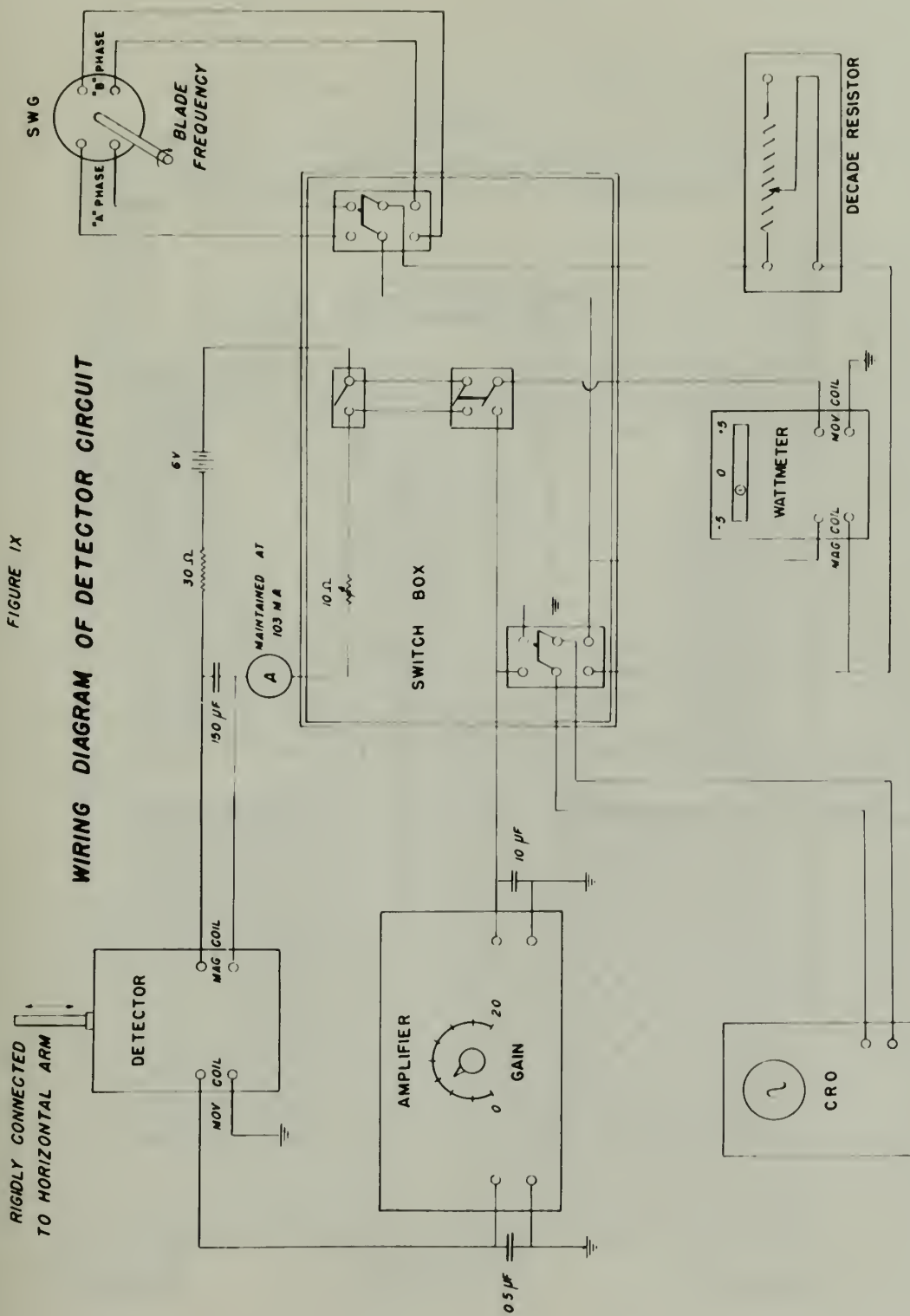


FIGURE X

DETECTOR

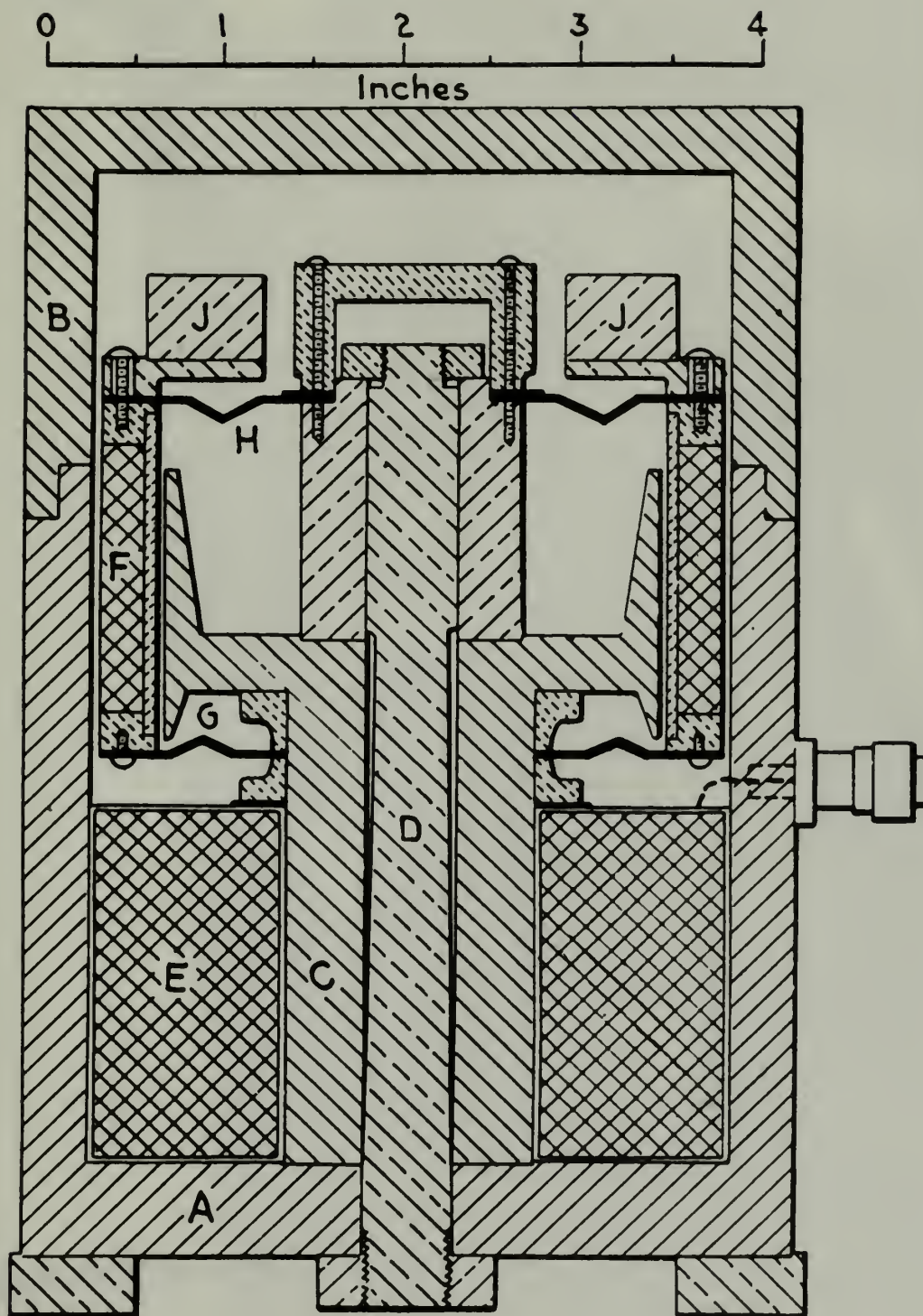




Fig. XI. Instrumentation Arrangement.

detector case by a pair of spring bronze flexures and is connected to the horizontal arm by a three-eighths inch rod as shown in Fig. III. The detector shown in Fig. X was modified to accommodate the three-eighths inch rod by replacing (J) with a cone-shaped piece and drilling a hole in the center of the case top. Energizing the fixed coil forces flux in the air gap between (A) and (C). Motion of the moveable coil therefore generates a voltage proportional to its velocity and the flux linkages.

Amplification of the detector signal was accomplished by means of a General Radio Co. voltage amplifier having the following characteristics:

Serial No.: 102

Model: 714A

Constant Gain: 20-6000 cps.

Mid-Band Gain: 910 maximum with variable gain control. Gain control dial subdivided into 20 divisions.

The output of the amplifier was fed to the moveable coil of a galvanometer. This galvanometer was manufactured by the Rubicon Company of Philadelphia, Pa. In the years following its purchase, Professor F.M. Lewis redesigned the galvanometer so that it is now best described as an alternating current galvanometer or a very sensitive wattmeter. The magnetizing coil of the galvanometer was

detector case by a pair of spring bronze flexures and is connected to the horizontal arm by a three-eighths inch rod as shown in Fig. III. The detector shown in Fig. X was modified to accommodate the three-eighths inch rod by reslicing (J) with a cone-shaped piece and drilling a hole in the center of the case top. Inserting the fixed coil forces flux in the air gap between (A) and (C). Motion of the movable coil therefore generates a voltage proportional to its velocity and the flux linkages. Amplification of the detector signal was accomplished by means of a General Radio Co. voltage amplifier having the following characteristics:

Serial No.: 102

Model: 714A

Constant Gain: 20-6000 cps.

Mid-Band Gain: 910 maximum with variable gain control. Gain control dial subdivided into 20 divisions.

The output of the amplifier was fed to the movable coil of a galvanometer. This galvanometer was manufactured by the Hubicon Company of Philadelphia, Pa. In the years following its purchase, Professor F.M. Lewis redesigned the galvanometer so that it is now best described as an alternating current galvanometer or a very sensitive wattmeter. The magnetizing coil of the galvanometer was

energized by a sine wave generator whose voltage output was a function of speed. Since the calibration runs were made at shaft speeds corresponding to those of measurement runs the only variable supplied to the galvanometer was the amplified detector signal. The galvanometer as modified actually performed as a wattmeter and read $EI \cos\beta$. A 110-6 volt transformer was used as a supply for the light source of the galvanometer.

The sine wave generator employed was model No. F-16, manufactured by The Electric Indicator Co. of Stamford, Conn. It is rated at 1.3 volts per 100 rpm and has two outputs which are 90° out of phase. This permitted reading $EI \cos\beta$, and $EI \cos(\beta + 90^\circ)$ or $EI \sin\beta$ with the galvanometer. $EI \cos\beta$ was designated as the A reading of the galvanometer and $EI \sin\beta$ as the B reading. The angle was designated β_1 or β_2 corresponding to a calibration run or a measurement respectively.

The wiring diagram indicates that the amplifier output was also fed to a cathode ray oscilloscope. The cathode ray oscilloscope was used to monitor the circuit. It could be switched to either the output of the sine wave generator or the amplifier. During the runs it was kept on the amplifier output and thus permitted a visual presentation of the signal generated in the detector and served as a warning system for malfunctioning of the equip-

energized by a sine wave generator whose voltage output
 was a function of speed. Since the calibration runs
 were made at shaft speeds corresponding to those of
 measurement runs the only variable applied to the gal-
 vanometer was the amplified detector signal. The
 galvanometer as modified actually performed as a watt-
 meter and read EI cos ϕ . A 110-0 volt transformer was used
 as a supply for the light source of the galvanometer.
 The sine wave generator employed was model No. E-16,
 manufactured by The Electric Indicator Co., of Stamford,
 Conn. It is rated at 1.5 volts per 100 rpm and has two
 outputs which are 90° out of phase. This permitted read-
 ing EI cos ϕ and EI cos ($\phi + 90^\circ$) or EI sin ϕ with the
 galvanometer. EI cos ϕ was designated as the A reading of
 the galvanometer and EI sin ϕ as the B reading. The angle
 was designated ϕ_1 or ϕ_2 corresponding to a calibration run
 or a measurement respectively.
 The wiring diagram indicates that the amplifier out-
 put was also fed to a cathode ray oscilloscope. The
 cathode ray oscilloscope was used to monitor the circuit.
 It could be switched to either the output of the sine wave
 generator or the amplifier. During the runs it was kept
 on the amplifier output and thus permitted a visual ver-
 ification of the signal generated in the detector and
 served as a warning system for malfunctioning of the ampli-

ment or circuit. Figure XI shows the amplifier, galvanometer, cathode ray oscilloscope, and switch box as used during the investigation. The switch box merely provided a convenient mounting for the various switches which were installed in the detector circuit for ease and flexibility of operation.

G. CALIBRATOR

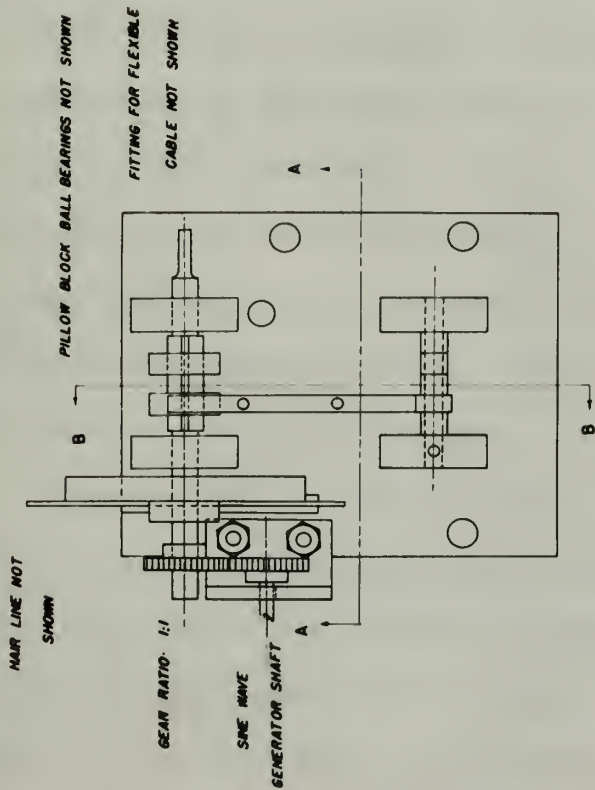
Figure XII shows the principal dimensions of the calibrator and Figure XIV shows the calibrator in position for a calibration run. This mechanism was used to calibrate the entire system so that the galvanometer reading could be related to the magnitude of the hydrodynamically induced vibratory forces. Basically, the calibration mechanism was designed to apply an excitation force of known magnitude and frequency to the bossing at a position assumed to correspond to the point of application of the actual vibratory force.

The calibrator consists of a cam actuated lever arm which is driven at four times propeller speed by shafting geared to the dynamometer. Connected to the lever arm is a wire-spring combination which in turn is connected to the bossing. The wire is normal to the bossing at a point whose distance from the propeller shaft axis is equal to 0.7 of the propeller radius. Longitudinally the point is located approximately two inches from the trailing edge of the bossing. See Fig. II.

ment or circuit. Figure XI shows the oscillator, amplifier, and switch mechanism, cathode ray oscilloscope, and switch box as used during the investigation. The switch box merely provided a convenient mounting for the various switches which were installed in the detector circuit for ease and flexibility of operation.

G. CALIBRATOR

Figure XII shows the principal dimensions of the calibrator and Figure XIII shows the calibrator in position for a calibration run. This mechanism was used to calibrate the entire system so that the galvanometer reading could be related to the magnitude of the hydrodynamically induced vibratory forces. Basically, the calibration mechanism was designed to apply an excitation force of known magnitude and frequency to the housing at a position assumed to correspond to the point of application of the actual vibratory force. The calibrator consists of a fan actuated lever arm which is driven at four times propeller speed by a shafting geared to the dynamometer. Connected to the lever arm is a wire-wound combination which in turn is connected to the housing. The wire is coiled in the housing at a point whose distance from the propeller shaft axis is equal to 0.7 of the propeller radius. Longitudinally the point is located approximately two inches from the trailing edge of the housing. See Fig. II.



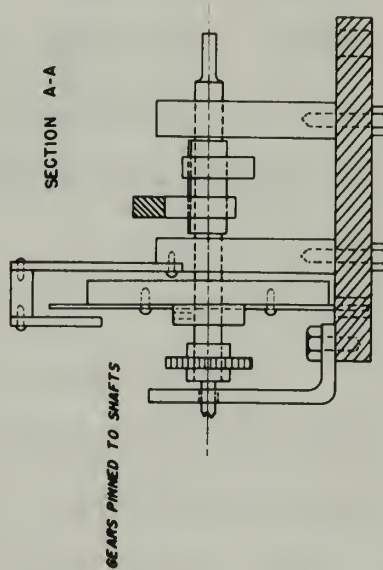
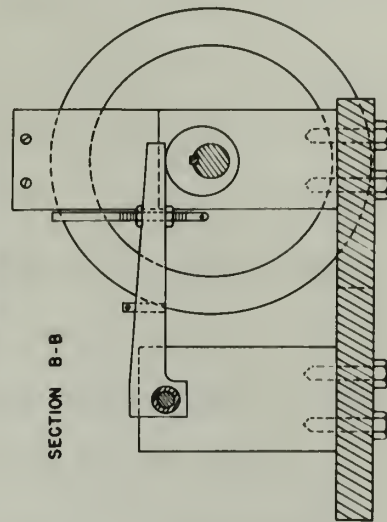
CALIBRATOR

MATERIAL:
ALL PARTS STEEL EXCEPT
ALUMINUM LEVER ARM



FIGURE XII

SINE WAVE GENERATOR MOUNTING
AND GEARING NOT SHOWN



Rotation of the cam shaft causes a sinusoidal displacement of the lever arm and consequently a sinusoidally varying elongation of the wire-spring combination. An excitation force equal in magnitude to the spring constant of the wire-spring combination times its elongation is thus applied to the bossing. The cam has a total throw of one-quarter inch causing a displacement of $3/32$ inches at the point of wire attachment to the lever arm.

To minimize flexural and torsional vibration of the cam shaft, a flywheel was attached to the shaft and a second cam was installed adjacent to first but 180° out of phase. Each cam actuated two lever arms, held in contact with the cam by springs. Only one of the four arms was connected to the wire running to the bossing. See Figs. XII, XIII, and XIV. It was found during the early calibration runs that the effect of the three extra lever arms was negligible in reducing torsional vibration, and they were therefore removed. This explains the additional cam shown in the illustrations.

Figure XIV is a photograph of the calibrator in position on the propeller tunnel hatch coaming for a calibration run. The various springs shown were attached directly to the lever arm by means of a tension regulating spindle. The wire then led from the spring to the point of attachment on the bossing. See Fig. XV. The wire used

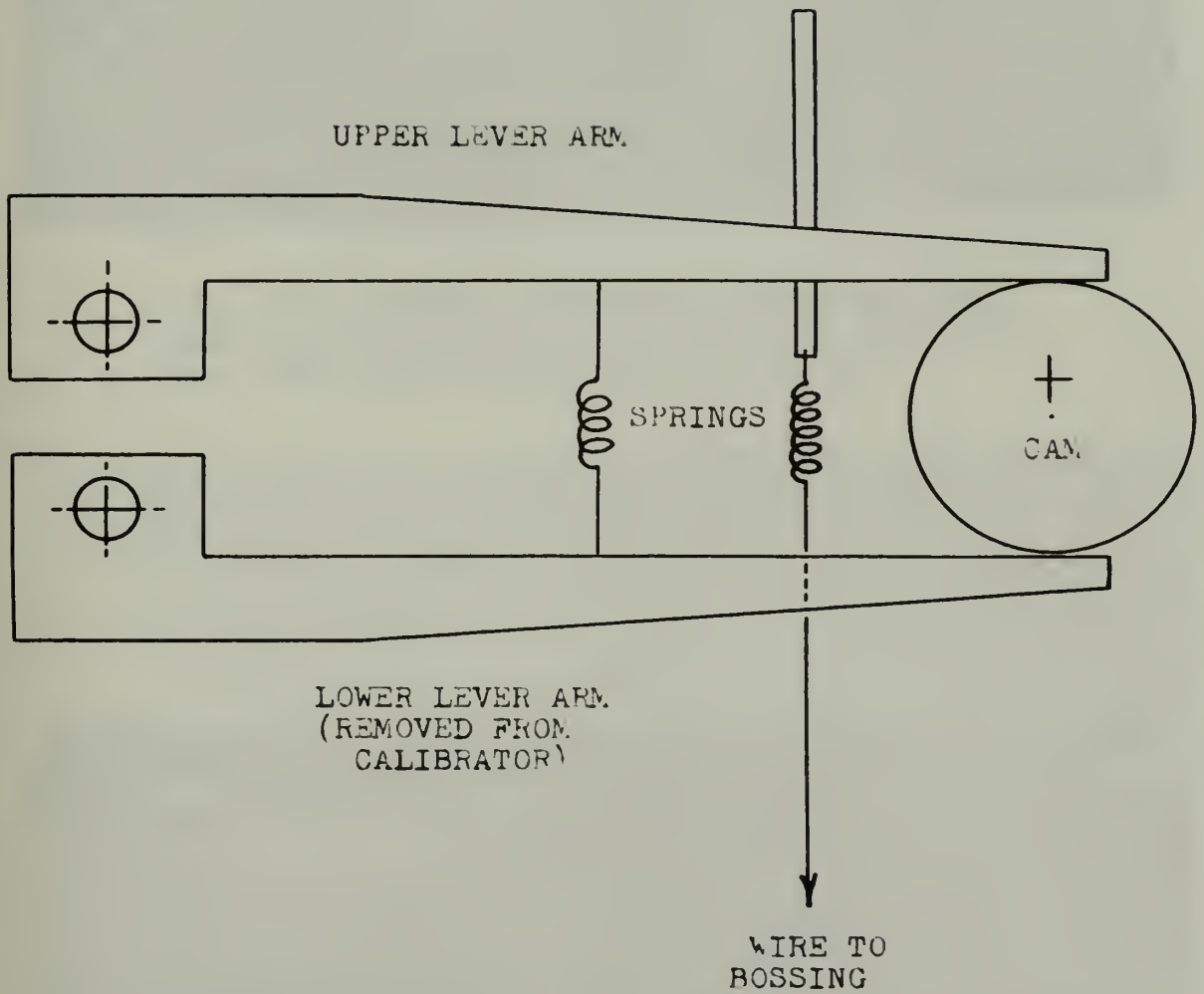
Rotation of the cam shaft caused a sinusoidal displacement of the lever arm and consequently a sinusoidal varying elongation of the wire-spring combination. An excitation force equal in magnitude to the spring constant of the wire-spring combination times its elongation is thus applied to the housing. The cam has a total throw of one-quarter inch causing a displacement of $\frac{1}{32}$ inches at the point of wire attachment to the lever arm.

To minimize flexural and torsional vibration of the cam shaft, a flywheel was attached to the shaft and a second cam was installed adjacent to first but 180° out of phase. Each cam actuated two lever arms, held in contact with the cam by springs. Only one of the four arms was connected to the wire running to the housing. See Figs. XII, XIII, and XIV. It was found during the early calibration runs that the effect of the three extra lever arms was negligible in reducing torsional vibration, and they were therefore removed. This explains the additional cam shown in the illustrations.

Figure XIV is a photograph of the calibrator in position on the propeller tunnel hatch coming for a calibration run. The various springs shown were attached directly to the lever arm by means of a tension regulating spindle. The wire then led from the spring to the point of attachment on the housing. See Fig. XV. The wire used

FIGURE XIII

LEVER ARMS





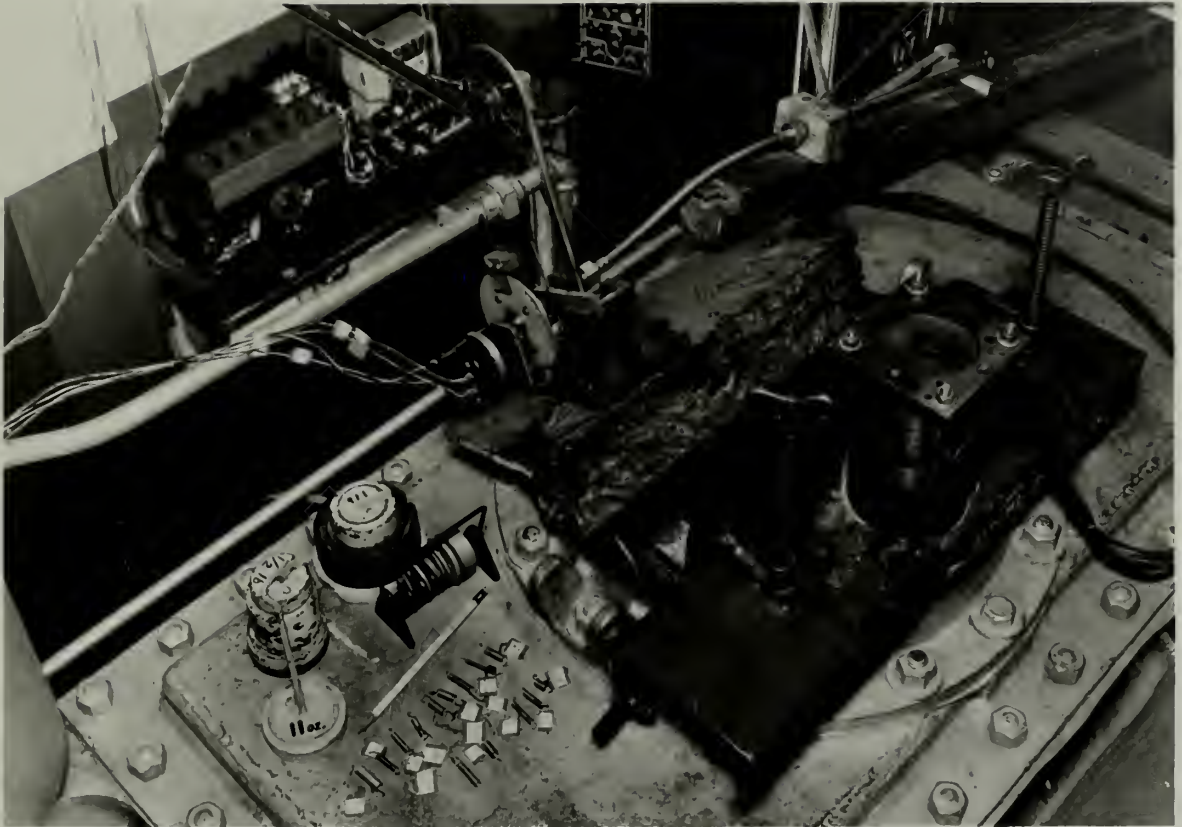


Fig. XIV. Propeller tunnel hatch showing detector mounting and calibrator in position for a calibration run. Note calibrating springs in foreground.

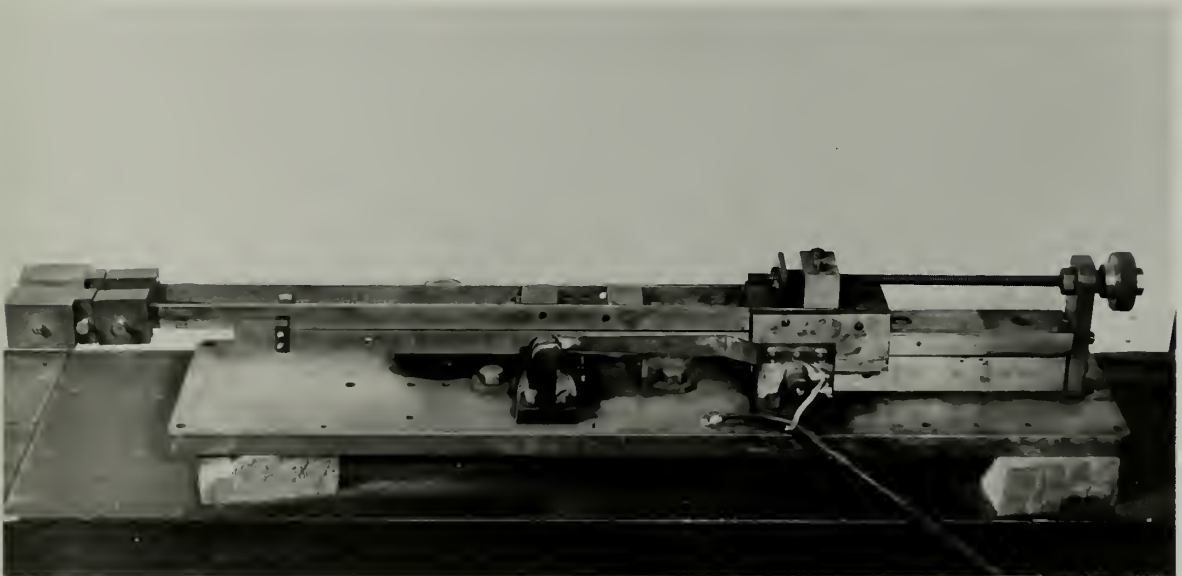


Fig. XIX. Tuning Fork.

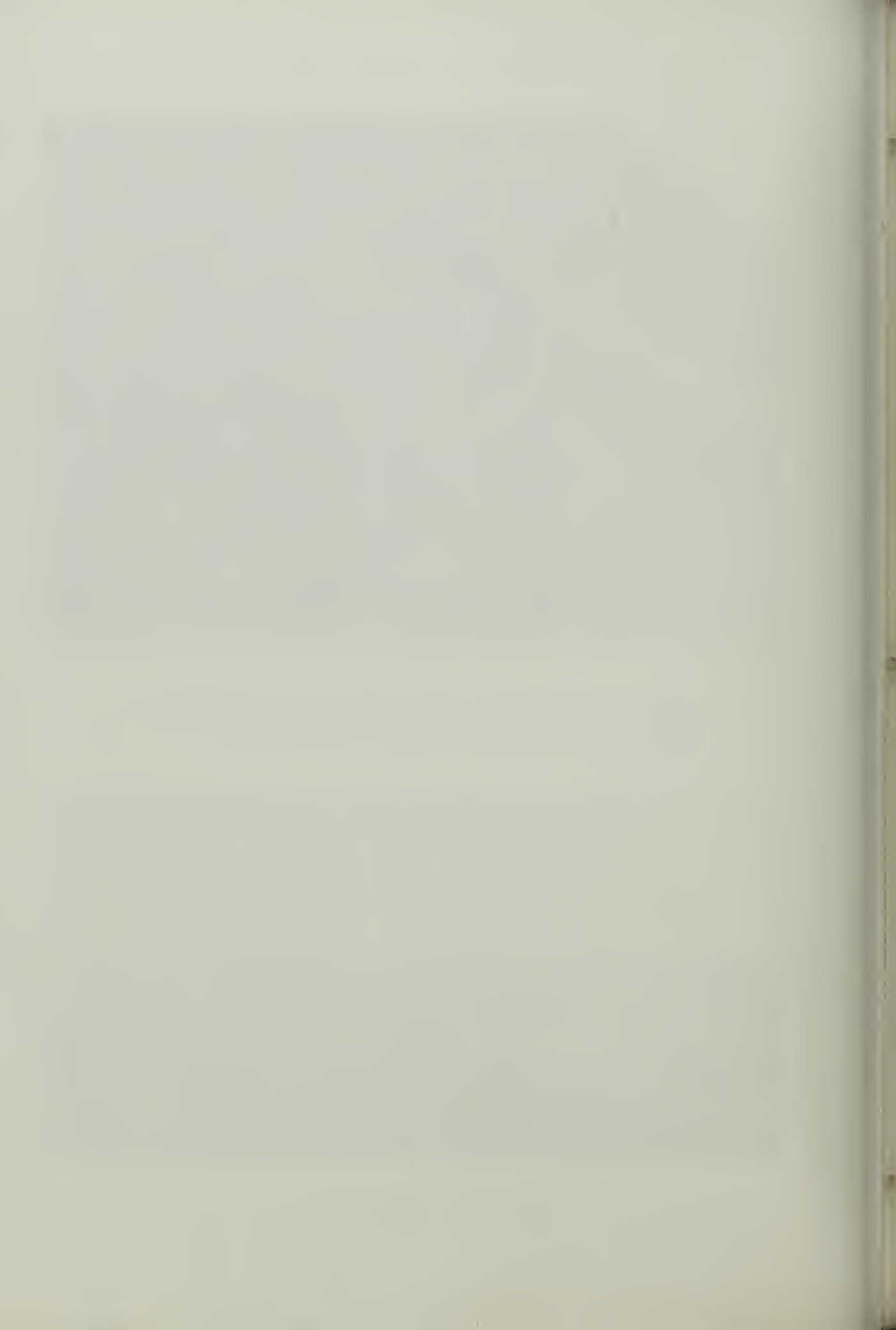
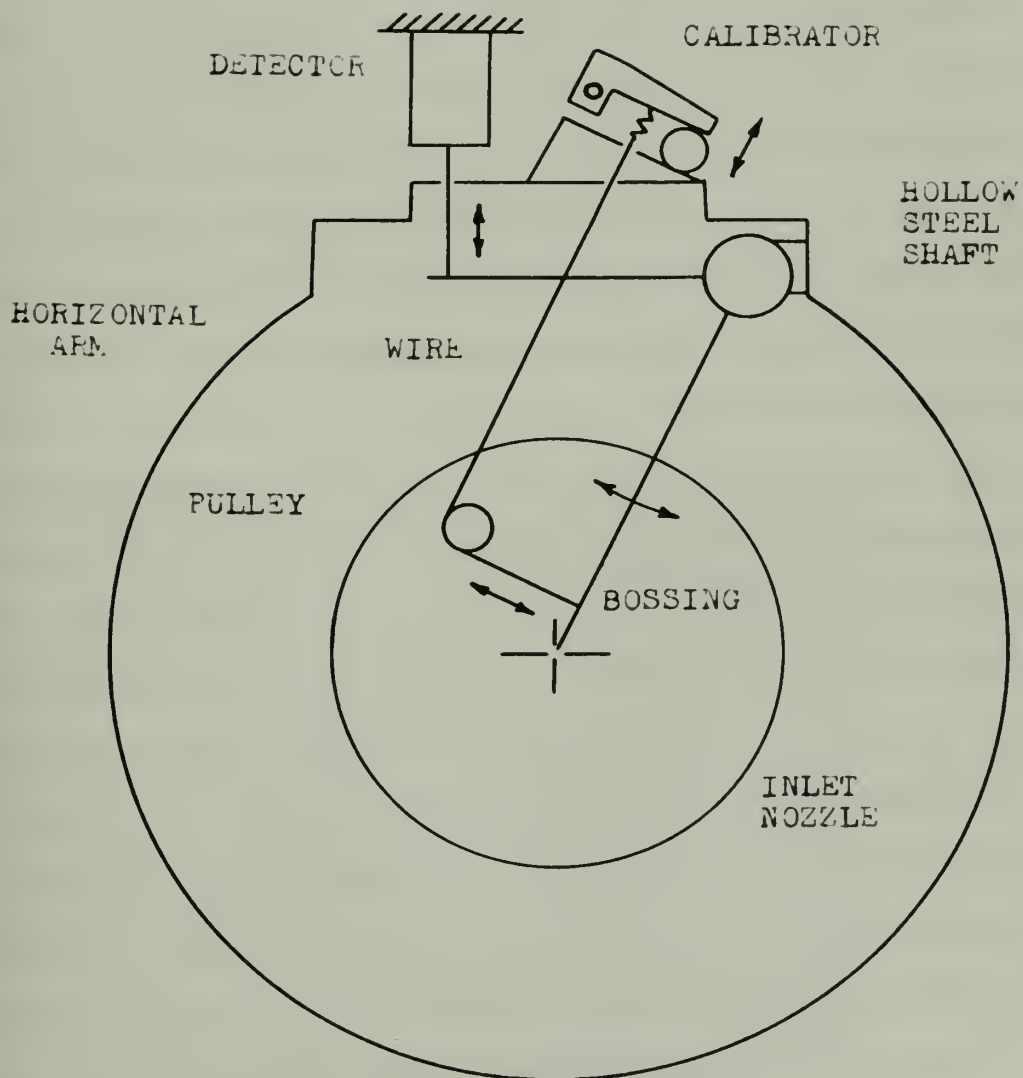


FIGURE XV

CALIBRATION SET-UP



LOOKING UPSTREAM TOWARD THE INLET NOZZLE

was 0.010 in. diameter piano wire. It was directed normal to the bossing surface by using a pulley with frictionless bearings positioned as shown in Fig. XV. Care was taken to insure that the wire had no kinks in order to maintain as nearly as possible a linear wire-spring combination.

As seen in the illustrations of the calibrator, the sine wave generator was mounted on the same base as the cam shaft and geared directly to the cam shaft. The only purpose in using a geared drive was to avoid an alignment problem between the cam shaft and the sine wave generator shaft. The flywheel, in addition to reducing torsional vibrations, provided a suitable location for the mounting of an indicator card used in phase angle determinations. The hair line and indicator card were adjusted so that a 0° reading on the card represented the high point of the actuating cam. This relationship is discussed in the Appendix. However, it should be mentioned here that the calibrator was designed in the above manner to provide flexibility of the system in physical positioning. As a packaged unit it was easily moved to a new location above the tunnel control panel during the actual measurement runs without disturbing the angular relationships between the sine wave generator phases, indicator card, and cam.

was 0.010 in. diameter piano wire. It was directed
 normal to the passing surface by using a pulley with
 frictionless bearings positioned as shown in Fig. XV.
 Care was taken to insure that the wire had no kinks
 in order to maintain as nearly as possible a linear
 wire-spring combination.

As seen in the illustrations of the calibrator,
 the sine wave generator was mounted on the same base
 as the cam shaft and geared directly to the cam shaft.
 The only purpose in using a gear drive was to avoid
 an alignment problem between the cam shaft and the sine
 wave generator shaft. The flywheel, in addition to re-
 ducing torsional vibrations, provided a suitable location
 for the mounting of an indicator card used in phase angle
 determinations. The hair line and indicator card were
 adjusted so that a 0° reading on the card represented
 the high point of the actuating cam. This relationship
 is discussed in the Appendix. However, it should be
 mentioned here that the calibrator was designed in the
 above manner to provide flexibility of the system in
 physical positioning. As a packaged unit it was easily
 moved to a new location above the tunnel control panel
 during the actual measurement runs without disturbing
 the angular relationship between the sine wave gen-
 erator phase, indicator card, and cam.

As originally designed the calibrator unit, when in position for a calibration run, was driven by a long flexible cable geared to the dynamometer shaft. Excessive torsional vibration made it necessary to use a solid shaft with short flexible cables at each end. See Fig. XIV. The gearing was four to one at the driven end so that the long shaft and cam shaft (calibrator) rotated at four times propeller shaft speed. When the calibrator was relocated above the control panel for measurement runs one of the short flexible cables was used to drive the calibrator from the same gears on the dynamometer shaft. Figure XVI shows the calibrator unit in position above the control panel for a measurement run.

H. PHASE SYSTEM.

Determination of the phase relationship between the time of occurrence of the measured force and the propeller blade position with respect to the trailing edge of the bossing is described in detail in the Appendix. The procedure consisted of determining three angles. Two of these angles were calculated directly from the galvanometer readings; one from the calibration runs and one from the measurement runs. The third angle was read directly on the calibrator indicator card during the measurement runs.

An originally designed the calibrator unit, when
 in position for a calibration run, was driven by a long
 flexible cable passing to the dynamometer shaft. (Fig. 14-
 cessive torsional vibration made it necessary to use a
 solid shaft with short flexible cables at each end. See
 Fig. XIV. The gearing was four to one at the driven end
 so that the long shaft and calibrator (calibrator)
 rotated at four times propeller shaft speed. When the
 calibrator was released above the control panel for a
 measurement runs one of the short flexible cables was
 used to drive the calibrator from the shaft gear on the
 dynamometer shaft. Figure XVI shows the calibrator unit
 in position above the control panel for a measurement run.
 The quantity of the measurement run was as high as
 100 ft. The phase system. The phase relationship between the
 time of occurrence of the measured force and the propeller
 blade position with respect to the trailing edge of the
 blade is described in detail in the Appendix. The mea-
 sure consisted of determining three angles. Two of
 these angles were calculated directly from the galvanometer
 readings; one from the calibration runs and was used as the
 measurement runs. The third angle was read directly on
 the calibrator indicator card during the measurement
 runs.



Fig. XVI. Calibrator and Strobe light in position for a measurement run.



Fig. XVII. Telescope mounted in test section window.

Essentially, then, the phase system consisted of the galvanometer, the indicator card on the flywheel of the calibrator, the phaser for timing of the strobe lights and a telescope. The telescope was mounted in a side window of the propeller tunnel as shown in Fig. XVII and used to correctly time firing of the strobe lights. One strobe light was mounted at a window in the test section and the other on the control panel for reading the indicator card. Both lights fired simultaneously.

I. TUNNEL SPEED CONTROL

For all constant speed runs, the propeller shaft was operated at a speed corresponding to a frequency close to the natural frequency of the bossing system. Increased sensitivity in force detection together with satisfactory phase angle determination was attained by operating the system just off the resonant peak. Such a frequency required that the control of the propeller shaft speed be extremely accurate. The principle of the Wenner speed controller was utilized.

The speed control circuit is discussed in detail in ⁽¹⁰⁾. Basically, speed control was obtained within very narrow limits by means of an adjustable frequency tuning fork acting in the motor field circuit as shown in Fig. XVIII. The tuning fork actually consists of a pair of tuning forks of different lengths and con-

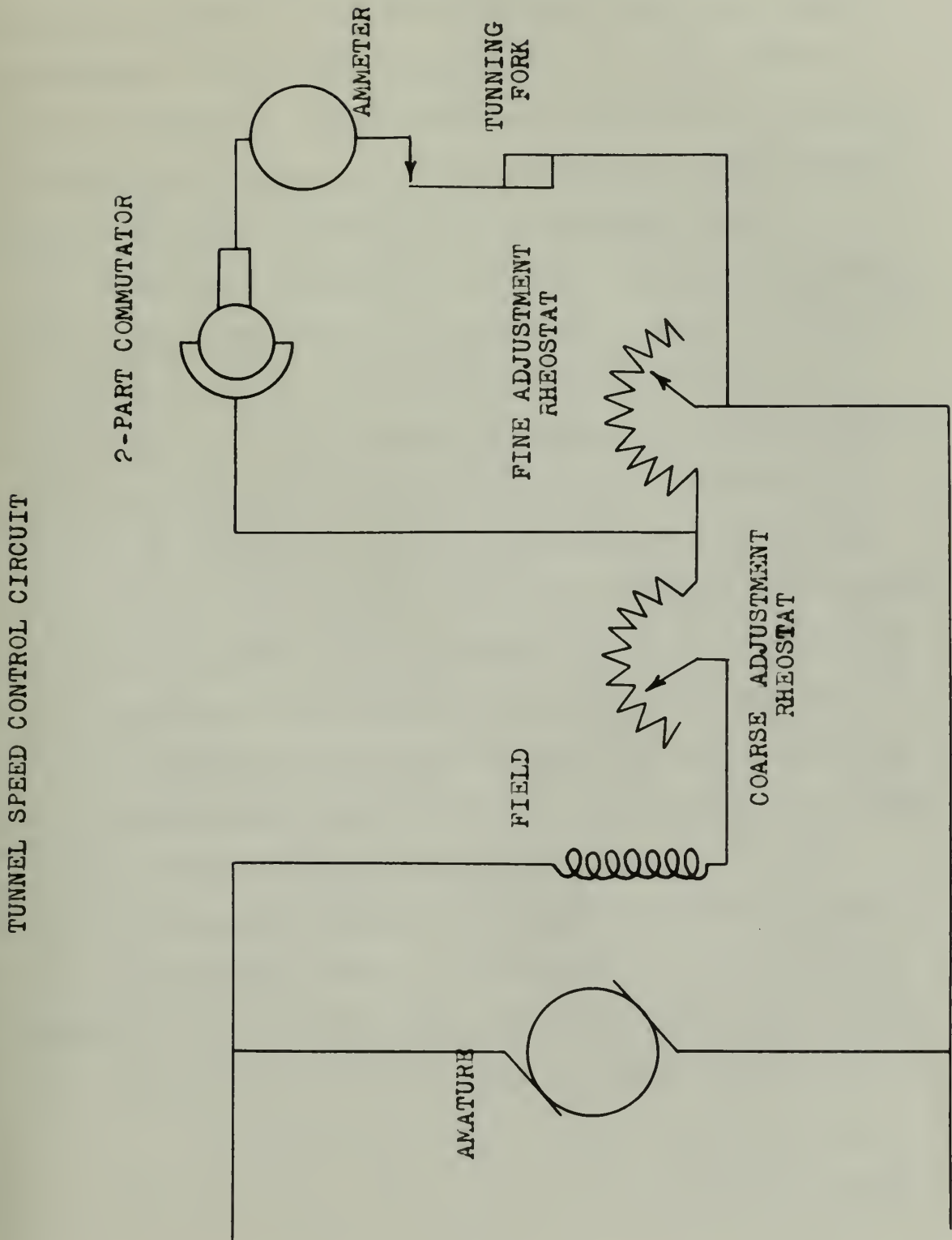
Essentially, then, the phase system consisted of the galvanometer, the indicator card on the flywheel of the calibrator, the phaser for timing of the strobe lights and a telescope. The telescope was mounted in a slide window of the propeller tunnel as shown in Fig. XVII and used to correctly time firing of the strobe lights. One strobe light was mounted at a window in the test section and the other on the control panel for reading the indicator card. Both lights fired simultaneously.

I. TUNNEL SPEED CONTROL

For all constant speed runs, the propeller shaft was operated at a speed corresponding to a frequency close to the natural frequency of the bearing system. Increased sensitivity in force detection together with satisfactory phase angle determination was attained by operating the system just off the resonant peak. Such a frequency required that the control of the propeller shaft speed be extremely accurate. The principle of the Wenner speed controller was utilized.

The speed control circuit is discussed in detail in (10). Basically, speed control was obtained within very narrow limits by means of an adjustable frequency tuning fork acting in the motor field circuit as shown in Fig. XVII. The tuning fork actually consists of a pair of tuning forks of different lengths and con-

FIGURE XVIII



sequently of different frequencies, mounted one over the other. The pair of forks were designed so that the relative position of the two could be varied by a screw adjustment. Clips near the ends constrain the forks to vibrate together. Rough frequency adjustment is attained by attaching weight sets to the fork tips. Finer adjustment is achieved by varying the adjustment screw.

A two-part commutator is geared to the dynamometer shaft. The commutator is constructed so that the circuit is closed for half a revolution and open for half a revolution. In series with the commutator is the tuning fork make-and-break contact maker which is adjusted so that it is closed for half a vibration and open for the other half. If the tuning fork and commutator are running in step the second field rheostat will be short circuited for a portion of each revolution. The field current will attain a certain value dependent upon the phase relation of the tuning fork and commutator. If the load or voltage changes the commutator speed, and therefore the phase relationship, the field current will then vary to return it to the desired value. A galvanometer in the circuit, mounted on the control panel, provides visual indication of synchronism of the commutator and tuning fork.

sequently of different frequencies, mounted one over the other. The pair of forks were designed so that the relative position of the two could be varied by a screw adjustment. Clips near the ends constrain the forks to vibrate together. Rough frequency adjustment is attained by attaching weight sets to the fork tines. Finer adjustment is achieved by varying the adjustment screw.

A two-part commutator is geared to the dynamometer shaft. The commutator is constructed so that the circuit is closed for half a revolution and open for half a revolution. In series with the commutator is the tuning fork make-and-break contact maker which is adjusted so that it is closed for half a vibration and open for the other half. If the tuning fork and commutator are running in step the second field rheostat will be short circuited for a portion of each revolution. The field current will attain a certain value dependent upon the phase relation of the tuning fork and commutator. If the load or voltage changes the commutator speed, and therefore the phase relationship, the field current will then vary to return it to the desired value. A galvanometer in the circuit, mounted on the control panel, provides visual indication of synchronism of the commutator and tuning fork.

III. PROCEDURE

Once the instrumentation and method of calibration were considered to be operationally acceptable, the procedure consisted of three basic steps which were repeated for each condition investigated. These were: (1) calibration, (2) measurement and (3) force and phase angle determination. Before the investigation could proceed, however, it was necessary to investigate the effects of certain variables, correct design defects, and obtain reproducible data. Since this initial procedure is confined to only the beginning of the investigation it will be omitted here and discussed instead in the Appendix.

Calibration consisted of applying a force of known magnitude and frequency to the bossing and recording the response of the system as galvanometer deflections. This was accomplished by using the calibrator described in Section II and a variety of wire-spring combinations. The wire from the calibrator was attached to the bossing at a position which was assumed to be the point of application of the hydrodynamically induced vibratory force. A variety of springs was used with the calibrator cover-

A variety of springs was used with the calibrator cover-
cation of the hydrodynamically induced vibratory force.

The wire from the calibrator was attached to the housing
in Section II and a variety of wire-spring combinations.
This was accomplished by using the calibrator described
response of the system as galvanometer deflections.
magnitude and frequency to the housing and recording the

Calibration consisted of applying a force of known

be omitted here and discussed instead in the appendix.

lined to only the beginning of the investigation it will

reproducible data. Since this initial procedure is con-

certain variables, correct design defects, and obtain

however, it was necessary to investigate the effects of

determination. Before the investigation could proceed,

dration, (1) measurement and (2) force and phase angle

for each condition investigated. These were: (1) cali-

cedure consisted of three basic steps which were repeated

were considered to be operationally acceptable, the pro-

Once the instrumentation and method of calibration

III. PROCEDURE

ing a range of forces from approximately 0.25 lbs. to 1.10 lbs. Enough wire-spring combinations were used to clearly define calibration curves of resultant galvanometer deflections vs. force.

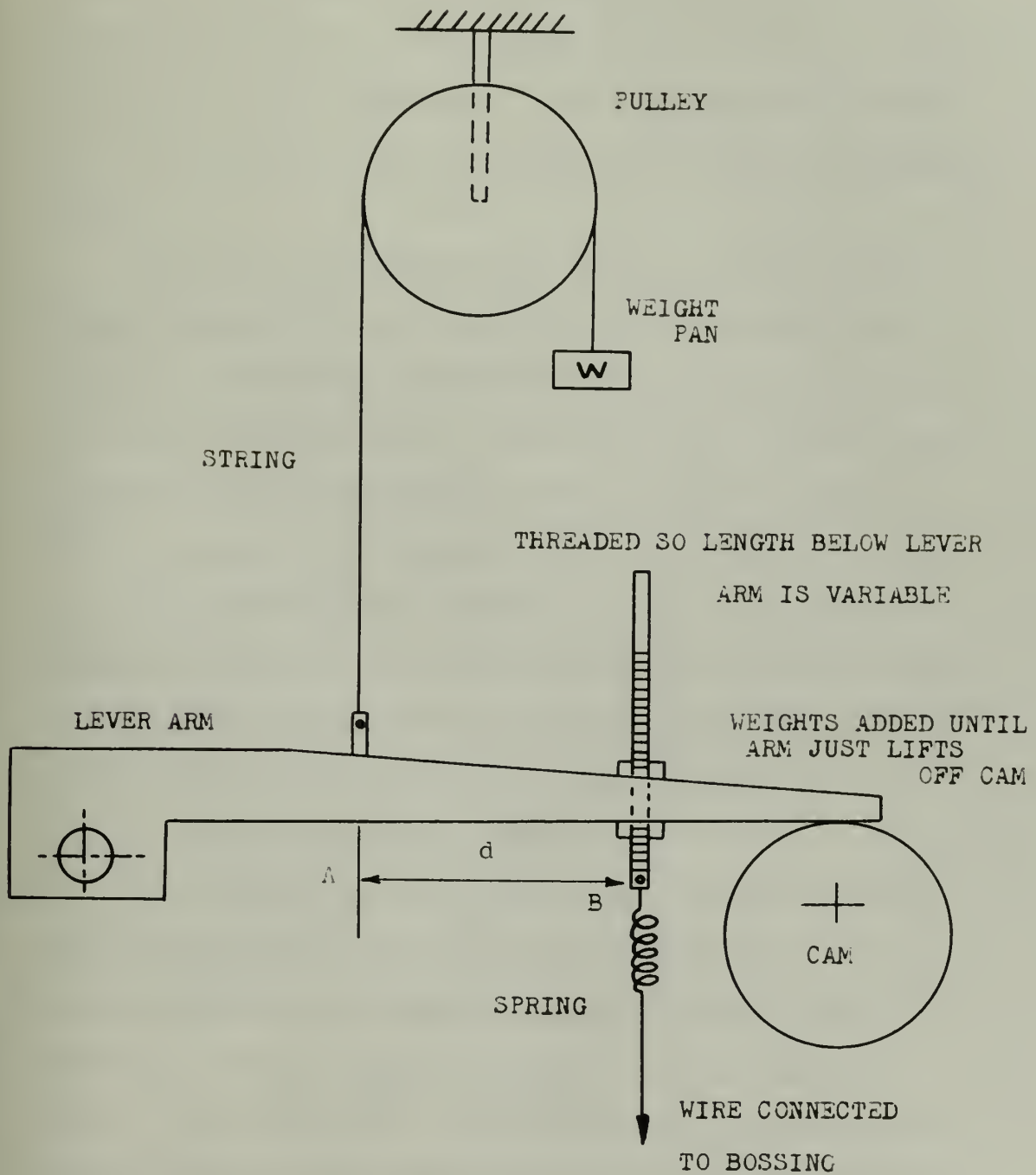
Once the desired spring was attached between the calibrator lever arm and the wire to the bossing, it was necessary to set the initial tension and determine the magnitude of the force which would be applied to the bossing. The initial tension was set by placing the desired weight on the weight pan and then adjusting the length of the wire-spring combination (the elongation of the spring) until the lever arm just lifted from the low point of the cam. See Figs. XVI and XX. The magnitude of the force applied to the bossing through the wire-spring combination was measured by adding weights to the weight pan until the lever arm just lifted off the high point of the cam. The weight pan was then disconnected from the lever arm and the tunnel run at the required speed. If the calibration was to be at a constant propeller speed, the tuning fork speed control circuit was used. For variable speed runs the tuning fork was disconnected. This procedure was repeated for a number of wire-spring combinations, the number used being determined by the number required to define a calibration curve. The end result of a calibration run was a plot of resultant galvanometer deflection readings against force.

ing a range of forces from approximately 0.25 lbs. to
 1.10 lbs. Enough wire-spring combinations were used
 to clearly define calibration curves of resultant gal-
 vanometer deflections vs. force.

Once the desired spring was attached between the
 calibrator lever arm and the wire to the passing, it
 was necessary to set the initial tension and determine
 the magnitude of the force which would be applied to
 the passing. The initial tension was set by placing
 the desired weight on the weight pan and then adjusting
 the length of the wire-spring combination (the elongation
 of the spring) until the lever arm just lifted from the
 low point of the cam. See Figs. XVI and XX. The magni-
 tude of the force applied to the passing through the
 wire-spring combination was measured by adding weights
 to the weight pan until the lever arm just lifted off
 the high point of the cam. The weight pan was then
 disconnected from the lever arm and the tunnel run at
 the required speed. If the calibration was to be at a
 constant propeller speed, the tuning fork speed control
 circuit was used. For variable speed runs the tuning
 fork was disconnected. This procedure was repeated for
 a number of wire-spring combinations, the number used
 being determined by the number required to define a
 calibration curve. The end result of a calibration run
 was a plot of resultant galvanometer deflection read-
 ings against force.

FIGURE XX

FORCE DETERMINATION



The response of the entire system was a function of the magnitude and frequency of the applied force and the natural frequency of the bossing. The natural frequency of the bossing system varied with clearance between the propeller and bossing, and the length of the nose piece used. Therefore, the calibration runs had to be made under the same conditions as the measurement runs.

For the measurement runs the wire of the wire-spring combination was removed from the bossing, the propeller installed, and the calibrator relocated on the tunnel control panel. See Fig. XVI. For the major portion of the investigation the propeller speed was held constant by the tuning fork speed control circuit and the water velocity changed to give the desired thrust variations. The remainder of the data was taken with either constant water velocity and variable RPM, or constant thrust and variable combinations of propeller RPM and water velocity.

In addition to recording the galvanometer deflection readings, as in the calibration runs, it was necessary to record propeller speed, thrust, water velocity, and the angle α , as read on the indicator card of the calibrator. The method of measuring propeller speed, thrust and water velocity is described in Section II.

The response of the entire system was a function of the magnitude and frequency of the applied force and the natural frequency of the boating. The natural frequency of the boating system varied with clearance between the propeller and boating, and the length of the nose piece used. Therefore, the calibration runs had to be made under the same conditions as the measurement runs.

For the measurement runs the wire of the wire-spring combination was removed from the boating, the propeller installed, and the calibrator relocated on the tunnel control panel. See Fig. XVI. For the major portion of the investigation the propeller speed was held constant by the tuning fork speed control circuit and the water velocity changed to give the desired thrust variations. The remainder of the data was taken with either constant water velocity and variable RPM, or constant thrust and variable combinations of propeller RPM and water velocity.

In addition to recording the galvanometer deflection readings, as in the calibration runs, it was necessary to record propeller speed, thrust, water velocity, and the angle α , as read on the indicator card of the calibrator. The method of measuring propeller speed, thrust and water velocity is described

in Section II.

The angle α is defined as the phase angle between the time the generating line of an arbitrarily selected propeller blade coincides with the trailing edge of the bossing, and the time the calibrator cam causes the maximum positive force to be applied to the bossing during calibration. The propeller shaft was marked so that the generating line of the chosen blade coincided with the trailing edge of the bossing when the cross hairs of the telescope were aligned with the mark. See Fig. XVII. During the measurement runs the timing of the strobe lights was adjusted until the scribe mark on the propeller shaft coincided with the telescope cross hairs. The angle α was then read on the calibrator indicator card.

Once both the calibration and measurement runs had been completed for a desired condition of investigation, the magnitude of the hydrodynamically induced force could be determined together with its phase relationship to the propeller blade position. From the galvanometer readings recorded during the calibration runs, resultant galvanometer readings and the angle β_1 were computed:

$$\text{Resultant reading} = \sqrt{A \text{ reading}^2 + B \text{ reading}^2}$$

$$\beta_1 = \tan^{-1} \frac{B \text{ reading}}{A \text{ reading}}$$

The resultant readings were plotted against the forces

The angle α is defined as the phase angle between the time the generating line of a arbitrarily selected propeller blade coincides with the trailing edge of the bossing, and the time the calibrator can cause the maximum positive force to be applied to the bossing during calibration. The propeller shaft was marked so that the generating line of the chosen blade coincided with the trailing edge of the bossing when the cross hairs of the telescope were aligned with the mark. See Fig. XVII. During the measurement runs the timing of the stroke lights was adjusted until the scribe mark on the propeller shaft coincided with the telescope cross hairs. The angle α was then read on the calibrator indicator card.

Once both the calibration and measurement runs had been completed for a desired condition of investigation, the magnitude of the hydrodynamically induced force could be determined together with its phase relationship to the propeller blade position. From the galvanometer readings recorded during the calibration runs, resultant galvanometer readings and the angles α were computed:

$$\text{Resultant Reading} = \sqrt{A^2 \text{ Reading}^2 + B^2 \text{ Reading}^2}$$

$$\beta = \tan^{-1} \frac{B \text{ Reading}}{A \text{ Reading}}$$

The resultant readings were plotted against the lateral

which produced them to give a curve of force vs. resultant galvanometer readings for the particular set of conditions employed.

The resultant galvanometer readings and the angle β_2 for the measurement runs were computed in a similar manner. The calibration curve was then entered with resultant readings and the magnitude of the forces determined. The phase relationship between the time of occurrence of the measured vibratory force and the time the propeller blade generating line coincided with the trailing edge of the bossing was then calculated. This relationship is represented by the angle γ , which is defined as the phase angle between the time the generating line of the arbitrarily selected propeller blade coincides with the trailing edge of the bossing and the occurrence of the measured hydrodynamically induced force normal to the bossing. The relationship for determination of γ is:

$$4\gamma = \beta_2 - (\beta_1 + \alpha)$$

where the following convention was adopted for β_1 and β_2 quadrant determination:

<u>A reading</u>	<u>B reading</u>	<u>Angle</u>
+	+	0 - 90°
-	+	90 - 180°
-	-	180 - 270°
+	-	270 - 360°

which produced them to give a curve of force vs. displacement
galvanometer readings for the particular set of conditions
employed.

The resultant galvanometer readings and the angle γ
for the measurement runs were computed in a similar manner.
The calibration curve was then entered with resultant read-
ings and the magnitude of the force determined. The phase
relationship between the time of occurrence of the measured
viscosity force and the time the propeller blade generating
line coincided with the trailing edge of the blade was
then calculated. This relationship is represented by the
angle γ , which is defined as the phase angle between the
time the generating line of the airfoil is selected and
the blade coincides with the trailing edge of the blade.
ing and the occurrence of the measured hydrodynamically
induced force normal to the housing. The relationship for
determination of γ is:

$$\gamma = \alpha_2 - (\alpha_1 + \alpha)$$

where the following convention was adopted for α_1 and α_2
constant determination:

Angle	B reading	A reading
0 - 90°	+	+
90 - 180°	+	-
180 - 270°	-	-
270 - 360°	-	+

A detailed description of the methods of force determination, phase angle determination, and the method of calculation is given in the Appendix.

A detailed description of the method of force determination, phase angle determination, and the method of calculation is given in the Appendix.

The first part of the report describes the method of force determination. The second part describes the method of phase angle determination. The third part describes the method of calculation. The fourth part describes the method of data reduction. The fifth part describes the method of error analysis. The sixth part describes the method of comparison with other methods. The seventh part describes the method of conclusion. The eighth part describes the method of references. The ninth part describes the method of appendix. The tenth part describes the method of index. The eleventh part describes the method of table of contents. The twelfth part describes the method of title page. The thirteenth part describes the method of preface. The fourteenth part describes the method of introduction. The fifteenth part describes the method of summary. The sixteenth part describes the method of acknowledgments. The seventeenth part describes the method of list of figures. The eighteenth part describes the method of list of tables. The nineteenth part describes the method of list of symbols. The twentieth part describes the method of list of abbreviations. The twenty-first part describes the method of list of acronyms. The twenty-second part describes the method of list of units. The twenty-third part describes the method of list of constants. The twenty-fourth part describes the method of list of variables. The twenty-fifth part describes the method of list of parameters. The twenty-sixth part describes the method of list of functions. The twenty-seventh part describes the method of list of operators. The twenty-eighth part describes the method of list of relations. The twenty-ninth part describes the method of list of equations. The thirtieth part describes the method of list of formulas. The thirty-first part describes the method of list of diagrams. The thirty-second part describes the method of list of figures. The thirty-third part describes the method of list of tables. The thirty-fourth part describes the method of list of symbols. The thirty-fifth part describes the method of list of abbreviations. The thirty-sixth part describes the method of list of acronyms. The thirty-seventh part describes the method of list of units. The thirty-eighth part describes the method of list of constants. The thirty-ninth part describes the method of list of variables. The fortieth part describes the method of list of parameters. The forty-first part describes the method of list of functions. The forty-second part describes the method of list of operators. The forty-third part describes the method of list of relations. The forty-fourth part describes the method of list of equations. The forty-fifth part describes the method of list of formulas. The forty-sixth part describes the method of list of diagrams. The forty-seventh part describes the method of list of figures. The forty-eighth part describes the method of list of tables. The forty-ninth part describes the method of list of symbols. The fiftieth part describes the method of list of abbreviations. The fifty-first part describes the method of list of acronyms. The fifty-second part describes the method of list of units. The fifty-third part describes the method of list of constants. The fifty-fourth part describes the method of list of variables. The fifty-fifth part describes the method of list of parameters. The fifty-sixth part describes the method of list of functions. The fifty-seventh part describes the method of list of operators. The fifty-eighth part describes the method of list of relations. The fifty-ninth part describes the method of list of equations. The sixtieth part describes the method of list of formulas. The sixty-first part describes the method of list of diagrams. The sixty-second part describes the method of list of figures. The sixty-third part describes the method of list of tables. The sixty-fourth part describes the method of list of symbols. The sixty-fifth part describes the method of list of abbreviations. The sixty-sixth part describes the method of list of acronyms. The sixty-seventh part describes the method of list of units. The sixty-eighth part describes the method of list of constants. The sixty-ninth part describes the method of list of variables. The seventieth part describes the method of list of parameters. The seventy-first part describes the method of list of functions. The seventy-second part describes the method of list of operators. The seventy-third part describes the method of list of relations. The seventy-fourth part describes the method of list of equations. The seventy-fifth part describes the method of list of formulas. The seventy-sixth part describes the method of list of diagrams. The seventy-seventh part describes the method of list of figures. The seventy-eighth part describes the method of list of tables. The seventy-ninth part describes the method of list of symbols. The eightieth part describes the method of list of abbreviations. The eighty-first part describes the method of list of acronyms. The eighty-second part describes the method of list of units. The eighty-third part describes the method of list of constants. The eighty-fourth part describes the method of list of variables. The eighty-fifth part describes the method of list of parameters. The eighty-sixth part describes the method of list of functions. The eighty-seventh part describes the method of list of operators. The eighty-eighth part describes the method of list of relations. The eighty-ninth part describes the method of list of equations. The ninetieth part describes the method of list of formulas. The ninety-first part describes the method of list of diagrams. The ninety-second part describes the method of list of figures. The ninety-third part describes the method of list of tables. The ninety-fourth part describes the method of list of symbols. The ninety-fifth part describes the method of list of abbreviations. The ninety-sixth part describes the method of list of acronyms. The ninety-seventh part describes the method of list of units. The ninety-eighth part describes the method of list of constants. The ninety-ninth part describes the method of list of variables. The hundredth part describes the method of list of parameters.

IV. RESULTS

The results of this investigation are best presented in graphical and tabular form. Figures XXI and XXII illustrate the variation of the vibratory force with thrust and clearance. Clearance values used refer to the clearance between the propeller leading edge and the bossing trailing edge at 0.7 radius. Since the propeller blade is slightly raked (8°), actual clearance varies from one-quarter inch at 0.2 radius to one and one-half inches at the blade tip. In examining these figures it should be remembered that the variation in thrust was obtained by a variation in water velocity at a constant propeller speed. It should also be pointed out that the normal operating point of the propeller used would correspond to a thrust of approximately 21 lbs.

Figure XXIII shows the variation in vibratory force with clearance for a thrust of 21 lbs. This figure clearly illustrates the affect of bossing length as well as clearance on the magnitude of the induced vibratory forces. Figure XXIV is the same information as Figure XXIII plotted on semi-log coordinates. It

IV. RESULTS

The results of this investigation are best presented in graphical and tabular form. Figures XVI and XVII illustrate the variation of the vibratory force with thrust and clearance. Clearance values used refer to the clearance between the propeller leading edge and the housing trailing edge at 0.7 radius. Since the propeller blade is slightly twisted (2°), actual clearance varies from one-quarter inch at 0.5 radius to one and one-half inches at the blade tip. In examining these figures it should be remembered that the variation in thrust was obtained by a variation in water velocity at a constant propeller speed. It should also be pointed out that the normal operating point of the propeller used would correspond to a thrust of approximately 11 lbs. Figure XVIII shows the variation in vibratory force with clearance for a thrust of 25 lbs. This figure clearly illustrates the effect of housing length as well as clearance on the magnitude of the induced vibratory forces. Figure XIX is the same information as Figure XVIII plotted on semi-log coordinates. It

should be emphasized here that Figs. XXII and XXIII are for one particular set of conditions. For example, these figures are for a thrust of 21 lbs. and a propeller speed of 548 RPM.

Figure XXV is another plot showing the variation of force with thrust for a particular value of clearance. However, in this figure water velocity was held constant and the propeller speed varied to obtain the desired thrust values. The upper curve was taken directly from Fig. XXI for purposes of comparison.

Figure XXVI is plotted using values obtained from Fig. XXV and illustrates the variation of force with water velocity.

The phase angle relationships resulting from the investigation are summarized in Tables XXXIII and XXXIV. The values of the phase angles for each measurement run are included on the measurement tables which appear in the Appendix. These tables show the maximum variation in the phase angle for the thrust range used at each value of the clearance. In addition, the value of the angle is given for a thrust of 21 lbs. which, as previously mentioned, corresponds to the average operating point of the propeller.

Table XXXV is a summary of the magnitude of the vibratory force and its phase angle relationships. The

should be emphasized here that Figs. XXII and XXIII
 are for one particular set of conditions. For example,
 these figures are for a thrust of 21 lbs. and a pro-
 peller speed of 148 RPM.
 Figure XXV is another plot showing the variation
 of force with thrust for a particular value of clearance.
 However, in this figure water velocity was held constant
 and the propeller speed varied to obtain the desired
 thrust values. The upper curve was taken directly from
 Fig. XXI for purposes of comparison.
 Figure XXVI is plotted using values obtained from
 Fig. XXV and illustrates the variation of force with
 water velocity.
 The phase angle relationships resulting from the
 investigation are summarized in Tables XXVII and XXVIII.
 The values of the phase angles for each measurement run
 are included on the measurement tables which appear in
 the Appendix. These tables show the maximum variation
 in the phase angle for the thrust range used at each
 value of the clearance. In addition, the value of the
 angle is given for a thrust of 21 lbs. which, as pre-
 viously mentioned, corresponds to the average operating
 point of the propeller.
 Table XXIX is a summary of the magnitude of the
 vibratory force and its phase angle relationships. The

force value has been reduced to a percentage of the thrust at the operating point.

The generally accepted law of similitude for bossing forces states that for equal values of the advance coefficient, J , the forces vary as the ratio of the propeller speed squared. ($F_2 = F_1 \left(\frac{N_2}{N_1}\right)^2$). Table XXXVI is an illustration of the values computed by this law as compared to the measured values. The table also gives the values computed by the same basic relationship but using a power of 2.75 rather than 2.00.

at the meeting point.

The generally accepted law of similitude for obtaining

efficient, i. the forces vary as the ratio of the parallel forces states that for equal values of the advance co-

Illustration of the values computed by this law as compared squared, $(\frac{M}{I})^2$. Table XXXVI is an

values computed by the same basic relationships but using
 pared to the measured values. The table also gives the

00.6 next to it 00.4 10 1000 0

Figure XXI

FORCE vs. THRUST

Short Bossing

RPM: 548

AMW 4/9/55 *WJ*

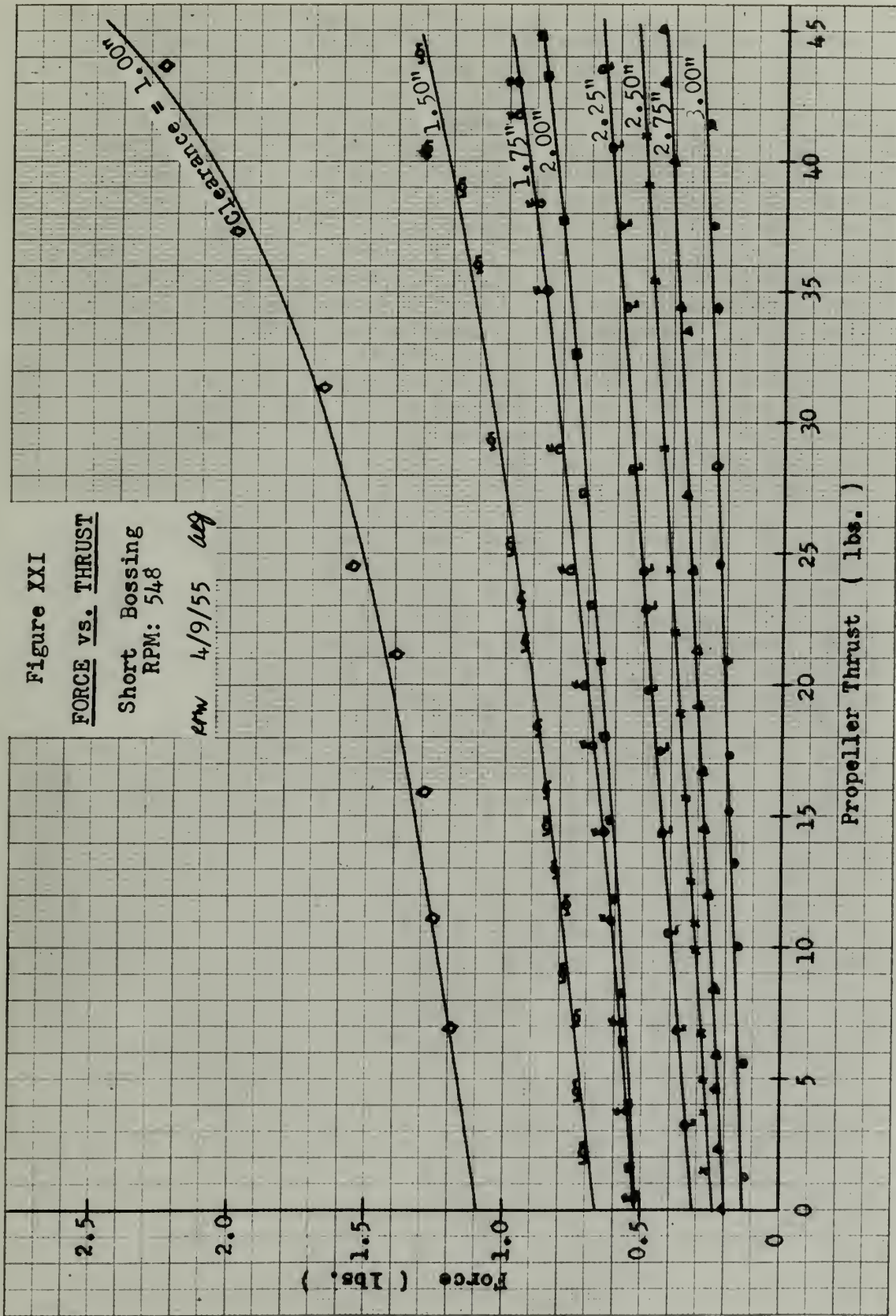


Figure XXII

FORCE vs. THRUST

Long Bossing
RPM: 548

27W 4/9/55 *avg*

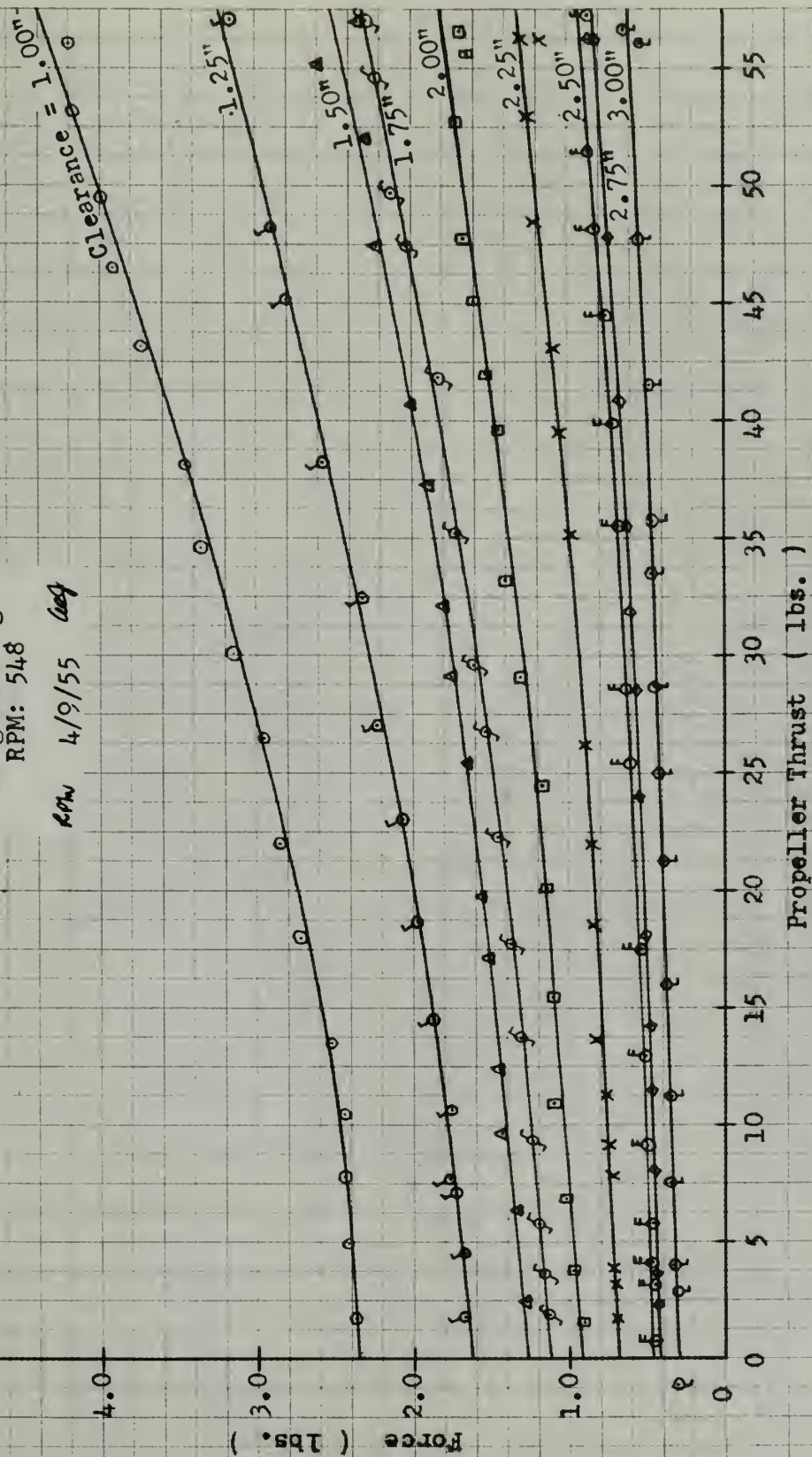


Figure XXIII

FORCE vs. CLEARANCE

RPM: 548

Rev 4/9/55 ref

Propeller Thrust = 21.0 lbs.

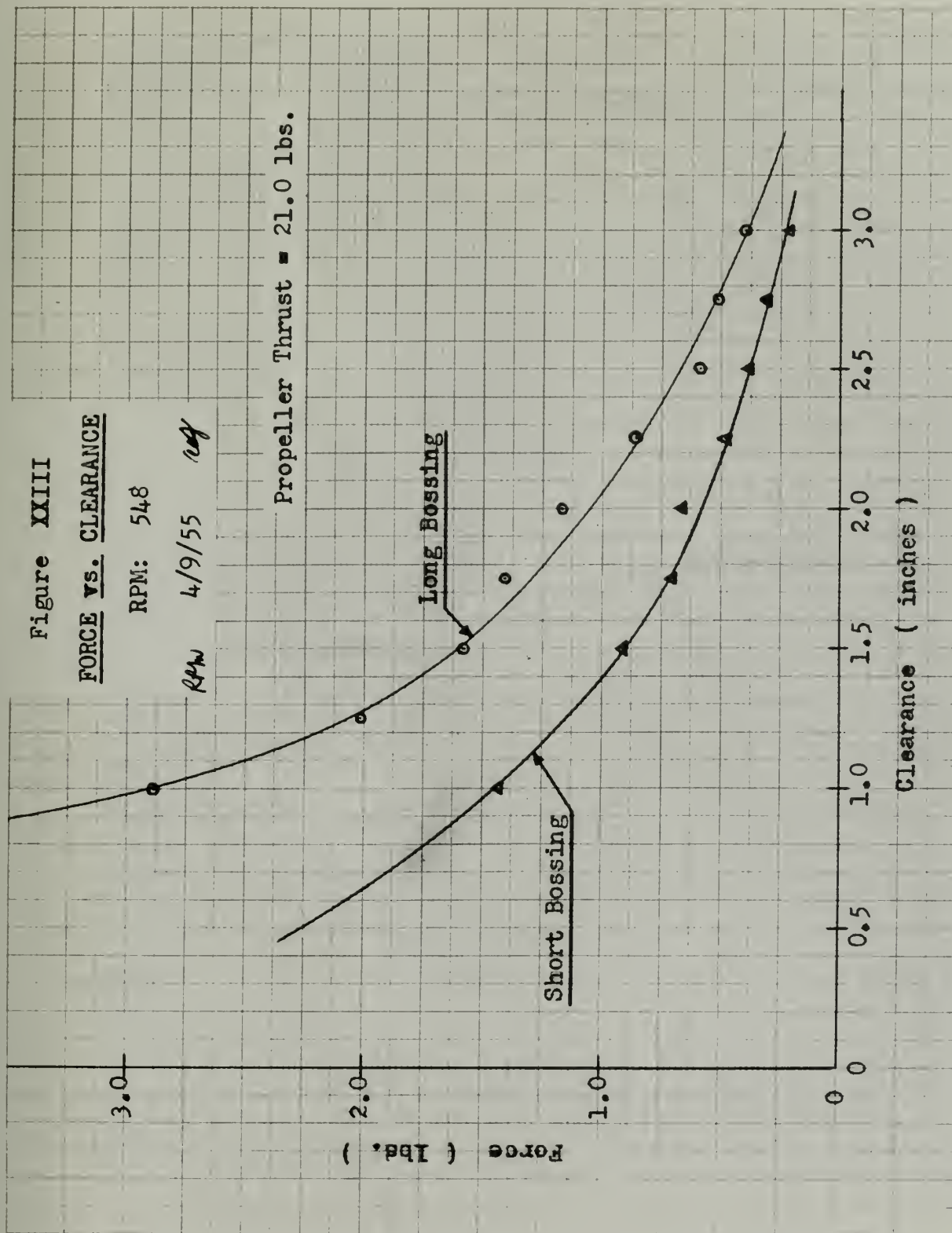
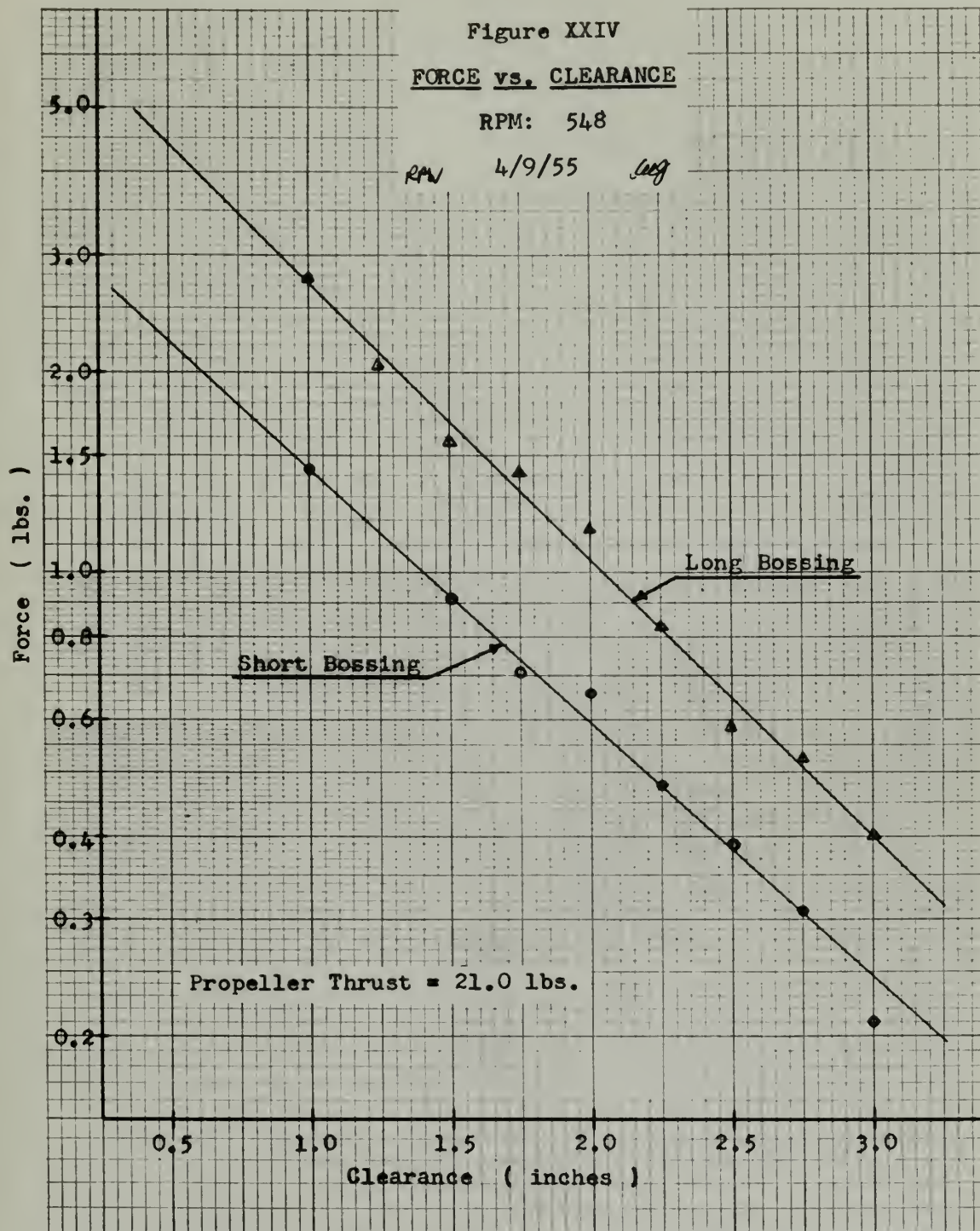


Figure XXIV

FORCE vs. CLEARANCE

RPM: 548

RAW 4/9/55 *leg*



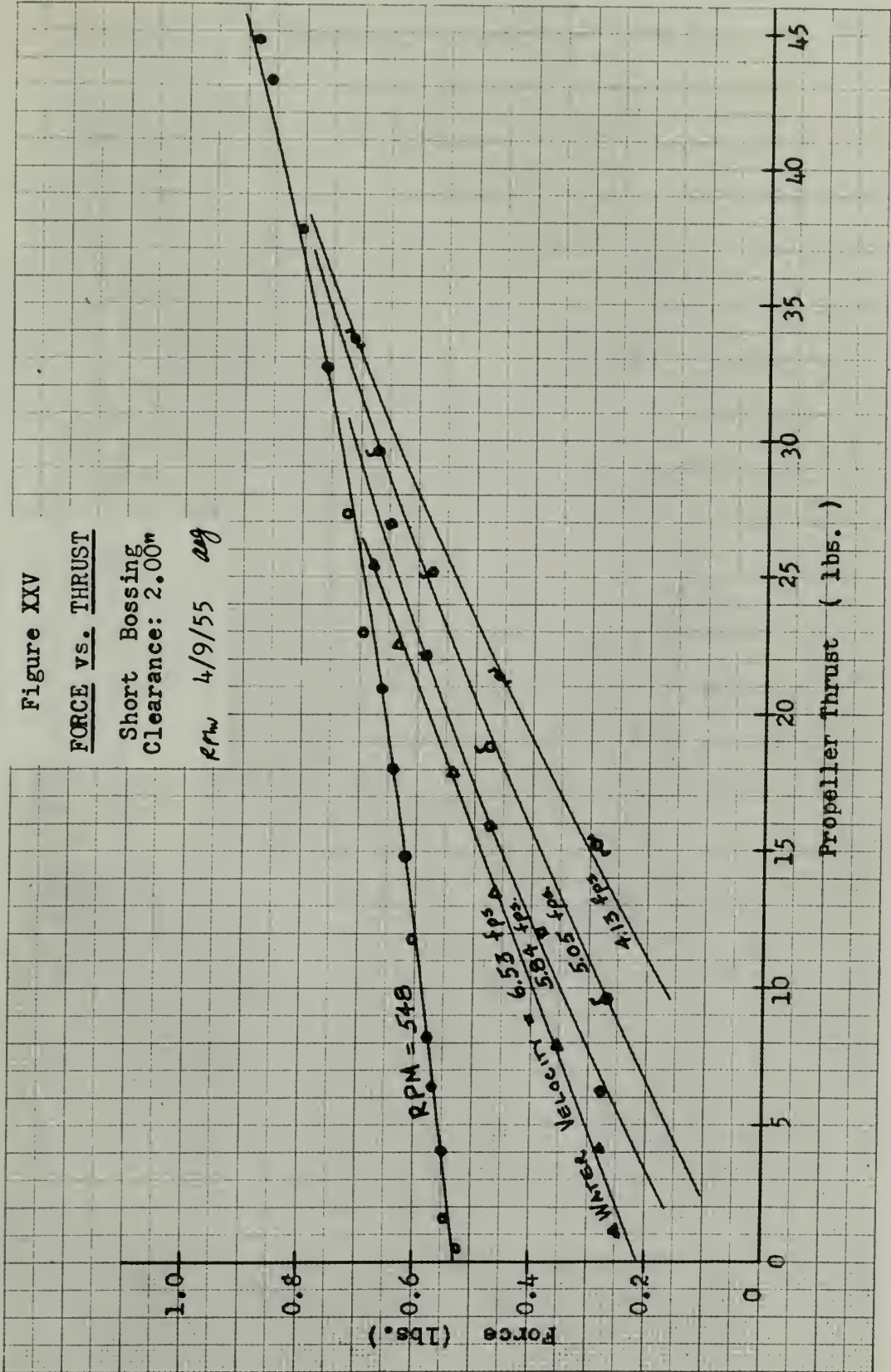


Figure XXVI

FORCE vs. WATER VELOCITY

Short Bossing
Propeller Thrust = 15.0 lbs.

Wg
4/9/55

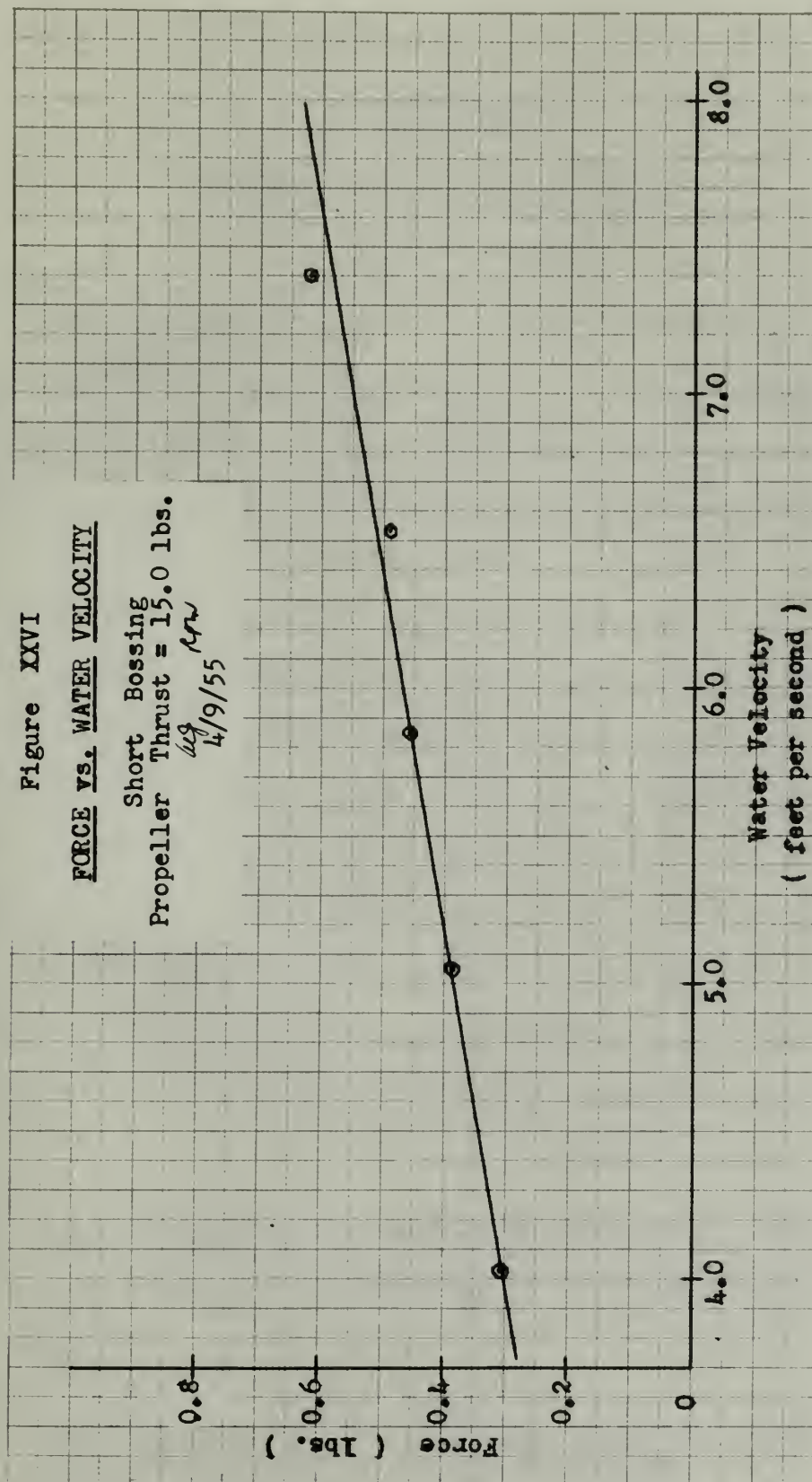


TABLE XXXIII

Summary of Phase Angle γ
for Short Bossing

Clear- ance	Clear- ance Prop. Diam.	γ_{min} (-)	γ_{max} (-)	$\Delta\gamma$	$\gamma_{T=21 \text{ lbs.}}$ (-)	$\gamma_{T=21 \text{ lbs.}}$ (+)
inches		deg	deg	deg	deg	deg
1	0.085	31.0	37.6	6.6	35.0	10.0
1.50	0.127	29.9	33.1	3.2	30.8	14.2
1.75	0.148	30.3	34.3	4.0	31.1	13.9
2.00	0.169	not computed				
2.25	0.190	31.5	34.4	2.9	32.5	12.5
2.50	0.211	32.5	37.3	4.8	34.8	10.2
2.75	0.232	33.5	37.6	4.1	35.4	9.6
3.00	0.250	30.8	35.6	4.8	32.0	13.0

$$Av. \Delta\gamma = 4.34^\circ$$

NOTE: γ_{min} generally corresponds to high thrust values.

γ_{max} generally corresponds to low thrust values.

$\Delta\gamma_{max}$ is maximum variation.

By Definition $+\gamma$ is the phase angle by which the force leads the propeller blade.

By definition γ is the phase angle by which the force lags the propeller blade.

ΔY_{\max} is maximum variation.

NOTE: Y_{\min} generally corresponds to high thrust values.
 Y_{\max} generally corresponds to low thrust values.

$$\Delta v. \Delta Y = 4.34\%$$

Clear- ance inches	Clear- ance Prop. diam.	Y_{\min} (-)	Y_{\max} (-)	ΔY	$Y_{\text{Test}} \text{ lbs.}$ (-)	$Y_{\text{Test}} \text{ lbs.}$ (+)
1	0.082	31.0	37.6	6.6	35.0	10.0
1.50	0.127	29.9	33.1	3.2	30.8	14.2
1.75	0.148	30.3	34.3	4.0	31.1	13.9
2.00	0.169	not computed				
2.25	0.190	31.2	34.4	3.2	32.2	12.2
2.50	0.211	32.2	37.3	4.6	34.8	10.2
2.75	0.232	33.2	37.6	4.1	32.4	7.6
3.00	0.250	30.8	32.6	4.8	32.0	13.0

Summary of Phase Angle γ
 for Short Bussing

TABLE XXXIII

TABLE XXXIV

Summary of Phase Angle γ
for Long Bossing

Clear- ance	Clear- ance Prop. Diam.	$\gamma_{\min.}$ (+)	$\gamma_{\max.}$ (+)	$\Delta\gamma$	$\gamma_{T=21 \text{ lbs.}}$ (+)
inches		deg	deg	deg	deg
1	0.085	23.9	26.0	2.1	25.1
1.25	0.106	24.9	26.1	1.2	25.9
1.50	0.127	24.3	26.1	1.8	26.0
1.75	0.148	22.9	23.9	1.0	23.8
2.00	0.169	22.9	24.5	1.6	24.5
2.25	0.190	21.9	24.3	2.4	24.0
2.50	0.211	21.9	23.5	1.6	23.0
2.75	0.232	21.6	25.5	3.9	25.0
3.00	0.250	22.2	25.9	3.7	25.2

Av. $\Delta\gamma = 2.14^\circ$

NOTE: γ_{\min} generally corresponds to high thrust values.
 γ_{\max} generally corresponds to low thrust values.
 $\Delta\gamma_{\max}$ is maximum variation.

By Definition $+\gamma$ is the phase angle by which the force leads the propeller blade.

TABLE XXXIV

SUMMARY OF TEST RESULTS
FOR LONG-BEARING

Distance inches	Distance inches	Y _{max.} (+)	Y _{min.} (+)	ΔY	Y _{max.} (+)	Y _{min.} (+)
1	0.0085	25.1	25.1	0.0	25.1	25.1
1.25	0.0106	25.1	25.1	0.0	25.1	25.1
1.50	0.0127	25.1	25.1	0.0	25.1	25.1
1.75	0.0148	25.1	25.1	0.0	25.1	25.1
2.00	0.0169	25.1	25.1	0.0	25.1	25.1
2.25	0.0190	25.1	25.1	0.0	25.1	25.1
2.50	0.0211	25.1	25.1	0.0	25.1	25.1
2.75	0.0232	25.1	25.1	0.0	25.1	25.1
3.00	0.0250	25.1	25.1	0.0	25.1	25.1

$$\Delta Y = 2.14$$

NOTE: Y_{max} generally corresponds to high thrust values.
Y_{min} generally corresponds to low thrust values.
ΔY is maximum variation.

By definition ΔY is the angle by which the force leads the pressure plate.

TABLE XXXV

Summary of Force and Phase Angle

Thrust = 21 lbs.

RPM = 548

Clear- ance	<u>SHORT BOSSING</u>				<u>LONG BOSSING</u>		
	<u>Clear- ance</u>	Force	% Thrust	Y (+)	Force	% Thrust	Y (+)
	<u>Prop. Diam.</u>						
inches		lbs		deg	lbs		deg
1.00	0.085	1.43	6.82	10.0	2.78	13.22	25.1
1.25	0.106	-----	-----	-----	2.03	9.68	25.9
1.50	0.127	0.91	4.33	14.2	1.58	7.52	26.0
1.75	0.148	0.71	3.48	13.9	1.42	6.77	23.8
2.00	0.169	0.66	3.14	-----	1.16	5.53	24.5
2.25	0.190	0.48	2.38	12.5	0.84	4.00	24.0
2.50	0.211	0.38	1.81	10.2	0.58	2.76	23.0
2.75	0.232	0.31	1.48	9.6	0.52	2.48	25.0
3.00	0.250	0.21	1.00	13.0	0.40	1.91	25.2

NOTE: By Definition +Y is the angle by which the force leads the propeller blade.

TABLE XXXV

Summary of Force and Phase Angle

Power = 240

Thrust = 21 lbs.

Clear- ance inches	SHORT SPACING			LONG SPACING		
	Force	Thrust	Y (+)	Force	Thrust	Y (+)
inches	lbs	lbs	deg	lbs	lbs	deg
1.00	0.065	1.45	6.52	10.0	1.73	15.12
1.25	0.106	---	---	---	2.03	15.68
1.50	0.127	0.91	4.33	14.2	1.58	16.00
1.75	0.148	0.71	3.48	17.9	1.42	16.77
2.00	0.169	0.66	3.14	---	1.16	17.53
2.25	0.190	0.48	2.38	12.5	0.84	18.00
2.50	0.211	0.38	1.81	10.5	0.68	18.76
2.75	0.232	0.31	1.48	9.6	0.53	19.18
3.00	0.250	0.21	1.00	13.0	0.40	19.91

NOTE: By definition Y is the angle by which the force lags the propeller blades as they rotate.

TABLE XXXVI

Comparison of Measured Values With Law
of Similitude

J	Thrust	Force meas- ured	N	$(N_2/N_1)^2$	Force comput- ed by square law	$(N_2/N_1)^{2.75}$	Force comput- ed by 2.75 law
v/nd	lbs.	lbs.	RPM		lbs.		lbs.
0.58	28.9	<u>0.655</u>	530	1.49	<u>0.56</u>	1.73	<u>0.657</u>
0.58	18.7	<u>0.38</u>	434				
0.62	22.3	<u>0.535</u>	496	1.49	<u>0.46</u>	1.727	<u>0.535</u>
0.62	15.2	<u>0.31</u>	407				
0.65	27.8	<u>0.680</u>	547	2.00	<u>0.510</u>	2.60	<u>0.662</u>
0.65	18.5	<u>0.460</u>	473	1.49	<u>0.382</u>	1.73	<u>0.441</u>
0.65	13.2	<u>0.255</u>	387				
0.70	25.0	<u>0.670</u>	568	1.66	<u>0.590</u>	2.015	<u>0.720</u>
0.70	19.9	<u>0.550</u>	506	1.32	<u>0.470</u>	1.47	<u>0.523</u>
0.70	13.5	<u>0.355</u>	440				
0.77	15.2	<u>0.490</u>	516	1.66	<u>0.440</u>	2.015	<u>0.534</u>
0.77	11.8	<u>0.385</u>	462	1.25	<u>0.330</u>	1.366	<u>0.362</u>
0.77	9.4	<u>0.265</u>	400				
0.85	7.2	<u>0.345</u>	468	1.25	<u>0.340</u>	1.366	<u>0.368</u>
0.85	6.4	<u>0.270</u>	418				

TABLE XXVII
Comparison of Observed Values With Low
of 1911-1912

[illegible]

V. DISCUSSION OF RESULTS

The factual statement of the results of this investigation has been presented in the preceding section. The purpose of this section is to discuss these results in order that they may be correctly interpreted and properly evaluated.

It has not been the purpose of this thesis to develop a new theory or to disprove existing theories, but rather to cast additional light on the mechanism of propeller excited vibratory forces. In an attempt to increase the existing factual knowledge of the phenomena, the influence of various parameters on the magnitude and phase angle of the vibratory force have been studied. In order that the results of these studies may be a significant contribution it becomes necessary to indicate their validity by an examination of the techniques employed in their determination. It is also imperative to re-emphasize some of the more subtle points which may be overlooked in analysis of the factual results.

The best method of insuring accurate interpretation of the measurement data was by comparison with calibration data corresponding in magnitude to the measurements. In

V. DISCUSSION OF RESULTS

The factual statement of the results of this investigation has been presented in the preceding section. The purpose of this section is to discuss these results in order that they may be correctly interpreted and properly evaluated.

It has not been the purpose of this thesis to develop a new theory or to disprove existing theories, but rather to cast additional light on the mechanism of oscillator excited vibratory forces. In an attempt to increase the existing factual knowledge of the phenomena, the influence of various parameters on the magnitude and phase angle of the vibratory force have been studied. In order that the results of these studies may be a significant contribution it becomes necessary to indicate their validity by an examination of the techniques employed in their derivation. It is also imperative to re-emphasize some of the more subtle points which may be overlooked in analysis of the factual results.

The best method of insuring accurate interpretation of the measurement data was by comparison with calibration data corresponding in magnitude to the measurements. In

determining the variation of vibratory force with thrust, it was impossible to use this method for all measurement runs, particularly in the analysis of data taken with the long bossing (long nose piece). (Fig. XXII). Forces obtained using the short nose piece, with the exception of 1" clearance data, were taken directly from either directly plotted or interpolated (1.75" and 2.5") calibration curves. (Figs. XXXV and XXI). The method employed for a clearance of 1.0 inch is considered valid although is recognized to be not as direct as having a calibration covering the ranges of measured force. For clearances of 1.75 and 2.50 inches the interpolation between existing calibration curves was linear. As shown in Fig. XXIV these two points are slightly off the straight line representing the variation of force with clearance. Closer correspondence of the data would have been obtained had a logarithmic interpolation been made between existing calibration curves. The ideal solution, of course, would have been the preparation of a separate calibration curve for each individual spacer arrangement. The overall error resulting from such calibration interpolation, however, is seen to be small, and therefore the procedure is considered justifiable.

Of the total of nine clearance runs made with the long nose piece, only four ($2\frac{1}{4}$ "-3") were possible to analyze directly from calibration curves.

determining the variation of vibratory force with time, it was impossible to use this method for all measurement runs, particularly in the analysis of data taken with the long nosed (long nose piece). (Fig. XII). Forces obtained using the short nose piece, with the exception of 1" clearance data, were taken directly from strain directly plotted or interpolated (1.75" and 2.5") calibration curves. (Figs. XXV and XXI). The method employed for a clearance of 1.0 inch is considered valid although it is recognized to be not as direct as having a calibration covering the range of measured force. For clearances of 1.75 and 2.50 inches the interpolation between existing calibration curves was linear. As shown in Fig. XIV these two points are slightly off the straight line representing the variation of force with clearance. Closer correspondence of the data would have been obtained had a logarithmic interpolation been made between existing calibration curves. The ideal solution, of course, would have been the preparation of a separate calibration curve for each individual test arrangement. The overall error resulting from such calibration interpolation, however, is seen to be small, and therefore the procedure is considered justifiable. Of the total of nine clearance runs made with the long nose piece, only four (2.5"-3") were possible to analyze directly from calibration curves.

Time did not permit a data reduction technique similar to that employed for a clearance of 1 inch with the short bossing. For the determination of forces measured which were outside the range of the calibration data, it was necessary to assume that the calibration curves were straight lines. This assumption permitted force determination for any galvanometer deflection by mere application of the calibration curve slope.

In addition, data for clearances of 1.25, 1.75, 2.25, and 2.75 inches for the long bossing were reduced by logarithmic interpolation between existing calibration curves. It should be noted that the calibration curves, as drawn, do not always intersect at the origin. (Figs. XLII and XLIII). The initial procedure and preliminary calibrations indicated that the galvanometer scale was not linear and, therefore, the calibration curves of resultant galvanometer readings vs. force possessed slight curvature. This was demonstrated in the short bossing calibration curves.

This discussion should emphasize that certain errors were accepted in the reduction of the data for the long bossing which were not present in the short bossing analysis. If it is assumed that the values of the force determined for clearances of 2.5" and 3.0" are correct, since they were derived directly from cal-

time did not permit a data reduction technique similar
 to that employed for a clearance of 1 inch with the
 short bearing. For the determination of forces measured
 which were outside the range of the calibration data, it
 was necessary to assume that the calibration curves were
 straight lines. This assumption permitted forces deter-
 mination for any galvanometer deflection by mere appli-
 cation of the calibration curve slope.
 In addition, data for clearances of 1.25, 1.75,
 2.25, and 2.75 inches for the long bearing were reduced
 by logarithmic interpolation between existing calibration
 curves. It should be noted that the calibration curves
 as drawn, do not always intersect at the origin.
 (Figs. XIII and XIV). The initial procedure and inter-
 mediate calibrations indicated that the galvanometer
 scale was not linear and, therefore, the calibration
 curves at resultant galvanometer readings vs. force
 possessed slight curvature. This was demonstrated in
 the short bearing calibration curves.
 This discussion should emphasize that certain
 errors were accepted in the reduction of the data for
 the long bearing which were not present in the short
 bearing analysis. It is assumed that the values of
 the force determined for clearances of 1.25 and 1.75
 are correct, since they were derived directly from cal-

ibration curves, the slope of the long bossing curve in Fig. XXIV could be reduced to a value corresponding to that of the short bossing. This would indicate that the values at smaller clearances as plotted, are high. If the calibration curves were of a shape similar to those of the short bossing these values would be smaller, and better agreement would exist between the slopes of the two curves. Despite these small discrepancies, the qualitative results indicate conclusively that for the longer bossing the magnitude of the force is at least 1.5 times as great as that for the corresponding conditions with the short bossing.

The curves of vibratory forces vs. clearance could be more clearly defined by measurement at clearances of less than 1 inch. The propeller selected for this investigation was designed with 8° rake so that a clearance of one inch at the 0.7 radius was the minimum value obtainable.

During the initial procedure and the exploratory runs it was discovered that lateral vibration of the wire-spring combination introduced a small error in the magnitude of the calibration force. The initial tension of the wire was increased to reduce this vibration, and several forms of dampers were used. These proved to be unsatisfactory, however, and were removed. Thus a small

ibration curves, the slope of the load-deflection curve in
 Fig. XIV could be reduced to a value corresponding to
 that of the short bearing. This would indicate that the
 values at smaller clearances are distorted, and also, if
 the calibration curves were of a shape similar to those
 of the short bearing these values would be similar, and
 better agreement would exist between the slopes of the
 two curves. Despite these small discrepancies, the
 qualitative results indicate conclusively that for the
 longer bearing the magnitude of the force is at least 1.5
 times as great as that for the corresponding conditions
 with the short bearing.

The curves of vibratory force vs. clearance could
 be more directly defined by measurement at clearances of
 less than 1 inch. The procedure selected for this in-
 vestigation was designed with the idea of that a clearance
 of one inch at the 0.7 radian was the minimum value ob-
 tainable.

During the initial procedure and the exploratory
 runs it was discovered that lateral vibration of the
 wire-spring connection introduced a small error in the
 magnitude of the calibration force. The initial tension
 of the wire was increased to reduce this vibration, and
 several forms of supports were used. These proved to be
 unsatisfactory, however, and were removed. Thus a small

but constant error existed for all data runs due to the lateral vibration of the wire-spring combination. The magnitude of this error is considered negligible for forces exceeding 0.4 lbs., but may be of some significance at lower values of force which correspond to the greater clearances.

Preliminary runs to determine the influence of certain parameters on the proposed calibration method revealed that self-excitation of the bossing system by the water was possible. The magnitude of the vibration varied directly with the water velocity while the frequency remained constant at the natural frequency of the bossing system. To increase the sensitivity of the detector system the investigation was conducted, for the most part, near the resonant peak. Thus the operating frequency corresponded closely to that of the natural frequency of the system and, therefore, the frequency of self-excitation. When compared with the vibratory forces, the influence of this phenomenon was found to be small at the water velocities anticipated. However small, it is possible that some slight error could have been introduced, particularly at low thrust values for the greater clearance runs.

Operation of the bossing system near the resonant peak made propeller speed control extremely critical.

but constant error existed for all tests due to the
 lateral vibration of the ultra-spring mechanism. The
 magnitude of this error is considered negligible for
 forces exceeding 0.4 lbs., but may be of some significance
 at lower values of force which correspond to the greater
 clearances. Preliminary runs to determine the influence of
 certain parameters on the proposed calibration method
 revealed that self-excitation of the testing system as
 the meter was possible. The magnitude of the vibration
 varied directly with the water velocity while the fre-
 quency remained constant at the natural frequency of the
 testing system. To increase the sensitivity of the de-
 tector system the investigation was conducted for the
 first test, near the resonant peak. Thus the operating
 frequency corresponded closely to that of the natural
 frequency of the system and, therefore, the frequency of
 self-excitation. When compared with the vibratory forces,
 the influence of this phenomenon was found to be small at
 the water velocities anticipated. However, still, it is
 possible that some slight error could have been introduced,
 particularly at low thrust values for the greater clearances.
 Operation of the testing system near the resonant
 peak adds rotational speed control entirely artificial.

Errors of 2 and 3 RPM in propeller speed caused relatively large errors in the magnitude of the measured force. To insure that such errors were kept to a minimum, constant attention had to be directed toward speed control. The magnitude of the errors introduced is felt, for the most part, to be negligible. However, this was only possible through constant adjustment of the speed control system. It is felt that the quantity of data taken could have been roughly doubled had speed control not been such a problem, either by having a more positive means of speed control available or by operating the system further from the resonant frequency.

Figure XXV illustrates the results of an investigation to determine the influence of water velocity on the vibratory force and to confirm the existing laws of similitude. For a constant value of thrust, the data clearly demonstrates the increase in the induced vibratory force with an increase in the water velocity past the bossing.

Correlation of this data was impossible with the existing laws of similitude, i.e. $F_2 = F_1 \left(\frac{N_2}{N_1} \right)^{2.00}$. As demonstrated in Table XXXVI, however, if the exponent of 2.00 is increased to 2.75, the results are in better agreement. It is suspected that the amplifier in the circuit was operating at or slightly below the linear

errors of 2 and 3 RPM in absolute speed versus relatively large errors in the magnitude of the measured force. To insure that such errors were kept to a minimum, constant attention had to be directed toward speed control. The magnitude of the errors introduced is felt, for the most part, to be negligible. However, this was only possible through constant adjustment of the speed control system. It is felt that the quantity of data taken could have been roughly doubled had speed control not been such a problem, either by having a more sensitive means of speed control available or by operating the system further from the resonant frequency.

Figure XXV illustrates the results of an investigation to determine the influence of water velocity on the vibratory force and to confirm the existing law of amplitude for a constant value of thrust, the data clearly demonstrates the increase in the induced vibratory force with an increase in the water velocity past the baseline.

Correlation of this data was impossible with the existing law of amplitude,
$$F = \sqrt{\frac{N}{W}} \cdot 2.00$$
 as demonstrated in Table XXVI, however, if the exponent of 1.00 is increased to 2.75, the results are in better agreement. It is suggested that the amplifier in the circuit was operating at or slightly below the linear

range of frequency vs. gain for these data runs. With a decrease in RPM the curves would drop off more sharply than they should. Thus the possibility exists that the effect represented here is somewhat exaggerated. The overall discrepancy is felt to be small, however, and qualitatively the data is valid.

Tables XXXIII and XXXIV are a summary of the phase angle relationships for the vibratory force. In calculating the values of the phase angle it was necessary to use measurements at a particular gain setting since it was found that the angle β_1 varied with gain. This was thought to be the results of operating the amplifier in the non-linear frequency range. The phase angle β_1 also varied in magnitude throughout a calibration run, but to a much lesser extent. Since a constant value of β_1 is essential for the evaluation of the phase angle γ , the average value of β_1 for each calibration run was used. For phase angle determination where the calibration curves had been derived by interpolation it was necessary to interpolate between the β_1 values also. It is felt that the phase angle relationships are of the correct order of magnitude but are subject to small errors which were introduced by the calculation procedure employed.

range of frequency vs. gain for these cases. With
a decrease in γ the curves would drop off more sharply
than they should. Thus the possibility exists that the
effect measured here is somewhat exaggerated. The
overall effect is felt to be small, however, and
qualitatively the data is valid.

Tables XXIII and XXIV are a summary of the phase
angle relationships for the various cases. In cal-
culating the values of the phase angle it was necessary
to use measurements at a constant gain setting since
it was found that the angle β_1 varied with gain. This
was thought to be the result of operating the amplifier
in the non-linear frequency range. The phase angle β_1
also varied in magnitude throughout a calibration run,
but to a much lesser extent. Since a constant value of
 β_1 is essential for the evaluation of the phase angle γ ,
the average value of β_1 for each calibration run was used.
For phase angle determination where the calibration curves
had been derived by interpolation it was necessary to in-
terpolate between the β_1 values also. It is felt that the
phase angle relationships are of the correct order of
magnitude but are subject to small errors which were in-
troduced by the calculation procedure employed.

VI. CONCLUSIONS

1. The induced vibratory force normal to the bossing is a function of the following variables:

- (a) Propeller thrust.
- (b) Water velocity.
- (c) Clearance between propeller blade and bossing.
- (d) Length of bossing.

2. For a constant value of propeller speed the vibratory force as a function of clearance may be represented by the following relationship:

$$F_2 = F_1 e^{-\mu(C_2 - C_1)}$$

where, F_2 and F_1 are the vibratory forces

μ is the slope of the semi-log plot of force vs. clearance, and

C_1 and C_2 are the clearances in inches at 0.7 radius.

3. The law of similitude for vibratory forces normal to the bossing corresponds more closely to the following relationship:

... VI. CONCLUSIONS ...

1. The induced vibratory force normal to the passing is a function of the following variables:

- (a) Propeller thrust.
- (b) Water velocity.
- (c) Clearance between propeller blade and passing.
- (d) Length of passing.

2. For a constant value of propeller speed the vibratory force as a function of clearance may be represented by the following relationship:

$$F_2 = F_1 e^{-u(C_1 - C_2)}$$

where, F_2 and F_1 are the vibratory forces

at the slope of the semi-log plot of force vs. clearance, and

C_1 and C_2 are the clearances in inches at 0.7 radius.

3. The law of magnitude for vibratory forces normal to the passing corresponds more closely to the following relationship:

for $J_2 = J_1$

$$F_2 = F_1 \left(\frac{N_2}{N_1} \right)^{2.75}$$

where F_1 and F_2 are the forces and N_1 and N_2 are the corresponding propeller speeds.

4. For design purposes a clearance equal to 1/3 the propeller diameter is recommended to minimize vibratory forces.

5. The phase angle, γ , defined as the angle between the time the generating line of an arbitrarily selected propeller blade coincides with the trailing edge of the bossing, and the occurrence of the measured hydrodynamically induced force normal to the bossing, is:

- (a) Independent of the clearance between propeller and bossing, and
- (b) A function of the bossing length and propeller thrust.

$$\text{for } J_2 = J_1$$

$$F_2 = F_1 \left(\frac{N_2}{N_1} \right)^{2.75}$$

where F_1 and F_2 are the forces and N_1 and N_2 are the corresponding propeller speeds.

4. For design purposes a clearance equal to 1% of the propeller diameter is recommended for relative vibratory forces.

5. The phase angle, γ , between the angle between the time the generating line of an arbitrarily selected propeller blade coincides with the trailing edge of the housing, and the occurrence of the measured hydrodynamically induced force normal to the housing, is:

- (a) Independent of the clearance between propeller and housing, and
- (b) A function of the housing length and propeller thrust.

VII. RECOMMENDATIONS

A. Redesign of Apparatus and Changes to Instrumentation:

1. Design a new calibrator capable of applying a force of at least 5 lbs. to the bossing and operating at much higher speeds.
2. Design a chain or geared drive for the increased capacity calibrator to eliminate torsional vibrations at higher loadings. The drive end of the system should be at the tunnel end of the dynamometer shaft. The new calibrator may still use a short flexible cable drive in the measurement run position.
3. Design a damper to eliminate lateral vibration of the spring-wire combination used for calibrating the system. In reducing lateral vibrations this damper should not be permitted to interfere with application of the calibrator force to the bossing.
4. Obtain a propeller with no rake in order to reduce minimum propeller clearances.
5. Obtain a voltage amplifier which is linear down to 10 cps; i.e. gain is independent of frequency down to 10 cps.

VII. RECOMMENDATIONS

A. Redesign of Apparatus and Changes to Instrumentation:

1. Design a new calibrator capable of applying a force of at least 5 lbs. to the housing and operating at much higher loads.
2. Design a chain or geared drive for the in-creased capacity calibrator to eliminate torsional vibrations at higher loadings. The drive end of the system should be at the tunnel end of the dynamometer shaft. The new calibrator may still use a short flexible cable drive in the measurement run position.
3. Design a device to eliminate lateral vibration of the spring-wire combination used for calibrating the system. In reducing lateral vibrations this device should not be permitted to interfere with application of the calibrator force to the housing.
4. Obtain a propeller with no gaps in order to reduce airframe propeller clearances.
5. Obtain a voltage amplifier which is linear down to 10 cps; i.e. gain is independent of frequency down to 10 cps.

6. Device a system which insures positive propeller tunnel speed control to within .5 RPM with little or no manual adjustment necessary. This may be accomplished by modification to the tuning fork circuit described herein.

7. Obtain an alternating current galvanometer or similar measuring instrument with a linear reading scale.

8. Rewind moveable coil of detector unit to give a larger number of turns. This will permit greater sensitivity and allow operation away from the resonant peak.

B. For Future Investigations:

1. Confirm assumption that vibratory force is applied at a distance from the propeller shaft corresponding to the 0.7 radius of the propeller. The possibility exists of accomplishing this by the use of strain gages.

2. Investigate the presently accepted law of similitude to confirm the results of this investigation.

3. Investigate more thoroughly the effects of bossing length on the induced force by running at least two additional series, each with different nose pieces.

4. Investigate more thoroughly the influence of water velocity on the induced vibratory forces.

6. Devise a system which induces positive pressure

on the tunnel speed control to within 5 RPM with little or no manual adjustment necessary. This may be accomplished by modification to the tuning fork circuit described herein.

7. Obtain an alternating current galvanometer or similar measuring instrument with a linear reading scale.

8. Rewind movable coil of detector unit to give a larger number of turns. This will permit greater sensitivity and allow operation away from the resonant peak.

B. For Future Investigations:

1. Confirm assumption that vibratory force is applied at a distance from the propeller shaft corresponding to the 0.7 radius of the propeller. The possibility exists of accomplishing this by the use of strain gauges.

2. Investigate the presently accepted law of similarity to confirm the results of this investigation.

3. Investigate more thoroughly the effects of passing length on the induced force by running at least two additional series, each with different nose pieces.

4. Investigate more thoroughly the influence of water velocity on the induced vibratory forces.

5. Confirm the phase angle relationship established in this thesis by additional investigation.

6. Investigate the influence of wake distribution on the magnitude and phase angle of the induced vibratory forces.

7. An alternate solution to the problem of designing a larger capacity calibrator and chain drive would be to use a smaller diameter propeller.

8. Utilize the bossing bearing installed in the hub to investigate bearing forces of blade frequency induced using similar parameters as in this thesis.

5. Confirm the phase angle relationship established

in this thesis by additional investigation.

6. Investigate the influence of wave distribution
on the magnitude and phase angle of the induced vibratory
forces.

7. An alternate solution to the problem of designing
a larger capacity collector and chain drive would be to
use a smaller diameter sprocket.

8. Utilize the bearing bearing installed in the
hub to investigate bearing forces of blade frequency in-
duced using similar parameters as in this thesis.

VIII. APPENDIX

VIII. APPENDIX

APPENDIX A

Detailed Procedure

1. Determination of an acceptable calibration and measurement procedure.

After the bossing system and the instrumentation were assembled and before the calibration and measurement runs could be commenced, many small, time-consuming problems had to be solved. The solution to these problems influenced the procedure finally adopted and therefore constitute a part of the initial procedure. The initial procedure may be subdivided into three groups of problems or investigations: (1) those concerning instrumentation, (2) those concerning the mechanical aspects of the bossing system as employed and (3) the effects of certain variables.

The instrumentation problems were actually simple in nature but are included for future reference. The amplifier characteristics were unknown at the start of the investigation. The major characteristics of the amplifier which were considered to be important were frequency response, linearity and amplification. These were determined by various techniques in the De Forrest Experimental Stress

APPENDIX A

Detailed Procedure

1. Determination of an acceptable calibration and measurement procedure.

After the testing system and the instrumentation were assembled and before the calibration and measurement runs could be commenced, many small, time-consuming problems had to be solved. The solution to these problems influenced the procedure finally adopted and therefore constitute a part of the initial procedure. The initial procedure may be subdivided into three groups of problems or investigations: (1) those concerning the mechanical aspects of the testing system as employed and (2) the effects of certain variables. The instrumentation problems were actually simple in nature but are included for future reference. The amplifier characteristics were unknown at the start of the investigation. The major characteristics of the amplifier which were considered to be important were frequency response, linearity and amplification. These were determined by various techniques in the De Forest Experimental Bureau.

Analysis Laboratory. A plot was made on semi-log paper of gain vs. gain dial setting with gain as the log coordinate. The plot was a straight line between settings of 6 to 11 inclusive, increased suddenly at settings of 5-1/2 and 11-1/2, and was curved above 12 and below 5. In order to utilize the relationship between gain and gain dial settings it was necessary to restrict the settings used between the values of 6 and 11. A plot was made of gain vs. frequency for various gain dial settings in order to determine the linear range of frequency response. A constant gain was obtained from approximately 20 cps to 6000 cps. Since 20 cps corresponds to a propeller speed of 300 RPM, if a four-bladed propeller is used, 300 RPM was considered to be the lowest possible shaft speed. Actually, it was found later in the investigation that with the amplifier in the detector circuit (Fig. IX) the linear range did not extend much below 35 cps. Thus the amplifier characteristics as originally determined restricted the flexibility of the measurement system to propeller speeds greater than 300 RPM, and gain dial settings of 6 to 11 inclusive.

Despite the fact that the linear range as originally measured was found to extend to as low as 20 cps, trouble was experienced with the phase angle relationships. It was found that the phase shift within the amplifier varied with gain. This probably was a result of operating at a

Analysis Laboratory. A plot was made on semi-log paper of gain vs. gain dial setting with gain as the log coordinate. The plot was a straight line between settings of 6 to 11 inclusive, increased suddenly at settings of 12-14 and 15-16, and was curved above 17 and below 5. In order to utilize the relationship between gain and gain dial settings it was necessary to restrict the settings used between the values of 6 and 11. A plot was made of gain vs. frequency for various gain dial settings in order to determine the linear range of frequency response. A constant gain was obtained from approximately 20 cps to 6000 cps. Since the curves tend to a propeller speed of 300 RPM, if a four-bladed propeller is used, 300 rpm was considered to be the lowest possible shaft speed. Actually, it was found later in the investigation that with the amplifier in the detector circuit (Fig. IX) the linear range did not extend much below 25 cps. Thus the amplifier characteristics as originally determined restricted the flexibility of the measurement system to propeller speeds greater than 300 RPM, and gain dial settings of 6 to 11 inclusive.

Despite the fact that the linear range is originally measured was found to extend to as low as 20 cps, trouble was experienced with the phase angle relationship. It was found that the phase shift within the amplifier varied with gain. This probably was a result of overloading at

frequency which was in the non-linear range of the amplifier. This condition was recognized early in the investigation. To correct it an amplifier of a lower frequency range was required. Such an amplifier was not available so the angles β_1 and β_2 became functions of the gain dial setting.

Being restricted to gain dial settings of 6 to 11 inclusive, it was necessary to decrease the magnitude of the galvanometer inputs by some other method when necessary to get on-scale readings. To accomplish this a resistance decade box was connected in series with the sine wave generator input to the galvanometer. Since the galvanometer multiplies the amplified detector output and the sine wave generator input together, a reduction in the sine wave generator input reduces the galvanometer sensitivity for a given detector output. Thus, the decade box functioned as an additional sensitivity control. The amount of resistance to use in a series of runs was usually established by making a preliminary measurement run to determine the magnitude of the signals to be expected. This was done because it was highly desirable to make both the measurement run and the calibration run at the same gain dial setting and thus avoid unduly complicated methods of data reduction.

frequency which was in the non-linear range of the amplifier. This condition was remedied very simply by the insertion of an amplifier of a lower frequency range was required. Such an amplifier was not available at the angles θ_1 and θ_2 because functions of the gain dial setting.

Being restricted to gain dial settings of 6 to 11 inclusive, it was necessary to decrease the magnitude of the galvanometer input by some other method when necessary to get on-scale readings. To accomplish this a resistance decade box was connected in series with the sine wave generator input to the galvanometer. Since the galvanometer multiplies the amplified detector output and the sine wave generator input together, a reduction in the sine wave generator input reduces the galvanometer sensitivity for a given detector output. Thus, the decade box functioned as an additional sensitivity control. The amount of assistance to use in a series of runs was usually established by making a preliminary measurement run to determine the magnitude of the signals to be expected. This was done because it was highly desirable to make both the measurement run and the calibration run at the same gain dial setting and thus avoid unduly complicated methods of data reduction.

The magnitude of the signal generated in the detector unit is a function of the velocity of the moveable coil and its flux linkages. The amount of flux linkage was controlled by the current in the fixed coil (E of Fig. X). Any fluctuations in this current would cause variations in the sensitivity of the detector system. Originally a 1.5 volt dry cell battery was used to energize this coil and was found to be unsatisfactory because its terminal voltage could not be maintained constant. To maintain the current in the fixed coil constant a lead acid storage battery was used. A variable resistor and ammeter were placed between the battery and the coil so that a constant current could be insured. An automobile battery charger was used to keep the storage battery in a constant state of charge.

During the early calibration runs a great deal of trouble was experienced with the reproducibility of data. The reasons for such difficulties were two-fold in that they arose from both instrumentation and mechanical sources. During the original calibration runs the galvanometer zero setting was arbitrarily chosen to facilitate acquiring on-scale readings. It was discovered that the response of the galvanometer to a signal of fixed magnitude and frequency was a function of the zero setting. In other words, the galvanometer was found to be non-linear.

The magnitude of the signal generated in the detector unit is a function of the velocity of the movable coil and its flux linkage. The amount of flux linkage was controlled by the current in the fixed coil (E of Fig. X). Any fluctuations in this current would cause variations in the sensitivity of the detector system. Originally a 1.5 volt dry cell battery was used to energize this coil and was found to be unsatisfactory because its terminal voltage could not be maintained constant. To maintain the current in the fixed coil constant a lead acid storage battery was used. A variable resistor and ammeter were placed between the battery and the coil so that a constant current could be insured. An automobile battery charger was used to keep the storage battery in a constant state of charge.

During the early calibration runs a great deal of trouble was experienced with the reproducibility of data. The reasons for such difficulties were two-fold in that they arose from both instrumentation and mechanical sources. During the original calibration runs the galvanometer was set at an arbitrarily chosen to facilitate recording on-scale readings. It was discovered that the response of the galvanometer to a signal of fixed magnitude and frequency was a function of the zero setting. In other words, the galvanometer was found to be non-linear.

After this discovery the same zero setting was used throughout the investigation and carefully checked at frequent intervals.

As previously mentioned, the bossing system operated in most conditions just off the resonant peak to give increased sensitivity. During the preliminary calibration runs the propeller shaft speed was checked at frequent intervals and corrected occasionally to the desired value. Subsequent measurements revealed that the response of the system was extremely critical with respect to propeller shaft speed and that the speed was not held constant enough by frequent manual adjustments. The tuning fork speed control circuit as described in Section II was then adopted. The tuning fork held the speed within approximately 1 RPM.

The first determinations of the phase angle γ relating the propeller blade position and the occurrence of the measured vibratory force revealed another instrumentation problem. It was possible to calculate two values of γ depending upon which phase of the sine wave generator appeared first in the time domain of the measurement system. By using a once per revolution contact maker and the cathode ray oscilloscope, it was established that the arbitrarily designated A reading preceded B reading in the measurement system used. This

After this discovery the same test setting was used throughout the investigation and carefully checked at frequent intervals.

As previously mentioned, the bearing system operated in most conditions just off the resonant gear to give increased sensitivity. During the preliminary calibration runs the propeller shaft speed was checked at frequent intervals and corrected occasionally to the desired value. Subsequent measurements revealed that the response of the system was extremely critical with respect to propeller shaft speed and that the speed was not held constant enough by frequent manual adjustments. The tuning fork speed control circuit as described in Section II was then adopted. The tuning fork held the speed within approximately 1 RPM.

The first determinations of the phase angle γ relating the propeller disk position and the occurrence of the measured vibratory force revealed another instrumentation problem. It was possible to calculate two values of γ depending upon which phase of the sine wave generator appeared first in the time domain of the measurement system. By using a wave generator connected to the cathode ray oscilloscope, it was established that the arbitrarily designated A working oscilloscope reading in the measurement system used. This

fact controls the definitions of β_1 and β_2 and the make-up of the phase angle determination method employed. Although a small problem, it is representative of the ones which lead to time delays in discovery and correction.

At the same time instrumentation troubles were being corrected and modified, the problems concerning the mechanical aspects of the bossing system were discovered. Preliminary calibration runs quickly showed the calibrator mechanism as originally designed and driven had to be modified to eliminate torsional vibrations. These torsional vibrations affected the calibration method in several ways. Since the sine wave generator was driven by the calibrator shaft, the torsional oscillations caused an unsteady sine wave generator output. Thus the sine wave generator input to the galvanometer was unsteady causing the galvanometer readings to oscillate. In addition, torsional vibration of the calibrator cam shaft produced a vibratory force whose frequency did not correspond to that of the hydrodynamically induced force, and therefore could not be used for construction of a representative calibration curve. The calibrator, when in position for a calibration run, was originally driven by a long flexible cable geared to the dynamometer shaft at the thrust meter end. To reduce the torsional vibration to an acceptable level, the major portion of

fact controls the definition of δ_1 and δ_2 and the make-up of the phase angle determination method employed. Although a small problem, it is representative of the ones which lead to time delays in discovery and correction. At the same time instrumentation troubles were being corrected and notified, the problems concerning the mechanical aspects of the bearing system were also covered. Eventually calibration runs quickly showed the calibrator mechanism as originally designed and driven had to be modified to eliminate torsional vibrations. These torsional vibrations affected the calibration method in several ways. Since the drive generator was driven by the calibrator shaft, the torsional oscillations caused an unstable sine wave generator output. Thus the sine wave generator input to the galvanometer was unstable causing the galvanometer readings to oscillate. In addition, torsional vibration of the calibrator can shaft produced a vibratory force whose frequency did not correspond to that of the hydrodynamically induced force, and therefore could not be used for construction of a representative calibration curve. The calibrator, when in position for a calibration run, was originally driven by a long flexible cable geared to the dynamometer shaft at the thrust meter end. To reduce the torsional vibration to an acceptable level, the major portion of

the flexible cable was replaced by a solid steel shaft. The shaft was mounted on a long 4" x 4" wooden beam and supported by bronze bearings. Short pieces of flexible cable were used at each end of the solid shaft. Figure XVI shows part of the shaft and one of the short flexible cables connected to the calibrator. It should be mentioned here that the three extra arms on the calibrator had a negligible effect in reducing vibration and were removed during the initial phase of the investigation.

Although the torsional vibration was greatly reduced by using the solid steel shaft, it still persisted. It was discovered that the alignment of the calibrator cam shaft and the sine wave generator shaft was not true. The two shafts had been coupled together with a solid steel coupling to prevent slippage and to preserve the phase angle relationships. To eliminate the alignment problem the sine wave generator was moved to one side and identical gears were pinned to each shaft. This is the reason for the sine wave generator gear drive.

In one of the many attempts to obtain reproducible data it was found that the sensitivity of the measurement system varied with the exact location of the detector unit. This was caused by rubbing of the moveable coil on the inside of the detector case. As seen in Fig. X the clearance between the moveable coil and the side is ex-

The flexible cable was replaced by a solid steel shaft.
 The shaft was mounted on a long 4" x 1/2" wooden base and
 supported by bronze bearings. Short pieces of flexible
 cable were used at each end of the solid shaft. Figure
 XVI shows part of the shaft and one of the short flexible
 cables connected to the calibrator. It should be mentioned
 here that the three extra arms on the calibrator had a
 negligible effect in reducing vibration and were removed
 during the initial phase of the investigation.
 Although the torsional vibration was greatly re-
 duced by using the solid steel shaft, it still persisted.
 It was discovered that the alignment of the calibrator
 cam shaft and the sine wave generator shaft was not true.
 The two shafts had been couled together with a solid
 steel coupling to prevent slippage and to preserve the
 phase angle relationship. To eliminate the alignment
 problem the sine wave generator was moved to one side
 and identical gears were pinned to each shaft. This
 is the reason for the sine wave generator gear drive.
 In one of the many attempts to obtain reproducible
 data it was found that the sensitivity of the resonant
 system varied with the exact location of the detector unit.
 This was caused by rubbing of the movable coil on the
 inside of the detector case. As seen in Fig. X the
 clearance between the movable coil and the side is ex-

tremely small. Therefore, unless the vertical rod connecting the horizontal arm to the moveable coil of the detector was correctly aligned, rubbing occurred and consequently greatly varying detector sensitivities resulted. To eliminate this variable the correct position of the detector unit was found and carefully marked to insure a reproducible location and thus a constant sensitivity. In addition the detector casing was re-machined to a larger internal diameter to provide greater clearance around the moveable coil. The final remedial measures taken in obtaining reproducible data focused themselves about the wire used between the calibrator lever arm and the bossing during the calibration runs. The wire which was originally selected for this function was black iron wire, of $1/32$ inch diameter. In selecting this wire, calculations were made to determine the influence of the weight of the wire on the spring constants of the springs used, and, on the time lag between the time the cam reached the high point and the time the bossing received the application of this maximum force. Both of these effects were calculated to be negligible. Initially, the force applied to the bossing by a particular spring was determined by measuring the elongation of the spring alone as a function of the required elongation force. These measurements were made for each

erely small. Therefore, only the vertical rod can-
necting the horizontal arm to the movable coil of the
detector was correctly aligned, rubbing occurred and
consequently greatly varying detector sensitivities re-
sulted. To eliminate this variable the contact position
of the detector unit was found and carefully marked so
that a reproducible location and thus a constant
sensitivity. In addition the detector casing was re-
machined to a larger internal diameter to provide greater
clearance around the movable coil. The final remedial
measures taken in obtaining reproducible data included
thoroughly about the wire used between the calibration
lever arm and the bearing during the calibration runs.
The wire which was originally selected for this function
was black iron wire, of 1/32 inch diameter. In selecting
this wire, calculations were made to determine the in-
fluence of the weight of the wire on the spring constants
of the springs used, and, on the time lag between the time
the cam reached the high point and the time the bearing
received the application of this maximum force. Both
of these effects were calculated to be negligible.
Initially, the force applied to the bearing by a positi-
vely spring was determined by measuring the elongation
of the spring alone as a function of the required
elongation force. These measurements were made for each

spring individually. It had been calculated that the spring constant of the wire was infinite compared to that of the spring and was therefore negligible. This method was found to be completely unsatisfactory. The first corrective step was to replace the wire then in use with 0.010" diameter steel piano wire. The use of piano wire reduced the number of kinks and small bends which ordinary wire inherently possesses. In addition, it reduced the spring action of the wire on the pulley, used to guide the wire to the bossing. This replacement of the original wire with piano wire still did not completely solve the problem of reproducible data. The system used to determine the force applied to the bossing was inadequate. Using the initial system the elongation of the wire was assumed to be zero, and the displacement of the bossing and pulley was assumed to be zero when the force was applied. The method finally adopted took these variables into account by determining the force applied to the bossing with the bossing and calibrator system assembled and the wire-spring combination attached in the exact manner in which it was to be used for calibration. The method is described in detail in the following section on force determination.

With adoption of the piano wire for the wire-spring combination another problem was inherited:

spring individually. It had been calculated that the
 spring constant of the wire was infinite compared to
 that of the spring and was therefore negligible. This
 method was found to be completely satisfactory. The
 first corrective step was to replace the wire then in
 use with 0.010" diameter steel piano wire. The use of
 piano wire reduced the number of kinks and small bends
 which previously were inherently present. In addition,
 it reduced the spring action of the wire on the pulley,
 used to guide the wire to the bearing. This reduction
 of the original wire with piano wire still did
 not completely solve the problem of reproducible data.
 The system used to determine the force applied to the
 bearing was inadequate. Using the initial system
 the elongation of the wire was assumed to be zero,
 and the displacement of the bearing and pulley was
 assumed to be zero when the force was applied. The
 method finally adopted took these variables into account
 by determining the force applied to the bearing with
 the bearing and calibrator system extended and the
 wire-spring combination attached in the exact manner
 in which it was to be used for calibration. The method
 is described in detail in the following section on
 force determination.

With addition of the piano wire to the wire-
 spring combination another problem was inherited:

lateral vibration of the wire in the span between the lever arm and the pulley. See Fig. XV. It was found that the amount of lateral vibration of the wire was a function of the initial tension applied to the wire-spring combination. The amount of lateral vibration affected the magnitude of the force applied to the bossing. By increasing the initial tension lateral vibrations were greatly reduced although not eliminated. Several attempts were made to eliminate these vibrations by using different types of dampers. The dampers not only tended to reduce the lateral vibration but also the longitudinal vibration and consequently, the magnitude of the force applied to the bossing. The effect of the lateral vibration at higher initial tensions was felt to be almost negligible when the precision of the overall assumptions were reconsidered. For this reason, rather than use some type of damper which would further complicate the calibration system, a small but constant error was accepted.

With an operationally acceptable system of measurement and calibration, there remained the problem of evaluating the effects of certain parameters on the calibration technique. Several of these have been mentioned in connection with the instrumentation and mechanical aspects of the initial procedure. The one remaining parameter to be mentioned is that of water

lateral vibration of the wire in the gap between the lever arm and the pulley. See Fig. 20. It was found that the amount of lateral vibration of the wire was a function of the initial tension applied to the wire-spring combination. The amount of lateral vibration affected the magnitude of the force applied to the bobbing. By increasing the initial tension lateral vibrations were greatly reduced although not eliminated. Several attempts were made to eliminate these vibrations by using different types of bobbings. The results were not only failed to reduce the lateral vibration but also the longitudinal vibration and consequently, the magnitude of the force applied to the bobbing. The effect of the lateral vibration at higher initial tension was felt to be almost negligible when the precision of the overall measurements was reconsidered. For this reason, rather than use some type of bobbing which would further complicate the calibration system, a small but constant error was accepted.

With an operationally acceptable system of measurement and calibration, there remained the problem of evaluating the effects of certain parameters on the calibration technique. Several of these have been mentioned in connection with the instrumentation and mechanical aspects of the initial procedure. The one remaining parameter to be mentioned is that of water

velocity. The calibration technique employed assumed the effect of water velocity to be negligible on the response of the bossing. It was found, however, that the bossing was sensitive to variations in water velocity. The phenomenon is similar to that of the self-excitation of airplane wings commonly known as wing flutter. The frequency of the vibration was constant but its amplitude was found to increase with increasing water velocity. A shift from the long nose piece to the short nose piece was accompanied by a shift in the frequency of the self excited vibration. The frequency measured coincided closely to the calculated natural frequency of the bossing system. This meant that the water velocity would affect the response of the system to a given force and frequency. To reduce this effect to a negligible quantity it was decided to accept a reduced sensitivity and operate away from the natural frequency of the bossing. Poor performance of the calibrator mechanism at propeller speeds greater than 625 RPM placed an upper limit on the frequency. (625 RPM corresponds to a calibrator speed of 2500 RPM). The lower limit was established at approximately 350 RPM because of the amplifier characteristics. A propeller shaft speed of 548 RPM was therefore selected as the basic speed at which a large portion of the investi-

velocity. The calibration technique employed assumed the effect of water velocity to be negligible on the response of the bearing. It was found, however, that the bearing was sensitive to variations in water velocity. The phenomenon is similar to that of the self-excitation of airplane wings commonly known as wing flutter. The frequency of the vibration was constant but the amplitude was found to increase with increasing water velocity. A shift from the long nose plate to the short nose plate was accompanied by a shift in the frequency of the self-excited vibration. The frequency measured coincided closely to the calculated natural frequency of the bearing system. This meant that the water velocity would affect the response of the system to a given force and frequency. To reduce this effect to a negligible quantity it was decided to select a reduced sensitivity and operate away from the natural frequency of the bearing. Test performance of the calibrator mechanism at propeller speeds greater than 625 RPM placed an upper limit on the frequency. (625 RPM corresponds to a calibrator speed of 2500 RPM). The lower limit was established at approximately 350 RPM because of the amplifier characteristics. A propeller shaft speed of 545 RPM was therefore selected as the basic speed at which a large portion of the investigation was conducted.

gation was conducted. At this propeller speed it was found that the water velocities required to cover the desired range of thrusts were sufficiently low to have a negligible effect on the system response. A small error is introduced at the higher water velocities but these correspond to negative thrust values which were not of interest in this investigation.

From this it can be seen that many assumptions have been made as to the magnitude of various sources of error. Refinement of the instrumentation, bossing system, calibration and measurement techniques could go on endlessly. As many refinements were made as considered compatible with the time allowed for the thesis. Whether more refined measurements would have been consistent with the basic assumptions used to permit the investigation is questionable.

tion was conducted. At this speed it was
 found that the water velocity required to cover the
 desired range of thrusts was sufficiently low to have
 a negligible effect on the system response. A small
 error is introduced at the higher water velocities but
 these correspond to negative thrust values which were
 not of interest in this investigation.
 From this it can be seen that many assumptions
 have been made as to the magnitude of various sources
 of error. Refinement of the instrumentation, bearing
 system, calibration and measurement techniques could
 be an aid. As many refinements were made as
 considered compatible with the time allowed for the
 thesis. Whether more refined measurements would have
 been consistent with the basic assumptions used to
 derive the investigation is questionable.

2. Details of Force Determination:

Determination of the magnitude of the hydro-dynamically induced vibratory force, was accomplished by preparation of a series of calibration curves. The response of the system to a vibratory force was a function of the frequency of the excitation force and the natural frequency of the bossing system. The frequency of the excitation force corresponds to four times the propeller shaft speed and, consequently, calibration was required for each speed used. The natural frequency of the bossing system was found to be a function of clearance and bossing length, i.e. which nose piece and spacer ring combination was in use. The term clearance refers to the distance between the propeller and bossing and the term length to the dimension parallel to the direction of water flow. See Fig. XXVII. The clearance between the propeller and bossing was varied by lengthening the cylindrical or hub section of the bossing. Lengthening was accomplished by inserting brass spacers at the after end of the cast aluminum hub section. See Fig. VI and Fig. XXVII. This additional weight altered the natural frequency of the bossing and thus the natural frequency of the entire bossing system comprising the bossing, hollow steel shaft, and horizontal arm. Addition of the brass spacers was accompanied by relocation of the point

2. Details of Force Determination:

Determination of the magnitude of the hydro-
dynamically induced vibratory force, was accomplished
by observation of a series of calibration curves. The
response of the system to a vibratory force was a
function of the frequency of the excitation force and the
natural frequency of the housing system. The frequency
of the excitation force corresponds to four times the pro-
peller shaft speed and, consequently, calibration was
required for each speed used. The natural frequency of
the housing system was found to be a function of clear-
ance and housing length, i.e., which nose piece and tower
ring combination was in use. The term clearance refers
to the distance between the propeller and housing and the
term length to the dimension parallel to the direction of
water flow. See Fig. XXVII. The clearance between the
propeller and housing was varied by lengthening the
cylindrical or non section of the housing. Lengthening
was accomplished by inserting brass spacers at the after
end of the cast aluminum non section. See Fig. VI and
Fig. XXVII. This sectional weight altered the natural
frequency of the housing and thus the natural frequency
of the entire housing system comprising the housing,
hollow steel shaft, and horizontal arm. Addition of the
brass spacers was accompanied by relocation of the point

FIGURE XXVII

BOSSING CLEARANCE

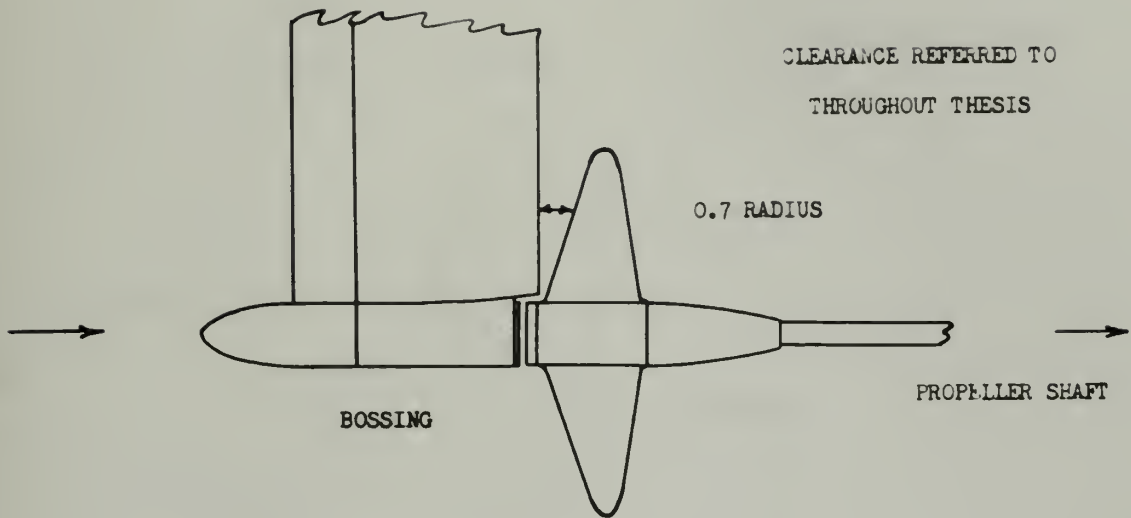


FIGURE XXVIII

FORCE MEASURED

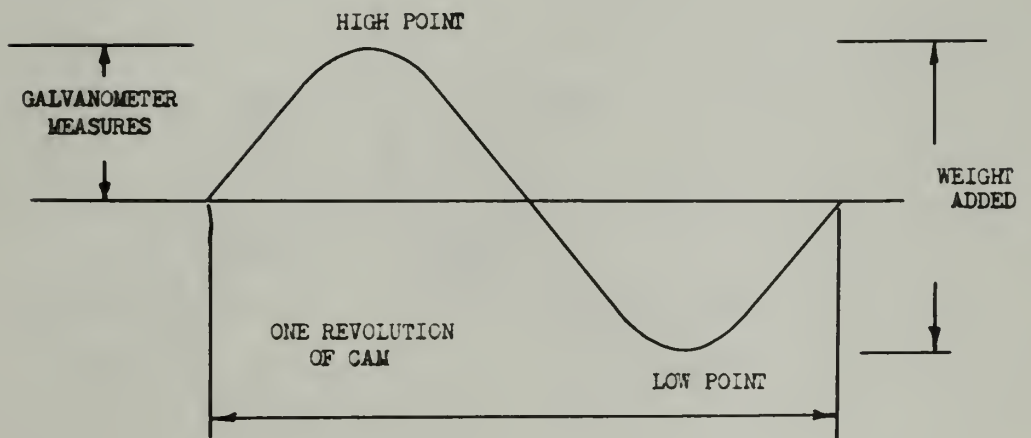
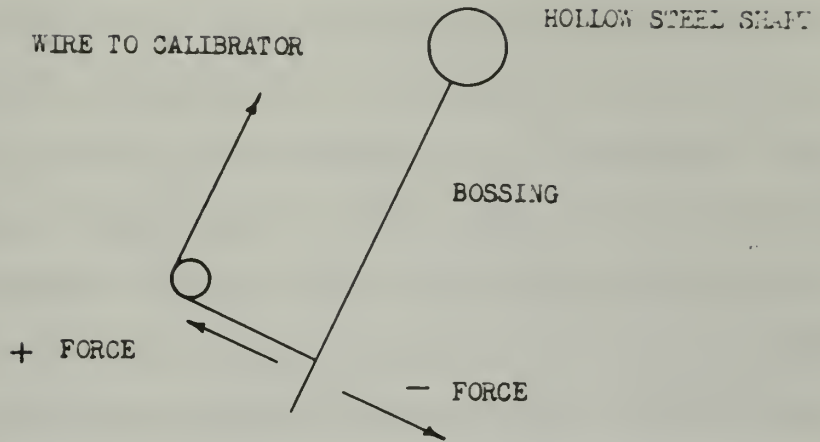
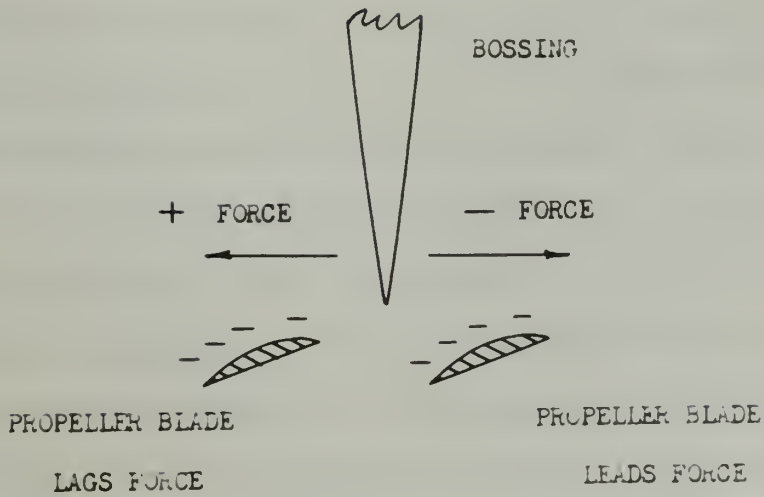


FIGURE XXIX

FORCE SIGN CONVENTION



FOR CALIBRATION



FOR MEASUREMENT

of attachment of the bossing to the hollow steel shaft. As a result the point of application of the alternating twisting moment was changed and this in turn changed the angular displacement of the hollow steel shaft and horizontal arm for a given vibratory force. For this reason it was necessary to calibrate the system for each clearance investigated and each length of bossing used. The shift in natural frequency of the bossing with a variation in length resulted from the fact that the inertia of the entrained water varies as the square of the bossing length.

Calibration was accomplished by means of the calibrator described in Section II. The appropriate nose piece and the piano wire were fastened to the bossing before it was placed in the test section. The bossing was placed at the desired location in the test section dependent upon the clearance under investigation. The propeller was not attached to the propeller shaft during the calibration runs because it was necessary to run the dynamometer shaft at the correct speed. This was necessary since the calibrator shaft was driven by the dynamometer. The piano wire was then run through a pulley with frictionless bearings to the calibrator where it was attached to the lever arm by means of a small helical spring. An assortment of springs provided a good range of spring constants. With the lever arm at the low point of the cam the initial tension was set by putting the desired

of attachment of the bearing to the hollow steel shaft. As a result the point of application of the alternating twisting moment was changed and this in turn changed the angular displacement of the hollow steel shaft and horizontal arm for a given vibratory force. For this reason it was necessary to calibrate the system for each clearance investigated and each length of bearing used. The shift in natural frequency of the bearing with a variation in length resulted from the fact that the inertia of the entrained water varies as the square of the bearing length. Calibration was accomplished by means of the cali-

brator described in Section II. The appropriate nose piece and the piano wire were fastened to the bearing before it was placed in the test section. The bearing was placed at the desired location in the test section dependent upon the clearance under investigation. The propeller was not attached to the propeller shaft during the calibration runs because it was necessary to run the dynamometer shaft at the correct speed. This was necessary since the calibrator shaft was driven by the dynamometer. The piano wire was then run through a pulley with frictionless bearings to the calibrator where it was attached to the lever arm by means of a small helical spring. An assortment of springs provided a good range of spring constants. With the lever arm at the low point of the cam the initial tension was set by cutting the desired

weight on the weight pan and then adjusting the length of the wire-spring combination until the lever arm just lifted off the cam. This amounted to varying the initial elongation of the spring. See Fig. XX. The same initial tension or force was applied to each spring depending upon stiffness. Having adjusted the initial tension to the desired value, the cam was rotated 180° to the high point. Weights were then added to the weight pan until the lever arm just lifted off the cam. This additional weight was the force applied to the bossing when corrected for the distance (d) between A and B in Fig. XX, the angle between the weight pan string and the arm, and the actual amplitude measured. See Fig. XXVIII.

Although the same springs and same diameter piano wire were used repeatedly for the various calibration runs, the spring constant was determined independently for each run.

Having determined the magnitude of the weights required, the weights were removed from the weight pan and the weight pan string removed from the lever arm. The propeller shaft was then run at the desired RPM and the galvanometer readings, A reading and B reading, recorded. The above process was then repeated for a sufficient number of springs to determine a calibration curve of force vs. resultant galvanometer reading, R reading.

weight on the weight pan and then adjusting the length of the wire-spring combination until the lever arm just lifted off the cam. This amounted to varying the initial elongation of the spring. See Fig. XX. The same initial tension of force was applied to each spring depending upon stiffness. Having adjusted the initial tension to the desired value, the cam was rotated 180° to the high point. Weights were then added to the weight pan until the lever arm just lifted off the cam. This additional weight was the force applied to the bearing when corrected for the distance (b) between A and B in Fig. XX, the angle between the weight pan string and the air, and the actual wall-tube measured. See Fig. XXVIII.

Although the same springs and same diameter wire were used repeatedly for the various calibration runs, the spring constant was determined independently for each run.

Having determined the magnitude of the weight required, the weights were removed from the weight pan and the weight pan string removed from the lever arm. The propeller shaft was then run at the desired RPM and the galvanometer readings, A reading and B reading, recorded. The above process was then repeated for a sufficient number of springs to determine a calibration curve of force vs. resultant galvanometer reading, B reading. See Fig. XXIX.

See sample calculations and a typical calibration curve.

The next phase of the procedure consisted of actual force measurements. Having sufficient data to plot a calibration curve the wire-spring combination was removed from the bossing, the propeller keyed to the propeller shaft in the marked angular position (see details of phase angle determination), and the calibrator relocated on the control panel. See Fig. XVI.

The results of previous investigations indicated that the magnitude of the bossing force was mainly a function of two variables: thrust and clearance. Consequently, for each set of conditions, measurements were made for a wide range of thrusts; from above the operating point to approximately zero. At the desired values of thrust the galvanometer readings were recorded and reduced to the corresponding force by means of the calibration curves.

Early calibration runs revealed that the maximum force which could be applied to bossing by the calibrator was approximately 1.1 lbs. (See Discussions of Results). Because the magnitudes of the forces were well above 1.1 lbs. for 1" clearances with the short bossing, and the calibration curves showed the system to be non-linear, it was necessary in this case to use a different cali-

See sample calculations and a typical calibration curve.

The next phase of the procedure consisted of actual force measurements. Having sufficient data to plot a calibration curve the wire-spring combination was removed from the housing, the propeller keyed to the propeller shaft in the raised angular position (see details of phase angle determination), and the calibrator relocated on the control panel. See Fig. XVI.

The results of previous investigations indicated that the magnitude of the bearing force was mainly a function of two variables: thrust and clearance. Consequently, for each set of conditions, measurements were made for a wide range of thrusts; from above the operating point to approximately zero. At the desired values of thrust the dynamometer readings were recorded and reduced to the corresponding force by means of the calibration curves.

Early calibration runs revealed that the maximum force which could be applied to bearing by the calibrator was approximately 1.1 lbs. (see Discussion of Results). Because the magnitudes of the forces were well above 1.1 lbs. for 1" clearances with the shaft bearing, and the calibration curves showed the system to be non-linear, it was necessary in this case to use a different cali-

bration technique. From this it should not be concluded that the bossing system was non-linear, but rather the measurement system; in particular the galvanometer or amplifier. For this reason the magnitude of the force could not be determined by linear extrapolation of the 1" calibration curve.

A calibration curve was made in the usual manner with the calibrator for an amplifier gain setting of 10. The measurements were made with an amplifier gain setting of 6. In addition to taking the calibration data with a gain setting of 10, data was recorded for gain settings from 6 to 11 inclusive. Lines of constant force were then plotted on semi-log paper with an ordinate of resultant galvanometer reading and an abscissa of gain setting. From this, lines of constant resultant reading were plotted using an ordinate of force and an abscissa of gain setting. The average slope of the constant resultant galvanometer readings was measured. The relationship to determine the magnitude of the force at other gain settings was found to be $F = F_0 e^{\mu(D_0 - D)}$, where D_0 and D are the amplifier gain settings, and μ is the slope. (For the 1" clearance runs $F_6 = F_{10} e^{4\mu}$). In other words, with the resultant galvanometer readings from the actual measurement runs, the force, F_{10} , is determined from the calibration curve. But the resultant

station technique. From this it should not be concluded that the housing system was non-linear, but rather the measurement system; in particular the galvanometer or amplifier. For this reason the magnitude of the force could not be determined by linear extrapolation of the 1" calibration curve.

A calibration curve was made in the usual manner with the calibrator for an amplifier gain setting of 10. The measurements were made with an amplifier gain setting of 6. In addition to taking the calibration data with a gain setting of 10, data was recorded for gain settings from 6 to 11 inclusive. Lines of constant force were then plotted on semi-log paper with an ordinate of resultant galvanometer reading and an abscissa of gain setting. From this, lines of constant resultant reading were plotted using an ordinate of force and an abscissa of gain setting. The average slope of the constant resultant galvanometer readings was measured. The relationship to determine the magnitude of the force at other gain settings was found to be $F = F_0 \cdot 10^{u(P-C)}$, where P and C are the amplifier gain settings, and u is the slope. (For the 1" clearance runs $F_0 = 10^{4.0}$.) In other words, with the resultant galvanometer readings from the actual measurement runs, the force, F_0 , is determined from the calibration curve. But the resultant

readings were taken with a gain setting of 6, therefore, it is necessary to run along a constant resultant reading line to a gain setting of 6 and read the force F_6 . The data for a clearance of 1" with the short bossing was the only data reduced in this manner. The magnitude of the forces for the other runs with the short bossing could be determined directly from a calibration curve.

The method employed to determine the magnitude of the forces when the long bossing was employed differed from that described above. These forces were much greater than had been anticipated inasmuch as it was originally considered that the bossing with the short nose piece attached was "very long" in comparison with the propeller diameter, chord lengths, etc. Consequently, the calibration runs were made in a manner similar to those used with the short nose piece at clearances greater than 1". For most clearances the forces measured were larger than 1.1 lbs. and therefore too large to be taken directly from the calibration curves. Linear extrapolation was therefore employed to reduce this data. The method is described in detail in the section on Sample Calculations.

readings were taken with a strain indicator of 0.1 mm. therefore, it is necessary to run along a constant resistance reading line to a point reading of 0.1 and read the force F_0 . The value for a clearance of 1.0 with the short bearing was the only data reduced in this manner. The magnitude of the forces for the other runs with the short bearing could be determined directly from a calibration curve. The method employed to determine the magnitude of the forces when the long bearing was subjected to three times that described above. These forces were much greater than had been anticipated inasmuch as it was originally considered that the bearing with the short nose piece attached was "very long" in comparison with the pinball diameter, cone length, etc. Consequently, the calibration runs were made in a manner similar to those used with the short nose piece at clearances greater than 1.0. For most clearances the forces measured were larger than 1.1 lbs. and therefore too large to be taken directly from the calibration curves. Linear extrapolation was therefore employed to reduce this data. The method is described in detail in the section on Sample Calculations.

3. Details of Phase Angle Determination

Phase angle determination involved the evaluation of four phase angles and the relationship between these angles. In this calculation all the phase angles are referred to the indicator card which is attached to the flywheel of the calibrator mechanism and rotates at four times propeller shaft speed. The four angles are defined as follows:

$$\beta_1 = \tan^{-1} \frac{B_{rdg1}}{A_{rdg1}} \quad \text{(Subscript one refers to calibration and two to measurement.)}$$

$$\beta_2 = \tan^{-1} \frac{B_{rdg2}}{A_{rdg2}}$$

α = the phase angle between the time the generating line of an arbitrarily selected propeller blade coincides with trailing edge of the bossing and the time the calibrator cam applies the maximum positive force to the bossing during calibration.

γ = the phase angle between the time the generating line of the arbitrarily selected propeller blade coincides with the trailing edge of the bossing and the occurrence of the measured hydrodynamically induced force normal to the bossing. A positive force acts in the same direction as the maximum calibrator force; i.e. in the same direction as the calibrator wire pulls on the bossing.

3. Details of Phase Angle Determination

Phase angle determination involved the evaluation of four phase angles and the relationships between these angles. In this calculation all the phase angles are referred to the indicator card which is attached to the flywheel of the calibrator mechanism and rotates at four times propeller shaft speed. The four angles are defined as follows:

$\alpha_1 = \tan^{-1} \frac{E_{1\text{rd}}}{A_{1\text{rd}}}$
(Substituting one reference to calibration and time for displacement.)

$$\alpha_2 = \tan^{-1} \frac{E_{2\text{rd}}}{A_{2\text{rd}}}$$

$\alpha =$ the phase angle between the time the generating line of an arbitrarily selected propeller blade coincides with trailing edge of the housing and the time the calibrator can apply the maximum positive force to the housing during calibration.

$\gamma =$ the phase angle between the time the generating line of the arbitrarily selected propeller blade coincides with the trailing edge of the housing and the occurrence of the measured hydrodynamically induced force normal to the housing. A positive force acts in the same direction as the maximum calibrator force; i.e. in the same direction as the calibrator wire pulls on the housing.

λ = the phase angle between the time of occurrence of the measured signal to the galvanometer and the applied bossing force; either calibrator or measured, since this angle was assumed to be constant.

δ = the phase angle between the time of occurrence of the A reading to the galvanometer and the time the calibrator cam applies the maximum positive force to the bossing.

The indicator card was attached to the calibrator flywheel so that a zero reading corresponded to the high point of the cam, or application of the maximum positive calibrator force. The time delay between extension of the spring and application of the force at the bossing was calculated to be negligible.

For convenience in the determination of β_1 and β_2 the following sign convention was adopted:

<u>A reading</u>	<u>B reading</u>	<u>Angle</u>
+	+	0 - 90°
-	+	90 - 180°
-	-	180 - 270°
+	-	270 - 360°

From Fig. XXXI the following relationship can be determined:

λ = the phase angle between the time of occurrence of the measured signal to the galvanometer and the applied forcing force; either calibrator or measured, since this angle was assumed to be constant.

δ = the phase angle between the time of occurrence of the λ reading to the galvanometer and the time the calibrator was applied the maximum positive force to the bearing.

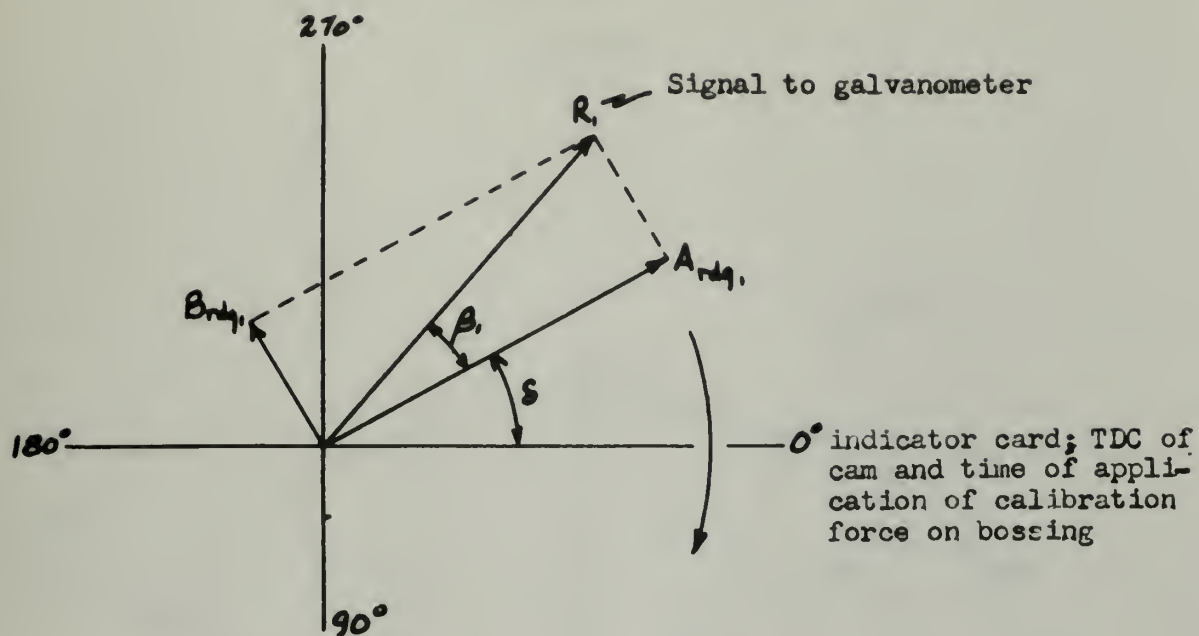
The indicator card was attached to the calibrator flange so that a zero reading corresponded to the right point of the cam, or application of the maximum positive calibrator force. The time delay between extension of the spring and application of the force at the bearing was calculated to be negligible.

For convenience in the determination of λ and δ , the following sign convention was adopted:

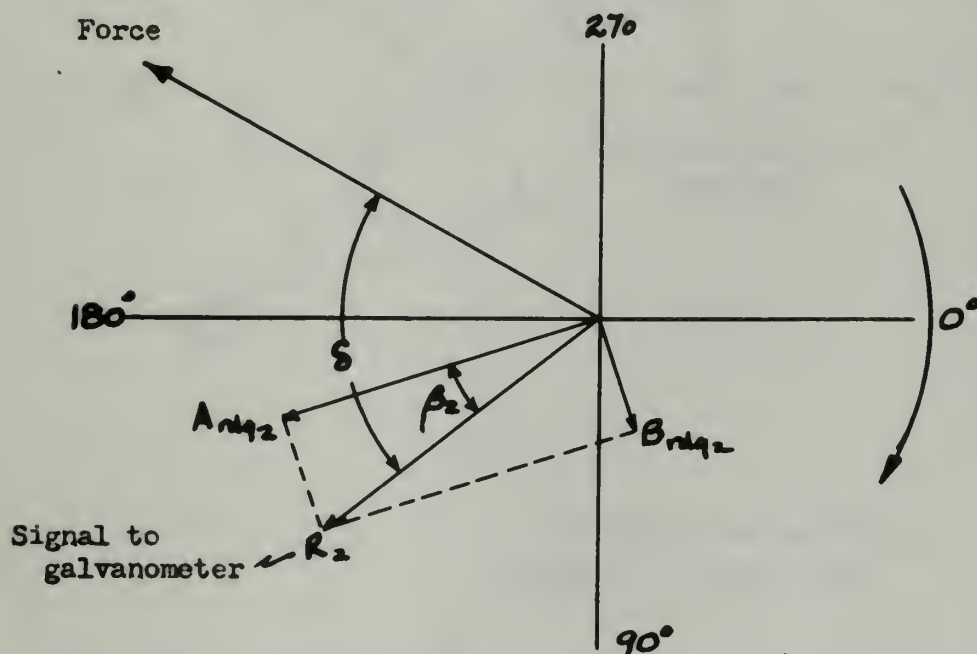
<u>A reading</u>	<u>B reading</u>	<u>Angle</u>
+	+	0 - 90°
-	+	90 - 180°
-	-	180 - 270°
+	-	270 - 360°

From Fig. XXXI, the following relationships can be determined:

Figure XXX



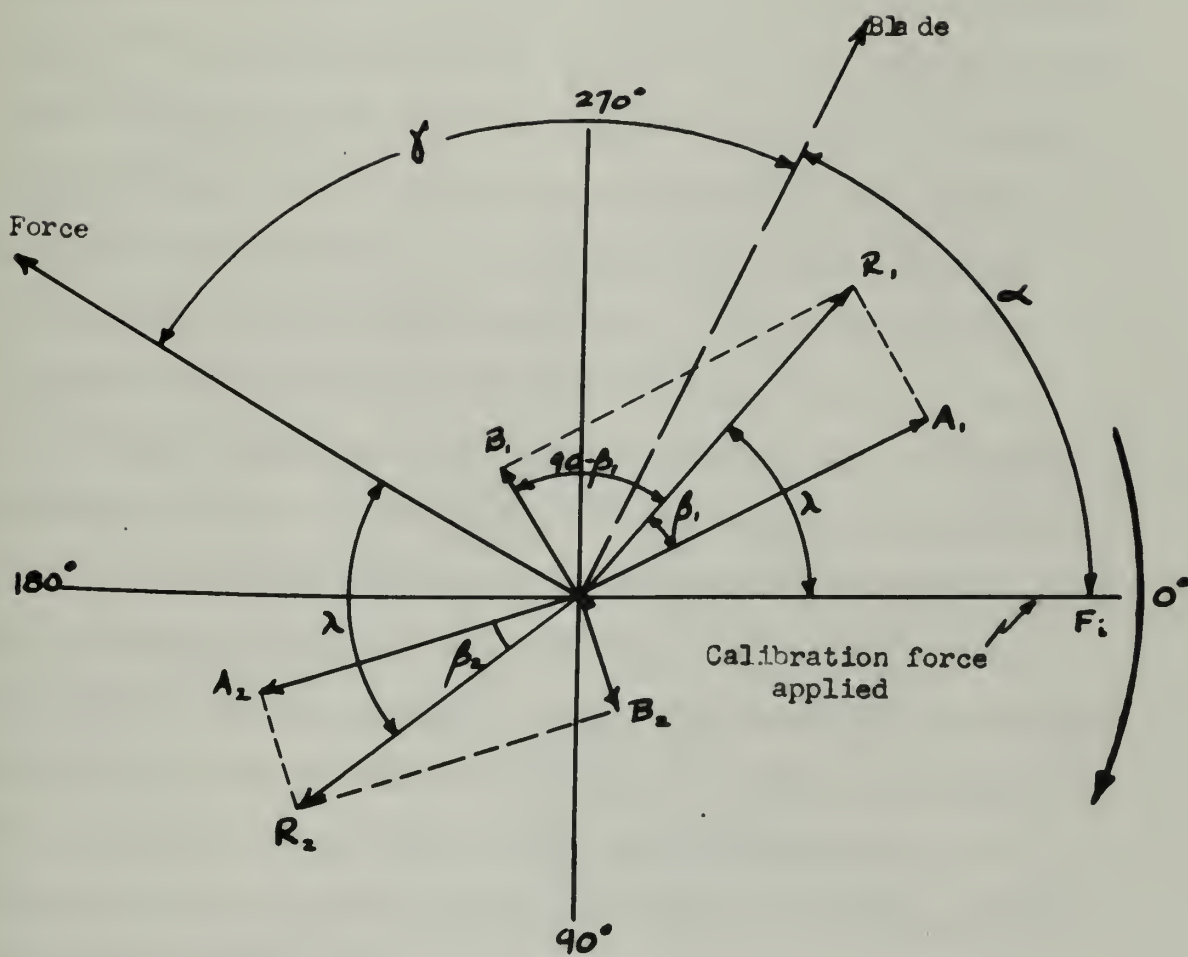
PHASE DIAGRAM FOR CALIBRATION RUNS



PHASE DIAGRAM FOR MEASUREMENT RUNS

(with negative readings)

Figure XXXI



Derived from combining
diagrams of Figure XXX

$$\gamma = 180 + \beta_2 - (\beta_1 + d)$$

or with the sign convention

$$\gamma = \beta_2 - (\beta_1 + d).$$

Since the above relationship has been referred to the indicator card which rotates at four times propeller speed, γ has to be divided by four to determine the relationship between force, propeller blade position and bossing. The angle is determined when the generating line of the propeller blade is in line with the trailing edge of the bossing. Therefore, on the phase diagram the bossing corresponds to the blade position. The force can be thought of as a rotating force vector rotating at four times shaft speed or at calibrator speed. The horizontal component of the force vector is the force applied to the bossing. For the case illustrated the measured force lags the propeller blade position by γ° . Since the force measured is in the negative sense, the positive force will lead the propeller blade by $\frac{180 - \gamma^\circ}{4}$. When referred to the propeller blade and bossing this means that the positive force occurs before the propeller blade reaches the position where the generating line and the trailing edge of the bossing coincide.

The method of measurement employed assumed the phase angle λ to be constant. δ , the angle between phase A of the sine wave generator and the high point

$$\gamma = 180 + \delta_2 - (\delta_1 + \delta)$$

or with the sign convention

$$\gamma = \delta_2 - (\delta_1 + \delta).$$

Since the above relationship has been referred to the indicator card which rotates at four times propeller speed, γ has to be divided by four to determine the relationship between force, propeller blade position and heading. The angle is determined when the generating line of the propeller blade is in line with the trailing edge of the heading. Therefore, on the phase diagram the heading corresponds to the blade position. The force can be thought of as a rotating force vector rotating at four times shaft speed or at calibrator speed. The horizontal component of the force vector is the force applied to the heading. For the case illustrated the measured force lags the propeller blade position by γ° . Since the force measured is in the negative sense, the positive force will lead the propeller blade by $\frac{180 - \gamma}{4}$. When referred to the propeller blade and heading this means that the positive force occurs before the propeller blade reaches the position where the generating line and the trailing edge of the heading coincide.

The method of measurement employed assumed the phase angle λ to be constant. δ , the angle between phase A of the sine wave generator and the high point

of the cam was also constant since the sine wave generator and cam shaft were geared together. Consequently, β_1 was theoretically a constant as long as the sine wave generator and cam shaft were not displaced angularly by uncoupling. The calibrator being a packaged unit permitted movement from the propeller tunnel hatch where it was used for calibration, to a new location during the measurement runs. For propeller shaft speeds of 548 RPM which corresponds to 36.5 cps, it was found that the angle λ was a function of the amplifier gain. As a result the angle β_1 had to be as a function of gain setting. The galvanometer reads $EI \cos \beta$, or $EI \cos (\beta + \pi/2)$ dependent upon which sine wave generator output is used in conjunction with the amplified signal from the detector. A switch permitted rapid switching of the sine wave generator input to the galvanometer from phase A to phase B. The A reading corresponds to the galvanometer reading with phase A of the sine wave generator as an input to the galvanometer; a measure of $EI \cos (\beta_1)$. The B reading corresponds to the galvanometer reading with phase B as the input; a measure of $EI \sin \beta_1$. Therefore, the signal to the galvanometer or resultant reading is:

of the cam was also constant since the sine wave gen-
 erator and cam shaft were geared together. Consequently,
 ϕ_1 was theoretically a constant as long as the sine wave
 generator and cam shaft were not displaced angularly by
 uncoupling. The calibrator being a packaged unit con-
 tained movement from the propeller tunnel hatch where it
 was used for calibration, to a new location during the
 measurement runs. For propeller shaft speeds of 348 RPM
 which corresponds to 36.5 cps, it was found that the
 angle λ was a function of the amplifier gain. As a
 result the angle ϕ_1 had to be as a function of gain.
 setting. The galvanometer reads $E_1 \cos \phi_1$ or $E_1 \sin \phi_1$
 $E_1 \cos (\lambda + \pi/2)$ dependent upon which sine wave gen-
 erator output is used in conjunction with the amplified
 signal from the detector. A switch permitted reading
 switching of the sine wave generator input to the gal-
 vanometer from phase A to phase B. The A reading corre-
 sponds to the galvanometer reading with phase A of the sine
 wave generator as an input to the galvanometer; a measure
 of $E_1 \cos (\phi_1)$. The B reading corresponds to the gal-
 vanometer reading with phase B as the input; a measure
 of $E_1 \sin \phi_1$. Therefore, the signal to the galvanometer
 or resultant reading is

$$\begin{aligned}
 \text{Resultant rdg} &= \sqrt{(A_{\text{rdg}})^2 + (B_{\text{rdg}})^2} \\
 &= \sqrt{(EI)^2 \cos^2 \beta_1 + (EI)^2 \sin^2 \beta_1} \\
 &= \sqrt{(EI)^2 (\sin^2 \beta_1 + \cos^2 \beta_1)} = EI
 \end{aligned}$$

$$\tan \beta_1 = \frac{B_{\text{rdg}}}{A_{\text{rdg}}} \quad \text{or} \quad \beta_1 = \tan^{-1} \frac{B_{\text{rdg}}}{A_{\text{rdg}}}$$

The resultant readings and β_1 were easily determined for each calibration run. In a similar manner for each measurement run, a resultant reading could be computed together with β_2 .

The phase angle, α , as previously defined was determined by means of the indicator card and two strobe lights. The generating line of an arbitrarily selected propeller blade was marked on the blade at the tip. The propeller was then placed on the propeller shaft in the test section of the tunnel and the propeller and shaft marked so that the propeller was always returned to the same angular location on the shaft after each removal. The marked propeller blade was then aligned with the trailing edge of the bossing and the propeller shaft marked so that the mark coincided with the cross hairs of a small telescope mounted outside the test chamber window. See Fig. XVII. By means of the phaser for

$$\text{Resistant } r_{0g} = \sqrt{(A_{r0g})^2 + (B_{r0g})^2}$$

$$\sqrt{(H_1)^2 \cos^2 \theta_1 + (H_1)^2 \sin^2 \theta_1}$$

$$\sqrt{(H_1)^2 (\cos^2 \theta_1 + \sin^2 \theta_1)} = H_1$$

$$\tan \theta_1 = \frac{B_{r0g}}{A_{r0g}} \quad \text{or } \theta_1 = \tan^{-1} \frac{B_{r0g}}{A_{r0g}}$$

The resistant readings and θ_1 were easily determined for each calibration run. In a similar manner for each measurement run, a resistant reading could be computed together with θ_1 .

The phase angle, ϕ , as previously defined was determined by means of the indicator card and two etched lights. The generating line of an arbitrarily selected propeller blade was marked on the blade at the tip. The propeller was then placed on the propeller shaft in the test section of the tunnel and the propeller and shaft marked so that the propeller was always returned to the same angular location on the shaft after each removal. The marked propeller blade was then aligned with the trailing edge of the housing and the propeller shaft marked so that the mark coincided with the cross hairs of a small telescope mounted outside the test chamber window. See Fig. XVII. By means of the phase for

timing of the strobe-lights, the strobe lights could be phased so that they "stopped" the propeller shaft when the scribe mark lined up with the cross hairs in the telescope (blade in line with bossing). A second strobe light, fired simultaneously with the first, was used to read the indicator card. The phase angle, α , was read directly from the card since 0° corresponded to the high point of the cam. Using the relationship $4\gamma = \beta_2 - (\beta_1 + \alpha)$ and the sign convention for determination of the quadrant β_1 and β_2 , the phase angle between force and blade position was determined.

timing of the stroke-light, the stroke light could
 be phased so that they "retarded" the parallel shift
 when the scribe mark lined up with the cross hairs in
 the telescope (blade in line with housing). A second
 stroke light, fired simultaneously with the first, was
 used to read the indicator card. The phase angle, ϕ ,
 was read directly from the card since 0° corresponded
 to the high point of the cam. Using the relationship

$$y = A_1 \sin(\omega t + \phi_1) + A_2 \sin(\omega t + \phi_2)$$
 and the sign convention for deter-
 mination of the constant ϕ , and ϕ_2 , the phase angle
 between force and blade position was determined.

APPENDIX B

SAMPLE CALCULATIONS

As discussed in Section III, analysis of the major portion of the data recorded involved three basic divisions: (1) calibration, (2) measurement, and (3) phase angle determination. To illustrate the calculations sequence, each step will be taken individually, using arbitrary data:

A. Calibration:

Data recorded:

Spring No.	R
Initial Tension:	4 lbs., 11 oz.
Weight:	3 lbs., 100 gms.
RPM:	548
Gain Setting:	6
Resistance:	1000 ohms
A reading	-1.39
B reading	-1.48

To obtain the force applied to the bossing by the wire-spring combination, the weight added to the weight pan is converted by a ratio of lever arms and the cosine of the angle of attachment of the weight pan string to the lever arm:

APPENDIX B

SAMPLE CALCULATION

As discussed in Section III, analysis of the major portion of the data recorded involved three basic divisions: (1) calibration, (2) measurement, and (3) phase angle determination. To illustrate the calculations necessary, each area will be taken individually, using arbitrary data:

A. Calibration:

Data recorded:

Spring No.	11
Initial Tension:	4 lbs., 11 oz.
Weight:	3 lbs., 100 gms.
RPM:	348
Gain Setting:	6
Resistance:	1000 ohms
Reading	-1.32
Reading	-1.48

To obtain the force applied to the bearing by the wire-spring combination, the weight added to the weight pan is converted by a ratio of lever arms and the cosine of the angle of attachment of the weight pan string to the lever arm:

$$\begin{aligned}
 \text{Force per one-half revolution} &= \frac{3 \text{ lbs.} \cdot 100 \text{ gms.}}{2} \cos 83^\circ 23' \\
 \text{of the cam} &= \frac{3.2205}{2} \times 0.99 \\
 &= 1.596 \text{ lbs.}
 \end{aligned}$$

This value represents the total change in force on the bossing while the cam travels through twice the amplitude. The excitation force, then, is just half of this value:

$$\text{Force} = 0.798 \text{ lbs.}$$

Since the galvanometer deflection readings recorded represent two perpendicular vectors, the resultant deflection:

$$\begin{aligned}
 R_{\text{rdg}}^2 &= A_{\text{rdg}}^2 + B_{\text{rdg}}^2 \\
 &= (1.39)^2 + (1.48)^2
 \end{aligned}$$

$$R_{\text{rdg}} = 2.02$$

With these two calculated values, a point on the calibration curve is determined for this set of data.

For use in the phase determination, β_1 , must be determined. By definition:

$$\begin{aligned}
 \beta_1 &= \tan^{-1} \frac{B_{\text{rdg}}}{A_{\text{rdg}}} \\
 &= \tan^{-1} \frac{-1.48}{-1.39} = 46.8^\circ + 180^\circ \\
 &= 226.8^\circ
 \end{aligned}$$

Force per one-half revolution of the cam

$$= \frac{1.16 \times 100 \text{ gms.} \times 3.14}{2} = 18.3 \text{ lbs.}$$

$$= \frac{1.16 \times 100}{2} = 58.0$$

$$= 1.296 \text{ lbs.}$$

This value represents the total change in force on the bearing while the cam travels through twice the amplitude. The reaction force, then, is just half of this value:

$$\text{Force} = 0.648 \text{ lbs.}$$

Since the displacement of the bearing is recorded, the resultant of the two perpendicular vectors, the resultant of

displacement:

$$\vec{R} = \vec{A} + \vec{B}$$

$$R = \sqrt{(1.16)^2 + (1.16)^2} = 1.63$$

With these two calculated values, a point on the cell-

displacement curve is determined for this set of data.

For use in the phase determination, the value of

determined by definition:

$$\phi = \tan^{-1} \frac{B}{A}$$

$$\phi = \tan^{-1} \frac{1.16}{1.16} = 45.8^\circ + 180^\circ$$

$$= 225.8^\circ$$

As discussed in Section III, the angle is determined to be between 180° and 270° by the sign convention adopted.

B. Measurement Run

Data Recorded:

Thrust, uncorr. :	26.4 lbs.
Thrust correction:	+0.7 lbs.
Press. column, H_1 :	184 mm.
RPM:	548
Gain Setting:	6
Resistance:	5000 ohms
A reading:	-0.72
B reading:	+1.92
α	327
Temperature:	80°F.

From this data we must determine the values of thrust, J , (advance coefficient) force on the bossing, and β_2 .

$$\text{Thrust, corrected} = 26.4 + 0.7 = 27.1 \text{ lbs.}$$

From propeller tunnel calibration data, the water velocity in the test section, in feet per second,

$$v = 0.41656 \sqrt{H_1 \times C_{\text{temp.}}}$$

where H_1 is the measured height of the bromo-benzene column, in mm.

and $C_{\text{temp.}}$ is a correction to the column reading to account for changes in atmospheric temperature. For 80°F., the value of $C_{\text{temp.}}$ is 0.985.

Thus,

$$\begin{aligned} v &= 0.41656 \sqrt{184 \times 0.985} \\ &= 5.60 \text{ fps.} \end{aligned}$$

as discussed in Section III, the angle is determined to be between 180° and 270° by the sign convention adopted.

5. Measurement Run

Data Recorded:

Thrust, uncorr.:	26.1 lbs.
Thrust correction:	+0.7 lbs.
Press. column, H_1 :	1.4 mm.
Gain setting:	548
Resistance:	6
Resistance:	8000 ohms
A reading:	-0.72
B reading:	+1.92
Temperature:	32.7
Temperature:	80°F.

From this data we must determine the values of thrust, T ,

(advance coefficient) force on the housing, and β .

Thrust, corrected = 26.1 + 0.7 = 27.1 lbs.

From propeller tunnel calibration data, the water

velocity in the test section, in feet per second,

$$v = 0.4165 \sqrt{H_1 \times C_{\text{corr.}}}$$

where H_1 is the measured height of the pressure

position column, in mm.

and $C_{\text{corr.}}$ is a correction to the column read-

ing to account for changes in

atmospheric temperature. For 80°F.,

the value of $C_{\text{corr.}}$ is 0.985.

$$v = 0.4165 \sqrt{1.4 \times 0.985}$$

Thus,

$$v = 5.60 \text{ ft.}$$

By definition,

$$J = v/nd$$

where n = rev. per sec.

d = diameter in feet.

v = water velocity in ft/sec.

$$J = 4.60 \times \frac{60}{548} \times \frac{12}{11.82} = 0.622$$

For the determination of the force, the resultant reading is first determined as before,

$$R_{rdg}^2 = (-0.72)^2 + (1.92)^2$$

$$R_{rdg} = 2.06$$

In the simplest case, the calibration curve for this arrangement of parameters is now entered with this resultant deflection, and the corresponding force read directly. This force, then, together with the corresponding thrust, is plotted.

As for the calibration data, by definition,

$$\begin{aligned}\beta_2 &= \tan^{-1} \frac{B_{rdg}}{A_{rdg}} \\ &= \tan^{-1} \frac{1.92}{-0.72} = 69.5^\circ\end{aligned}$$

In this particular instance, the sign convention determines that β_2 has a value between 90° and 180° . Thus,

$$\beta_2 = 180 - 69.5 = 110.5^\circ$$

by definition,
 $J = v \sqrt{\rho d}$

where $n = 100$ per cent,
 $d =$ diameter in feet,
 $v =$ water velocity in ft/sec.

$$J = 0.0044 \times \frac{11}{11.33} \times 0.612 = 0.00412$$

For the determination of the force, the resultant
 velocity is first determined as before,

$$R_{100} = (-0.71)^2 + (1.92)^2$$

$$R_{100} = 1.96$$

In the above case, the calibration curve for this
 arrangement of parameters is now entered with this re-
 sultant velocity, and the corresponding force read
 directly. This force, then, together with the corre-
 sponding thrust, is plotted.

As for the calibration data, by definition,

$$\frac{R}{A} = \tan^{-1} \frac{V_{100}}{V_{100}}$$

$$\frac{R}{A} = \tan^{-1} \frac{1.96}{0.71} = 69.4^\circ$$

In this particular instance, the sign convention determines
 that R has a value between 90° and 180° . Thus,
 $R = 180 - 69.4 = 110.6^\circ$

As previously discussed, the calibration data directly represents only forces between 0 and 1.1 lbs. For some combinations of nose pieces and clearances, the actual measured force exceeds this range. In such cases two methods of extrapolation were employed. The first, and simplest, was employed exclusively in reducing the data taken with the long nose piece. It consists of merely determining the slope of the calibration curve for the data taken, and thus obtaining a constant relationship between resultant deflection readings and force applied. This method involves the assumption of linear response of the bossing system to the applied forces over the full range of forces experienced. In general, the relationship is

$$\text{Force} = K + S \times R_{\text{rdg}}$$

where K = the base intercept
of the calibration
curve, and

S = slope of the cali-
bration curve.

The second method, based precisely on the data taken, was employed in the analysis of a part of the short bossing data. Use is made of variable amplifier gain. A detailed description of this method may be found in the section on Detailed Procedure. See Section V for a discussion of the two methods.

As previously discussed, the calibration data directly represents only forces between 0 and 1.1 lbs. For some combinations of nose pieces and clearances, the actual measured force exceeds this range. In such cases two methods of extrapolation were employed. The first, and simplest, was employed exclusively in reducing the data taken with the 1/8 inch nose piece. It consisted of merely determining the slope of the calibration curve for the data taken, and then obtaining a constant relationship between resultant deflection readings and force applied. This pattern involves the assumption of linear response of the bearing system to the applied forces over the full range of forces experienced. In general, the relationship is

$$\text{Force} = K + S \times R$$

where K = the nose intercept of the calibration curve, and

S = slope of the calibration curve.

The second method, based precisely on the data taken, was employed in the analysis of a part of the short bearing data. Use is made of variable modified gain. A detailed description of this method may be found in the section on Fitted Procedure. See Section V for a discussion of the two methods.

C. Phase Determination.

The method of phase determination is discussed in detail in Appendix A. For the example given above,

$$\beta_1 = 226.8^\circ$$

$$\beta_2 = 110.5^\circ$$

$$\alpha = 327^\circ$$

$$360 - \alpha = 33^\circ$$

In accordance with the development in Appendix A,

$$4\gamma = \beta_2 - (\beta_1 + \alpha)$$

$$= 110.5 - (226.8 + 33) = -149.3^\circ$$

$$\gamma = 37.3^\circ$$

where γ is defined as the phase angle between the time the generating line of an arbitrarily selected propeller blade coincides with the trailing edge of the bossing and the occurrence of the measured hydrodynamically induced force normal to the bossing.

C. Phase Determination.

The method of phase determination is discussed in detail in Appendix A. For the example given above, $\phi_1 = 25.6^\circ$, $\phi_2 = 110.5^\circ$, $\phi_3 = 227^\circ$, $\phi_4 = 300^\circ = 36^\circ$.

In accordance with the development in Appendix A, $\Delta y = \frac{1}{2} (y_1 + y_2)$, $y = 110.5^\circ - (25.6^\circ + 36^\circ) = -149.3^\circ$, $y = 37.3^\circ$.

where y is defined as the phase angle between the time the generating line of an arbitrarily selected parallel blade coincides with the trailing edge of the passing and the occurrence of the associated hydrodynamically induced force normal to the passing.

The phase angle ϕ is defined as the angle between the time the generating line of an arbitrarily selected parallel blade coincides with the trailing edge of the passing and the occurrence of the associated hydrodynamically induced force normal to the passing.

APPENDIX C

Original Data and Calculations

THE UNIVERSITY OF CHICAGO

THE DEPARTMENT OF CHEMISTRY

REPORT OF THE

COMMISSIONERS OF THE

BOARD OF CHURCHES

APPENDIX C

THE CHURCHES OF THE

Original List and Collection

THE CHURCHES OF THE

THE CHURCHES OF THE

THE CHURCHES OF THE

THE CHURCHES OF THE

THE CHURCHES OF THE

THE CHURCHES OF THE

THE CHURCHES OF THE

TABLE I

Calibration Run No. I

Nose Piece: Short
Resistance: 1000 ohms

RPM = 548

Amplifier Gain Setting: Variable

Spring Letter Design- ation	I.F.		W		F	G.S. Amplifier		A rdg	B rdg	R rdg
	lbs + oz	lbs + oz	lbs + oz	lbs		Gain Setting	(+)			
N	2 - 11	4 + 200	1.10			6	0.55	1.00	1.14	
						7	0.65	1.20	1.37	
						8	0.82	1.67	1.86	
						9	1.05	2.18	2.42	
						10	1.25	2.61	2.89	
						11	1.60	3.48	3.83	
K	4 - 11	2.5 + 40	0.639			6	0.38	0.62	0.73	
						7	0.41	0.75	0.86	
						8	0.52	0.95	1.07	
						9	0.61	1.20	1.35	
						10	0.71	1.47	1.63	
						11	0.89	1.80	2.10	
P	3 - 11	4.0 + 125	1.06			6	0.50	0.92	1.05	
						7	0.55	1.05	1.19	
						8	0.70	1.55	1.70	
						9	0.92	2.25	2.43	
						10	1.12	2.48	2.72	
						11	1.38	3.35	3.62	

(continued)

Classification No. 1

From: 2701
residence: 1000 cps

[illegible]

(General)

TABLE I
(continued)

Calibration Run No. 1

Nose Piece: Short Resistance: 1000 ohms		Clearance 1"		RPM = 548 Amplifier Gain Setting:		Variable	
Spring Letter Design- ation	I.F. lbs + oz	W lbs + qms	F lbs	G.S. Amplifier Gain Setting	A rdg (+)	B rdg (+)	R rdg
M	4 - 11	2 + 80	0.50	6	0.28	0.50	0.57
				7	0.30	0.58	0.65
				8	0.36	0.78	0.86
				9	0.45	0.97	1.07
				10	0.54	1.19	1.31
V	4 - 11	3 + 140	0.82	11	0.65	1.55	1.68
				6	0.40	0.69	0.80
				7	0.47	0.80	0.93
				8	0.62	1.15	1.31
				9	0.76	1.46	1.64
H	1.5 - 11	2.5 + 30	0.64	10	0.90	1.79	2.00
				11	1.15	2.40	2.66
				6	0.41	0.65	0.77
				7	0.45	0.75	0.87
				8	0.60	1.02	1.19
				9	0.70	1.29	1.47
				10	0.80	1.57	1.76
				11	1.05	2.05	2.30

I. ON POLYMERIS

old my : pld m d = all com

[illegible]

- 111 -

TABLE II

Calibration Run No. 2

Nose Piece: Short
Resistance: 1000 ohms

Clearance 1"

RPM: 548

Amplifier Gain Setting: 10

Spring	I.F.	W	F	A rdg	B rdg	R rdg	* β_1
Letter Design- ation	lbs + oz	lbs. + gms.	lbs.	(+)	(+)		deg.
I	1 - 11	0.5 + 110	0.19	0.39	0.59	0.71	50.4
L	3 - 11	1.5 + 160	0.46	0.62	1.15	1.30	57.5
R	3 - 11	3.0 + 170	0.84	1.05	2.00	2.26	57.1
N	2 - 11	4.0 + 200	1.10	1.25	2.61	2.89	61.2
K	4 - 11	2.5 + 40	0.64	0.71	1.47	1.63	58.6
P	3 - 11	4.0 + 125	1.06	1.12	2.48	2.72	61.6
M	4 - 11	2.0 + 80	0.50	0.54	1.19	1.31	61.9
C	1.5 - 11	1.0 + 20	0.26	0.26	0.59	0.65	58.4
V	4 - 11	3.0 + 140	0.82	0.90	1.79	2.00	60.0
H	1.5 - 11	2.5 + 30	0.64	0.80	1.57	1.76	57.8

Average $\beta_1 = 59.1^\circ$ * Note: β_1 is for an Amplifier Gain
Setting of 6.

II TABLE

Continued from No. 1

HAZ : WIND
VELOCITY : 10

Clearance 1

From :
To :
Note : 1000 ft

HAZ	WIND	VELOCITY	Clearance 1	From	To	Note
HAZ	WIND	VELOCITY	Clearance 1	From	To	Note
1.00	10.0	10.0	10.0	10.0	10.0	10.0
2.00	20.0	20.0	20.0	20.0	20.0	20.0
3.00	30.0	30.0	30.0	30.0	30.0	30.0
4.00	40.0	40.0	40.0	40.0	40.0	40.0
5.00	50.0	50.0	50.0	50.0	50.0	50.0
6.00	60.0	60.0	60.0	60.0	60.0	60.0
7.00	70.0	70.0	70.0	70.0	70.0	70.0
8.00	80.0	80.0	80.0	80.0	80.0	80.0
9.00	90.0	90.0	90.0	90.0	90.0	90.0
10.00	100.0	100.0	100.0	100.0	100.0	100.0

HAZ : WIND
VELOCITY : 10

TABLE III

Measurement Run No. 1

Water Temperature: 77°F.
Nose Piece : Short
Thrust Correction: -2.0 lbs.

Clearance 1"

RPM : 548
Amplifier Gain Setting: 6
Resistance : 1000 ohms

T _{rdg} lbs.	T _{corr} lbs.	H ₁ rdg	v fns	J v/nd	A _{rdg}	B _{rdg}	R _{rdg}	F (10) lbs.	F lbs.	β ₂ deg	β ₁ deg	α _{rdg} deg	α ₁ deg	4γ deg	γ deg
64.0	62.0	0	0	0	+0.90	-3.40	3.52	1.350	3.65	255.2	255.2	288	72	124.1	31
63.0	61.0	13	1.46	0.162	-0.70	-3.25	3.32	1.272	3.44	257.8	257.8	290	70	128.7	32.1
56.8	54.8	42	2.68	0.297	-0.65	-2.85	2.93	1.125	3.04	257.7	257.7	288	72	128.6	31.7
51.6	49.6	79	3.68	0.408	-0.50	-2.45	2.50	0.958	2.60	258.5	258.5	288	72	127.4	31.9
45.7	43.7	117	4.47	0.495	-0.35	-2.15	2.18	0.833	2.26	260.6	260.6	287	73	128.5	32.1
39.3	37.3	165	5.32	0.591	-0.25	-1.90	1.92	0.733	1.99	362.5	362.5	284	76	127.4	31.9
33.3	31.3	220	6.13	0.682	-0.15	-1.60	1.62	0.617	1.67	264.7	264.7	287	73	132.6	33.1
26.5	24.5	279	6.90	0.767	-0.05	-1.50	1.51	0.575	1.56	268.0	268.0	285	75	135.9	33.4
23.1	21.1	314	7.33	0.814	+0.02	-1.35	1.35	0.515	1.40	270.8	270.8	285	75	136.7	34.1
17.9	15.9	377	8.03	0.892	+0.10	-1.25	1.26	0.480	1.30	274.5	274.5	287	73	142.4	35.6
13.1	11.1	433	8.60	0.954	+0.20	-1.20	1.22	0.465	1.26	279.5	279.5	290	70	150.4	37.6
8.9	6.9	491	9.16	1.018	+0.20	-1.15	1.17	0.443	1.20	280.0	280.0	288	72	148.9	37.2

1. PM cell from 11/11/40

[illegible]

• 777 : 901800 JI 10120
Jeds : 0210 0100
- 9010.5 - : 00100000 10000

- 112 -

TABLE IV

Calibration Run No. 3

Nose Piece: Short
Resistance: 1000 ohmsRPM: 548
Amplifier Gain Setting: 10

Clearance 1-1/2"

Spring	I.F.	W	F	A rdg	B rdg	R rdg	B ₁
Letter Design- ation	lbs. + oz.	lbs. + qms	lbs.	(+)	(+)		deg.
P	4 - 11	3.5 + 200	0.88	1.85	3.55	4.00	62.5
				1.90	3.58	4.05	62.0
N	4 - 11	4 + 22	1.05	1.85	3.45	3.81	61.8
				1.85	3.55	4.00	62.5
V	4 - 11	3 + 40	0.77	1.35	2.52	2.96	61.8
				1.28	2.48	2.79	62.6
R	4 - 11	3 + 170	0.84	1.35	2.78	3.09	64.2
				1.35	2.70	3.02	63.5
L	4 - 11	2 + 0	0.50	0.72	1.55	1.71	65.0
				0.71	1.53	1.69	65.0
Q	4 - 11	2.5 + 50	0.66	1.04	2.04	2.39	63.0
				1.05	2.09	2.34	63.3
W	4 - 11	2.0 + 50	0.53	0.92	1.79	2.01	62.8
				0.93	1.78	1.99	62.5
X	4 - 11	1.5 + 190	0.48	0.82	1.60	1.80	62.8
				0.85	1.60	1.81	62.0
M	4 - 11	2.0 + 20	0.51	0.69	1.60	1.74	66.7
				0.75	1.60	1.77	65.0
C	3 - 11	1.0 + 20	0.26	0.39	0.80	0.89	64.0
				0.40	0.82	0.91	64.0
I	3 - 11	1.0 + 30	0.27	0.40	0.81	0.90	63.7
				0.42	0.82	0.92	63.0

Average B₁ = 63.3°

016917066 J-T/211

1000 gms 1000 gms

id	phr A	phr B	phr A	3	M	T.I	phr B
2.22	00.4	22.3	22.1	87.0	003 + 2.3	11 - A	Q
0.22	20.4	22.3	00.1				
8.10	18.3	22.3	28.1	20.1	53 + A	11 - A	M
2.22	00.4	22.3	20.1				
8.10	20.3	22.3	27.1	27.0	04 + E	11 - A	V
0.22	00.4	22.3	25.1				
2.22	20.3	22.3	22.1	48.0	04 + E	11 - A	M
0.22	17.1	22.1	17.0	02.0	0 + S	11 - A	J
0.22	00.1	22.1	40.1	20.0	02 + E.5	11 - A	D
2.22	10.3	27.1	29.1	22.0	02 + 0.5	11 - A	N
0.22	00.1	27.1	25.0	26.0	001 + 2.1	11 - A	X
0.22	18.1	27.1	22.0	12.0	02 + 0.5	11 - A	M
0.22	00.1	27.1	27.0	24.0	02 + 0.1	11 - E	D
0.22	00.0	27.0	24.0	75.0	02 + 0.1	11 - E	I

TABLE V

Measurement Run No. 2

Water Temperature: 76°F.
 Nose Piece : Short
 Thrust Correction: -2.0 lbs.

RPM : 548
 Amplifier Gain Setting: 10
 Resistance : 1000 ohms

Clearance 1-1/2"

T _{tdg} lbs.	T _{corr} lbs.	H ₁ in	v fps	J v/nd	A _{rdg}	B _{rdg}	R _{rdg}	F lbs	β ₂ deg	β ₁ deg	α _{rdg} deg	360-α ₁ deg	4γ deg	-γ deg
51.0	49.0	23	1.99	0.221	-1.85	-4.30	4.68	1.31	247.3		303	57	127.0	31.8
46.1	44.1	41	2.63	0.295	-1.95	-4.30	4.74	1.33	245.6		301	59	123.3	30.8
42.5	40.5	59	3.18	0.354	-1.85	-4.25	4.63	1.30	246.6		302	58	125.3	31.3
41.0	39.0	70	3.48	0.384	-1.80	-4.05	4.43	1.18	246.0		300	60	122.7	30.6
38.0	36.0	90	3.92	0.436	-1.70	-3.85	4.20	1.12	246.2		300	60	122.9	30.7
31.3	29.3	127	4.66	0.518	-1.50	-3.65	3.94	1.06	247.8		295	65	119.5	29.9
27.3	25.3	154	5.13	0.570	-1.32	-3.40	3.64	0.985	248.8		298	62	123.5	30.9
25.4	23.2	173	5.45	0.605	-1.19	-3.28	3.49	0.945	250.2		295	65	121.9	30.4
23.6	21.6	189	5.68	0.632	-1.15	-3.22	3.42	0.930	250.3		295	65	122.0	30.5
20.4	18.4	217	6.10	0.678	-1.02	-3.07	3.24	0.885	251.6		295	65	123.3	30.8
18.0	16.0	239	6.40	0.711	-0.98	-2.95	3.11	0.850	251.7		295	65	123.4	30.8
16.6	14.6	254	6.63	0.737	-0.98	-2.95	3.11	0.850	251.7		295	65	123.4	30.8
15.0	13.0	274	6.85	0.761	-0.89	-2.85	2.99	0.820	252.7		295	65	124.4	31.1
13.6	11.6	290	7.06	0.784	-0.80	-2.75	2.86	0.790	253.7		295	65	125.4	31.4
11.0	9.0	313	7.33	0.815	-0.75	-2.75	2.86	0.790	254.8		295	65	126.5	31.6
9.3	7.3	340	7.62	0.848	-0.62	-2.60	2.67	0.740	256.5		295	65	128.2	32.1
6.5	4.5	365	7.90	0.879	-0.55	-2.55	2.62	0.730	257.8		295	65	129.5	32.4
4.2	2.2	387	8.14	0.903	-0.40	-2.50	2.53	0.705	260.9		295	65	132.6	33.1

TABLE VI

Measurement Run No. 3

Water Temperature: 76°F.
 Nose Piece: Short
 Thrust Correction: -2.0 lbs.

Clearance 1-3/4"

RPM : 548
 Amplifier Gain Setting: 10
 Resistance : 1000 ohms

T lbs.	I lbs.	corr lbs.	H rdg.	v fps	J v/nd	A rdg	B rdg	R rdg	F lbs.	β_2 deg.	β_1 deg.	a rdg	360-a deg.	-Y deg.
55.1	53.1	1	0.414	0.046	-1.30	-4.10	4.30	1.097	252.4	304	56	132.1	33.0	
53.1	51.1	14	1.55	0.172	-1.65	-3.95	4.29	1.096	247.4	303	57	126.1	31.5	
48.3	46.3	32	2.34	0.260	-1.45	-3.85	4.11	1.051	259.4	302	58	137.1	34.3	
45.0	43.0	45	2.78	0.309	-1.45	-3.50	3.79	0.976	247.5	301	59	124.2	31.0	
43.8	41.8	53	3.01	0.334	-1.45	-3.45	3.75	0.968	247.2	301	59	123.9	30.9	
40.4	38.4	68	3.41	0.379	-1.32	-3.15	3.41	0.890	247.2	299	61	121.9	30.4	
37.0	35.0	93	4.00	0.445	-1.20	-3.05	3.28	0.860	248.6	299	61	123.3	30.8	
31.0	29.0	122	4.57	0.508	-1.12	-2.85	3.06	0.810	248.6	297	63	121.3	30.3	
8.79														
26.4	24.4	165	5.32	0.591	-0.99	-2.68	2.89	0.770	248.8	297	63	121.5	30.4	
22.0	20.0	205	5.93	0.659	-0.85	-2.50	2.62	0.710	251.3	296	64	123.0	30.7	
19.7	17.7	233	6.32	0.702	-0.75	-2.40	2.51	0.680	252.7	296	64	124.4	31.1	
16.4	14.4	264	6.73	0.747	-0.65	-2.25	2.35	0.640	253.9	296	64	125.6	31.4	
13.0	11.0	293	7.09	0.788	-0.55	-2.17	2.24	0.610	255.7	296	64	127.4	31.8	
9.1	7.1	341	7.65	0.850	-0.35	-2.05	2.08	0.572	260.3	296	64	132.0	33.0	
5.9	3.9	380	8.06	0.896	-0.20	-1.95	1.97	0.545	264.1	296	64	135.8	33.9	
2.4	0.4	422	8.50	0.944	-0.15	-1.85	1.86	0.520	265.4	296	64	137.1	34.3	

TABLE VII

Calibration Run No. A

Nose Piece: Short

Resistance: 1000 ohms

RPM
Amplifier Gain Setting: 10
: Variable

Spring Letter Design.	I.F. lbs. + oz.	W lbs. + gms	F lbs.	A Idg (+)	B Idg (+)	R Idg	β 1 deg. *	RPM
M	4.5 + 11	2.0 + 0	0.495	0.31	0.50	0.588		396
				0.35	0.59	0.686		426
				0.40	0.72	0.825		462
				0.47	0.85	0.972		482
				0.52	1.09	1.21		510
				0.61	1.49	1.61		536
				0.70	1.75	1.89		549
				0.80	2.19	2.33		560
				1.10	3.32	3.50		580
				1.22	3.90	4.08		584
Q	4.5 + 11	2.5 + 70	0.660	0.35	0.59	0.685		379
				0.36	0.63	0.726		391
				0.40	0.70	0.805		408
				0.44	0.79	0.904		425
				0.49	0.86	0.989		445
				0.50	0.95	1.075		458
				0.58	1.08	1.225		479
				0.60	1.25	1.39		496
				0.68	1.36	1.52		506
				0.85	1.91	2.09		535
				1.17	2.48	2.74		552
				1.30	3.80	4.00		569
				1.42	4.40	4.63		576

(continued)

TABLE VII
(continued)

Calibration Run No. 4

Nose Piece: Short Resistance: 1000 ohms		Clearance 2"		RPM Amplifier Gain Setting: 10		: Variable	
Spring	I.F.	W	A	B	β ₁		RPM
Letter Design.	lbs. + oz.	lbs. + oms.	lbs.	Rdg	Rdg	deg. *	
V	4.5 + 11	3.0 + 60	0.778	0.45 0.49 0.51 0.51 0.66 0.75 0.85 1.15 1.31 1.41 1.78 1.90	0.72 0.78 0.84 0.90 1.15 1.30 1.55 2.10 2.45 2.75 3.66 4.85		382 396 408 416 458 474 491 522 536 546 560 570

* Note: β₁ not computed.

607-1700

75-057087-1

1990: 1990
 1991: 1991
 1992: 1992
 1993: 1993
 1994: 1994
 1995: 1995
 1996: 1996
 1997: 1997
 1998: 1998
 1999: 1999
 2000: 2000
 2001: 2001
 2002: 2002
 2003: 2003
 2004: 2004
 2005: 2005
 2006: 2006
 2007: 2007
 2008: 2008
 2009: 2009
 2010: 2010
 2011: 2011
 2012: 2012
 2013: 2013
 2014: 2014
 2015: 2015
 2016: 2016
 2017: 2017
 2018: 2018
 2019: 2019
 2020: 2020
 2021: 2021
 2022: 2022
 2023: 2023
 2024: 2024
 2025: 2025
 2026: 2026
 2027: 2027
 2028: 2028
 2029: 2029
 2030: 2030
 2031: 2031
 2032: 2032
 2033: 2033
 2034: 2034
 2035: 2035
 2036: 2036
 2037: 2037
 2038: 2038
 2039: 2039
 2040: 2040
 2041: 2041
 2042: 2042
 2043: 2043
 2044: 2044
 2045: 2045
 2046: 2046
 2047: 2047
 2048: 2048
 2049: 2049
 2050: 2050
 2051: 2051
 2052: 2052
 2053: 2053
 2054: 2054
 2055: 2055
 2056: 2056
 2057: 2057
 2058: 2058
 2059: 2059
 2060: 2060
 2061: 2061
 2062: 2062
 2063: 2063
 2064: 2064
 2065: 2065
 2066: 2066
 2067: 2067
 2068: 2068
 2069: 2069
 2070: 2070
 2071: 2071
 2072: 2072
 2073: 2073
 2074: 2074
 2075: 2075
 2076: 2076
 2077: 2077
 2078: 2078
 2079: 2079
 2080: 2080
 2081: 2081
 2082: 2082
 2083: 2083
 2084: 2084
 2085: 2085
 2086: 2086
 2087: 2087
 2088: 2088
 2089: 2089
 2090: 2090
 2091: 2091
 2092: 2092
 2093: 2093
 2094: 2094
 2095: 2095
 2096: 2096
 2097: 2097
 2098: 2098
 2099: 2099
 2100: 2100
 2101: 2101
 2102: 2102
 2103: 2103
 2104: 2104
 2105: 2105
 2106: 2106
 2107: 2107
 2108: 2108
 2109: 2109
 2110: 2110
 2111: 2111
 2112: 2112
 2113: 2113
 2114: 2114
 2115: 2115
 2116: 2116
 2117: 2117
 2118: 2118
 2119: 2119
 2120: 2120
 2121: 2121
 2122: 2122
 2123: 2123
 2124: 2124
 2125: 2125
 2126: 2126
 2127: 2127
 2128: 2128
 2129: 2129
 2130: 2130
 2131: 2131
 2132: 2132
 2133: 2133
 2134: 2134
 2135: 2135
 2136: 2136
 2137: 2137
 2138: 2138
 2139: 2139
 2140: 2140
 2141: 2141
 2142: 2142
 2143: 2143
 2144: 2144
 2145: 2145
 2146: 2146
 2147: 2147
 2148: 2148
 2149: 2149
 2150: 2150
 2151: 2151
 2152: 2152
 2153: 2153
 2154: 2154
 2155: 2155
 2156: 2156
 2157: 2157
 2158: 2158
 2159: 2159
 2160: 2160
 2161: 2161
 2162: 2162
 2163: 2163
 2164: 2164
 2165: 2165
 2166: 2166
 2167: 2167
 2168: 2168
 2169: 2169
 2170: 2170
 2171: 2171
 2172: 2172
 2173: 2173
 2174: 2174
 2175: 2175
 2176: 2176
 2177: 2177
 2178: 2178
 2179: 2179
 2180: 2180
 2181: 2181
 2182: 2182
 2183: 2183
 2184: 2184
 2185: 2185
 2186: 2186
 2187: 2187
 2188: 2188
 2189: 2189
 2190: 2190
 2191: 2191
 2192: 2192
 2193: 2193
 2194: 2194
 2195: 2195
 2196: 2196
 2197: 2197
 2198: 2198
 2199: 2199
 2200: 2200
 2201: 2201
 2202: 2202
 2203: 2203
 2204: 2204
 2205: 2205
 2206: 2206
 2207: 2207
 2208: 2208
 2209: 2209
 2210: 2210
 2211: 2211
 2212: 2212
 2213: 2213
 2214: 2214
 2215: 2215
 2216: 2216
 2217: 2217
 2218: 2218
 2219: 2219
 2220: 2220
 2221: 2221
 2222: 2222
 2223: 2223
 2224: 2224
 2225: 2225
 2226: 2226
 2227: 2227
 2228: 2228
 2229: 2229
 2230: 2230
 2231: 2231
 2232: 2232
 2233: 2233
 2234: 2234
 2235: 2235
 2236: 2236
 2237: 2237
 2238: 2238
 2239: 2239
 2240: 2240
 2241: 2241
 2242: 2242
 2243: 2243
 2244: 2244
 2245: 2245
 2246: 2246
 2247: 2247
 2248: 2248
 2249: 2249
 2250: 2250
 2251: 2251
 2252: 2252
 2253: 2253
 2254: 2254
 2255: 2255
 2256: 2256
 2257: 2257
 2258: 2258
 2259: 2259
 2260: 2260
 2261: 2261
 2262: 2262

Received Jan 14 1959

TABLE VIII

Calibration Run No. 4

Nose Piece: Short Resistance: 1000 ohms		Clearance 2"		RPM Amplifier Gain Setting: 10		: Variable	
Spring	I.F.	W	F	A _{ldg}	B _{ldg}	R _{ldg}	β _l
Letter Design.	lbs. + oz.	lbs. + gms	lbs.	(+)	(+)		deg. *
R	4.5 + 11	3.0 + 200	0.856	0.45	0.66	0.800	
				0.55	0.72	0.905	358
				0.49	0.79	0.930	368
				0.55	0.91	1.062	390
				0.69	1.13	1.325	410
				0.76	1.34	1.54	450
				0.79	1.40	1.61	468
				0.89	1.59	1.82	477
				0.95	1.79	2.03	492
				1.09	2.03	2.30	504
				1.19	2.35	2.63	515
				1.41	3.11	3.42	524
				1.62	3.39	3.76	544
				1.68	3.85	4.20	552
				1.85	4.70	5.05	555
							566
C	4.0 + 11	4.0 + 50	1.021	0.59	0.85	1.035	365
				0.62	0.91	1.11	380
				0.65	1.00	1.19	394
				0.73	1.11	1.33	412
				0.84	1.28	1.53	432
				0.90	1.46	1.72	453
				1.04	1.70	1.99	471
				1.10	1.79	2.10	480
				1.35	2.25	2.62	502
				1.63	2.56	3.20	514
				1.70	2.85	3.32	522
				1.85	3.10	3.60	532
				2.10	3.95	4.47	545
				2.35	4.75	5.30	554

(continued)

0

—

3

TABLE VIII
(continued)

Calibration Run No. 4

Nose Piece: Short Resistance: 1000 ohms		Clearance 2"		RPM Amplifier Gain Setting: 10		: Variable	
I.F. lbs. + oz.	W lbs. + oms lbs.	F	A rdg (+)	B rdg (+)	R rdg	β_1 deg. *	RPM
Spring							
Letter Design.	4.0 + 11	1.0 + 90	0.298				
I							
			0.20	0.30	0.360		379
			0.25	0.33	0.413		395
			0.25	0.36	0.438		430
			0.25	0.45	0.515		461
			0.39	0.65	0.758		519
			0.48	0.86	0.985		545
			0.59	1.10	1.25		560
			0.62	1.42	1.55		576
			0.59	1.82	1.91		584
			0.55	1.73	1.81		583
			0.70	2.85	2.94		596
			0.65	4.35	4.40		602

* Note: β_1 not computed.

TABLE IX

Measurement Run No. 8

Water Temperature: 77°F.
 Nose Piece : Short
 Thrust Correction: -7.5 lbs.

RPM : 548
 Amplifier Gain Setting: 10
 Resistance : 1000 ohms

Clearance 2"

T _{rdg} lbs.	T _{corr} lbs.	H ₁ rdg	v fps	J v/nd	A _{rdg} (+)	B _{rdg} (+)	R _{rdg}	F lbs	32 deg
59.5	52.0	26	2.11	0.234	4.10	1.30	4.29	0.950	17.6
55.0	47.5	45	2.78	0.308	3.85	1.20	4.03	0.910	17.3
52.2	44.7	59	3.2	0.355	3.75	1.02	3.89	0.885	15.2
50.7	43.2	74	3.58	0.398	3.60	1.00	3.74	0.860	15.5
45.2	37.7	105	4.26	0.473	3.30	0.98	3.44	0.805	16.5
40.1	32.6	144	5.00	0.555	3.05	0.92	3.18	0.760	16.8
30.5	23.0	217	6.13	0.681	2.70	0.88	2.83	0.695	18.0
34.8	27.3	183	5.63	0.626	2.85	0.90	2.99	0.725	17.5
28.4	20.9	248	6.56	0.730	2.50	0.88	2.65	0.660	19.3
25.5	18.0	278	6.95	0.772	2.41	0.88	2.57	0.640	20.0
22.3	14.8	315	7.40	0.820	2.29	0.89	2.45	0.620	21.4
19.3	11.8	347	7.75	0.862	2.20	0.92	2.39	0.605	22.7
15.7	8.2	386	8.19	0.910	2.04	0.96	2.26	0.580	25.3
13.9	6.4	417	8.50	0.945	2.00	0.95	2.22	0.570	25.5
11.5	4.0	444	8.76	0.975	1.92	0.93	2.13	0.550	26.0
9.1	1.6	478	9.10	1.011	1.87	0.95	2.09	0.545	27.0
8.0	0.5	491	9.24	1.025	1.82	0.95	2.05	0.525	27.6

Note: γ not computed for this run;

1_{rdg} = 42° for run and necessary information for
 calculation of γ is in thesis.

5/2 :
01 :
001 :

[illegible]

TABLE X

Calibration Run No. 5

Nose Piece: Short
Resistance: 1000 ohms

Clearance 2-1/4"

RPM = 548
Amplifier Gain Setting: 10

Spring	I.F.	W	F	A rdg	B rdg	R rdg	β_1
Letter Design- ation	lbs. + oz.	lbs. + gms	lbs.	(+)	(+)		deg.
Q	4 - 11	2.5 + 70	0.66	1.21 1.25	2.47 2.45	2.75 2.75	64.0 63.0
X	4 - 11	2.0 + 10	0.50	0.80 0.83	1.81 1.79	1.98 1.97	66.0 65.2
G	3 - 11	1.0 + 40	0.27	0.40 0.43	1.02 1.03	1.10 1.12	68.5 67.5
R	4 - 11	3.0 + 160	0.84	1.65 1.59	3.15 3.15	3.56 3.52	62.5 63.2
M	4 - 11	1.5 + 250	0.51	0.78 0.78	1.85 1.81	2.01 1.97	67.2 66.7
W	4 - 11	2.0 + 10	0.50	0.77 0.79	1.81 1.85	1.95 2.01	66.7 66.8
L	4 - 11	1.5 + 220	0.49	0.70 0.69	1.77 1.74	1.90 1.87	68.3 68.3
C	3 - 11	0.5 + 220	0.25	0.30 0.31	0.85 0.84	0.90 0.90	70.5 69.7
N	4 - 11	4.0 + 100	1.05	2.05 2.03	4.05 4.10	4.53 4.58	63.0 63.5
V	4 - 11	3.0 + 40	0.77	1.51 1.51	2.89 2.86	3.26 3.24	62.5 62.2
Average β_1 =							65.3°

3144 : 33019 33019
4444 0001 : 33019 33019

- 155 -

TABLE XI

Measurement Run No. 4

Water Temperature: 76°F.
 Nose Piece : Short
 Thrust Correction: -2.0 lbs.

RPM : 548
 Amplifier Gain Setting: 10
 Resistance : 1000 ohms

Clearance 2-1/4"

T	I	H	V	J	A	B	R	F	B	B	α	4Y	-Y
rdg	corr	l	v	j	rdg	rdg	rdg	lbs	deg	deg	deg	deg	deg
lbs.	lbs.	rdg	fps	v/nd									
53.5	51.5	0	0	0	-1.05	-2.90	3.09	0.745	250.0	303	57	127.7	31.9
53.0	51.0	17	1.71	0.190	-1.10	-2.90	3.10	0.752	249.3	302	58	126.0	31.5
52.5	50.5	21	1.90	0.211	-0.90	-2.85	2.95	0.720	252.5	302	58	129.2	32.3
47.7	45.7	36	2.48	0.276	-0.85	-2.70	2.83	0.695	252.5	302	58	129.2	32.3
45.5	43.5	45	2.78	0.309	-0.85	-2.60	2.73	0.675	252.0	301	59	127.7	31.9
42.5	40.5	62	3.26	0.362	-0.74	-2.40	2.51	0.630	252.8	301	59	128.5	32.1
39.5	37.5	78	3.65	0.406	-0.72	-2.28	2.39	0.600	252.5	299	61	126.2	31.6
36.4	34.4	101	4.16	0.462	-0.63	-2.15	2.24	0.570	253.7	298	62	126.4	31.6
30.2	28.2	133	4.77	0.530	-0.61	-2.05	2.14	0.550	253.5	298	62	126.2	31.6
26.3	24.3	168	5.36	0.596	-0.51	-1.87	1.94	0.500	254.7	298	62	127.4	31.9
24.9	22.9	179	5.53	0.614	-0.50	-1.87	1.93	0.495	255.0	299	61	128.7	32.1
21.8	19.8	208	5.96	0.663	-0.43	-1.85	1.90	0.490	257.0	299	61	130.7	32.6
19.5	17.5	230	6.26	0.697	-0.41	-1.65	1.70	0.445	256.0	299	61	129.7	32.4
16.3	14.3	263	6.72	0.746	-0.35	-1.60	1.64	0.435	257.7	300	60	132.4	33.1
12.5	10.5	305	7.23	0.804	-0.30	-1.51	1.54	0.410	258.7	301	59	134.4	33.6
8.8	6.8	347	7.70	0.856	-0.24	-1.40	1.42	0.380	260.3	301	59	136.0	34.0
5.2	3.2	388	8.15	0.906	-0.21	-1.30	1.32	0.355	260.8	302	58	137.5	34.4

TABLE XII

Measurement Run No. 5

Water Temperature: 76°F.														RPM : 548													
Nose Piece : Short														Amplifier Gain Setting: 10													
Thrust Correction: -2.0 lbs.														Resistance : 1000 ohms													
Clearance 2-1/2"																											
T	T	H ₁	v	J	A	B	R	F	β ₁	β ₂	α	Y	-Y														
rdg	corr	rdg	fps	v/nd	rdg	rdg	rdg	lbs	deg	deg	deg	deg	deg														
lbs.	lbs.																										
52.5	50.5	2	0.585	0.065	-0.75	-2.50	2.61	0.615	253.3	304	56	130.3	32.5														
52.0	50.0	12	1.43	0.159	-0.75	-2.50	2.61	0.615	253.3	305	55	131.3	32.8														
48.0	46.0	31	2.30	0.256	-0.60	-2.30	2.38	0.570	255.3	305	55	133.3	33.2														
43.0	41.0	54	3.04	0.338	-0.52	-2.06	2.12	0.515	255.8	306	54	134.8	33.7														
41.1	39.1	65	3.34	0.371	-0.50	-1.98	2.04	0.495	255.8	306	54	134.8	33.7														
37.4	35.4	90	3.93	0.437	-0.43	-1.85	1.90	0.465	257.0	306	54	136.0	34.0														
31.0	29.0	124	4.61	0.513	-0.39	-1.72	1.77	0.440	257.3	306	54	136.3	34.1														
26.4	24.4	164	5.30	0.589	-0.31	-1.60	1.63	0.410	259.0	306	54	138.0	34.5														
24.0	22.0	187	5.66	0.630	-0.28	-1.50	1.53	0.385	259.5	306	54	138.5	34.6														
														0.79													
20.9	18.9	213	6.05	0.672	-0.25	-1.45	1.47	0.372	260.3	306	54	139.3	34.8														
17.7	15.7	248	6.51	0.723	-0.22	-1.35	1.37	0.350	260.7	306	54	139.7	34.9														
14.5	12.5	276	6.87	0.763	-0.16	-1.25	1.26	0.325	262.7	306	54	141.7	35.4														
12.9	10.9	298	7.15	0.794	-0.13	-1.20	1.21	0.311	263.8	306	54	142.8	35.6														
11.9	9.9	309	7.26	0.808	-0.13	-1.19	1.20	0.310	263.7	306	54	142.7	35.6														
8.7	6.7	343	7.67	0.852	-0.09	-1.11	1.12	0.290	265.3	307	53	145.3	36.3														
6.9	4.9	366	7.92	0.880	-0.05	-1.05	1.06	0.280	267.3	307	53	147.3	36.8														
5.7	3.7	382	8.10	0.900	-0.05	-1.05	1.06	0.280	267.3	307	53	147.3	36.8														
3.5	1.5	407	8.35	0.930	-0.03	-1.05	1.05	0.275	269.4	307	53	149.4	37.3														

IX 310AT

2.0M null instruction

BAR :
OI : null instruction
endo 0001 :

ES/1-2 construction

.300V : request to be
from :
sel 0.1- : instruction to be

Y-	Y2	Y3	Y4	Y5	Y6	Y7	Y8	Y9	Y10	Y11	Y12	Y13	Y14	Y15	Y16	Y17	Y18	Y19	Y20	Y21	Y22	Y23	Y24	Y25	Y26	Y27	Y28	Y29	Y30	Y31	Y32	Y33	Y34	Y35	Y36	Y37	Y38	Y39	Y40	Y41	Y42	Y43	Y44	Y45	Y46	Y47	Y48	Y49	Y50	Y51	Y52	Y53	Y54	Y55	Y56	Y57	Y58	Y59	Y60	Y61	Y62	Y63	Y64	Y65	Y66	Y67	Y68	Y69	Y70	Y71	Y72	Y73	Y74	Y75	Y76	Y77	Y78	Y79	Y80	Y81	Y82	Y83	Y84	Y85	Y86	Y87	Y88	Y89	Y90	Y91	Y92	Y93	Y94	Y95	Y96	Y97	Y98	Y99	Y100	Y101	Y102	Y103	Y104	Y105	Y106	Y107	Y108	Y109	Y110	Y111	Y112	Y113	Y114	Y115	Y116	Y117	Y118	Y119	Y120	Y121	Y122	Y123	Y124	Y125	Y126	Y127	Y128	Y129	Y130	Y131	Y132	Y133	Y134	Y135	Y136	Y137	Y138	Y139	Y140	Y141	Y142	Y143	Y144	Y145	Y146	Y147	Y148	Y149	Y150	Y151	Y152	Y153	Y154	Y155	Y156	Y157	Y158	Y159	Y160	Y161	Y162	Y163	Y164	Y165	Y166	Y167	Y168	Y169	Y170	Y171	Y172	Y173	Y174	Y175	Y176	Y177	Y178	Y179	Y180	Y181	Y182	Y183	Y184	Y185	Y186	Y187	Y188	Y189	Y190	Y191	Y192	Y193	Y194	Y195	Y196	Y197	Y198	Y199	Y200	Y201	Y202	Y203	Y204	Y205	Y206	Y207	Y208	Y209	Y210	Y211	Y212	Y213	Y214	Y215	Y216	Y217	Y218	Y219	Y220	Y221	Y222	Y223	Y224	Y225	Y226	Y227	Y228	Y229	Y230	Y231	Y232	Y233	Y234	Y235	Y236	Y237	Y238	Y239	Y240	Y241	Y242	Y243	Y244	Y245	Y246	Y247	Y248	Y249	Y250	Y251	Y252	Y253	Y254	Y255	Y256	Y257	Y258	Y259	Y260	Y261	Y262	Y263	Y264	Y265	Y266	Y267	Y268	Y269	Y270	Y271	Y272	Y273	Y274	Y275	Y276	Y277	Y278	Y279	Y280	Y281	Y282	Y283	Y284	Y285	Y286	Y287	Y288	Y289	Y290	Y291	Y292	Y293	Y294	Y295	Y296	Y297	Y298	Y299	Y300	Y301	Y302	Y303	Y304	Y305	Y306	Y307	Y308	Y309	Y310	Y311	Y312	Y313	Y314	Y315	Y316	Y317	Y318	Y319	Y320	Y321	Y322	Y323	Y324	Y325	Y326	Y327	Y328	Y329	Y330	Y331	Y332	Y333	Y334	Y335	Y336	Y337	Y338	Y339	Y340	Y341	Y342	Y343	Y344	Y345	Y346	Y347	Y348	Y349	Y350	Y351	Y352	Y353	Y354	Y355	Y356	Y357	Y358	Y359	Y360	Y361	Y362	Y363	Y364	Y365	Y366	Y367	Y368	Y369	Y370	Y371	Y372	Y373	Y374	Y375	Y376	Y377	Y378	Y379	Y380	Y381	Y382	Y383	Y384	Y385	Y386	Y387	Y388	Y389	Y390	Y391	Y392	Y393	Y394	Y395	Y396	Y397	Y398	Y399	Y400	Y401	Y402	Y403	Y404	Y405	Y406	Y407	Y408	Y409	Y410	Y411	Y412	Y413	Y414	Y415	Y416	Y417	Y418	Y419	Y420	Y421	Y422	Y423	Y424	Y425	Y426	Y427	Y428	Y429	Y430	Y431	Y432	Y433	Y434	Y435	Y436	Y437	Y438	Y439	Y440	Y441	Y442	Y443	Y444	Y445	Y446	Y447	Y448	Y449	Y450	Y451	Y452	Y453	Y454	Y455	Y456	Y457	Y458	Y459	Y460	Y461	Y462	Y463	Y464	Y465	Y466	Y467	Y468	Y469	Y470	Y471	Y472	Y473	Y474	Y475	Y476	Y477	Y478	Y479	Y480	Y481	Y482	Y483	Y484	Y485	Y486	Y487	Y488	Y489	Y490	Y491	Y492	Y493	Y494	Y495	Y496	Y497	Y498	Y499	Y500	Y501	Y502	Y503	Y504	Y505	Y506	Y507	Y508	Y509	Y510	Y511	Y512	Y513	Y514	Y515	Y516	Y517	Y518	Y519	Y520	Y521	Y522	Y523	Y524	Y525	Y526	Y527	Y528	Y529	Y530	Y531	Y532	Y533	Y534	Y535	Y536	Y537	Y538	Y539	Y540	Y541	Y542	Y543	Y544	Y545	Y546	Y547	Y548	Y549	Y550	Y551	Y552	Y553	Y554	Y555	Y556	Y557	Y558	Y559	Y560	Y561	Y562	Y563	Y564	Y565	Y566	Y567	Y568	Y569	Y570	Y571	Y572	Y573	Y574	Y575	Y576	Y577	Y578	Y579	Y580	Y581	Y582	Y583	Y584	Y585	Y586	Y587	Y588	Y589	Y590	Y591	Y592	Y593	Y594	Y595	Y596	Y597	Y598	Y599	Y600	Y601	Y602	Y603	Y604	Y605	Y606	Y607	Y608	Y609	Y610	Y611	Y612	Y613	Y614	Y615	Y616	Y617	Y618	Y619	Y620	Y621	Y622	Y623	Y624	Y625	Y626	Y627	Y628	Y629	Y630	Y631	Y632	Y633	Y634	Y635	Y636	Y637	Y638	Y639	Y640	Y641	Y642	Y643	Y644	Y645	Y646	Y647	Y648	Y649	Y650	Y651	Y652	Y653	Y654	Y655	Y656	Y657	Y658	Y659	Y660	Y661	Y662	Y663	Y664	Y665	Y666	Y667	Y668	Y669	Y670	Y671	Y672	Y673	Y674	Y675	Y676	Y677	Y678	Y679	Y680	Y681	Y682	Y683	Y684	Y685	Y686	Y687	Y688	Y689	Y690	Y691	Y692	Y693	Y694	Y695	Y696	Y697	Y698	Y699	Y700	Y701	Y702	Y703	Y704	Y705	Y706	Y707	Y708	Y709	Y710	Y711	Y712	Y713	Y714	Y715	Y716	Y717	Y718	Y719	Y720	Y721	Y722	Y723	Y724	Y725	Y726	Y727	Y728	Y729	Y730	Y731	Y732	Y733	Y734	Y735	Y736	Y737	Y738	Y739	Y740	Y741	Y742	Y743	Y744	Y745	Y746	Y747	Y748	Y749	Y750	Y751	Y752	Y753	Y754	Y755	Y756	Y757	Y758	Y759	Y760	Y761	Y762	Y763	Y764	Y765	Y766	Y767	Y768	Y769	Y770	Y771	Y772	Y773	Y774	Y775	Y776	Y777	Y778	Y779	Y780	Y781	Y782	Y783	Y784	Y785	Y786	Y787	Y788	Y789	Y790	Y791	Y792	Y793	Y794	Y795	Y796	Y797	Y798	Y799	Y800	Y801	Y802	Y803	Y804	Y805	Y806	Y807	Y808	Y809	Y810	Y811	Y812	Y813	Y814	Y815	Y816	Y817	Y818	Y819	Y820	Y821	Y822	Y823	Y824	Y825	Y826	Y827	Y828	Y829	Y830	Y831	Y832	Y833	Y834	Y835	Y836	Y837	Y838	Y839	Y840	Y841	Y842	Y843	Y844	Y845	Y846	Y847	Y848	Y849	Y850	Y851	Y852	Y853	Y854	Y855	Y856	Y857	Y858	Y859	Y860	Y861	Y862	Y863	Y864	Y865	Y866	Y867	Y868	Y869	Y870	Y871	Y872	Y873	Y874	Y875	Y876	Y877	Y878	Y879	Y880	Y881	Y882	Y883	Y884	Y885	Y886	Y887	Y888	Y889	Y890	Y891	Y892	Y893	Y894	Y895	Y896	Y897	Y898	Y899	Y900	Y901	Y902	Y903	Y904	Y905	Y906	Y907	Y908	Y909	Y910	Y911	Y912	Y913	Y914	Y915	Y916	Y917	Y918	Y919	Y920	Y921	Y922	Y923	Y924	Y925	Y926	Y927	Y928	Y929	Y930	Y931	Y932	Y933	Y934	Y935	Y936	Y937	Y938	Y939	Y940	Y941	Y942	Y943	Y944	Y945	Y946	Y947	Y948	Y949	Y950	Y951	Y952	Y953	Y954	Y955	Y956	Y957	Y958	Y959	Y960	Y961	Y962	Y963	Y964	Y965	Y966	Y967	Y968	Y969	Y970	Y971	Y972	Y973	Y974	Y975	Y976	Y977	Y978	Y979	Y980	Y981	Y982	Y983	Y984	Y985	Y986	Y987	Y988	Y989	Y990	Y991	Y992	Y993	Y994	Y995	Y996	Y997	Y998	Y999	Y1000	Y1001	Y1002	Y1003	Y1004	Y1005	Y1006	Y1007	Y1008	Y1009	Y1010	Y1011	Y1012	Y1013	Y1014	Y1015	Y1016	Y1017	Y1018	Y1019	Y1020	Y1021	Y1022	Y1023	Y1024	Y1025	Y1026	Y1027	Y1028	Y1029	Y1030	Y1031	Y1032	Y1033	Y1034	Y1035	Y1036	Y1037	Y1038	Y1039	Y1040	Y1041	Y1042	Y1043	Y1044	Y1045	Y1046	Y1047	Y1048	Y1049	Y1050	Y1051	Y1052	Y1053	Y1054	Y1055	Y1056	Y1057	Y1058	Y1059	Y1060	Y1061	Y1062	Y1063	Y1064	Y1065	Y1066	Y1067	Y1068	Y1069	Y1070	Y1071	Y1072	Y1073	Y1074	Y1075	Y1076	Y1077	Y1078	Y1079	Y1080	Y1081	Y1082	Y1083	Y1084	Y1085	Y1086	Y1087	Y1088	Y1089	Y1090	Y1091	Y1092	Y1093	Y1094	Y1095	Y1096	Y1097	Y1098	Y1099	Y1100	Y1101	Y1102	Y1103	Y1104	Y1105	Y1106	Y1107	Y1108	Y1109	Y1110	Y1111	Y1112	Y1113	Y1114	Y1115	Y1116	Y1117	Y1118	Y1119	Y1120	Y1121	Y1122	Y1123	Y1124	Y1125	Y1126	Y1127	Y1128	Y1129	Y1130	Y1131	Y1132	Y1133	Y1134	Y1135	Y1136	Y1137	Y1138	Y1139	Y1140	Y1141	Y1142	Y1143	Y1144	Y1145	Y1146	Y1147	Y1148	Y1149	Y1150	Y1151	Y1152	Y1153	Y1154	Y1155	Y1156	Y1157	Y1158	Y1159	Y1160	Y1161	Y1162	Y1163	Y1164	Y1165	Y1166	Y1167	Y1168	Y1169	Y1170	Y1171	Y1172	Y1173	Y1174	Y1175	Y1176	Y1177	Y1178	Y1179	Y1180	Y1181	Y1182	Y1183	Y1184	Y1185	Y1186	Y1187	Y1188	Y1189	Y1190	Y1191	Y1192	Y1193	Y1194	Y1195	Y1196	Y1197	Y1198	Y1199	Y1200	Y1201	Y1202	Y1203	Y1204	Y1205	Y1206	Y1207	Y1208	Y1209	Y1210	Y1211	Y1212	Y1213	Y1214	Y1215	Y1216	Y1217	Y1218	Y1219	Y1220	Y1221	Y1222	Y1223	Y1224	Y1225	Y1226	Y1227	Y1228	Y1229	Y1230	Y1231	Y1232	Y1233	Y1234	Y1235	Y1236	Y1237	Y1238	Y1239	Y1240	Y1241	Y1242	Y1243	Y1244	Y1245	Y1246	Y1247	Y1248	Y1249	Y1250	Y1251	Y1252	Y1253	Y1254	Y1255	Y1256	Y1257	Y1258	Y1259	Y1260	Y1261	Y1262	Y1263	Y1264	Y1265	Y1266	Y1267	Y1268	Y1269	Y1270	Y1271	Y1272	Y1273	Y1274	Y1275	Y1276	Y1277	Y1278	Y1279	Y1280	Y1281	Y1282	Y1283	Y1284	Y1285	Y1286	Y1287	Y1288	Y1289	Y1290	Y1291	Y1292	Y1293	Y1294	Y1295	Y1296	Y1297	Y1298	Y1299	Y1300	Y1301	Y1302	Y1303	Y1304	Y1305	Y1306	Y1307	Y1308	Y1309	Y1310	Y1311	Y1312	Y1313	Y1314	Y1315	Y1316	Y1317	Y1318	Y1319	Y1320	Y1321	
----	----	----	----	----	----	----	----	----	-----	-----	-----	-----	-----	-----	-----	-----	-----	-----	-----	-----	-----	-----	-----	-----	-----	-----	-----	-----	-----	-----	-----	-----	-----	-----	-----	-----	-----	-----	-----	-----	-----	-----	-----	-----	-----	-----	-----	-----	-----	-----	-----	-----	-----	-----	-----	-----	-----	-----	-----	-----	-----	-----	-----	-----	-----	-----	-----	-----	-----	-----	-----	-----	-----	-----	-----	-----	-----	-----	-----	-----	-----	-----	-----	-----	-----	-----	-----	-----	-----	-----	-----	-----	-----	-----	-----	-----	-----	-----	------	------	------	------	------	------	------	------	------	------	------	------	------	------	------	------	------	------	------	------	------	------	------	------	------	------	------	------	------	------	------	------	------	------	------	------	------	------	------	------	------	------	------	------	------	------	------	------	------	------	------	------	------	------	------	------	------	------	------	------	------	------	------	------	------	------	------	------	------	------	------	------	------	------	------	------	------	------	------	------	------	------	------	------	------	------	------	------	------	------	------	------	------	------	------	------	------	------	------	------	------	------	------	------	------	------	------	------	------	------	------	------	------	------	------	------	------	------	------	------	------	------	------	------	------	------	------	------	------	------	------	------	------	------	------	------	------	------	------	------	------	------	------	------	------	------	------	------	------	------	------	------	------	------	------	------	------	------	------	------	------	------	------	------	------	------	------	------	------	------	------	------	------	------	------	------	------	------	------	------	------	------	------	------	------	------	------	------	------	------	------	------	------	------	------	------	------	------	------	------	------	------	------	------	------	------	------	------	------	------	------	------	------	------	------	------	------	------	------	------	------	------	------	------	------	------	------	------	------	------	------	------	------	------	------	------	------	------	------	------	------	------	------	------	------	------	------	------	------	------	------	------	------	------	------	------	------	------	------	------	------	------	------	------	------	------	------	------	------	------	------	------	------	------	------	------	------	------	------	------	------	------	------	------	------	------	------	------	------	------	------	------	------	------	------	------	------	------	------	------	------	------	------	------	------	------	------	------	------	------	------	------	------	------	------	------	------	------	------	------	------	------	------	------	------	------	------	------	------	------	------	------	------	------	------	------	------	------	------	------	------	------	------	------	------	------	------	------	------	------	------	------	------	------	------	------	------	------	------	------	------	------	------	------	------	------	------	------	------	------	------	------	------	------	------	------	------	------	------	------	------	------	------	------	------	------	------	------	------	------	------	------	------	------	------	------	------	------	------	------	------	------	------	------	------	------	------	------	------	------	------	------	------	------	------	------	------	------	------	------	------	------	------	------	------	------	------	------	------	------	------	------	------	------	------	------	------	------	------	------	------	------	------	------	------	------	------	------	------	------	------	------	------	------	------	------	------	------	------	------	------	------	------	------	------	------	------	------	------	------	------	------	------	------	------	------	------	------	------	------	------	------	------	------	------	------	------	------	------	------	------	------	------	------	------	------	------	------	------	------	------	------	------	------	------	------	------	------	------	------	------	------	------	------	------	------	------	------	------	------	------	------	------	------	------	------	------	------	------	------	------	------	------	------	------	------	------	------	------	------	------	------	------	------	------	------	------	------	------	------	------	------	------	------	------	------	------	------	------	------	------	------	------	------	------	------	------	------	------	------	------	------	------	------	------	------	------	------	------	------	------	------	------	------	------	------	------	------	------	------	------	------	------	------	------	------	------	------	------	------	------	------	------	------	------	------	------	------	------	------	------	------	------	------	------	------	------	------	------	------	------	------	------	------	------	------	------	------	------	------	------	------	------	------	------	------	------	------	------	------	------	------	------	------	------	------	------	------	------	------	------	------	------	------	------	------	------	------	------	------	------	------	------	------	------	------	------	------	------	------	------	------	------	------	------	------	------	------	------	------	------	------	------	------	------	------	------	------	------	------	------	------	------	------	------	------	------	------	------	------	------	------	------	------	------	------	------	------	------	------	------	------	------	------	------	------	------	------	------	------	------	------	------	------	------	------	------	------	------	------	------	------	------	------	------	------	------	------	------	------	------	------	------	------	------	------	------	------	------	------	------	------	------	------	------	------	------	------	------	------	------	------	------	------	------	------	------	------	------	------	------	------	------	------	------	------	------	------	------	------	------	------	------	------	------	------	------	------	------	------	------	------	------	------	------	------	------	------	------	------	------	------	------	------	------	------	------	------	------	------	------	------	------	------	------	------	------	------	------	------	------	------	------	------	------	------	------	------	------	------	------	------	------	------	------	------	------	------	------	------	------	------	------	------	------	------	------	------	------	------	------	------	------	------	------	------	------	------	------	------	------	------	------	------	------	------	------	------	------	------	------	------	------	------	------	------	------	------	------	------	------	------	------	------	------	------	------	------	------	------	------	------	------	------	------	------	------	------	------	------	-------	-------	-------	-------	-------	-------	-------	-------	-------	-------	-------	-------	-------	-------	-------	-------	-------	-------	-------	-------	-------	-------	-------	-------	-------	-------	-------	-------	-------	-------	-------	-------	-------	-------	-------	-------	-------	-------	-------	-------	-------	-------	-------	-------	-------	-------	-------	-------	-------	-------	-------	-------	-------	-------	-------	-------	-------	-------	-------	-------	-------	-------	-------	-------	-------	-------	-------	-------	-------	-------	-------	-------	-------	-------	-------	-------	-------	-------	-------	-------	-------	-------	-------	-------	-------	-------	-------	-------	-------	-------	-------	-------	-------	-------	-------	-------	-------	-------	-------	-------	-------	-------	-------	-------	-------	-------	-------	-------	-------	-------	-------	-------	-------	-------	-------	-------	-------	-------	-------	-------	-------	-------	-------	-------	-------	-------	-------	-------	-------	-------	-------	-------	-------	-------	-------	-------	-------	-------	-------	-------	-------	-------	-------	-------	-------	-------	-------	-------	-------	-------	-------	-------	-------	-------	-------	-------	-------	-------	-------	-------	-------	-------	-------	-------	-------	-------	-------	-------	-------	-------	-------	-------	-------	-------	-------	-------	-------	-------	-------	-------	-------	-------	-------	-------	-------	-------	-------	-------	-------	-------	-------	-------	-------	-------	-------	-------	-------	-------	-------	-------	-------	-------	-------	-------	-------	-------	-------	-------	-------	-------	-------	-------	-------	-------	-------	-------	-------	-------	-------	-------	-------	-------	-------	-------	-------	-------	-------	-------	-------	-------	-------	-------	-------	-------	-------	-------	-------	-------	-------	-------	-------	-------	-------	-------	-------	-------	-------	-------	-------	-------	-------	-------	-------	-------	-------	-------	-------	-------	-------	-------	-------	-------	-------	-------	-------	-------	-------	-------	-------	-------	-------	-------	-------	-------	-------	-------	-------	-------	-------	-------	-------	-------	-------	-------	-------	-------	-------	-------	-------	-------	-------	-------	-------	-------	-------	-------	-------	-------	-------	-------	-------	-------	-------	-------	-------	-------	-------	-------	-------	-------	-------	-------	-------	-------	-------	-------	-------	-------	-------	-------	-------	-------	--

TABLE XIII

Calibration Run No. 6

Nose Piece: Short
Resistance: 1000 ohms

RPM = 548
Amplifier Gain Setting: 10

Spring	I.F.	W	F	A rdg	B rdg	R rdg	β_1
Letter Design- ation	lbs. + oz.	lbs. + ozs	lbs.	(+)	(+)		deg.
L	4 - 11	1.5 + 200	0.48	0.80	2.05	2.20	68.7
R	4 - 11	3.0 + 200	0.86	1.87 1.89	3.65 3.62	4.10 4.08	62.8 62.5
M	4 - 11	2.0 + 60	0.53	0.79 0.81	2.11 2.15	2.25 2.30	69.5 69.3
V	4 - 11	2.5 + 220	0.74	1.51 1.55	3.28 3.38	3.61 3.71	65.3 65.3
X	4 - 11	2.0 + 50	0.53	0.81 0.82	2.05 2.05	2.20 2.21	68.5 68.5
W	4 - 11	1.5 + 230	0.50	0.76 0.78	2.15 2.11	2.28 2.25	70.5 69.7
Q	4 - 11	2.0 + 250	0.64	1.19 1.29	2.80 2.80	3.04 3.08	68.0 65.3
C	3 - 11	0.5 + 240	0.26	0.27 0.29	0.95 0.96	0.99 1.00	74.0 73.2

Average β_1 = 68.6°

rich : 1951 2000
1950 1951 : 1952 1953

TABLE XIV

Measurement Run No. 6

Water Temperature: 76°F.
 Nose Piece : Short
 Thrust Correction: -2.0 lbs.

Clearance 2-3/4"

RPM : 548
 Amplifier Gain Setting: 10
 Resistance : 1000 ohms

T	T	H ₁	v	J	A	B	R	F	B ₂	B ₁	360-1	4Y	-Y
lbs.	lbs.	rdg	fps	v/nd	Rdg	Bdg	Rdg	lbs.	deg	deg	deg	deg	deg
54.4	52.4	18	1.76	0.196	-0.40	-2.30	2.34	0.520	260.2	306	54	137.6	34.4
53.0	51.0	3	0.72	0.080	-0.90	-2.10	2.28	0.510	246.8	305	55	123.2	30.8
51.5	49.5	28	2.19	0.244	-0.40	-2.15	2.19	0.495	259.5	307	53	137.9	34.4
51.3	49.3	32	2.34	0.261	-0.40	-2.10	2.14	0.485	259.2	306	54	136.6	34.1
47.0	45.0	47	2.74	0.317	-0.45	-1.90	1.95	0.450	256.7	306	54	134.1	33.5
45.0	43.0	54	3.04	0.339	-0.40	-1.85	1.90	0.440	258.0	306	54	135.4	33.9
42.4	40.0	71	3.49	0.388	-0.40	-1.70	1.74	0.410	256.8	306	54	134.2	33.6
36.4	34.4	110	4.35	0.483	-0.26	-1.58	1.60	0.380	260.7	306	54	138.1	34.5
35.5	33.5	121	4.56	0.507	-0.25	-1.47	1.49	0.355	260.4	306	54	137.8	34.4
29.2	27.2	154	5.16	0.573	-0.25	-1.45	1.47	0.350	260.3	306	54	137.7	34.4
26.3	24.3	187	5.69	0.632	-0.21	-1.32	1.34	0.325	261.0	306	54	138.4	34.6
23.5	21.3	211	6.03	0.670	-0.20	-1.27	1.29	0.315	261.1	306	54	138.5	34.6
21.2	19.2	244	6.51	0.723	-0.15	-1.22	1.23	0.300	263.0	306	54	140.4	35.1
18.7	16.7	263	6.74	0.750	-0.12	-1.15	1.16	0.285	264.0	306	54	141.4	35.4
16.5	14.5	278	6.94	0.771	-0.09	-1.12	1.12	0.280	265.5	306	54	142.9	35.7
14.0	12.0	315	7.39	0.820	-0.05	-1.05	1.06	0.260	267.3	306	54	144.7	36.1
10.4	8.4	356	7.85	0.871	-0.05	-0.95	0.96	0.240	267.0	306	54	144.4	36.1
7.9	5.9	387	8.19	0.910	+0.05	-0.92	0.93	0.233	273.0	306	54	150.4	37.6
6.6	4.6	413	8.45	0.940	0.00	-0.95	0.95	0.235	270.0	306	54	147.4	36.9
4.3	2.3	430	8.65	0.960	+0.02	-0.85	0.86	0.220	271.5	306	54	148.9	37.2
2.0	0.0	466	9.00	1.00	0	-0.85	0.85	0.215	270.0	306	54	147.4	37.6

2. -M and J14-15

7087
from ?
-P.L.-

- 151 -

TABLE XV

Calibration Run No. 7

Nose Piece: Short Resistance: 1000 ohms		Clearance 3"		RPM = 548 Amplifier Gain Setting: 10					
Spring Letter Desig- nation	I.F. lbs. + oz.	W lbs. + oz.	F lbs.	A rdg (+)	B rdg (+)	R rdg	β_1 deg.		
L	4 - 11	2.0 + 0	0.49	0.55	1.45	1.55	69.2		
M	4 - 11	2.0 + 50	0.52	0.52	1.60	1.68	72.0		
V	4 - 11	3.0 + 20	0.75	0.92	2.55	2.71	70.2		
N	4 - 11	4.0 + 200	1.10	1.60 1.55	4.20 4.10	4.49 4.38	69.2 69.4		
C	2.5 - 11	1.0 + 0	0.25	0.35	0.70	0.78	63.5		
Q	3 - 11	2.5 + 90	0.67	0.82	2.25	2.39	70.0		
R	4 - 11	3.5 + 30	0.88	1.20	2.95	3.19	68.0		
P	4 - 11	4.5 + 90	1.16	1.70	4.10	4.34	67.5		

Average $\beta_1 = 68.8^\circ$

7. 2nd July 1911

01 : nitro - methyl

Find : 9241 9000
 and 6001 : 9240 9100

Удостоверение № 100-100

TABLE XVI

Measurement Run No. 7

Water Temperature: 76°F.
Nose Piece : Short
Thrust Correction: -2.0 lbs. Clearance 3"

RPM : 548
Amplifier Gain Setting: 10
Resistance : 1000 ohms

T	I	T	H	v	J	A	B	R	F	β	β	α	360-α	4Y	-Y
lbs.	lbs.	lbs.	lbs.	lbs.	v/nd	A	B	R	lbs.	deg	deg	deg	deg	deg	deg
62.5	60.0	0	0	0	0	-0.40	-1.10	1.17	0.385	250.0	302	58	123.2	30.8	
55.2	53.2	23	1.99	0.221	0.221	-0.20	-1.05	1.07	0.360	259.3	301	59	131.5	32.9	
50.9	48.9	35	2.45	0.272	0.272	-0.24	-0.95	0.98	0.335	255.8	301	59	128.0	32.0	
48.8	46.8	45	2.77	0.308	0.308	-0.22	-0.95	0.97	0.330	257.0	301	59	129.2	32.3	
43.4	41.4	71	3.49	0.388	0.388	-0.18	-0.77	0.79	0.280	257.8	301	59	130.0	32.5	
39.5	37.5	95	4.03	0.448	0.448	-0.15	-0.71	0.73	0.262	258.0	301	59	130.2	32.6	
36.4	34.4	124	4.61	0.512	0.512	-0.14	-0.65	0.67	0.245	257.8	298	62	127.0	31.8	
30.3	28.3	144	4.97	0.552	0.552	-0.12	-0.66	0.67	0.245	259.7	298	62	128.9	32.2	
26.6	24.6	173	5.44	0.605	0.605	-0.13	-0.60	0.61	0.225	257.7	297	63	125.9	31.5	
22.9	20.9	207	5.94	0.660	0.660	-0.11	-0.51	0.52	0.200	257.8	297	63	126.0	31.5	
19.3	17.3	242	6.44	0.716	0.716	-0.09	-0.50	0.51	0.190	259.8	297	63	128.0	32.0	
17.2	15.2	261	6.68	0.743	0.743	-0.08	-0.50	0.51	0.190	261.0	298	62	130.2	32.5	
15.7	13.2	282	6.94	0.772	0.772	-0.06	-0.46	0.46	0.175	262.5	298	62	131.7	32.9	
12.0	10.0	327	7.48	0.830	0.830	-0.04	-0.40	0.40	0.155	264.0	298	62	133.2	33.3	
7.6	5.6	372	7.97	0.885	0.885	0.00	-0.35	0.35	0.135	270.0	298	62	139.2	34.8	
3.2	1.2	417	8.45	0.940	0.940	+0.02	-0.35	0.35	0.135	273.5	298	62	142.7	35.6	

S. M. J. J. J. J. J.

• 1957 : 1957-1958
• 1958 : 1958-1959
• 1959 : 1959-1960
• 1960 : 1960-1961
• 1961 : 1961-1962
• 1962 : 1962-1963
• 1963 : 1963-1964
• 1964 : 1964-1965
• 1965 : 1965-1966
• 1966 : 1966-1967
• 1967 : 1967-1968
• 1968 : 1968-1969
• 1969 : 1969-1970
• 1970 : 1970-1971
• 1971 : 1971-1972
• 1972 : 1972-1973
• 1973 : 1973-1974
• 1974 : 1974-1975
• 1975 : 1975-1976
• 1976 : 1976-1977
• 1977 : 1977-1978
• 1978 : 1978-1979
• 1979 : 1979-1980
• 1980 : 1980-1981
• 1981 : 1981-1982
• 1982 : 1982-1983
• 1983 : 1983-1984
• 1984 : 1984-1985
• 1985 : 1985-1986
• 1986 : 1986-1987
• 1987 : 1987-1988
• 1988 : 1988-1989
• 1989 : 1989-1990
• 1990 : 1990-1991
• 1991 : 1991-1992
• 1992 : 1992-1993
• 1993 : 1993-1994
• 1994 : 1994-1995
• 1995 : 1995-1996
• 1996 : 1996-1997
• 1997 : 1997-1998
• 1998 : 1998-1999
• 1999 : 1999-2000
• 2000 : 2000-2001
• 2001 : 2001-2002
• 2002 : 2002-2003
• 2003 : 2003-2004
• 2004 : 2004-2005
• 2005 : 2005-2006
• 2006 : 2006-2007
• 2007 : 2007-2008
• 2008 : 2008-2009
• 2009 : 2009-2010
• 2010 : 2010-2011
• 2011 : 2011-2012
• 2012 : 2012-2013
• 2013 : 2013-2014
• 2014 : 2014-2015
• 2015 : 2015-2016
• 2016 : 2016-2017
• 2017 : 2017-2018
• 2018 : 2018-2019
• 2019 : 2019-2020
• 2020 : 2020-2021
• 2021 : 2021-2022
• 2022 : 2022-2023
• 2023 : 2023-2024
• 2024 : 2024-2025
• 2025 : 2025-2026
• 2026 : 2026-2027
• 2027 : 2027-2028
• 2028 : 2028-2029
• 2029 : 2029-2030
• 2030 : 2030-2031
• 2031 : 2031-2032
• 2032 : 2032-2033
• 2033 : 2033-2034
• 2034 : 2034-2035
• 2035 : 2035-2036
• 2036 : 2036-2037
• 2037 : 2037-2038
• 2038 : 2038-2039
• 2039 : 2039-2040
• 2040 : 2040-2041
• 2041 : 2041-2042
• 2042 : 2042-2043
• 2043 : 2043-2044
• 2044 : 2044-2045
• 2045 : 2045-2046
• 2046 : 2046-2047
• 2047 : 2047-2048
• 2048 : 2048-2049
• 2049 : 2049-2050
• 2050 : 2050-2051
• 2051 : 2051-2052
• 2052 : 2052-2053
• 2053 : 2053-2054
• 2054 : 2054-2055
• 2055 : 2055-2056
• 2056 : 2056-2057
• 2057 : 2057-2058
• 2058 : 2058-2059
• 2059 : 2059-2060
• 2060 : 2060-2061
• 2061 : 2061-2062
• 2062 : 2062-2063
• 2063 : 2063-2064
• 2064 : 2064-2065
• 2065 : 2065-2066
• 2066 : 2066-2067
• 2067 : 2067-2068
• 2068 : 2068-2069
• 2069 : 2069-2070
• 2070 : 2070-2071
• 2071 : 2071-2072
• 2072 : 2072-2073
• 2073 : 2073-2074
• 2074 : 2074-2075
• 2075 : 2075-2076
• 2076 : 2076-2077
• 2077 : 2077-2078
• 2078 : 2078-2079
• 2079 : 2079-2080
• 2080 : 2080-2081
• 2081 : 2081-2082
• 2082 : 2082-2083
• 2083 : 2083-2084
• 2084 : 2084-2085
• 2085 : 2085-2086
• 2086 : 2086-2087
• 2087 : 2087-2088
• 2088 : 2088-2089
• 2089 : 2089-2090
• 2090 : 2090-2091
• 2091 : 2091-2092
• 2092 : 2092-2093
• 2093 : 2093-2094
• 2094 : 2094-2095
• 2095 : 2095-2096
• 2096 : 2096-2097
• 2097 : 2097-2098
• 2098 : 2098-2099
• 2099 : 2099-2100
• 2100 : 2100-2101
• 2101 : 2101-2102
• 2102 : 2102-2103
• 2103 : 2103-2104
• 2104 : 2104-2105
• 2105 : 2105-2106
• 2106 : 2106-2107
• 2107 : 2107-2108
• 2108 : 2108-2109
• 2109 : 2109-2110
• 2110 : 2110-2111
• 2111 : 2111-2112
• 2112 : 2112-2113
• 2113 : 2113-2114
• 2114 : 2114-2115
• 2115 : 2115-2116
• 2116 : 2116-2117
• 2117 : 2117-2118
• 2118 : 2118-2119
• 2119 : 2119-2120
• 2120 : 2120-2121
• 2121 : 2121-2122
• 2122 : 2122-2123
• 2123 : 2123-2124
• 2124 : 2124-2125
• 2125 : 2125-2126
• 2126 : 2126-2127
• 2127 : 2127-2128
• 2128 : 2128-2129
• 2129 : 2129-2130
• 2130 : 2130-2131
• 2131 : 2131-2132
• 2132 : 2132-2133
• 2133 : 2133-2134
• 2134 : 2134-2135
• 2135 : 2135-2136
• 2136 : 2136-2137
• 2137 : 2137-2138
• 2138 : 2138-2139
• 2139 : 2139-2140
• 2140 : 2140-2141
• 2141 : 2141-2142
• 2142 : 2142-2143
• 2143 : 2143-2144
• 2144 : 2144-2145
• 2145 : 2145-2146
• 2146 : 2146-2147
• 2147 : 2147-2148
• 2148 : 2148-2149
• 2149 : 2149-2150
• 2150 : 2150-2151
• 2151 : 2151-2152
• 2152 : 2152-2153
• 2153 : 2153-2154
• 2154 : 2154-2155
• 2155 : 2155-2156
• 2156 : 2156-2157
• 2157 : 2157-2158
• 2158 : 2158-2159
• 2159 : 2159-2160
• 2160 : 2160-2161
• 2161 : 2161-2162
• 2162 : 2162-2163
• 2163 : 2163-2164
• 2164 : 2164-2165
• 2165 : 2165-2166
• 2166 : 2166-2167
• 2167 : 2167-2168
• 2168 : 2168-2169
• 2169 : 2169-2170
• 2170 : 2170-2171
• 2171 : 2171-2172
• 2172 : 2

-158-

TABLE XVII

Measurement Run No. 9

Water Temperature: 79°F.
 Nose Piece : Short
 Thrust Correction: -7.5 lbs.

RPM : Variable
 Amplifier Gain Setting: 10
 Resistance : 1000 ohms

Clearance 2"

Trdg lbs.	T corr lbs.	H ₁ rdg	v fps	J v/nd	Ardg (+)	Brdg (+)	Rrdg	F lbs	RPM
22.0	14.5	92	4.44	0.629	0.85	0.32	0.906	0.630	430
"	"	145	4.96	0.646	1.07	0.40	1.142	0.645	467
"	"	127	4.65	0.605	1.10	0.42	1.175	0.665	468
"	"	167	5.33	0.658	1.45	0.52	1.54	0.715	494
"	"	215	6.05	0.730	1.49	0.58	1.60	0.680	504
"	"	191	5.70	0.682	1.65	0.60	1.76	0.700	508
"	"	238	6.37	0.731	2.02	0.75	2.15	0.675	530
"	"	317	7.35	0.815	2.35	0.95	2.53	0.625	549
"	"	280	6.90	0.763	2.62	1.01	2.81	0.635	550
"	"	354	7.76	0.823	3.69	2.15	4.26	0.640	574
"	"	392	8.17	0.855	4.05	2.50	4.75	-----	582

TABLE XVIII

Measurement Run No. 10

Water Temperature: 78°F.
Nose Piece : Short
Thrust Correction: +0.5 lbs.

RPM : Variable
Amplifier Gain Setting: 10
Resistance : 1000 ohms

Clearance 2"

T rdg lbs.	T corr lbs.	H1 rdg	v fps	J v/nd	A rdg (+)	B rdg (-)	R rdg	F lbs.	RPM
24.9	25.4	250	6.53	0.696	2.70	3.70	4.58	0.680	572
22.0	22.5			0.719	1.45	2.40	2.80	0.635	554
17.4	17.9			0.756	0.87	1.30	1.57	0.540	526
13.0	13.5			0.785	0.65	0.85	1.07	0.465	506
7.4	7.9			0.854	0.41	0.42	0.586	0.355	464
3.6	4.1			0.940	0.35	0.14	0.376	0.280	423
0.6	1.1			1.00	0.29	0.05	0.294	0.250	397
26.4	26.9	200	5.84	0.655	1.12	2.10	2.37	0.650	543
21.6	22.1			0.683	0.82	1.35	1.58	0.580	520
15.4	15.9			0.731	0.55	0.75	0.93	0.475	486
11.5	12.0			0.768	0.42	0.45	0.615	0.375	463
5.7	6.2			0.854	0.33	0.18	0.376	0.280	416
29.1	29.6	150	5.05	0.575	1.02	1.95	2.20	0.670	534
24.7	25.2			0.605	0.72	1.30	1.49	0.575	508
18.3	18.8			0.647	0.50	0.71	0.867	0.473	475
9.1	9.6			0.767	0.29	0.15	0.326	0.270	401
33.2	33.7	100	4.13	0.481	0.96	1.85	2.08	0.730	522
26.3	26.8			0.518	0.59	1.09	1.24	0.620	486
20.9	21.4			0.556	0.40	0.59	0.711	0.460	452
14.7	15.2			0.620	0.29	0.25	0.382	0.290	406

[illegible]

ОГЛАВЛЕНИЕ

1957 : 1958, 1959 : 1960 : 1961 : 1962 : 1963 : 1964 : 1965 : 1966 : 1967 : 1968 : 1969 : 1970 : 1971 : 1972 : 1973 : 1974 : 1975 : 1976 : 1977 : 1978 : 1979 : 1980 : 1981 : 1982 : 1983 : 1984 : 1985 : 1986 : 1987 : 1988 : 1989 : 1990 : 1991 : 1992 : 1993 : 1994 : 1995 : 1996 : 1997 : 1998 : 1999 : 2000 : 2001 : 2002 : 2003 : 2004 : 2005 : 2006 : 2007 : 2008 : 2009 : 2010 : 2011 : 2012 : 2013 : 2014 : 2015 : 2016 : 2017 : 2018 : 2019 : 2020 : 2021 : 2022 : 2023 : 2024 : 2025 : 2026 : 2027 : 2028 : 2029 : 2030 : 2031 : 2032 : 2033 : 2034 : 2035 : 2036 : 2037 : 2038 : 2039 : 2040 : 2041 : 2042 : 2043 : 2044 : 2045 : 2046 : 2047 : 2048 : 2049 : 2050 : 2051 : 2052 : 2053 : 2054 : 2055 : 2056 : 2057 : 2058 : 2059 : 2060 : 2061 : 2062 : 2063 : 2064 : 2065 : 2066 : 2067 : 2068 : 2069 : 2070 : 2071 : 2072 : 2073 : 2074 : 2075 : 2076 : 2077 : 2078 : 2079 : 2080 : 2081 : 2082 : 2083 : 2084 : 2085 : 2086 : 2087 : 2088 : 2089 : 2090 : 2091 : 2092 : 2093 : 2094 : 2095 : 2096 : 2097 : 2098 : 2099 : 2100 : 2101 : 2102 : 2103 : 2104 : 2105 : 2106 : 2107 : 2108 : 2109 : 2110 : 2111 : 2112 : 2113 : 2114 : 2115 : 2116 : 2117 : 2118 : 2119 : 2120 : 2121 : 2122 : 2123 : 2124 : 2125 : 2126 : 2127 : 2128 : 2129 : 2130 : 2131 : 2132 : 2133 : 2134 : 2135 : 2136 : 2137 : 2138 : 2139 : 2140 : 2141 : 2142 : 2143 : 2144 : 2145 : 2146 : 2147 : 2148 : 2149 : 2150 : 2151 : 2152 : 2153 : 2154 : 2155 : 2156 : 2157 : 2158 : 2159 : 2160 : 2161 : 2162 : 2163 : 2164 : 2165 : 2166 : 2167 : 2168 : 2169 : 2170 : 2171 : 2172 : 2173 : 2174 : 2175 : 2176 : 2177 : 2178 : 2179 : 2180 : 2181 : 2182 : 2183 : 2184 : 2185 : 2186 : 2187 : 2188 : 2189 : 2190 : 2191 : 2192 : 2193 : 2194 : 2195 : 2196 : 2197 : 2198 : 2199 : 2200 : 2201 : 2202 : 2203 : 2204 : 2205 : 2206 : 2207 : 2208 : 2209 : 2210 : 2211 : 2212 : 2213 : 2214 : 2215 : 2216 : 2217 : 2218 : 2219 : 2220 : 2221 : 2222 : 2223 : 2224 : 2225 : 2226 : 2227 : 2228 : 2229 : 2230 : 2231 : 2232 : 2233 : 2234 : 2235 : 2236 : 2237 : 2238 : 2239 : 2240 : 2241 : 2242 : 2243 : 2244 : 2245 : 2246 : 2247 : 2248 : 2249 : 2250 : 2251 : 2252 : 2253 : 2254 : 2255 : 2256 : 2257 : 2258 : 2259 : 2260 : 2261 : 2262 : 2263 : 2264 : 2265 : 2266 : 2267 : 2268 : 2269 : 2270 : 2271 : 2272 : 2273 : 2274 : 2275 : 2276 : 2277 : 2278 : 2279 : 2280 : 2281 : 2282 : 2283 : 2284 : 2285 : 2286 : 2287 : 2288 : 2289 : 2290 : 2291 : 2292 : 2293 : 2294 : 2295 : 2296 : 2297 : 2298 : 2299 : 2300 : 2301 : 2302 : 2303 : 2304 : 2305 : 2306 : 2307 : 2308 : 2309 : 2310 : 2311 : 2312 : 2313 : 2314 : 2315 : 2316 : 2317 : 2318 : 2319 : 2320 : 2321 : 2322 : 2323 : 2324 : 2325 : 2326 : 2327 : 2328 : 2329 : 2330 : 2331 : 2332 : 2333 : 2334 : 2335 : 2336 : 2337 : 2338 : 2339 : 2340 : 2341 : 2342 : 2343 : 2344 : 2345 : 2346 : 2347 : 2348 : 2349 : 2350 : 2351 : 2352 : 2353 : 2354 : 2355 : 2356 : 2357 : 2358 : 2359 : 2360 : 2361 : 2362 : 2363 : 2364 : 2365 : 2366 : 2367 : 2368 : 2369 : 2370 : 2371 : 2372 : 2373 : 2374 : 2375 : 2376 : 2377 : 2378 : 2379 : 2380 : 2381 : 2382 : 2383 : 2384 : 2385 : 2386 : 2387 : 2388 : 2389 : 2390 : 2391 : 2392 : 2393 : 2394 : 2395 : 2396 : 2397 : 2398 : 2399 : 2400 : 2401 : 2402 : 2403 : 2404 : 2405 : 2406 : 2407 : 2408 : 2409 : 2410 : 2411 : 2412 : 2413 : 2414 : 2415 : 2416 : 2417 : 2418 : 2419 : 2420 : 2421 : 2422 : 2423 : 2424 : 2425 : 2426 : 2427 : 2428 : 2429 : 2430 : 2431 : 2432 : 2433 : 2434 : 2435 : 2436 : 2437 : 2438 : 2439 : 2440 : 2441 : 2442 : 2443 : 2444 : 2445 : 2446 : 2447 : 2448 : 2449 : 2450 : 2451 : 2452 : 2453 : 2454 : 2455 : 2456 : 2457 : 2458 : 2459 : 2460 : 2461 : 2462 : 2463 : 2464 : 2465 : 2466 : 2467 : 2468 : 2469 : 2470 : 2471 : 2472 : 2473 : 2474 : 2475 : 2476 : 2477 : 2478 : 2479 : 2480 : 2481 : 2482 : 2483 : 2484 : 2485 : 2486 : 2487 : 2488 : 2489 : 2490 : 2491 : 2492 : 2493 : 2494 : 2495 : 2496 : 2497 : 2498 : 2499 : 2500 : 2501 : 2502 : 2503 : 2504 : 2505 : 2506 : 2507 : 2508 : 2509 : 2510 : 2511 : 2512 : 2513 : 2514 : 2515 : 2516 : 2517 : 2518 : 2519 : 2520 : 2521 : 2522 : 2523 : 2524 : 2525 : 2526 : 2527 : 2528 : 2529 : 2530 : 2531 : 2532 : 2533 : 2534 : 2535 : 2536 : 2537 : 2538 : 2539 : 2540 : 2541 : 2542 : 2543 : 2544 : 2545 : 2546 : 2547 : 2548 : 2549 : 2550 : 2551 : 2552 : 2553 : 2554 : 2555 : 2556 : 2557 : 2558 : 2559 : 2560 : 2561 : 2562 : 2563 : 2564 : 2565 : 2566 : 2567 : 2568 : 2569 : 2570 : 2571 : 2572 : 2573 : 2574 : 2575 : 2576 : 2577 : 2578 : 2579 : 2580 : 2581 : 2582 : 2583 : 2584 : 2585 : 2586 : 2587 : 2588 : 2589 : 2590 : 2591 : 2592 : 2593 : 2594 : 2595 : 2596 : 2597 : 2598 : 2599 : 2600 : 2601 : 2602 : 2603 : 2604 : 2605 : 2606 : 2607 : 2608 : 2609 : 2610 : 2611 : 2612 : 2613 : 2614 : 2615 : 2616 : 2617 : 2618 : 2619 : 2620 : 2621 : 2622 : 2623 : 2624 : 2625 : 2626 : 2627 : 2628 : 2629 : 2630 : 2631 : 2632 : 2633 : 2634 : 2635 : 2636 : 2637 : 2638 : 26

[illegible]

TABLE XIX

Calibration Run No. 8

Nose Piece: Long
Resistance: 5000 ohmsRPM : 548
Amplifier Gain Setting: 6

Spring Letter Design- ation	I.F.		W	F		Ar dq		Br dq		Krdq		β_1
	lbs. + oz.	lbs. + ozs		lbs.	lbs.	(-)	(-)	(-)	(-)	(-)	deg.	
L	4 - 11	2 - 20		0.505	0.35	0.44	0.561	231.6				
I	2 - 11	1 - 30		0.265	0.15	0.22	0.266	235.9				
V	4 - 11	2 $\frac{1}{2}$ - 220		0.740	0.52	0.65	0.830	231.5				
C	3 - 11	1 $\frac{1}{2}$ - 190		0.228	0.13	0.21	0.246	238.4				
R	4 - 11	3 - 150		0.821	0.58	0.75	0.945	232.5				
N	4 - 11	4 - 40		1.007	0.72	0.90	1.150	231.5				
Q	4 - 11	2 $\frac{1}{2}$ - 40		0.641	0.54	0.56	0.775	226.1				
G	3 - 11	1 - 70		0.286	0.13	0.25	0.271	242.7				
M	3 - 11	2 - 0		0.495	0.33	0.49	0.590	236.2				
P	4 - 11	4 - 60		1.020	0.72	0.95	1.190	233.0				
W	4 - 11	1 $\frac{1}{2}$ - 200		0.480	0.31	0.46	0.555	236.1				
X	3 - 11	1 $\frac{1}{2}$ - 180		0.470	0.28	0.45	0.529	238.3				

5. on my first day

Digitized by Google

CI=92,000 Y.

2000 0100
 2000 0100

- 131 -

TABLE XX

Nose Piece: Long

Calibration Run No. 9

RPM
Amplifier Gain Setting: 6 : 548

Clearance 1-1/2"

Spring Letter Design.	I.F. lbs. + oz	W lbs. + qms	F lbs.	Resis. ohms	A. Rdg (-)	B. Rdg (-)	R. Rdg	θ deg.
P	4 - 11	4 - 70	1.03	1000 5000	1.83 0.45	1.65 0.72	2.45 0.85	221.9 238.1
M	4 - 11	2 - 0	0.496	1000 5000	0.70 0.19	0.96 0.34	1.18 0.39	234.0 240.9
Q	4 - 11	2 1/2 - 40	0.641	1000 5000	1.05 0.29	1.22 0.45	1.61 0.53	229.4 237.4
L	4 - 11	2 - 10	0.500	1000 5000	0.76 0.20	0.90 0.34	1.18 0.39	230.0 239.7
W	4 - 11	2 - 20	0.505	1000 5000	0.76 0.21	0.94 0.35	1.20 0.41	231.2 239.2
G	4 - 11	1 - 40	0.270	1000 5000	0.41 0.08	0.54 0.19	0.68 0.21	233.0 247.1
R	4 - 11	3 - 100	0.800	1000 5000	1.39 0.35	1.48 0.59	2.04 0.69	226.9 239.5
I	3 - 11	1 - 10	0.254	1000 5000	0.32 0.04	0.50 0.18	0.59 0.19	237.5 257.5
V	4 - 11	3 - 0	0.745	1000 5000	1.18 0.32	1.40 0.52	1.82 0.61	230.0 238.5
X	3 - 11	2 - 0	0.495	1000 5000	0.74 0.17	0.90 0.33	1.16 0.37	230.7 242.8
N	4 - 11	4 - 70	1.03	1000 5000	1.65 0.45	1.85 0.70	2.28 0.83	228.4 237.4

TABLE XXI

Calibration Run No. 10

Nose Piece: Long
Resistance: 1000 ohmsRPM : 548
Amplifier Gain Setting: 6

Spring Letter Design.	I.F. lbs. + oz.	W lbs. + gms.	F lbs.	A _{ldg} (-)	B _{ldg} (-)	R _{ldg}	β l deg.
L	3 - 11	2 - 0	0.495	0.59	0.80	0.995	233.6
I	3 - 11	4 - 240	0.255	0.24	0.35	0.425	235.6
C	4 - 11	2 1/2 - 50	0.648	0.83	1.04	1.33	231.4
M	4 - 11	2 - 0	0.495	0.55	0.72	0.910	232.6
W	4 - 11	1 1/2 - 200	0.480	0.54	0.81	0.971	236.4
R	4 - 11	3 - 120	0.810	0.94	1.20	1.53	231.9
P	4 - 11	4 - 60	1.02	1.48	1.48	2.09	225.0
V	4 - 11	3 - 0	0.745	0.95	1.05	1.42	227.8
N	4 - 11	4 - 60	1.02	1.29	1.48	1.96	229.0
X	3 - 11	2 - 0	0.495	0.55	0.65	0.85	229.9
G	2 - 11	1 - 40	0.270	0.25	0.30	0.39	230.3

Ol. est multum in

[illegible]

Prod. : 50215 5704
Série 0001 : 00000000000000000000

- 133 -

TABLE XXII

Calibration Run No. 11

RPM: 548

Nose Piece: Long
Resistance: 1000 ohms

Clearance 2-1/2"

Spring Letter Design.	I.F. lbs. + oz.	W lbs. + gms	F lbs.	Setting	Ardg (-)	Brdg (-)	Rrdg	β deg.
V	4 - 11	3 - 0	0.745	6 8	0.91 1.80	1.00 2.10	1.35 2.76	227.9 229.4
N	4 - 11	4 - 50	1.01	6 8	1.27 2.50	1.45 2.72	1.93 3.69	228.9 227.5
W	4 - 11	2 - 40	0.520	6 8	0.55 1.10	0.67 1.42	0.87 2.10	230.7 232.3
X	3 - 11	1 1/2 - 200	0.480	6 8	0.53 1.06	0.66 1.33	0.845 1.70	231.4 231.5
L	4 - 11	2 - 10	0.500	6 8	0.55 1.12	0.67 1.35	0.870 1.75	230.6 230.4
R	4 - 11	3 - 100	0.800	6 8	1.04 2.00	1.19 2.30	1.60 3.05	228.0 229.0
G	3 - 11	1 - 40	0.270	6 8	0.26 0.60	0.35 0.75	0.435 0.960	233.5 231.4
C	4 - 11	2 1/2 - 0	0.620	6 8	0.75 1.60	0.96 1.85	1.22 2.44	232.1 229.3
P	4 - 11	4 - 100	1.04	6 8	1.45 2.67	1.52 2.92	2.10 3.97	226.5 228.0
C	3 - 11	1/2 - 200	0.233	6 8	0.18 0.50	0.31 0.71	0.359 0.869	240.0 235.0
I	3 - 11	1 - 20	0.260	6 8	0.23 0.50	0.32 0.72	0.393 0.885	234.4 234.6

Il est mort de la rage!

21-1-1956

[illegible]

- 481 -

TABLE XXIII

Calibration Run No. 12

Nose piece: Long Resistance: 1000 ohms		Clearance 3"		RPM Amplifier Gain Setting: 8			
Spring Letter Design.	I.F. lbs. + oz.	W lbs. + gms	F lbs.	A rdg (-)	B rdg (-)	R rdg	31 deg.
M	4 - 11	2 - 0	0.495	0.75	1.25	1.46	239.0
G	3 - 11	1 - 40	0.270	0.35	0.72	0.80	244.2
W	3 - 11	2 - 40	0.520	1.05	1.40	1.74	233.3
C	3 - 11	1 - 200	0.233	0.25	0.65	0.695	249.0
V	4 - 11	2 1/4 - 220	0.740	1.42	2.20	2.62	237.2
P	4 - 11	4 - 100	1.04	2.48	2.75	3.70	228.0
I	3 - 11	1 - 30	0.565	0.35	0.62	0.711	240.6
Q	4 - 11	2 1/4 - 40	0.641	1.44	1.79	2.29	231.3
R	4 - 11	3 - 120	0.810	1.92	2.25	2.96	229.6
L	3 - 11	2 - 20	0.505	1.00	1.38	1.70	234.1
N	4 - 11	4 - 40	1.007	2.35	2.75	3.63	229.5

El. of nat. philology

8 : n l t a n l e i l l o m

Classical

3000 0001 : 2001 12 21

1912年

- 132 -

TABLE XXIV

Measurement Pun No. 11

Water Temperature: 80°F.
Nose Piece : Long
Thrust Correction: +0.7 lbs.

RPM : 548
Amplifier Gain Setting: 6
Resistance : 5000 ohms

Clearance 1"

T lbs.	T lbs.	T corr lbs.	H ₁ rdg	v fps	J v/nd	A rdg (-)	B rdg (+)	R rdg	F lbs	β ₂ deg	β ₁ deg	α rdg deg	Δy (-)	y (+)
57.0	57.7	0	0	0	0	2.00	4.75	5.15	4.52	102.7	233.9	332	104.2	26.0
55.5	56.2	15	1.59	0.177		2.00	4.35	4.79	4.20	104.6		332	101.3	25.3
52.5	53.2	28	2.17	0.241		1.95	4.35	4.77	4.19	104.1		331	100.8	25.2
48.8	49.2	45	2.75	0.306		1.78	4.18	4.55	3.99	103.0		331	101.9	25.5
45.8	46.5	53	2.99	0.331		1.75	4.10	4.46	3.91	103.0		331	101.9	25.5
42.5	43.2	70	3.43	0.381		1.70	3.90	4.25	3.73	103.5		331	101.4	25.4
37.5	38.2	115	4.39	0.489		1.60	3.63	3.96	3.47	103.7		332	102.2	25.5
34.0	34.7	129	4.66	0.518		1.60	3.50	3.84	3.36	104.4		332	101.5	25.4
29.4	30.1	165	5.27	0.585		1.55	3.25	3.60	3.16	105.4		332	100.5	25.1
25.7	26.4	203	5.85	0.650		1.49	3.00	3.35	2.94	106.3		332	99.6	24.9
21.4	22.1	238	6.32	0.705		1.45	2.90	3.24	2.84	106.5		333	100.4	25.1
17.3	18.0	277	6.81	0.759		1.38	2.79	3.10	2.72	105.9		333	101.0	25.2
12.8	13.5	321	7.38	0.819		1.38	2.55	2.90	2.54	108.3		333	98.6	24.7
9.6	10.3	360	7.79	0.863		1.42	2.40	2.79	2.44	110.5		333	96.4	24.1
7.1	7.8	389	8.09	0.899		1.40	2.42	2.79	2.44	110.0		332	95.9	24.5
4.2	4.9	429	8.50	0.944		1.37	2.40	2.76	2.42	109.6		332	96.3	26.6
1.0	1.7	461	8.80	0.979		1.38	2.35	2.72	2.38	110.3		332	95.6	23.9

TABLE XXV

Measurement Run No. 12

Water Temperature: 80°F.
 Nose Piece : Long
 Thrust Correction: +0.7 lbs.

Clearance 1-1/4"

RPM : 548
 Amplifier Gain Setting: 6
 Resistance : 5000 ohms

T rdg lbs.	I corr lbs.	H ₁ rdg	v fps	J v/nd	A rdg (-)	B rdg (+)	R rdg	F lbs	β ₂ deg	β ₁ deg	¹ r dg deg	4Y (-) ^o	Y (+) ^o
57.8	58.5	0	0	0	1.10	2.80	3.01	3.24	101.4	237.7	326	102.3	25.6
56.5	57.2	14	1.54	0.171	1.05	2.75	2.95	3.17	100.8			102.9	25.7
47.5	48.2	45	2.75	0.306	0.95	2.52	2.70	2.90	100.6			103.1	25.8
44.5	45.2	59	3.15	0.350	0.92	2.45	2.62	2.81	100.4		327	104.3	26.1
37.5	38.2	96	4.03	0.447	0.85	2.25	2.40	2.58	100.7			104.0	26.0
31.7	32.5	148	4.99	0.555	0.75	2.02	2.15	2.31	100.4			104.3	26.1
26.4	27.1	184	5.55	0.618	0.72	1.92	2.05	2.21	100.3			104.4	26.1
22.3	23.0	204	5.85	0.651	0.70	1.80	1.92	2.06	101.2		325	103.5	25.9
18.0	18.7	267	6.70	0.740	0.65	1.72	1.84	1.98	100.7			104.0	26.0
13.8	14.5	303	7.16	0.797	0.66	1.61	1.74	1.87	102.2			102.5	25.6
9.9	10.6	351	7.69	0.852	0.65	1.51	1.65	1.77	103.3			101.4	25.4
7.0	7.7	378	7.97	0.886	0.66	1.52	1.66	1.78	103.2		326	101.5	25.4
6.5	7.2	394	8.14	0.906	0.70	1.45	1.61	1.73	105.7			99.0	24.8
3.8	4.5	424	8.45	0.940	0.66	1.40	1.55	1.67	105.2			99.5	24.9
1.1	1.8	449	8.69	0.967	0.64	1.42	1.56	1.68	104.2			100.5	25.1

51. 07 NOT IN RECORDS

7-1-1 1/4

Corrected + original : 80 lbs.
: Long
: end

- 137 -

TABLE XXVI

Measurement Run No. 13

Water Temperature: 80°F.

Nose Piece : Long

Thrust Correction: +0.7 lbs.

Clearance 1-1/2"

 RPM : 548
 Amplifier Gain Setting: 6
 Resistance : 5000 ohms

T	I	T	H	V	J	A	B	R	F	B	B	a	4	Y
rdg	corr	l	rdg	fps	v/nd	rdg	rdg	rdg	lbs	deg	deg	rdg	deg	°
lbs.	lbs.	lbs.	lbs.	lbs.	lbs.	(-)	(+)						(-)	(+)
56.3	57.0	3	0.71	0.03	0.55	1.80	1.89	2.34	107.1	241.6	323	97.5	24.4	
54.5	55.2	15	1.54	0.171	0.62	2.00	2.09	2.59	107.3			97.3	24.3	
52.0	52.7	25	2.05	0.228	0.60	1.75	1.85	2.29	109.0		322	94.5	24.4	
46.7	47.4	45	2.75	0.306	0.50	1.71	1.79	2.21	106.4			97.1	24.3	
40.0	40.7	79	3.64	0.405	0.41	1.55	1.61	1.99	104.8			98.7	24.7	
36.5	37.2	102	4.15	0.461	0.39	1.48	1.53	1.89	104.8			98.7	24.7	
31.5	32.2	131	4.70	0.522	0.37	1.40	1.45	1.80	104.8		325	101.7	25.4	
28.4	29.1	169	5.32	0.592	0.35	1.37	1.42	1.76	104.3			102.2	25.5	
23.6	24.3	205	5.88	0.652	0.28	1.29	1.32	1.63	102.2			104.3	26.1	
19.1	19.8	246	6.42	0.715	0.28	1.22	1.26	1.56	102.9			103.6	25.9	
16.4	17.1	288	6.97	0.772	0.31	1.19	1.23	1.52	104.6		324	100.0	25.2	
11.7	12.4	329	7.45	0.828	0.30	1.13	1.17	1.45	104.8			100.7	25.2	
9.0	9.7	354	7.73	0.859	0.32	1.10	1.16	1.42	106.2			99.3	24.8	
5.6	6.3	394	8.14	0.907	0.30	1.03	1.08	1.34	106.2			99.3	24.8	
1.7	2.4	441	8.61	0.959	0.29	0.99	1.04	1.29	106.2			99.3	24.8	

TABLE XXVII

Measurement Run No. 14

Water Temperature: 80°F.
 Nose piece : Long
 Thrust Correction: +0.7 lbs.

Clearance 1-3/4"

RPM : 548
 Amplifier Gain Setting: 6
 Resistance : 1000 ohms

T _{tdg} lbs.	T _{corr} lbs.	H ₁ rdg	v fps	J v/nd	A _{rdg} (-)	B _{rdg} (+)	R _{rdg} lbs	B ₂ deg	B ₁ deg	α _{rdg} deg	Δy deg	Y (+)
56.5	57.2	0	0	0	1.0	5.0	5.1	101.3	230.7	322	91.4	22.9
54.0	54.7	16	1.64	0.183	1.0	4.8	4.9	101.8		323	91.9	23.0
49.0	49.7	35	3.43	0.270	0.88	4.6	4.68	100.8		323	92.9	23.2
46.8	47.5	45	2.75	0.307	0.80	4.40	4.48	100.3		324	94.4	23.6
41.0	41.7	77	3.60	0.400	0.70	3.95	4.01	100.0		324	94.7	23.7
34.5	35.2	116	4.42	0.592	0.60	3.75	3.80	99.1		324	95.6	23.9
29.0	29.7	150	5.01	0.559	0.55	3.50	3.55	98.9		324	95.8	23.9
26.0	26.7	180	5.50	0.611	0.50	3.35	3.39	98.5		323	95.2	23.8
21.6	22.3	220	6.09	0.676	0.48	3.15	3.19	98.7		323	95.0	23.8
17.0	17.7	260	6.61	0.736	0.48	3.00	3.05	99.1		323	94.6	23.7
13.0	13.7	303	7.16	0.979	0.44	2.82	2.86	98.9		323	94.8	23.7
8.6	9.3	346	7.61	0.849	0.45	2.65	2.69	99.6		322	93.1	23.2
5.0	5.7	375	7.95	0.882	0.46	2.55	2.60	100.2		322	92.5	23.1
3.0	3.7	402	8.23	0.916	0.45	2.50	2.55	100.2		322	92.5	23.1
1.2	1.9	416	8.36	0.930	0.53	2.42	2.48	102.3		322	90.4	22.6

At. 5th Ave. 2000-1900

[illegible]

01/02/00 7-3/70

IMMIGRANT COLLECTION; 40.5 mps.
MUSE, FACE; 100.2
MUSE FOR IMMIGRANTS; 100.2

- 931 -

TABLE XXVIII

Measurement Run No. 15

Water Temperature: 80°F. RPM : 548
 Nose Piece : Long Amplifier Gain Setting: 6
 Thrust Correction: +0.7 lbs. Clearance 2" Resistance : 1000 ohms

T _{tdg} lbs.	T _{corr} lbs.	H ₁ rdg	v fps	J v/nd	A _{rdg} (-)	B _{rdg} (+)	R _{rdg} lbs	F lbs	β ₂ deg	β ₁ deg	α _{rdg} deg	4Y deg	Y (+)
56.0	56.7	1	0.41	0.046	0.70	3.50	3.57	1.70	101.3	231.2	322	91.9	23.0
55.0	55.7	14	1.53	0.171	0.70	3.40	3.47	1.64	101.6		322	91.6	22.9
52.0	52.7	27	2.13	0.237	0.70	3.55	3.62	1.72	101.1		322	92.1	23.0
47.0	47.7	45	2.75	0.306	0.50	3.45	3.50	1.66	98.2		321	96.0	24.0
44.5	45.2	57	3.09	0.344	0.45	3.32	3.36	1.60	97.7		321	96.5	24.1
41.3	42.0	73	3.50	0.390	0.38	3.15	3.19	1.52	96.9		321	97.3	24.3
39.0	29.7	89	3.87	0.430	0.39	3.00	3.04	1.45	97.4		321	96.8	24.2
32.5	33.2	130	4.68	0.520	0.31	2.79	2.92	1.40	96.3		321	97.9	24.5
28.4	29.1	166	5.29	0.588	0.25	2.72	2.74	1.31	95.3		322	97.9	24.5
23.8	24.5	207	5.89	0.656	0.25	2.45	2.47	1.19	95.8		322	97.4	24.4
19.4	20.1	240	6.35	0.707	0.21	2.38	2.40	1.16	95.0		322	98.2	24.5
14.8	15.5	284	6.91	0.769	0.15	2.28	2.30	1.11	93.8		322	99.4	24.9
10.2	10.9	327	7.40	0.822	0.25	2.25	2.27	1.10	96.3		322	97.9	24.5
6.2	6.9	368	7.88	0.874	0.31	2.10	2.12	1.03	98.4		322	94.8	23.7
3.1	3.8	404	8.26	0.919	0.29	2.15	2.17	1.05	97.7		322	95.5	23.9
1.4	2.1	419	8.39	0.932	0.25	2.00	2.02	0.98	97.1		322	96.1	24.0

LIVELY

21. COM. 2003 + 2004

BAC : 0001 : 9306181000

Clarendon 30

INFLUENZA COLLECTION: 10.1.1933.
NOTE: Bica : 1000.
NETHER INFLUENZA: 1000.

Y	Y _h	ph ₁	I'	z _h	z	ph ₂	ph ₃	ph ₄	ph ₅	ph ₆	ph ₇	L	V	I _h	TI02	ph ₁
(+)	ph ₀	ph ₀	ph ₀	ph ₀	ph ₀	(+)	(-)	ph ₁	ph ₁	ph ₁	ph ₁	ph ₁	ph ₁	ph ₁	ph ₁	ph ₁
0.00	0.10	5.00	0.100	0.101	0.101	0.101	0.101	0.101	0.101	0.101	0.101	0.101	0.101	0.101	0.101	0.101
0.00	0.10	5.00	0.100	0.101	0.101	0.101	0.101	0.101	0.101	0.101	0.101	0.101	0.101	0.101	0.101	0.101
0.00	0.10	5.00	0.100	0.101	0.101	0.101	0.101	0.101	0.101	0.101	0.101	0.101	0.101	0.101	0.101	0.101
0.00	0.10	5.00	0.100	0.101	0.101	0.101	0.101	0.101	0.101	0.101	0.101	0.101	0.101	0.101	0.101	0.101
0.00	0.10	5.00	0.100	0.101	0.101	0.101	0.101	0.101	0.101	0.101	0.101	0.101	0.101	0.101	0.101	0.101
0.00	0.10	5.00	0.100	0.101	0.101	0.101	0.101	0.101	0.101	0.101	0.101	0.101	0.101	0.101	0.101	0.101
0.00	0.10	5.00	0.100	0.101	0.101	0.101	0.101	0.101	0.101	0.101	0.101	0.101	0.101	0.101	0.101	0.101
0.00	0.10	5.00	0.100	0.101	0.101	0.101	0.101	0.101	0.101	0.101	0.101	0.101	0.101	0.101	0.101	0.101
0.00	0.10	5.00	0.100	0.101	0.101	0.101	0.101	0.101	0.101	0.101	0.101	0.101	0.101	0.101	0.101	0.101
0.00	0.10	5.00	0.100	0.101	0.101	0.101	0.101	0.101	0.101	0.101	0.101	0.101	0.101	0.101	0.101	0.101
0.00	0.10	5.00	0.100	0.101	0.101	0.101	0.101	0.101	0.101	0.101	0.101	0.101	0.101	0.101	0.101	0.101
0.00	0.10	5.00	0.100	0.101	0.101	0.101	0.101	0.101	0.101	0.101	0.101	0.101	0.101	0.101	0.101	0.101
0.00	0.10	5.00	0.100	0.101	0.101	0.101	0.101	0.101	0.101	0.101	0.101	0.101	0.101	0.101	0.101	0.101
0.00	0.10	5.00	0.100	0.101	0.101	0.101	0.101	0.101	0.101	0.101	0.101	0.101	0.101	0.101	0.101	0.101
0.00	0.10	5.00	0.100	0.101	0.101	0.101	0.101	0.101	0.101	0.101	0.101	0.101	0.101	0.101	0.101	0.101
0.00	0.10	5.00	0.100	0.101	0.101	0.101	0.101	0.101	0.101	0.101	0.101	0.101	0.101	0.101	0.101	0.101
0.00	0.10	5.00	0.100	0.101	0.101	0.101	0.101	0.101	0.101	0.101	0.101	0.101	0.101	0.101	0.101	0.101
0.00	0.10	5.00	0.100	0.101	0.101	0.101	0.101	0.101	0.101	0.101	0.101	0.101	0.101	0.101	0.101	0.101
0.00	0.10	5.00	0.100	0.101	0.101	0.101	0.101	0.101	0.101	0.101	0.101	0.101	0.101	0.101	0.101	0.101
0.00	0.10	5.00	0.100	0.101	0.101	0.101	0.101	0.101	0.101	0.101	0.101	0.101	0.101	0.101	0.101	0.101
0.00	0.10	5.00	0.100	0.101	0.101	0.101	0.101	0.101	0.101	0.101	0.101	0.101	0.101	0.101	0.101	0.101
0.00	0.10	5.00	0.100	0.101	0.101	0.101	0.101	0.101	0.101	0.101	0.101	0.101	0.101	0.101	0.101	0.101
0.00	0.10	5.00	0.100	0.101	0.101	0.101	0.101	0.101	0.101	0.101	0.101	0.101	0.101	0.101	0.101	0.101
0.00	0.10	5.00	0.100	0.101	0.101	0.101	0.101	0.101	0.101	0.101	0.101	0.101	0.101	0.101	0.101	0.101
0.00	0.10	5.00	0.100	0.101	0.101	0.101	0.101	0.101	0.101	0.101	0.101	0.101	0.101	0.101	0.101	0.101
0.00	0.10	5.00	0.100	0.101	0.101	0.101	0.101	0.101	0.101	0.101	0.101	0.101	0.101	0.101	0.101	0.101
0.00	0.10	5.00	0.100	0.101	0.101	0.101	0.101	0.101	0.101	0.101	0.101	0.101	0.101	0.101	0.101	0.101
0.00	0.10	5.00	0.100	0.101	0.101	0.101	0.101	0.101	0.101	0.101	0.101	0.101	0.101	0.101	0.101	0.101
0.00	0.10	5.00	0.100	0.101	0.101	0.101	0.101	0.101	0.101	0.101	0.101	0.101	0.101	0.101	0.101	0.101
0.00	0.10	5.00	0.100	0.101	0.101	0.101	0.101	0.101	0.101	0.101	0.101	0.101	0.101	0.101	0.101	0.101
0.00	0.10	5.00	0.100	0.101	0.101	0.101	0.101	0.101	0.101	0.101	0.101	0.101	0.101	0.101	0.101	0.101
0.00	0.10	5.00	0.100	0.101	0.101	0.101	0.101	0.101	0.101	0.101	0.101	0.101	0.101	0.101	0.101	0.101
0.00	0.10	5.00	0.100	0.101	0.101	0.101	0.101	0.101	0.101	0.101	0.101	0.101	0.101	0.101	0.101	0.101
0.00	0.10	5.00	0.100	0.101	0.101	0.101	0.101	0.101	0.101	0.101	0.101	0.101	0.101	0.101	0.101	0.101
0.00	0.10	5.00	0.100	0.101	0.101	0.101	0.101	0.101	0.101	0.101	0.101	0.101	0.101	0.101	0.101	0.101
0.00	0.10	5.00	0.100	0.101	0.101	0.101	0.101	0.101	0.101	0.101	0.101	0.101	0.101	0.101	0.101	0.101
0.00	0.10	5.00	0.100	0.101	0.101	0.101	0.101	0.101	0.101	0.101	0.101	0.101	0.101	0.101	0.101	0.101
0.00	0.10	5.00	0.100	0.101	0.101	0.101	0.101	0.101	0.101	0.101	0.101	0.101	0.101	0.101	0.101	0.101
0.00	0.10	5.00	0.100	0.101	0.101	0.101	0.101	0.101	0.101	0.101	0.101	0.101	0.101	0.101	0.101	0.101
0.00	0.10	5.00	0.100	0.101	0.101	0.101	0.101	0.101	0.101	0.101	0.101	0.101	0.101	0.101	0.101	0.101
0.00	0.10	5.00	0.100	0.101	0.101	0.101	0.101	0.101	0.101	0.101	0.101	0.101	0.101	0.101	0.101	0.101
0.00	0.10	5.00	0.100	0.101	0.101	0.101	0.101	0.101	0.101	0.101	0.101	0.101	0.101	0.101	0.101	0.101
0.00	0.10	5.00	0.100	0.101	0.101	0.101	0.101	0.101	0.101	0.101	0.101	0.101	0.101	0.101	0.101	0.101
0.00	0.10	5.00	0.100	0.101	0.101	0.101	0.101	0.101	0.101	0.101	0.101	0.101	0.101	0.101	0.101	0.101
0.00	0.10	5.00	0.100	0.101	0.101	0.101	0.101	0.101	0.101	0.101	0.101	0.101	0.101	0.101	0.101	0.101
0.00	0.10	5.00	0.100	0.101	0.101	0.101	0.101	0.101	0.101	0.101	0.101	0.101	0.101	0.101	0.101	0.101
0.00	0.10	5.00	0.100	0.101	0.101	0.101	0.101	0.101	0.101	0.101	0.101	0.101	0.101	0.101	0.101	0.101
0.00	0.10	5.00	0.100	0.101	0.101	0.101	0.101	0.101	0.101	0.1						

TABLE XXIX

Measurement Run No. 16

Water Temperature: 80°F.
 Nose Piece : Long
 Thrust Correction: +0.7 lbs.

RPM : 548
 Amplifier Gain Setting: 6
 Resistance : 1000 ohms

Clearance 2-1/4"

T _{rdg} lbs.	T _{corr} lbs.	H ₁ rdg	v fps	J v/nd	A _{rdg} (-)	B _{rdg} (+)	R _{rdg}	F lbs	β ₂ deg	β ₁ deg	α _{rdg} deg	4Y deg	Y (+)
55.5	56.2	1	0.410	0.046	0.50	2.55	2.60	1.295	101.0	231.3	325	95.3	23.8
55.6	56.3	15	1.54	0.171	0.75	2.25	2.38	1.195	108.4		325	87.9	22.0
52.2	52.9	28	2.17	0.241	0.65	2.45	2.54	1.265	104.8		321	87.5	21.9
47.7	48.4	45	2.75	0.306	0.54	2.35	2.42	1.215	102.9		321	89.4	22.4
42.3	43.0	72	3.47	0.387	0.41	2.12	2.17	1.095	100.9		321	91.4	22.9
38.7	39.4	97	4.04	0.449	0.40	2.00	2.04	1.040	101.3		323	93.0	23.2
34.4	35.1	125	4.59	0.505	0.34	1.88	1.92	0.980	100.2		323	94.1	23.5
25.5	26.2	193	5.70	0.635	0.30	1.73	1.75	0.900	99.8		323	94.5	23.6
21.2	21.9	228	6.20	0.690	0.24	1.65	1.67	0.865	98.3		323	96.0	24.0
17.8	18.5	255	6.55	0.729	0.25	1.60	1.62	0.840	98.9		325	97.4	24.3
13.9	13.6	294	7.04	0.783	0.25	1.55	1.57	0.815	99.1		325	97.2	24.3
10.5	11.2	325	7.40	0.822	0.24	1.46	1.48	0.775	99.3		325	97.0	24.2
8.4	9.1	348	7.64	0.849	0.22	1.44	1.46	0.765	98.7		324	96.6	24.1
7.1	7.8	364	7.82	0.870	0.25	1.37	1.39	0.730	100.3		324	95.0	23.8
3.1	3.8	404	8.25	0.918	0.24	1.36	1.38	0.725	100.0		324	95.3	23.8
2.5	3.2	419	8.39	0.932	0.24	1.31	1.34	0.705	100.4		324	94.9	23.7
1.0	1.7	431	8.51	0.945	0.25	1.31	1.34	0.705	100.8		324	94.5	23.6

di. on the 10th

CLASSIC 8-11-14

1907
 1908
 1909
 1910
 1911
 1912
 1913
 1914
 1915
 1916
 1917
 1918
 1919
 1920
 1921
 1922
 1923
 1924
 1925
 1926
 1927
 1928
 1929
 1930
 1931
 1932
 1933
 1934
 1935
 1936
 1937
 1938
 1939
 1940
 1941
 1942
 1943
 1944
 1945
 1946
 1947
 1948
 1949
 1950
 1951
 1952
 1953
 1954
 1955
 1956
 1957
 1958
 1959
 1960
 1961
 1962
 1963
 1964
 1965
 1966
 1967
 1968
 1969
 1970
 1971
 1972
 1973
 1974
 1975
 1976
 1977
 1978
 1979
 1980
 1981
 1982
 1983
 1984
 1985
 1986
 1987
 1988
 1989
 1990
 1991
 1992
 1993
 1994
 1995
 1996
 1997
 1998
 1999
 2000
 2001
 2002
 2003
 2004
 2005
 2006
 2007
 2008
 2009
 2010
 2011
 2012
 2013
 2014
 2015
 2016
 2017
 2018
 2019
 2020
 2021
 2022
 2023
 2024
 2025
 2026
 2027
 2028
 2029
 2030
 2031
 2032
 2033
 2034
 2035
 2036
 2037
 2038
 2039
 2040
 2041
 2042
 2043
 2044
 2045
 2046
 2047
 2048
 2049
 2050
 2051
 2052
 2053
 2054
 2055
 2056
 2057
 2058
 2059
 2060
 2061
 2062
 2063
 2064
 2065
 2066
 2067
 2068
 2069
 2070
 2071
 2072
 2073
 2074
 2075
 2076
 2077
 2078
 2079
 2080
 2081
 2082
 2083
 2084
 2085
 2086
 2087
 2088
 2089
 2090
 2091
 2092
 2093
 2094
 2095
 2096
 2097
 2098
 2099
 2100
 2101
 2102
 2103
 2104
 2105
 2106
 2107
 2108
 2109
 2110
 2111
 2112
 2113
 2114
 2115
 2116
 2117
 2118
 2119
 2120
 2121
 2122
 2123
 2124
 2125
 2126
 2127
 2128
 2129
 2130
 2131
 2132
 2133
 2134
 2135
 2136
 2137
 2138
 2139
 2140
 2141
 2142
 2143
 2144
 2145
 2146
 2147
 2148
 2149
 2150
 2151
 2152
 2153
 2154
 2155
 2156
 2157
 2158
 2159
 2160
 2161
 2162
 2163
 2164
 2165
 2166
 2167
 2168
 2169
 2170
 2171
 2172
 2173
 2174
 2175
 2176
 2177
 2178
 2179
 2180
 2181
 2182
 2183
 2184
 2185
 2186
 2187
 2188
 2189
 2190
 2191
 2192
 2193
 2194
 2195
 2196
 2197
 2198
 2199
 2200
 2201
 2202
 2203
 2204
 2205
 2206
 2207
 2208
 2209
 2210
 2211
 2212
 2213
 2214
 2215
 2216
 2217
 2218
 2219
 2220
 2221
 2222
 2223
 2224
 2225
 2226
 2227
 2228
 2229
 2230
 2231
 2232
 2233
 2234
 2235
 2236
 2237
 2238
 2239
 2240
 2241
 2242
 2243
 2244
 2245
 2246
 2247
 2248
 2249
 2250
 2251
 2252
 2253
 2254
 2255
 2256
 2257
 2258
 2259
 2260
 2261
 2262
 2263
 2264
 2265
 2266
 2267
 2268
 2269
 2270
 2271
 2272
 2273
 2274
 2275
 2276
 2277
 2278
 2279
 2280
 2281
 2282
 2283
 2284
 2285
 2286
 2287
 2288
 2289
 2290
 2291
 2292
 2293
 2294
 2295
 2296
 2297
 2298
 2299
 2300
 2301
 2302
 2303
 2304
 2305
 2306
 2307
 2308
 2309
 2310
 2311
 2312
 2313
 2314
 2315
 2316
 2317
 2318
 2319
 2320
 2321
 2322
 2323
 2324
 2325
 2326
 2327
 2328
 2329
 2330
 2331
 2332
 2333
 2334
 2335
 2336
 2337
 2338
 2339
 2340
 2341
 2342
 2343
 2344
 2345
 2346
 2347
 2348
 2349
 2350
 2351
 2352
 2353
 2354
 2355
 2356
 2357
 2358
 2359
 2360
 2361

- 141 -

TABLE XXX

Measurement Run No. 17

Water Temperature: 80°F.
 Nose Piece : Long
 Thrust Correction: +0.7 lbs.

Clearance 2-1/2"

RPM : 548
 Amplifier Gain Setting: 8
 Resistance : 1000 ohms

T rdg lbs.	T corr lbs.	H ₁ rdg	v fps	J v/nd	A rdg (-)	B rdg (+)	R rdg	F lbs	β ₂ deg	β ₁ deg	a rdg deg	Δγ deg	γ (+)
56.6	57.3	1	0.41	0.046	0.70	3.10	3.18	0.840	102.7	230.7	324	92.0	23.0
56.3	57.0	15	1.59	0.177	1.00	3.20	3.35	0.888	107.3		324	87.4	21.9
50.9	51.6	33	2.36	0.263	0.82	3.15	3.26	0.865	104.6		324	90.1	22.5
47.5	48.2	45	2.75	0.306	0.72	3.00	3.09	0.820	103.4		324	91.3	22.8
39.2	39.9	92	3.93	0.438	0.60	2.60	2.67	0.710	108.0		324	91.7	22.9
43.8	44.5	66	3.34	0.371	0.69	2.80	2.88	0.765	103.8		324	90.9	22.7
35.0	35.7	120	4.49	0.500	0.55	2.49	2.55	0.683	102.4		322	90.3	22.6
27.8	28.5	169	5.33	0.593	0.45	2.28	2.34	0.625	101.1		322	91.6	22.9
24.7	25.4	202	5.82	0.649	0.37	2.19	2.22	0.600	99.6		322	93.1	23.2
16.8	17.5	273	6.79	0.752	0.35	1.95	1.98	0.535	100.2		322	92.5	23.1
12.2	12.9	315	7.29	0.810	0.31	1.88	1.91	0.578	99.3		322	93.4	23.4
8.4	9.1	356	7.73	0.860	0.29	1.80	1.83	0.500	99.1		322	93.6	23.4
5.1	5.8	392	8.13	0.907	0.30	1.65	1.68	0.455	100.3		322	92.4	23.1
3.5	4.2	405	8.26	0.919	0.30	1.70	1.73	0.475	100.0		322	92.7	23.2
2.4	3.1	421	8.41	0.935	0.29	1.65	1.67	0.455	99.9		322	92.8	23.2
0	0.7	446	8.67	0.962	0.25	1.65	1.67	0.455	98.6		322	94.1	23.5

TABLE XXXI

Measurement Run No. 18

Water Temperature: 80°F.

Nose piece : Long

Thrust Correction: +0.7 lbs.

Clearance 2-3/4"

RPM : 548

Amplifier Gain Setting: 8

Resistance : 1000 ohms

Trdg lbs.	Y corr. lbs.	H ₁ rdg	V fps	J v/nd	Ardg (-)	Brdg (+)	Rrdg	F lbs	B ₂ deg	B ₁ deg	Yrdg deg	ΔY deg	Y (+)
55.5	56.2	3	0.71	0.079	0.85	3.00	3.11	0.864	105.7	233.3	325	92.6	23.1
55.5	56.2	18	1.74	0.194	1.10	2.75	2.97	0.824	111.7		325	86.6	21.6
47.2	47.9	45	2.75	0.306	0.60	2.60	2.67	0.774	103.0		325	95.3	23.3
40.1	40.8	85	3.78	0.421	0.45	2.28	2.32	0.655	101.2		325	97.1	24.3
34.9	35.6	119	4.48	0.598	0.37	2.15	2.18	0.620	99.8		325	98.5	24.6
31.2	31.9	140	4.85	0.539	0.33	2.11	2.14	0.600	98.9		324	98.4	24.6
27.9	28.6	170	5.34	0.593	0.29	1.99	2.02	0.578	98.3		324	99.0	24.7
23.2	23.9	210	5.94	0.661	0.22	1.88	1.90	0.548	96.7		324	100.6	25.1
17.5	18.2	260	6.61	0.735	0.21	1.75	1.77	0.513	96.8		324	100.5	25.1
13.5	14.2	293	7.02	0.782	0.15	1.68	1.69	0.492	95.1		324	102.2	25.5
10.8	11.5	328	7.41	0.824	0.15	1.64	1.66	0.485	95.2		324	102.1	25.5
7.4	8.1	363	7.82	0.869	0.15	1.55	1.56	0.460	95.5		324	101.8	25.4
2.9	3.6	412	8.32	0.926	0.15	1.50	1.52	0.450	95.7		324	101.6	25.4
1.6	2.3	428	8.49	0.943	0.15	1.45	1.46	0.433	95.9		324	101.4	25.3

TABLE XXXII

Measurement Run No. 19

Water Temperature: 80°F.
 Nose Piece : Long
 Thrust Correction: +0.7 lbs.

Clearance 3"

RPM : 548
 Amplifier Gain Setting: 8
 Resistance : 1000 ohms

T rdg lbs.	T corr lbs.	H ₁ rdg	v fps	J v/nd	A rdg (-)	B rdg (+)	R rdg	F lbs	β_2 deg	β_1 deg	α rdg deg	4Y deg	Y deg
56.0	56.7	1	0.41	0.046	0.70	2.0	2.12	0.617	109.2	235.9	323	89.7	22.4
55.5	56.2	17	1.69	0.188	0.70	1.90	2.03	0.538	110.2		323	88.7	22.2
47.0	47.7	45	2.75	0.306	0.55	1.80	1.88	0.551	107.0		323	91.9	23.0
40.8	41.5	85	3.78	0.421	0.36	1.52	1.56	0.470	103.3		323	95.6	23.9
35.0	35.7	120	4.49	0.499	0.34	1.49	1.53	0.462	102.8		323	96.1	24.0
32.8	33.5	138	4.82	0.536	0.31	1.45	1.48	0.448	102.1		325	98.8	24.7
28.0	28.7	178	5.48	0.609	0.28	1.39	1.42	0.432	101.4		325	99.5	24.9
24.3	25.0	206	5.89	0.653	0.25	1.31	1.34	0.410	100.8		325	100.1	25.0
20.5	21.2	242	6.38	0.709	0.22	1.25	1.27	0.395	100.0		325	100.9	25.2
15.3	16.0	285	6.91	0.770	0.21	1.19	1.21	0.380	100.0		325	100.9	25.2
10.5	11.2	327	7.40	0.823	0.15	1.10	1.11	0.353	97.2		325	103.7	25.9
6.9	7.6	365	7.84	0.870	0.19	1.00	1.02	0.330	100.7		325	100.2	25.1
3.3	4.0	400	8.20	0.912	0.14	1.00	1.01	0.328	97.9		325	103.0	25.8
2.1	2.8	415	8.36	0.928	0.15	0.97	0.98	0.320	98.8		325	102.1	25.5
-1.8	-1.1	469	8.89	0.988	0.13	0.98	0.99	0.323	97.6		325	103.3	25.8

El. de mod. fructuolam

CL 100.1925 20

1008
 1009
 1010
 1011
 1012
 1013
 1014
 1015
 1016
 1017
 1018
 1019
 1020
 1021
 1022
 1023
 1024
 1025
 1026
 1027
 1028
 1029
 1030
 1031
 1032
 1033
 1034
 1035
 1036
 1037
 1038
 1039
 1040
 1041
 1042
 1043
 1044
 1045
 1046
 1047
 1048
 1049
 1050
 1051
 1052
 1053
 1054
 1055
 1056
 1057
 1058
 1059
 1060
 1061
 1062
 1063
 1064
 1065
 1066
 1067
 1068
 1069
 1070
 1071
 1072
 1073
 1074
 1075
 1076
 1077
 1078
 1079
 1080
 1081
 1082
 1083
 1084
 1085
 1086
 1087
 1088
 1089
 1090
 1091
 1092
 1093
 1094
 1095
 1096
 1097
 1098
 1099
 1100
 1101
 1102
 1103
 1104
 1105
 1106
 1107
 1108
 1109
 1110
 1111
 1112
 1113
 1114
 1115
 1116
 1117
 1118
 1119
 1120
 1121
 1122
 1123
 1124
 1125
 1126
 1127
 1128
 1129
 1130
 1131
 1132
 1133
 1134
 1135
 1136
 1137
 1138
 1139
 1140
 1141
 1142
 1143
 1144
 1145
 1146
 1147
 1148
 1149
 1150
 1151
 1152
 1153
 1154
 1155
 1156
 1157
 1158
 1159
 1160
 1161
 1162
 1163
 1164
 1165
 1166
 1167
 1168
 1169
 1170
 1171
 1172
 1173
 1174
 1175
 1176
 1177
 1178
 1179
 1180
 1181
 1182
 1183
 1184
 1185
 1186
 1187
 1188
 1189
 1190
 1191
 1192
 1193
 1194
 1195
 1196
 1197
 1198
 1199
 1200
 1201
 1202
 1203
 1204
 1205
 1206
 1207
 1208
 1209
 1210
 1211
 1212
 1213
 1214
 1215
 1216
 1217
 1218
 1219
 1220
 1221
 1222
 1223
 1224
 1225
 1226
 1227
 1228
 1229
 1230
 1231
 1232
 1233
 1234
 1235
 1236
 1237
 1238
 1239
 1240
 1241
 1242
 1243
 1244
 1245
 1246
 1247
 1248
 1249
 1250
 1251
 1252
 1253
 1254
 1255
 1256
 1257
 1258
 1259
 1260
 1261
 1262
 1263
 1264
 1265
 1266
 1267
 1268
 1269
 1270
 1271
 1272
 1273
 1274
 1275
 1276
 1277
 1278
 1279
 1280
 1281
 1282
 1283
 1284
 1285
 1286
 1287
 1288
 1289
 1290
 1291
 1292
 1293
 1294
 1295
 1296
 1297
 1298
 1299
 1300
 1301
 1302
 1303
 1304
 1305
 1306
 1307
 1308
 1309
 1310
 1311
 1312
 1313
 1314
 1315
 1316
 1317
 1318
 1319
 1320
 1321
 1322
 1323
 1324
 1325
 1326
 1327
 1328
 1329
 1330
 1331
 1332
 1333
 1334
 1335
 1336
 1337
 1338
 1339
 1340
 1341
 1342
 1343
 1344
 1345
 1346
 1347
 1348
 1349
 1350
 1351
 1352
 1353
 1354
 1355
 1356
 1357
 1358
 1359
 1360
 1361
 1362
 1363
 1364
 1365
 1366
 1367
 1368
 1369
 1370
 1371
 1372
 1373
 1374
 1375
 1376
 1377
 1378
 1379
 1380
 1381
 1382
 1383
 1384
 1385
 1386
 1387
 1388
 1389
 1390
 1391
 1392
 1393
 1394
 1395
 1396
 1397
 1398
 1399
 1400
 1401
 1402
 1403
 1404
 1405
 1406
 1407
 1408
 1409
 1410
 1411
 1412
 1413
 1414
 1415
 1416
 1417
 1418
 1419
 1420
 1421
 1422
 1423
 1424
 1425
 1426
 1427
 1428
 1429
 1430
 1431
 1432
 1433
 1434
 1435
 1436
 1437
 1438
 1439
 1440
 1441
 1442
 1443
 1444
 1445
 1446
 1447
 1448
 1449
 1450
 1451
 1452
 1453
 1454
 1455
 1456
 1457
 1458
 1459
 1460
 1461
 1462

— 441 —

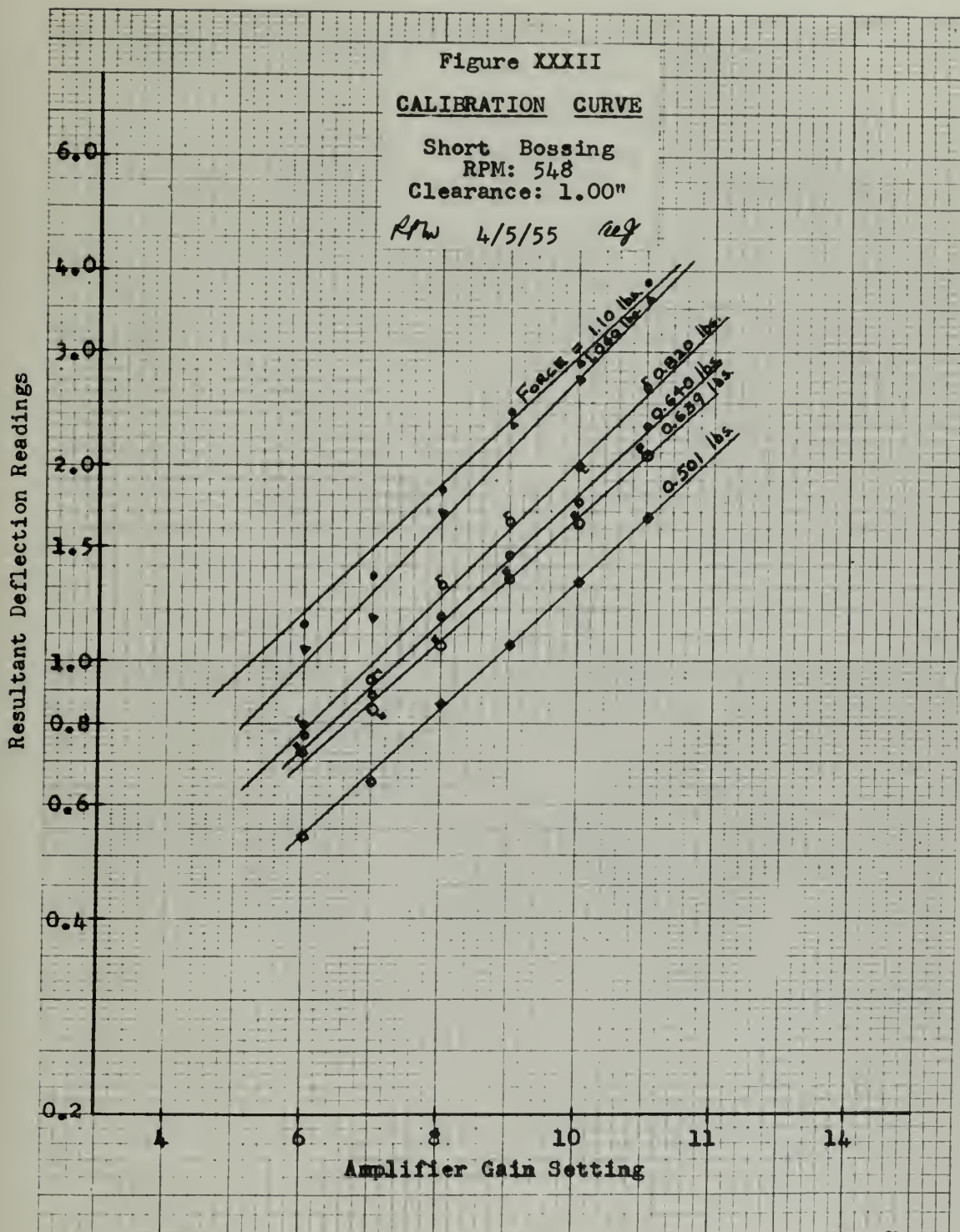


Figure XXXIII

CALIBRATION CURVE

Short Bossing

RPM: 548

Clearance: 1.00"

RMW 4/5/55 aeg

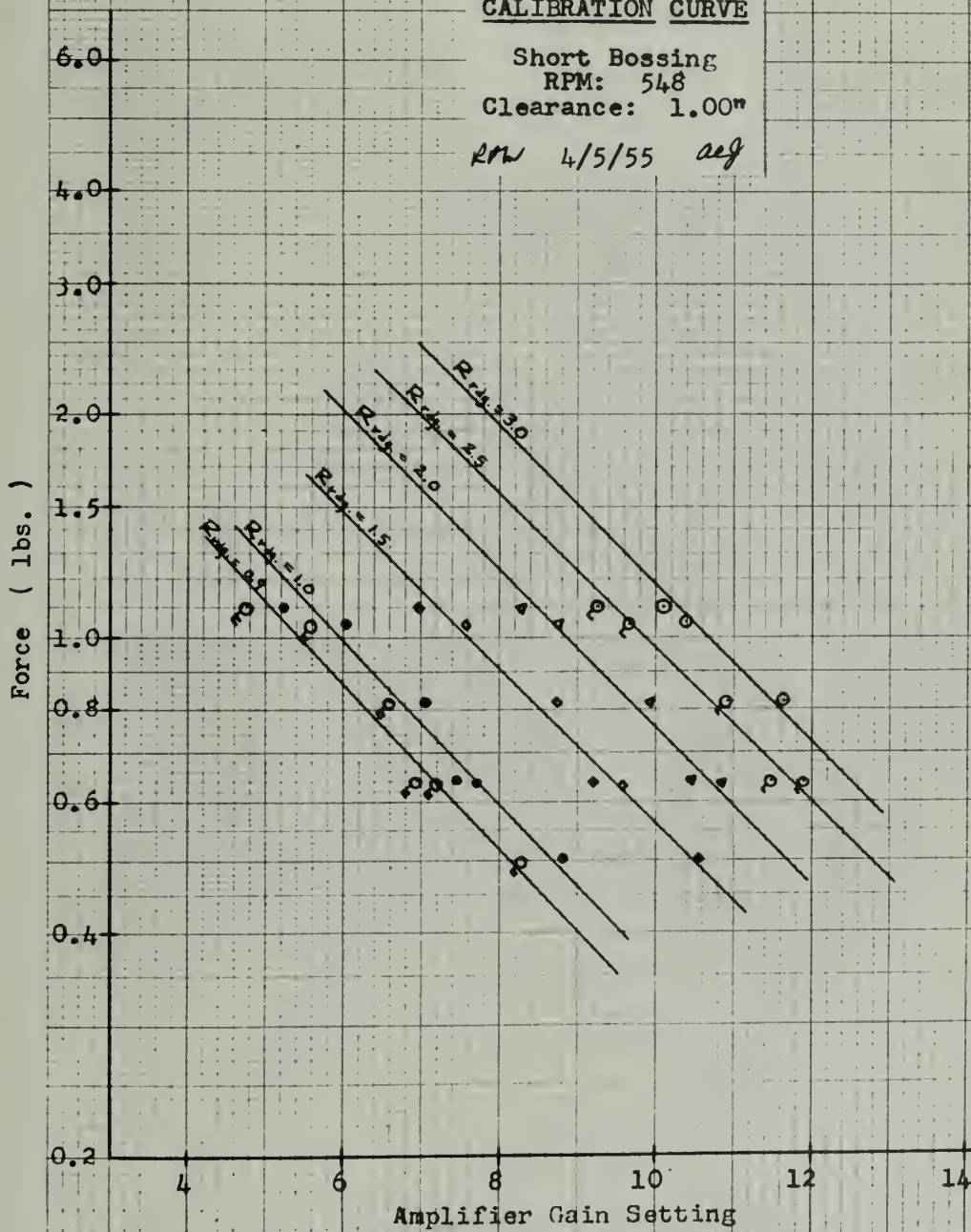
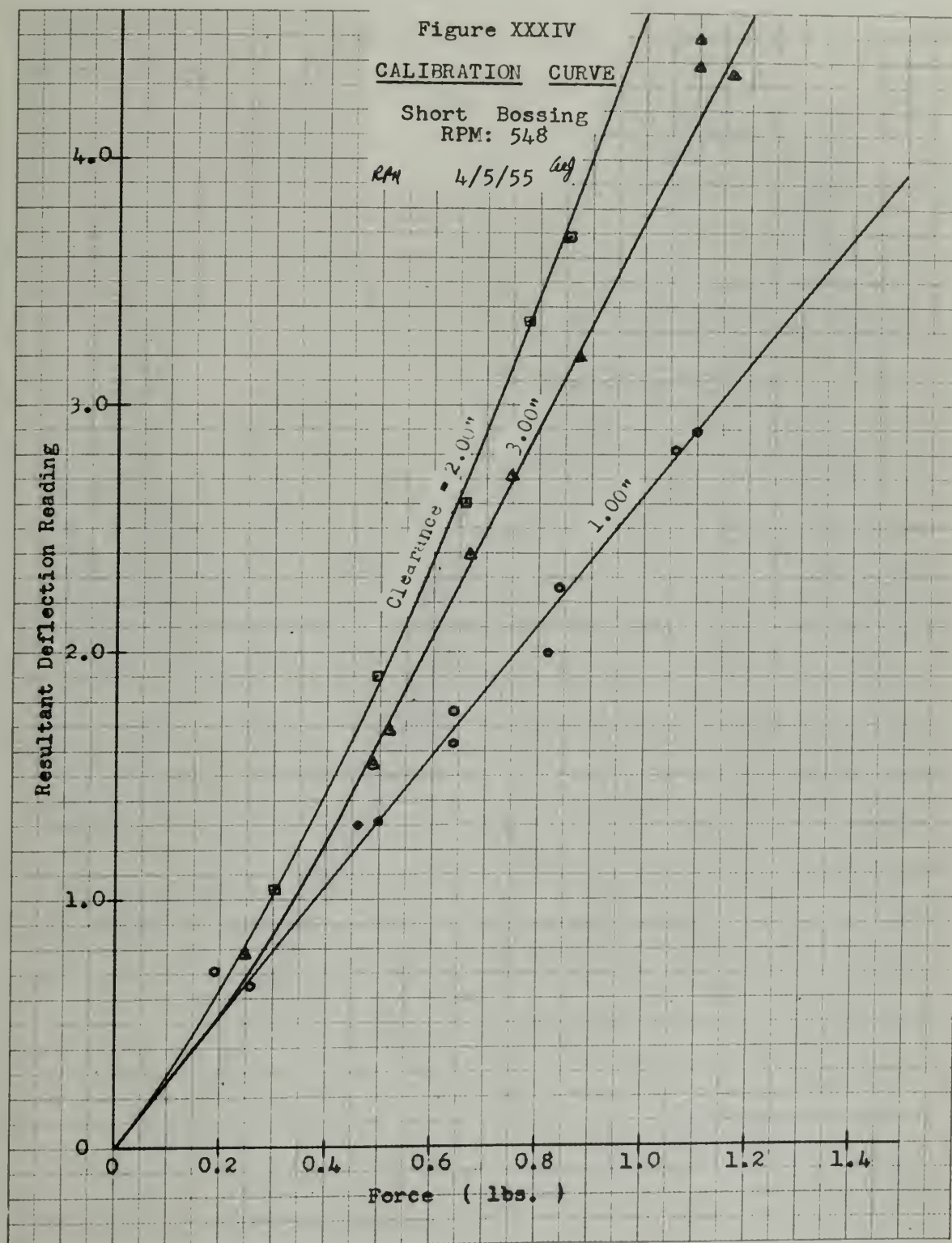


Figure XXXIV

CALIBRATION CURVE

Short Bossing
RPM: 548

RAH 4/5/55 *Wag*



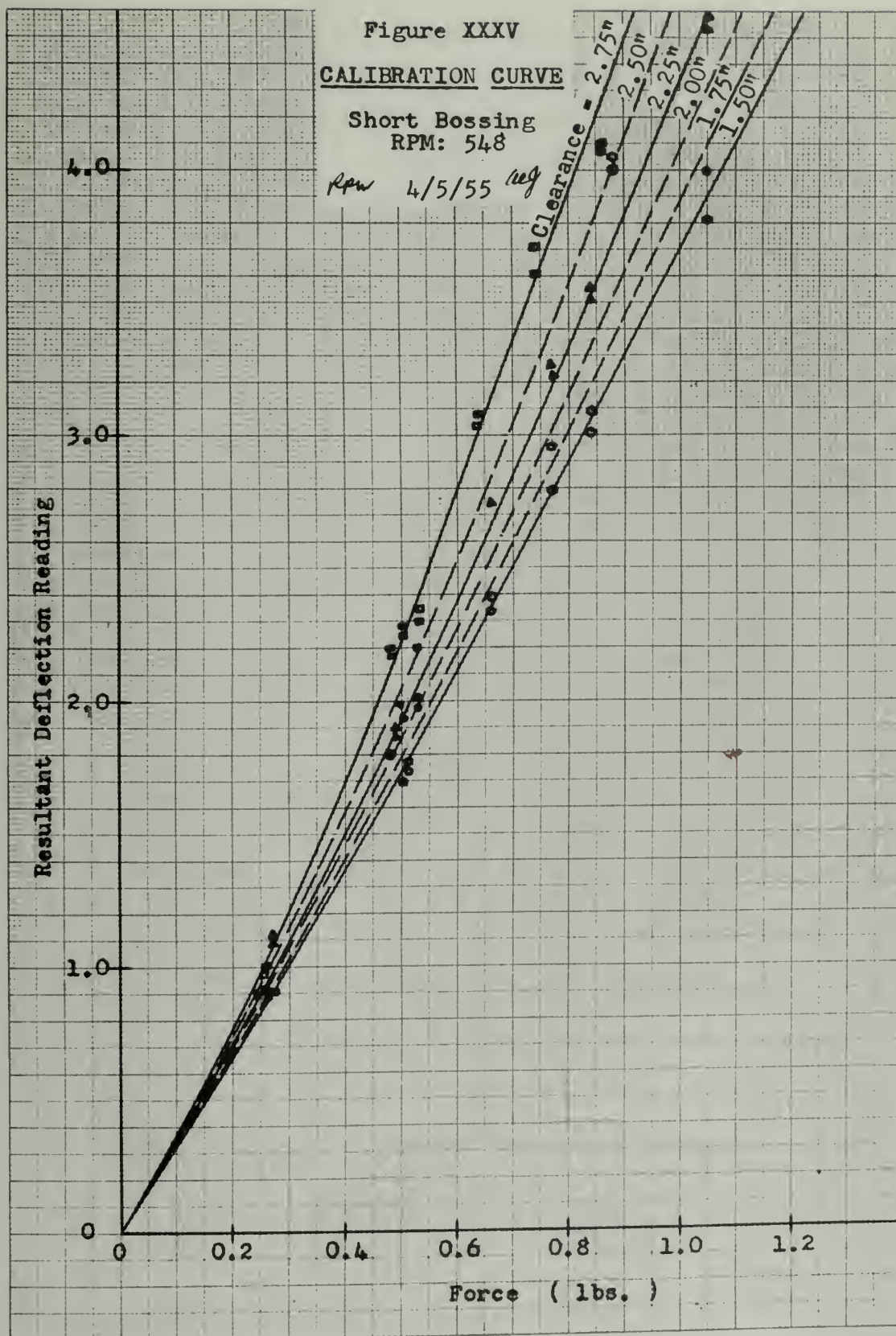


Figure XXXVI

CALIBRATION CURVE

Short Bossing

RPM: 548

Clearance: 2.00"

Row 4/5/55 leg

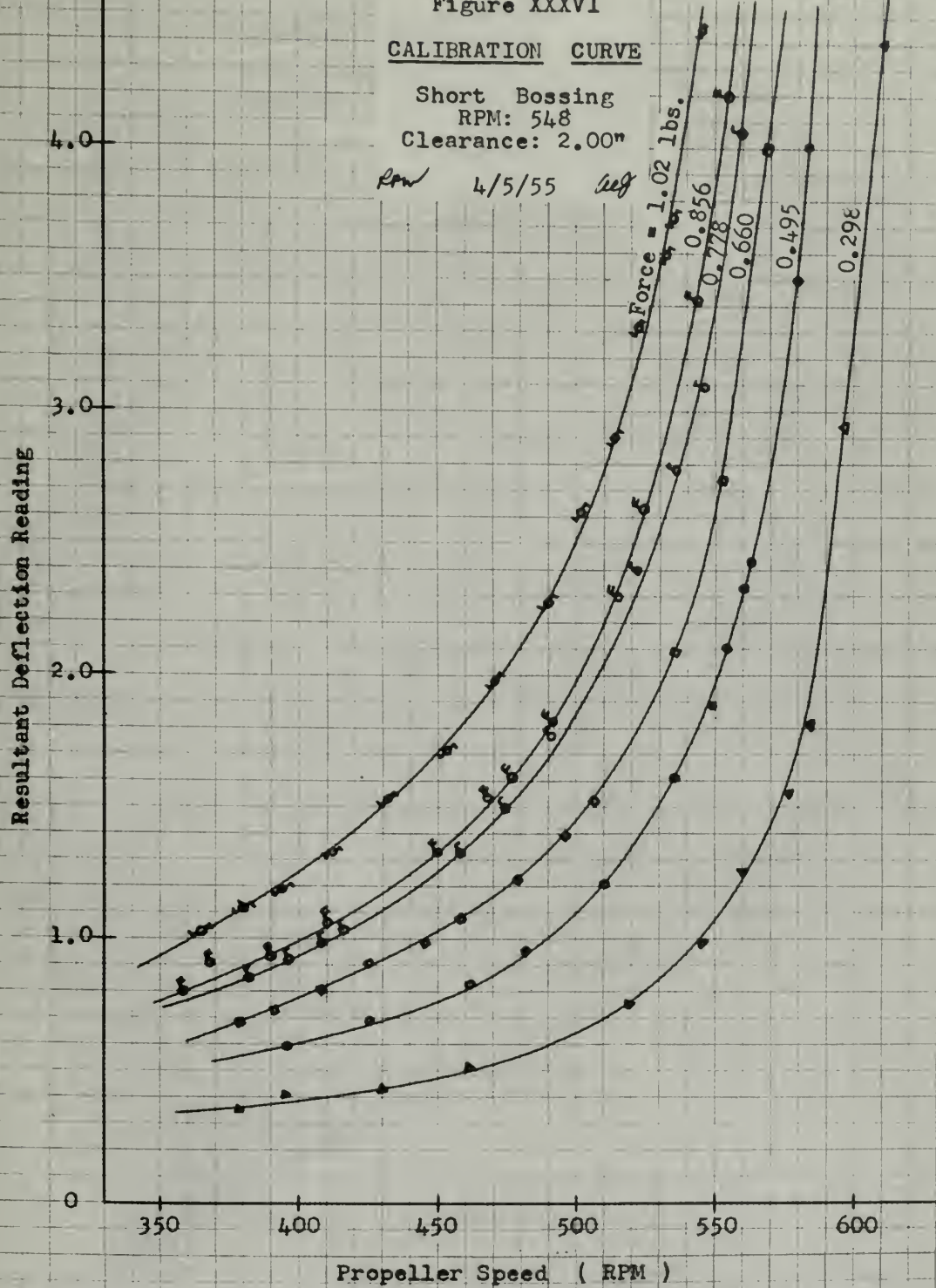


Figure XXXVII

CALIBRATION CURVE

Short Bossing
Clearance: 2.00"

Law 4/5/55 (leg)

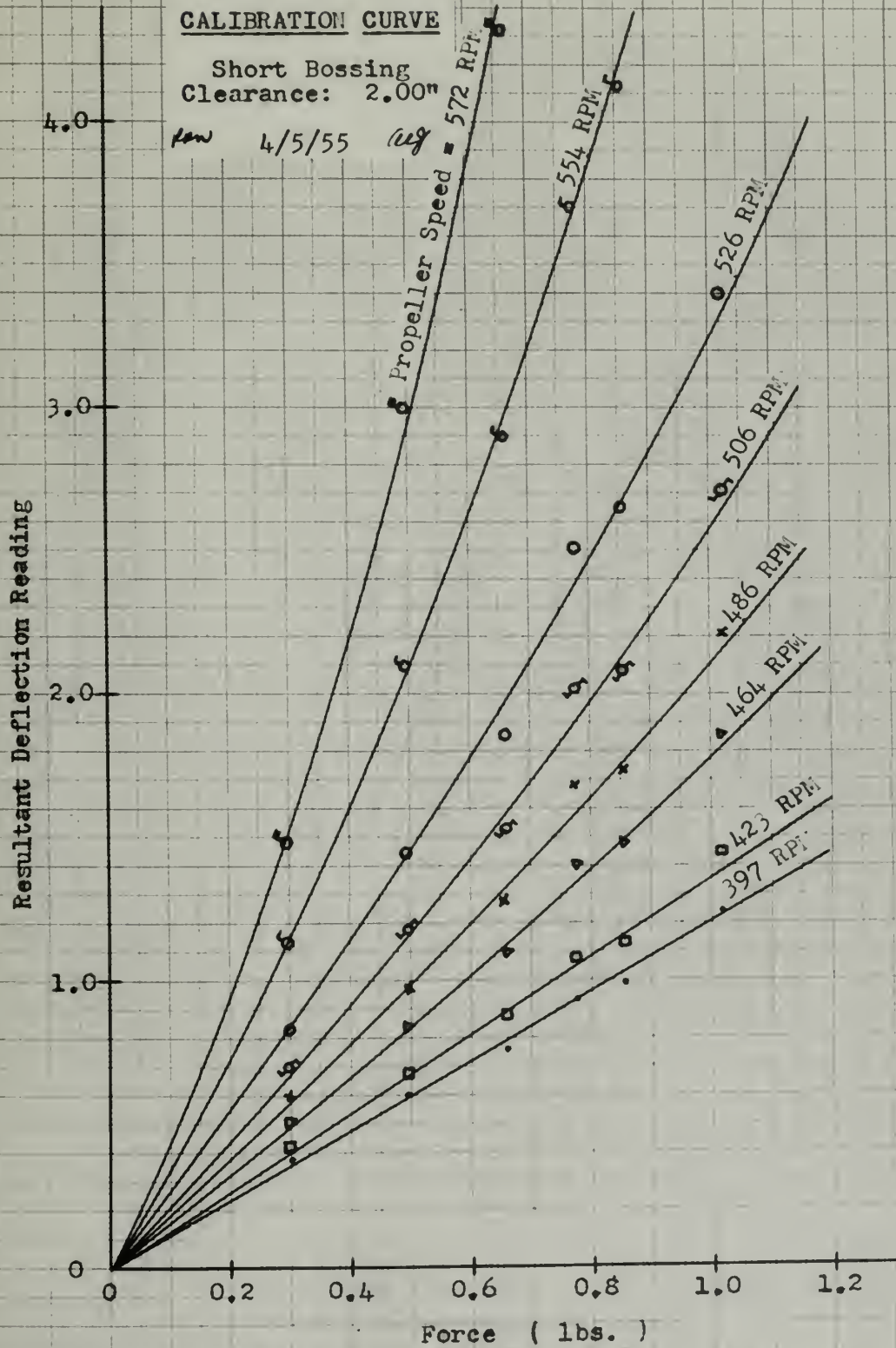


Figure XXXVIII

CALIBRATION CURVE

Short Bossing
Clearance: 2.00"

HW 4/5/55 *leg*

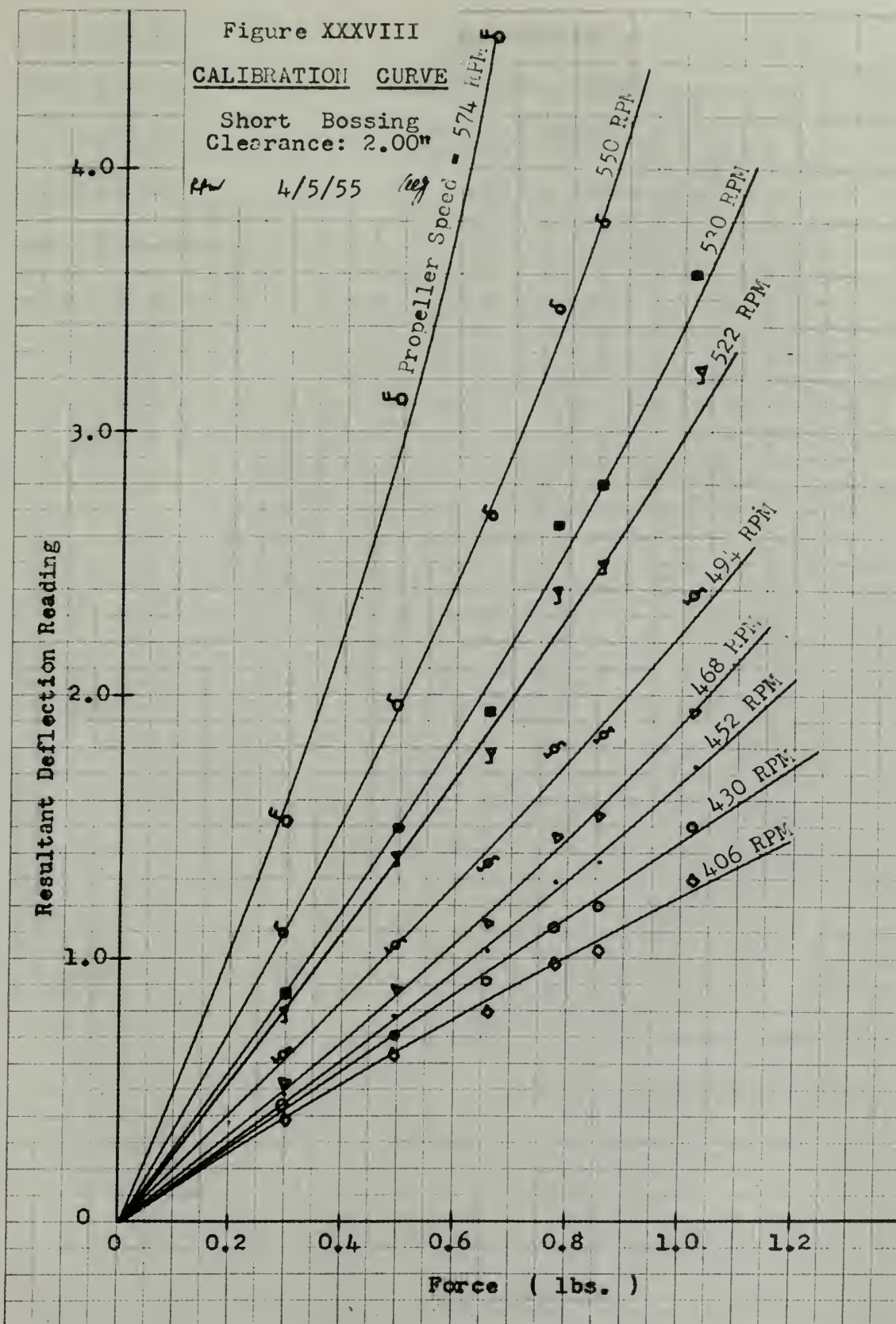


Figure XXXIX

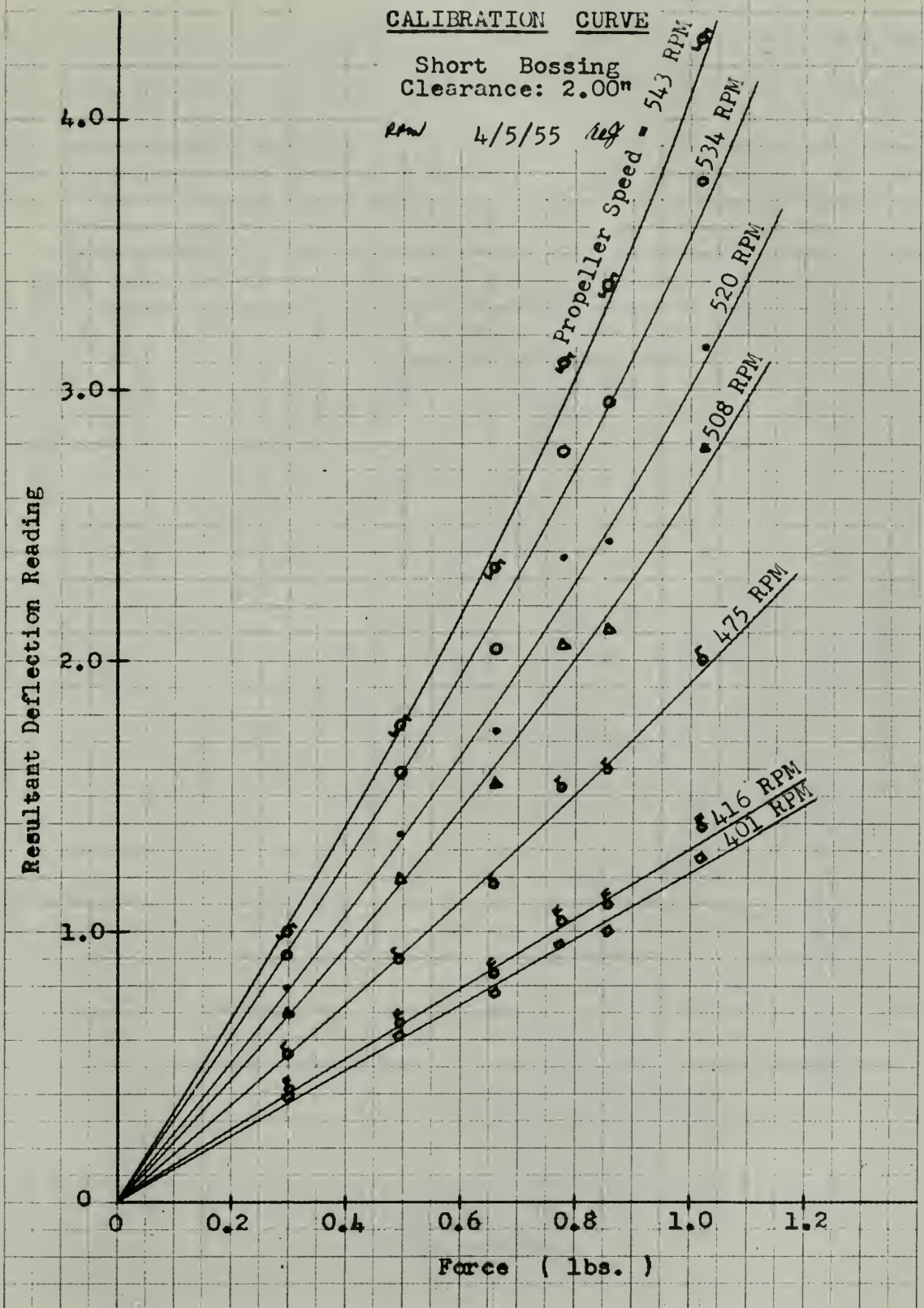
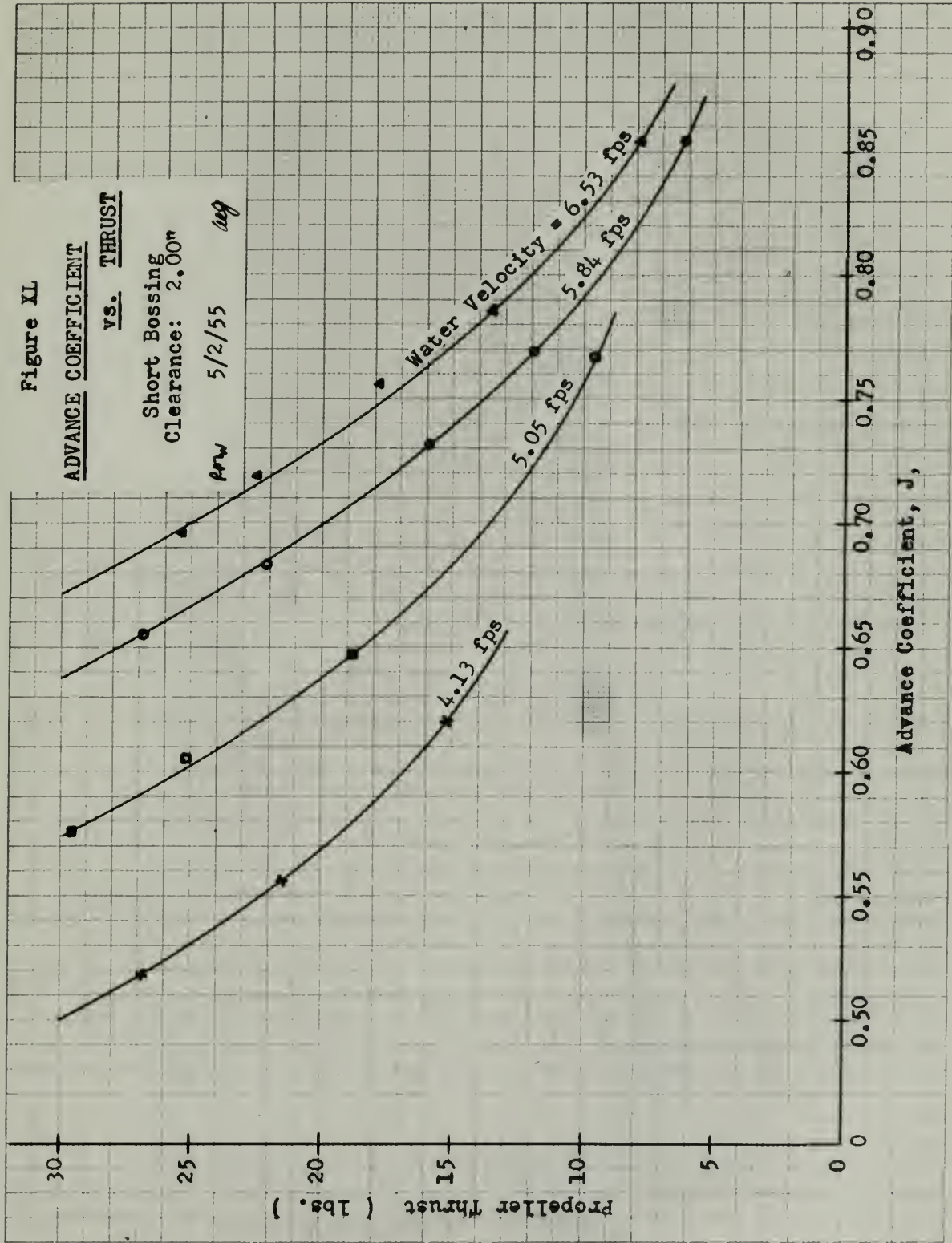


Figure XL

ADVANCE COEFFICIENT
vs. THRUST

Short Bossing
Clearance: 2.00"

5/2/55 *avg*



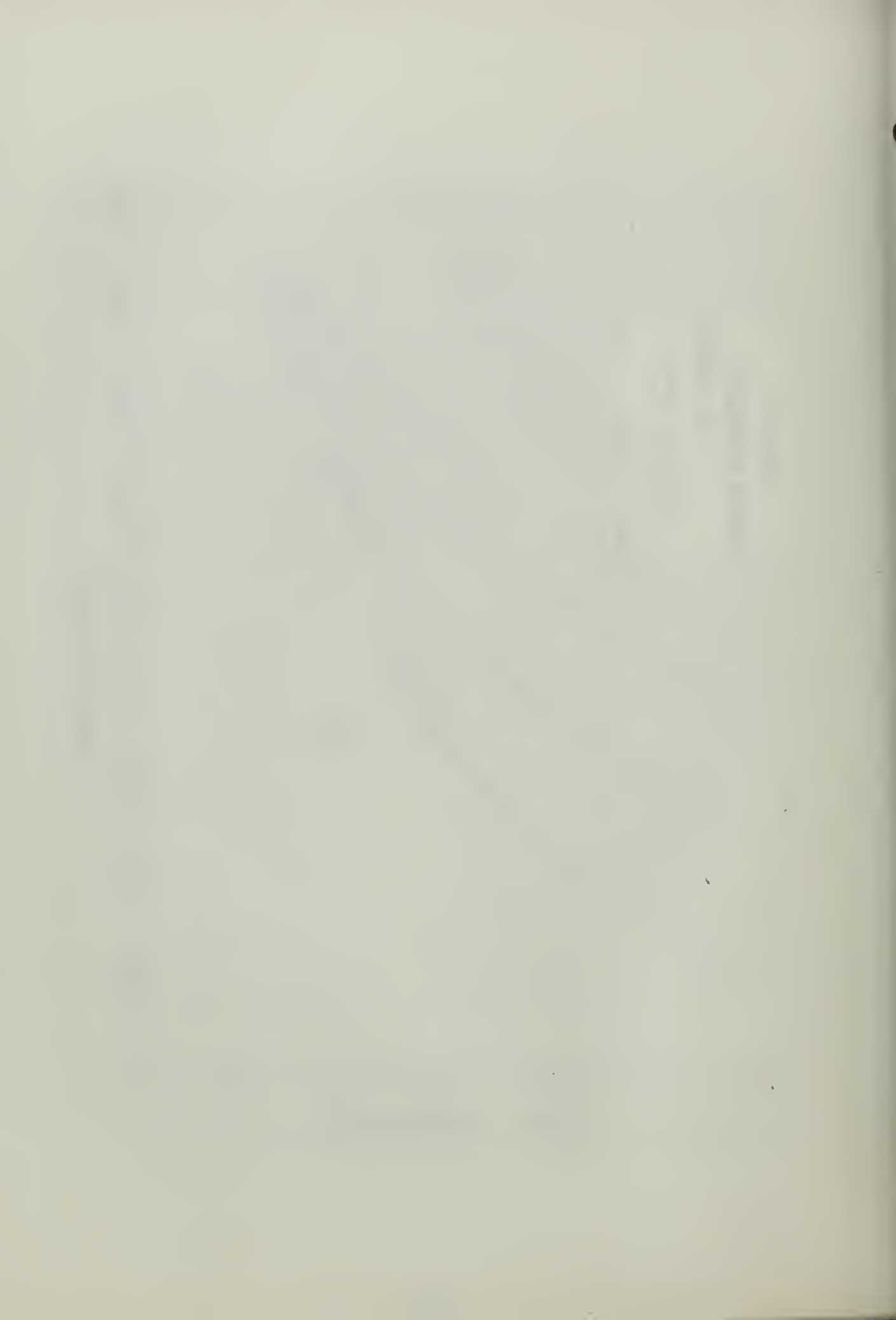
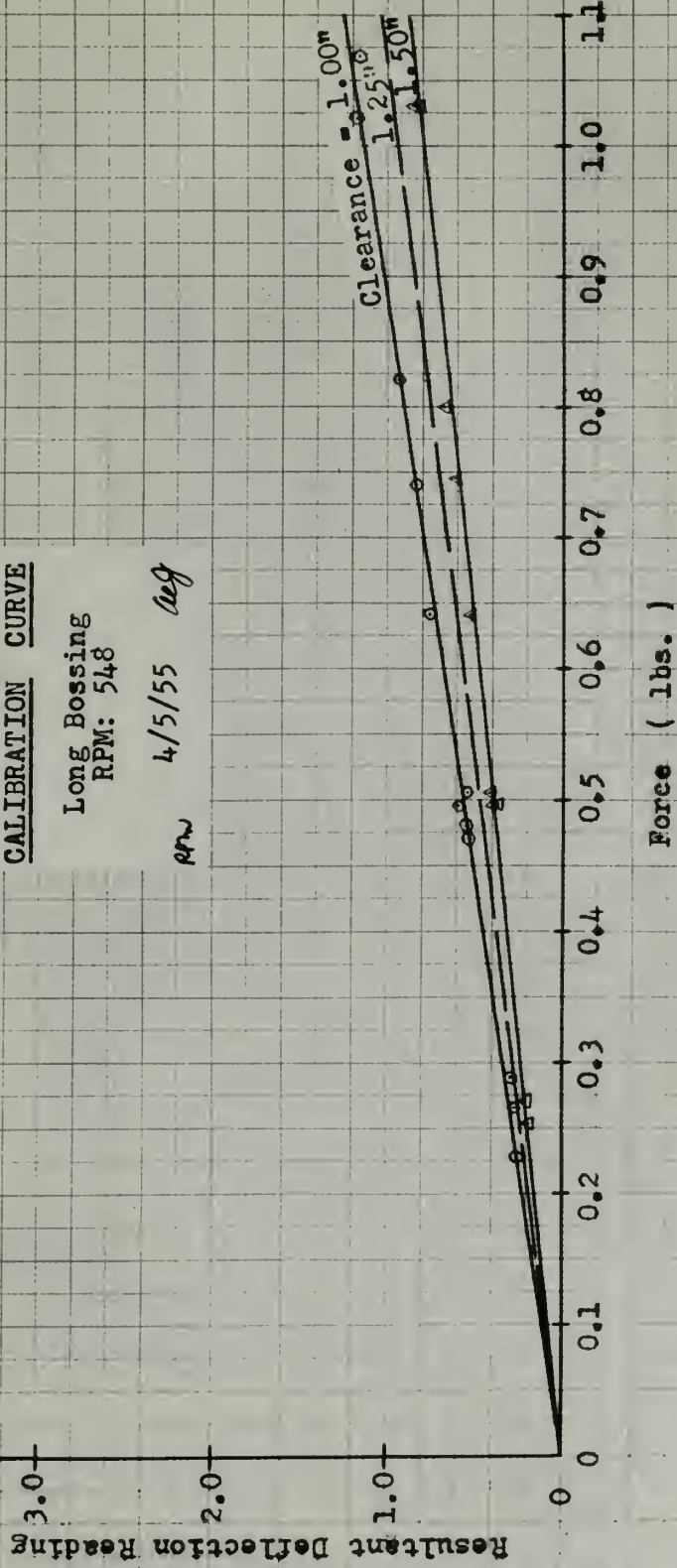


Figure XLI

CALIBRATION CURVE

Long Bossing
RPM: 548

4/5/55 *avg*



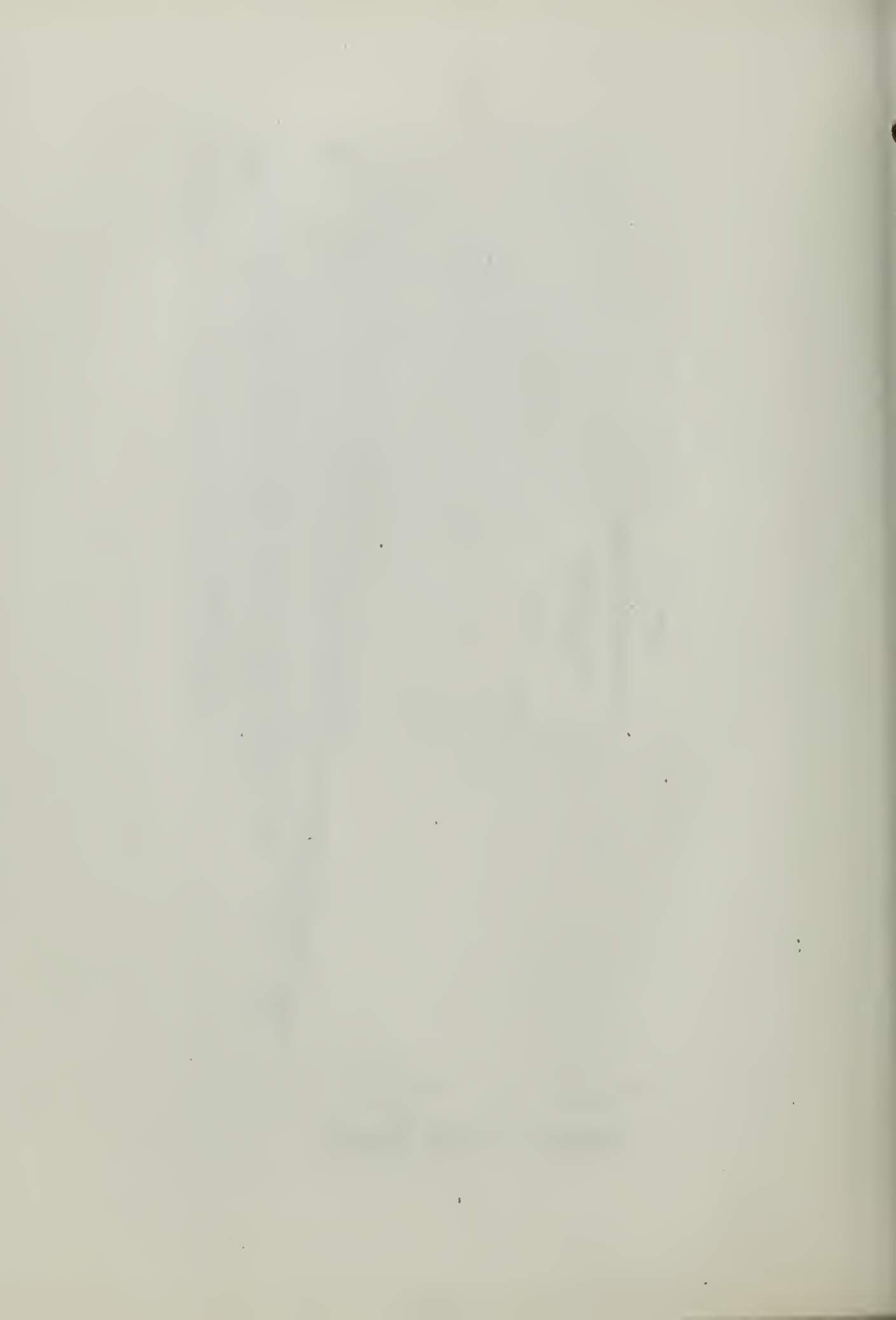
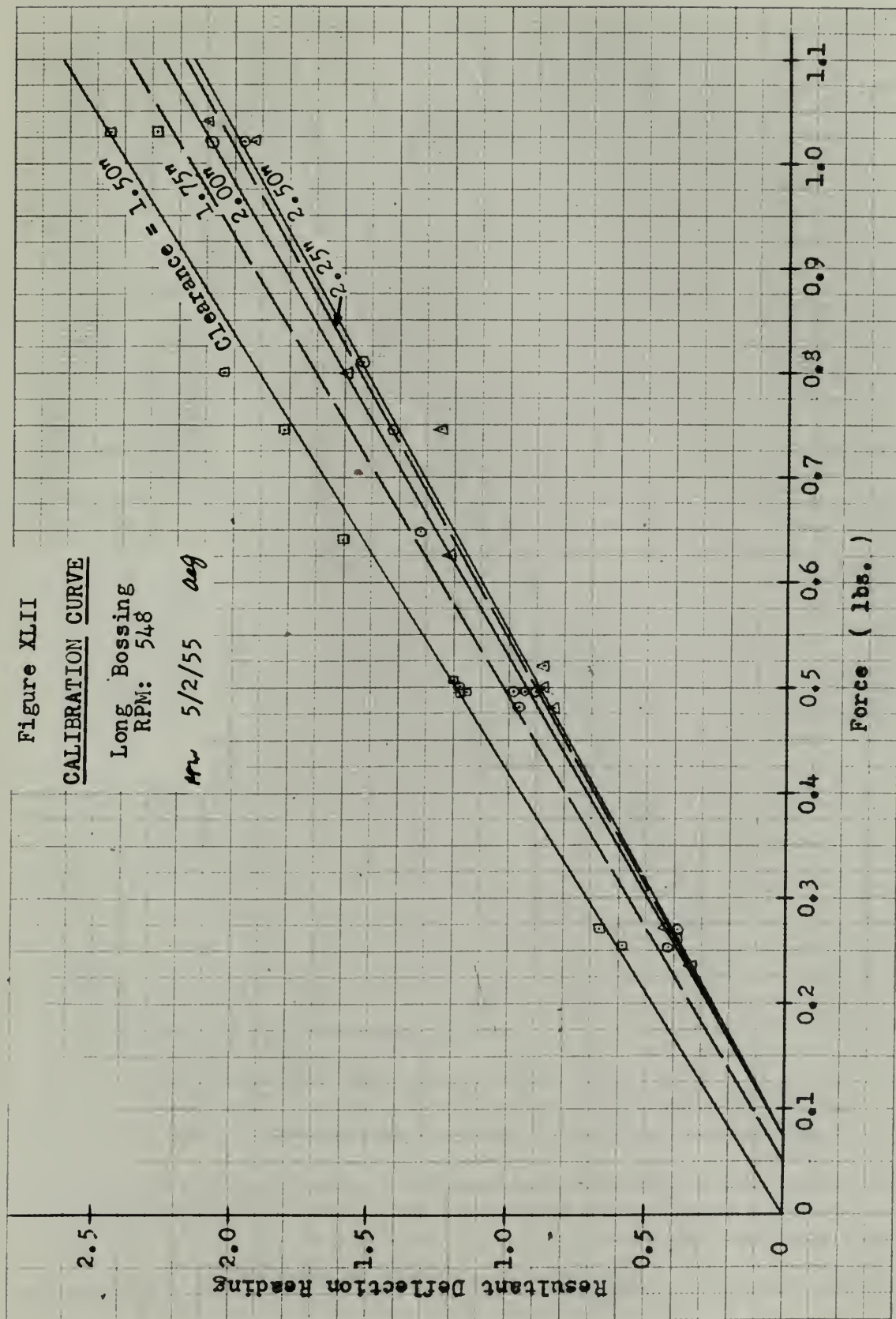


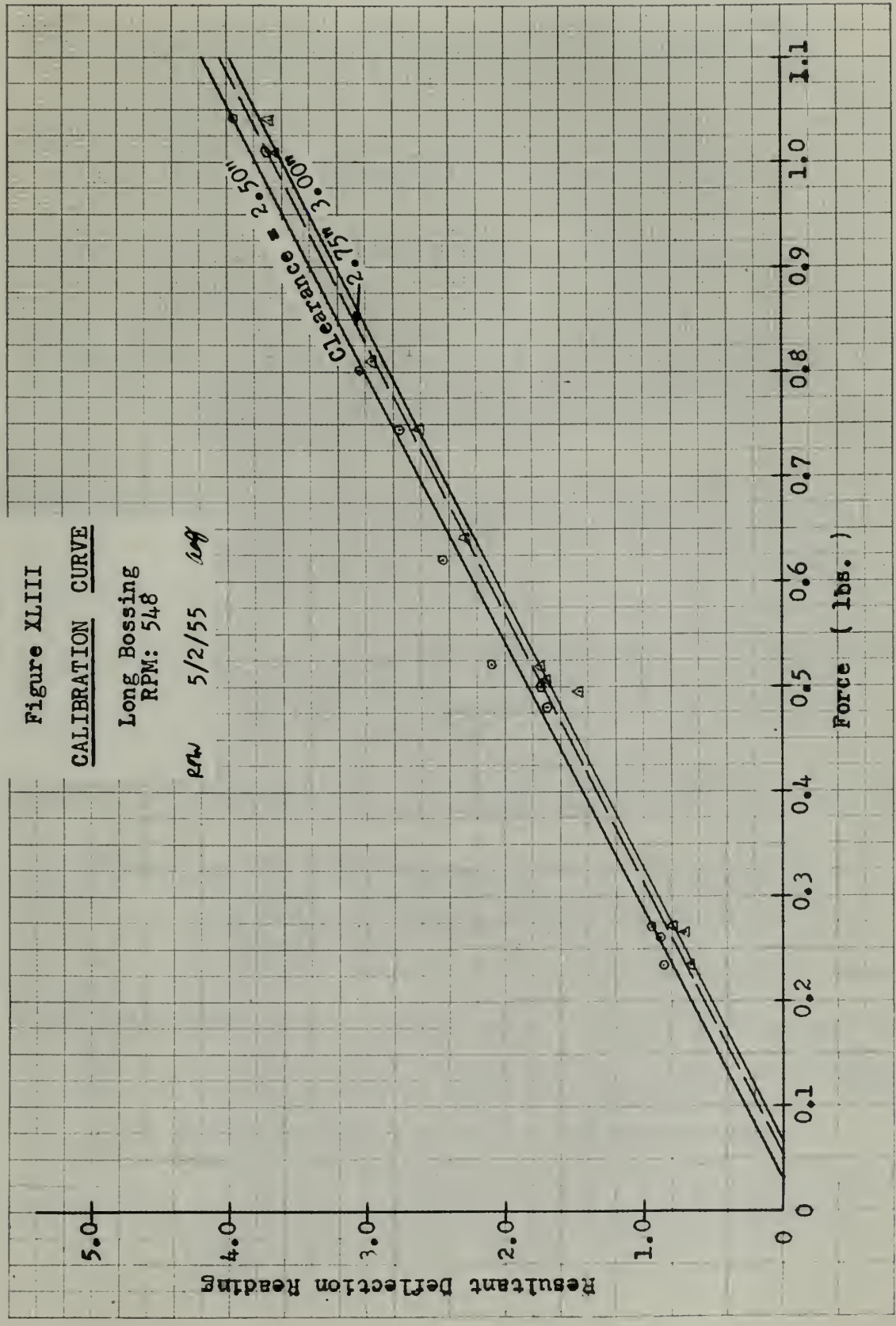
Figure XLII

CALIBRATION CURVE

Long Bossing
RPM: 548

Mr 5/2/55 *avg*





APPENDIX D

Bibliography

1. Brown, T.W.F., "Vibration Problems from the Marine Engineering Point of View," Transactions of the North East Coast Institution of Engineers and Shipbuilders, Vol. 55, 1938-1939.
2. Burrill, L.C., "Ship Vibration: Simple Methods of Estimating Critical Frequencies," Transactions of the North East Coast Institution of Engineers and Shipbuilders, Vol. 51, 1934-1935.
3. Calderwood, J., "Some General Observations on Vibration," Transactions of the North East Coast Institution of Engineers and Shipbuilders, Vol. 57, 1940-1941.
4. Constantini, "Vibration of Ships," Transactions of the Institution of Naval Architects, April 1938.
5. Coqueret, F., and Romano, P., "Some Particulars Concerning the Design of the 'Normandie' and the Elimination of Vibration," Transactions of The Society of Naval Architects and Marine Engineers, 1936.
6. Dinsmore, J.R., and Hooper, F.A., "Measurement of Hydrodynamic Vibratory Forces of a Model Propeller," Department of Naval Architecture and Marine Engineering Thesis, M.I.T., 1944.
7. Ellis, J.R., and Henderson, D.B., "Distribution of Hydrodynamic Vibratory Propeller Forces on a Model Propeller Bossing," Department of Naval Architecture and Marine Engineering Thesis, M.I.T., 1943.

APPENDIX D

Bibliography

1. Brown, T.W.L., "Vibration Problems from the Marine Engineering Point of View," Transactions of the North East Coast Institution of Engineers and Shipbuilders, Vol. 55, 1958-1959.
2. Gurtill, L.C., "Ship Vibration: Some Methods of Estimating Critical Frequencies," Transactions of the North East Coast Institution of Engineers and Shipbuilders, Vol. 51, 1934-1935.
3. Calderwood, J., "Some General Observations on Vibration," Transactions of the North East Coast Institution of Engineers and Shipbuilders, Vol. 57, 1940-1941.
4. Constantini, "Vibration of Ships," Transactions of the Institution of Naval Architects, April 1918.
5. Couvret, F., and Laroche, B., "Some Particulars Concerning the Design of the 'Inertance' and the Elimination of Vibration," Transactions of The Society of Naval Architects and Marine Engineers, 1916.
6. Glasstone, J.K., and Hooper, E.B., "Measurement of Hydrodynamic Vibration Forces on a Model Propeller," Report of Naval Architecture and Marine Engineering Thesis, N.I.T., 1944.
7. Ellis, J.H., and Anderson, E.H., "Distribution of Hydrodynamic Vibration Forces on a Naval Propeller Housing," Report of Naval Architecture and Marine Engineering Thesis, N.I.T., 1945.

8. Inglis, "A Suggested Method of Minimizing Vibration in Ships," Transactions of The Institution of Naval Architects, 1933.
9. Lewis, F.M., "Propeller Testing Tunnel at the Massachusetts Institute of Technology," Transactions of The Society of Naval Architects and Marine Engineers, 1939.
10. Lewis, F.M., "Propeller Vibration," Transactions of the Society of Naval Architects and Marine Engineers, 1935 and 1936.
11. Lewis, F.M., and Tachmindji, A.J., A paper presented at the Annual Meeting of The Society of Naval Architects and Marine Engineers, November 1954.
12. Mallock, A., "A Method of Preventing Vibration in Certain Classes of Steamships," Transactions of The Institute of Naval Architects, 1905.
13. McClure, A.C., and Mavor, J.W., "Hydrodynamic Vibratory Forces Generated by a Ship's Propeller," Department of Naval Architecture and Marine Engineering Thesis, M.I.T., 1950.
14. Pinkerton, D.F., and Arnold, H.A., "Vibratory Hydrodynamic Forces from Ship's Propellers," Department of Naval Architecture and Marine Engineering Thesis, M.I.T., 1941.
15. Reece, H.B., and Lansdowne, F.M., "Further Investigation of Hydrodynamic Vibratory Propeller Forces," Department of Naval Architecture and Marine Engineering Thesis, M.I.T., 1941.
16. Taylor, J. Lockwood, "Vibration of Ships," Transactions of the Institution of Naval Architects, 1930.
17. Taylor, J. Lockwood, "Ship Vibration Periods," Transactions of the North East Coast Institution of Engineers and Shipbuilders, Vol. 44, 1927-1928.
18. Todd, F.H., "Some Measurements of Ship Vibrations," Transactions of the North East Coast Institution of Engineers and Shipbuilders, Vol. 48, 1931-1932.

9. Indle, "A suggested method of minimizing vibration in ships," Transactions of the Institution of Naval Architects, 1933.

9. Lewis, F.M., "Propeller Testing Journal of the Massachusetts Institute of Technology," Transactions of the Society of Naval Architects and Marine Engineers, 1939.

10. Lewis, F.M., "Propeller Vibration," Transactions of the Society of Naval Architects and Marine Engineers, 1932 and 1933.

11. Lewis, F.M., and Tachibana, J., "A paper presented at the Annual Meeting of the Society of Naval Architects and Marine Engineers, November 1934.

12. Mallock, A., "A method of preventing vibration in certain classes of steamships," Transactions of the Institution of Naval Architects, 1905.

13. McCure, A.C., and Miller, J.W., "Hydrodynamic Vibration Forces Generated by a Ship's Propeller," Department of Naval Architecture and Marine Engineering Thesis, M.I.T., 1930.

14. Pinkerton, E.F., and Arnold, H.A., "Vibro-sonic Hydrodynamic Forces from Ship's Propellers," Department of Naval Architecture and Marine Engineering Thesis, M.I.T., 1941.

15. Rees, H.R., and Leshman, F.M., "Further investigation of hydrodynamic vibration generated by ship's propellers," Department of Naval Architecture and Marine Engineering Thesis, M.I.T., 1941.

16. Taylor, J. Lockwood, "Vibration of ships," Transactions of the Institution of Naval Architects, 1930.

17. Taylor, J. Lockwood, "Ship Vibration Periods," Transactions of the Institution of Naval Architects, Vol. 44, 1902-1903.

18. Todd, F.M., "The measurement of ship vibration," Transactions of the Institution of Naval Architects, Vol. 48, 1906-1907.

19. Todd, F.H., "Ship Vibration--A Comparison of Measured with Calculated Frequencies," Transactions of the North East Coast Institution of Engineers and Shipbuilders, Vol. 49, 1932-1933.

191. Todd, E. H. "Radio Migration--A Comparison of Migrations
with Calculated Expectations," Transactions
of the North West Coast Institute of
Invertebrate and Vertebrate, Vol. 49,

1931-1932.

192. Todd, E. H. "The Migrations of the
Invertebrate Animals of the North West Coast
of British Columbia," Transactions, 1931.

193. Todd, E. H. "The Migrations of the
Invertebrate Animals of the North West Coast
of British Columbia," Transactions, 1931.

194. Todd, E. H. "The Migrations of the
Invertebrate Animals of the North West Coast
of British Columbia," Transactions, 1931.

195. Todd, E. H. "The Migrations of the
Invertebrate Animals of the North West Coast
of British Columbia," Transactions, 1931.

196. Todd, E. H. "The Migrations of the
Invertebrate Animals of the North West Coast
of British Columbia," Transactions, 1931.

197. Todd, E. H. "The Migrations of the
Invertebrate Animals of the North West Coast
of British Columbia," Transactions, 1931.

198. Todd, E. H. "The Migrations of the
Invertebrate Animals of the North West Coast
of British Columbia," Transactions, 1931.

199. Todd, E. H. "The Migrations of the
Invertebrate Animals of the North West Coast
of British Columbia," Transactions, 1931.

200. Todd, E. H. "The Migrations of the
Invertebrate Animals of the North West Coast
of British Columbia," Transactions, 1931.

201. Todd, E. H. "The Migrations of the
Invertebrate Animals of the North West Coast
of British Columbia," Transactions, 1931.

J46

Jenks
Propeller excited
bossing forces.

28785

Jenks

J46

Jenks
Propeller excited bossing
forces.

28785

thesJ46

Propeller excited bossing forces /



3 2768 002 10744 3

DUDLEY KNOX LIBRARY